THE SYNTHESIS AND METABOLISM OF NOVEL 4-AMINOQUINOLINE ANTIMALARIALS

Thesis submitted in the accordance with the requirements of the University of Liverpool for the degree of Doctor of Philosophy.

Alison Emily Shone
MChem University of Liverpool
July 2007

DECLARATION

This thesis is the result of my own work. The material contained in the thesis has not been presented, nor is currently being presented, either wholly or in part for any other degree or other qualification.

Alison Emily Shone

This research was carried out in the Department of Chemistry and the Department of Pharmacology and Therapeutics at The University of Liverpool.

ACKNOWLEDGEMENTS

I owe a great deal to my supervisors Professor Paul O'Neill and Professor Kevin Park for, firstly, the fantastic opportunity to do this PhD and secondly, for all their help, encouragement and advice.

I am particularly grateful to Phill Roberts for all his help with the animal work in this thesis and also to Dr James Maggs whose assistance and knowledge of LC-MS has proved invaluable. Many thanks go to all the technical staff of the University of Liverpool.

I must express my gratitude to the MMV and to GlaxoSmithKline for funding these studies and for all the useful data and input (GSK).

All metabolism and distributional data for amodiaquine and isoquine were taken from a dissertation by Laura E. Randle.

To all my friends in chemistry, past and present: Zeyn, Vicky, Chi, Bénédicte, Peter "D'arcy" Gibbons, Inder, Louise, Stevie H, Paul S, Eddie, Nick "Mad-dog" Reilly and all members of the Paul O'Neill group – thanks for making these years so much fun! In particular I really appreciate the help Gibbo, Inder and Dave gave proof-reading chapters one and two and Paul Stocks for looking at chapter five. Special thanks go to the residents of Calton Avenue: Sarah, Kearnsy, Tobo and Mikey J – my best friends. To "the musketeers", Giancarlo and Dave, at the School of Tropical Medicine, thanks for all your help and advice and friendship – here's hoping I might one day be allowed into the clan! Charlie and Karen, you've been great.

Finally, on a personal note I would like to thank my parents, Elizabeth and also Matt. I am forever indebted to the constant understanding and support you have given me. Matt, the encouragement you have given me has been infallible –this book is for you, I love you.

CONTENTS

ABSTRACT

The developing world is desperate for new, safe, effective and affordable antimalarial drugs and has been since the demise of chloroquine (CQ) due to PfCRT-mediated parasite resistance, which emerged in the 1960s. Regarded as one of the most important chemotherapeutic agents in history, CQ is now largely ineffective in many areas of the world prompting studies into alternative treatments for malaria.

Using the related amodiaquine (AQ) as our template, we have developed simple routes to novel rationally designed analogues that are highly effective against CQ-resistant and CQ-sensitive parasites.

This thesis explores the metabolism and dispositional fate in rats of three such novel compounds; *N-tert* butyl isoquine (NTBISQ), *N-tert* butyl fluoro amodiaquine (FAQ-4) and *N-tert* butyl chloro amodiaquine (ClAQ-4), making comparisons with CQ, AQ and isoquine (ISQ).

Interchange of the 4'hydroxyl and 3'Mannich side-chain function of AQ has been found to block toxic quinone imine formation *in vivo* and replacement of the diethylamino side-chain with a *tert* butyl group has prevented P450 dealkylation. In addition to this, it has also been found that replacement of the 4'hydroxyl group of AQ with a halogen atom such as chlorine or fluorine can also inhibit metabolic activation to toxic quinone imine metabolites. After administration of [^{3}H]-NTBISQ to rats, the compound underwent direct glucuronidation to form the phenolic glucuronide (89.88 ± 2.31 %), this was in stark contrast to AQ which undergoes phase II gluthathione conjugation. [^{3}H]-ClAQ-4 was observed to undergo extensive metabolism to a side-chain carboxylic acid analogue (60.76 ± 2.34 %), whilst the main metabolite of [^{3}H]-FAQ-4 remains unresolved.

All three compounds were found to have excellent *in vitro* activity against a number of strains of *P. falciparum*. *In vivo* studies showed NTBISQ to have activity similar to that of AQ, with an ED_{50} value of 2.6 mg/kg. ClAQ-4 however, had surprisingly low *in vivo* activity (25 mg/kg) which was attributed to it undergoing rapid first-pass metabolism, due to its increased lipophilicity (LogP = 5.50 ± 0.59).

The results of this work have provided us with three compounds with potential for use in the treatment of malaria; NTBISQ in particular has been shown to be the stand-out candidate. Concerns over accumulation-based toxicity of these compounds still remain. The ability of this class of compounds to cause effects such as phospholipidosis and cardiotoxicity still hasn't been fully dissociated from efficacy. However we are confident that with its excellent pharmacokinetic and metabolic profile that NTBISQ is comparable, if not superior to piperaquine and pyronaridine, two drugs in phase III clinical trials at present. Indeed, NTBISQ is now due to enter phase I clinical trials in man.

ABBREVIATIONS

%	Percent
^{13}C	Carbon 13
^{1}H	Proton
[^{3}H]	Tritiated
ACN	Acetonitrile
ACTs	Artemisinin-based combination therapies
ADME	Absorption, Distribution, Metabolism and Excretion
ADR	Adverse drug reaction
amu	Atomic mass units
AQ	Amodiaquine
AQQI	Amodiaquine quinone imine
C	Degrees Celsius
Ci	Curies
Cl	Chloro
ClAQ-4	*N-tert* butyl chloro amodiaquine
cpm	Counts per minute
CQ	Chloroquine
CYP	Cytochrome P450
DCM	Dichloromethane
desAQ	Desethyl amodiaquine
desCQ	Desethyl chloroquine
DMSO	Dimethylsulfoxide
dpm	Disintegration per minute
DV	Digestive Vacuole
ED_{50}	The concentration at which response *in vivo* is 50 % of control levels
eq	Equivalents
EtOH	Ethanol
F %	Oral bioavailability
F	Fluoro
FAQ-4	*N-tert* butyl fluoro amodiaquine
Fe	Iron
g	Grams
GSH	Glutathione
GSK	GlaxoSmithKline
h	Hours
H_2O	Water

HCl	Hydrochloric acid
HPLC	High-performance liquid chromatography
Hz	Hertz
i.p.	Intraperitoneal injection
IR	Infra-red spectroscopy
i.v.	Intravenous injection
IC_{50}	The concentration at which response *in vitro* is 50 % of control levels
^{i}PrOH	Isopropanol
ISQ	Isoquine
J	Coupling constant
kg	Kilogram
L	Litre
LC-MS	Liquid chromatography-linked mass spectrometry
m/z	Mass to charge ratio
mCi	Millicuries
MeOH	Methanol
MFO	Mixed function oxidase system
mg	Milligrams
min	Minutes
mL	Millilitres
mmol	Millimoles
MMV	Medicines for Malaria Venture
mol	Moles
mp	Melting point
MPO	Myeloperoxidase
NaOH	Sodium hydroxide
NAPQI	*N*-acetyl-*p*-amino benzoquinone imine
nM	Nanomolar
nmol	Nanomoles
NMR	Nuclear magnetic resonance
NTBISQ	*N-tert* butyl isoquine
O_2	Oxygen
p	Probability
p.o.	By mouth
PfCRT	*Plasmodium falciparum* chloroquine resistance transporter
PQ	Piperaquine
Rt	Retention time
s	Seconds
Sn	Tin
$T_{1/2}$	Half-life

TLC	Thin-layer chromatography
µCi	Microcuries
µL	Microlitres
µmol	Micromoles
USA	United States of America
UV	Ultra-violet
v/v	Volume by volume
w/v	Weight by volume
WHO	World Health Organisation

CHAPTER 1

AN INTRODUCTION TO MALARIA AND THE 4-AMINOQUINOLINE CLASS OF ANTIMALARIALS

CONTENTS

1.1 INTRODUCTION TO MALARIA

1.1.1 Epidemiology

Malaria remains one of the most important disease problems in the world. Despite the greatest efforts to eradicate the disease in the 1950s and 1960s, malaria has not only prevailed but has made a dramatic resurgence within the past two decades. Morbidity and mortality rates are at almost unprecedented levels, with more than 90 countries affected. Malaria is responsible for approximately 515 million clinical episodes and 2 million deaths a year (Bell *et al.*, 2004; Olliaro *et al.*, 1996; Snow *et al.*, 2005).

Malaria is thought to be both a disease of poverty and a cause of poverty. It is largely a disease of the tropics, with the majority of cases occurring in sub-Saharan Africa, however, it also occurs in many sub-tropical locations. The effects of the disease mean that a substantial proportion of the population of sub-Saharan Africa is ill for a large part of the year. This makes sustained economic development very difficult to achieve and thus the global effects of the disease are a threat to public health and productivity, impeding the progress of many countries toward democracy and prosperity (www.rbm.who.int, 2001-2010).

Even with the important advances in our understanding of the disease, malaria continues to be one of the greatest causes of serious illness and death. The majority of deaths tend to be pregnant woman and children, with a child dying from the disease every 10 seconds (Oaks *et al.*, 1991; Rosenthal, 2001).

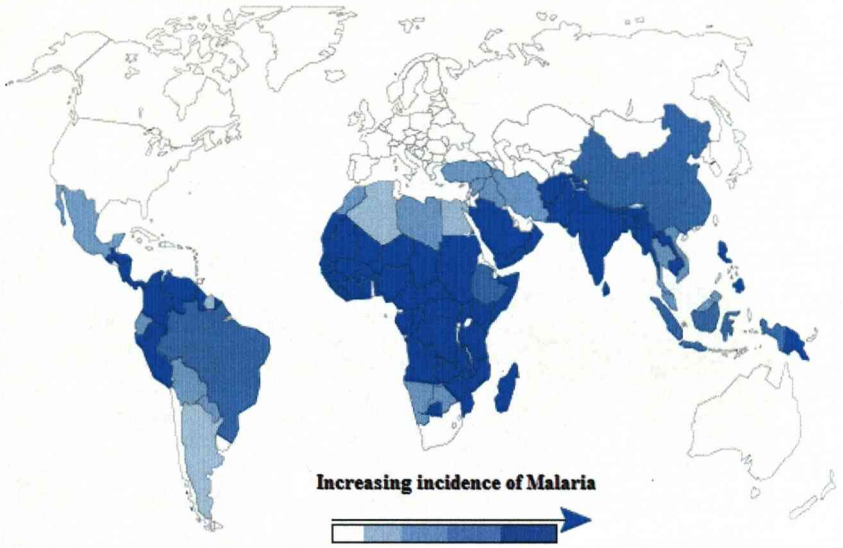

Figure 1.1 Geographical distribution of malaria. (Map from Roll back Malaria partnership, WHO).

1.1.2 The Malarial Pathogen

Humans become infected with malaria after a bite from the female anopheline mosquito harbouring plasmodial sporozoites. Four sub-species of *Plasmodium* exist causing human disease. *Plasmodium falciparum* is, by far, the most important species, often causing death through coma or anaemia; it uniquely infects erythrocytes of all ages. Infection by this species produces malignant *tertian malaria* – 'tertian' because the fever is said to recur every third day, 'malignant' because it is the most severe form of malaria and can be fatal. *P. falciparum* has demonstrated the ability to develop resistance to most available antimalarial drugs. *P. vivax*, also very common, is one of the most important causes of morbidity among parasite infections but rarely kills (Bell *et al.*, 2004; Rang *et al.*, 1999). Drug resistance to this species of malaria has only recently been recognised but it is increasing, with cases resistant to chloroquine (CQ) and other antimalarials noted in Southeast Asia, Oceania, India

and South America (Olliaro *et al.*, 2003). *P. malariae* and *P. ovale* infections are relatively uncommon causes of human malaria.

1.1.2.1 The Parasite Lifecycle

The lifecycle consists of a sexual stage, which takes place within the mosquito, and an asexual stage, which occurs in man (Figure 1.2) (Rang *et al.*, 1999; Rosenthal, 2001). During a blood meal the mosquito injects a relatively small number of sporozoites into the bloodstream. Within 30 minutes the immature parasites are cleared from the blood and enter the parenchymal cells of the liver. It is here, over the next 10 - 14 days that an asymptomatic pre-erythrocytic stage of parasite multiplication and development occurs. At the end of this stage the parasitised liver cells rupture and merozoites are released into the systemic circulation. These merozoites can then bind to and enter the erythrocytes whereby the parasites undergo asexual multiplication. This phase is responsible for the clinical manifestations of malaria. As the parasite matures it remodels the host cell by inserting parasitic proteins and phospholipids into the red cell membrane. Haemoglobin is digested by the parasite, using a system of proteases, and is transported into the parasite digestive vacuole (DV) (Pagola *et al.*, 2000). Here it is converted into monomeric haem and an amino acid source essential for further parasite growth (Figure 1.3) (Francis *et al.*, 1997; Olliaro *et al.*, 1995). Free haem is toxic to the parasite (Orjih *et al.*, 1981) and can cause enzyme inhibition, peroxidation of membranes, production of oxygen free-radicals and impaired leukocyte function. All *Plasmodium* species have a unique capability to render the haem harmless within the parasite DV by a process of biomineralization resulting in a crystalline structure known as haemazoin, or malarial pigment (Figure 1.3) (Ridley

et al., 1997). The structure of this non-toxic pigment has remained speculative, despite the numerous spectroscopic tools used in attempts at characterisation (Bohle *et al.*, 1997; Fitch *et al.*, 1987). It is now believed to consist of haem subunits paired together as dimers by two reciprocal iron-oxygen bonds (Pagola *et al.*, 2000)

At the end of the parasite multiplication the red blood cell ruptures and merozoites are released into the bloodstream which can then bind to, and enter fresh red cells, thus beginning the cell cycle again.

In certain forms of malaria, some of the sporozoites entering the liver cells can form hypnozoites, a resting form of the parasite. These hypnozoites can remain dormant for months or even years, but can be reactivated to continue an exoerythrocytic cycle of multiplication leading to relapses of malaria.

Some merozoites can differentiate into male and female gametocytes, which can subsequently infect mosquitoes that suck on the blood of an infected host, allowing completion of the sexual stage of the life cycle.

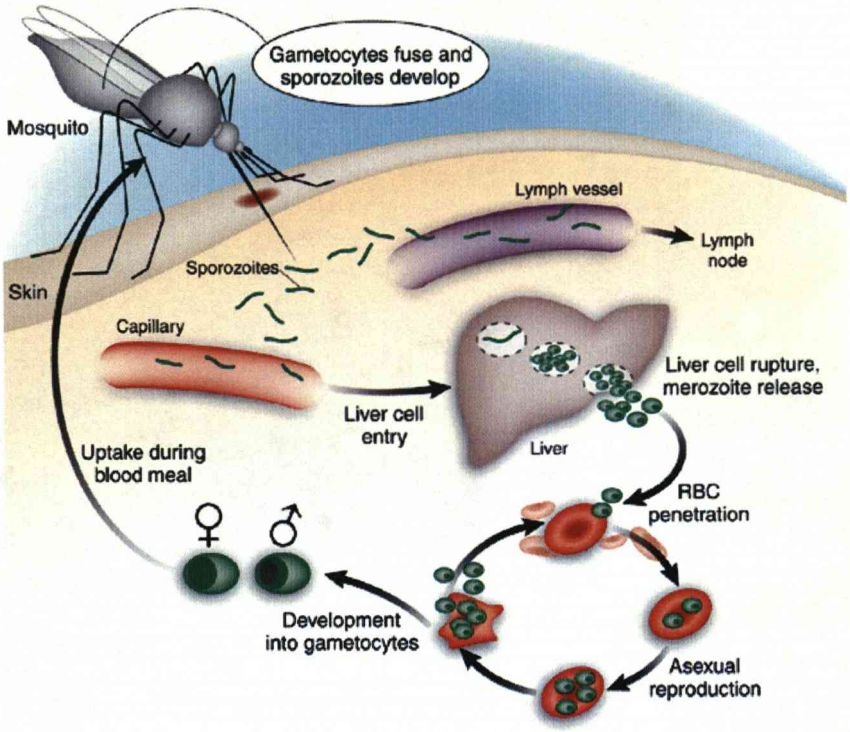

Figure 1.2 The life cycle of the malarial parasite (Jones *et al.*, 2006).

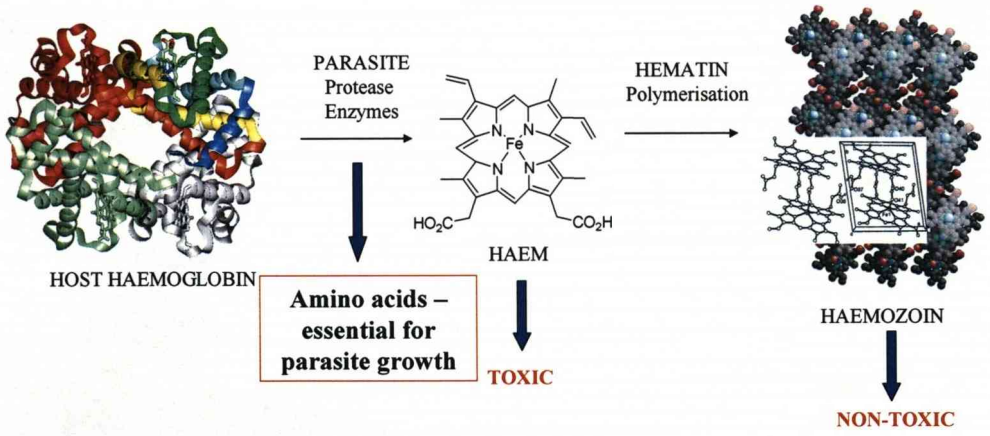

Figure 1.3 Schematic showing the degradation of human haemoglobin by the malaria parasite to form free haem, followed by polymerisation to the non-toxic malarial pigment, haemazoin.

1.1.3 Failure to Eradicate Malaria

In 1955, the World Health Organisation launched a programme to eradicate malaria using powerful 'residual' insecticides and highly effective antimalarial

agents which had become available (Mabaso *et al.*, 2004). The effort initially appeared to be a success owing to the incidence of malaria declining dramatically by the end of the 1950s. However, over more recent decades, morbidity and mortality caused by malaria have increased in many parts of the world and now 40% of the world's population remains at risk of contracting the disease.

Numerous factors contribute to the persistence of this severe, worldwide problem of malaria. Firstly, efforts to control mosquito vectors, which were quite successful in some areas many years ago, have been limited by financial constraints and insecticide resistance. Secondly, programmes to treat and control malaria have been severely limited by poverty in most endemic regions. Thirdly, despite significant efforts, an effective malaria vaccine is not yet available. Fourthly, people with no natural immunity to the disease are now exposed due to migration, climatic change and creation of new habitats. Finally, and from a medicinal chemist's point of view, more importantly, the malaria parasites have consistently demonstrated the ability to develop resistance to available drugs. The pace of this developing resistance is grossly imbalanced by the development of new compounds, thus the efficacy of current compounds in the field has been reduced (Morgan *et al.*, 2005; Olliaro *et al.*, 2003; White, 1992; White, 1998). This is best exemplified with chloroquine (CQ), a member of the 4-aminoquinoline class of antimalarials (Figure 1.4) (discussed Chapter 1 Section 1.2.2).

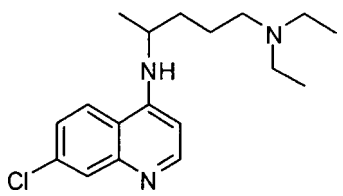

Figure 1.4 Chemical structure of Chloroquine

1.2 THE 4-AMINOQUINOLINE CLASS OF ANTIMALARIALS

1.2.1 Introduction

Quinoline-containing antimalarial drugs, such as CQ, quinine and mefloquine (Figure 1.5) have been used for years as key tools in the fight against malaria (Foley *et al.*, 1998). The synthetic 4-aminoquinoline, CQ was introduced during World War II for the treatment of malaria (Loeb *et al.*, 1946). Due to its low toxicity and for many years, effectiveness as an antimalarial, CQ became a mainstay in the chemotherapeutic armoury against malaria. The appearance of CQ resistance prompted the initiation of massive screening programmes in the USA, resulting in the production of three new drugs; the 4-aminoquinoline, amodiaquine (AQ); the quinolinemethanol, mefloquine, and the phenathrene methanol, halofantrine (Figure 1.5). Unfortunately, problems such as resistance and toxicity have limited the use of these drugs and for the first time in 300 years, we are in danger of having no effective quinolines in the fight against malaria.

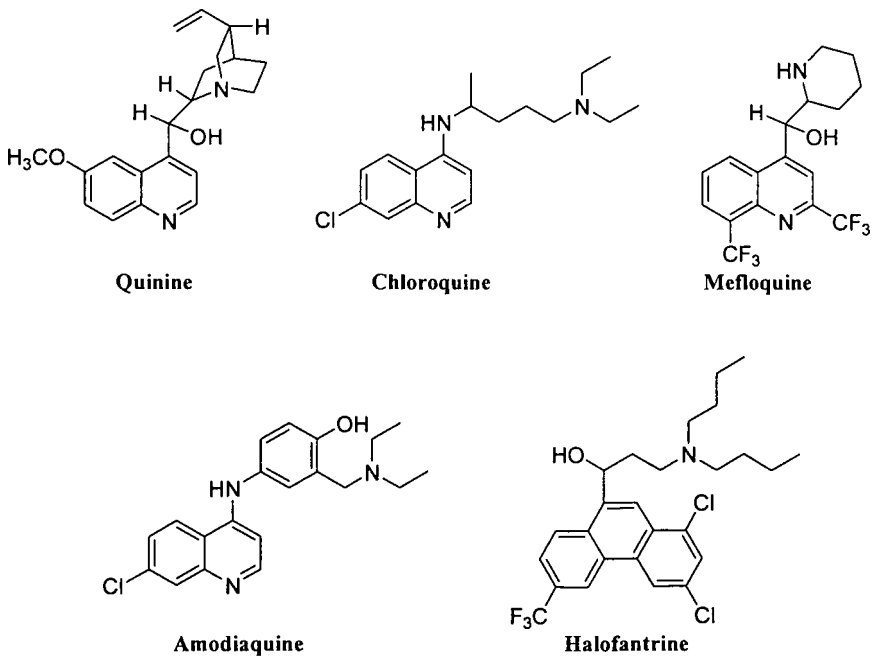

Figure 1.5 Structures of some quinoline-based antimalarial drugs

1.2.2 Mechanism of Action

CQ is active against only the erythrocytic stages of malaria parasites. It is not active against pre-erythrocytic parasites, hypnozoite-stage parasites in the liver, or against gametocytes. It is thought that the antimalarial activities of CQ and other quinoline-type compounds are a function of both the ability of the drug to interfere with the crystallisation process of haemazoin and the ability of the drug to accumulate to pharmacologically relevant concentrations at the site of drug action (Hawley *et al.*, 1998). This is supported by ultrastructural studies, which showed the first observable changes in malarial parasites treated with pharmacologically relevant concentrations of CQ to be swelling of the DV and accumulation of undigested haemoglobin in endocytic vesicles (Rosenthal, 2001). Thus, the ability of the 4-aminoquinolines to target such a parasite-specific process explains the selectivity of these drugs.

1.2.2.1 Accumulation of CQ in the Parasite DV

A major hypothesis for CQ accumulation suggests that it is driven by an "ion trapping" mechanism. CQ is taken up only to a very limited extent (to concentrations about two-fold those in plasma) by uninfected erythrocytes (Graph 1.1) (Macomber *et al.*, 1966). However, in contrast, the drug is concentrated several thousand-fold inside the parasitised erythrocyte.

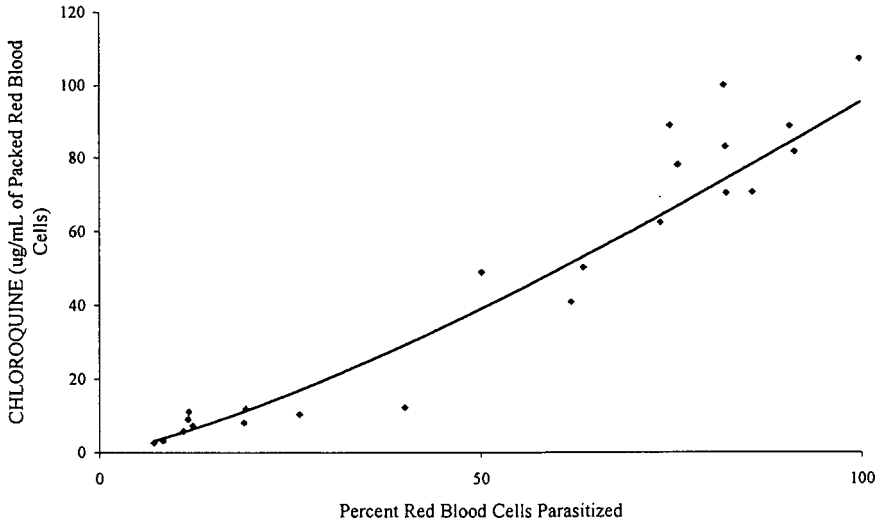

Graph 1.1 Correlation between parasitemia and uptake of chloroquine by erthyrocytes. Mice, 2-4 days after inoculation with CQ-sensitive *P. berghei* and uninfected mice treated *i.p.* with [^{14}C]-CQ (40 mg/kg) (Macomber *et al.*, 1966)

CQ is a diprotic weak base (pK_{a1} = 10.2, pK_{a2} = 8.1) and according to the weak base model, an unprotonated form can readily cross the membranes of the parasitised red cell and move along the pH gradient to accumulate within the acidic DV (pH 5-5.2) (Saliba *et al.*, 1998; Yayon *et al.*, 1984). As the drug moves down this pH gradient it becomes protonated, rendering it membrane impermeable and trapped within the acidic compartment of the DV. The level of accumulation has been reported to be higher within the DVs of malaria-infected red blood cells than in acidic compartments of mammalian cells, suggesting that there may be additional mechanisms for uptake of quinolines in parasite-infected erythrocytes, such as receptor binding (Saliba *et al.*, 1998).

1.2.2.2 The Binding of CQ to Free Haem

The mature human erythrocyte is perceived by the parasite, essentially as a "sack" of haemoglobin, providing it with a ready supply of amino acids and other nutrients (Francis *et al.*, 1997). However, as haemoglobin is degraded by the parasite, free haem (ferriprotoporphyrin IX, FP) is generated *via* haem auto-

oxidation. FP is fairly innocuous in the ferrous form within haemoglobin but becomes toxic upon release from globin. The parasite lacks the machinery for enzymatic degradation of the potentially lytic FP and is faced with a significant toxic-waste problem. As mentioned earlier, the parasite has a unique ability to crystallise the free haem to form the malarial pigment haemazoin, the process of which is essential for the survival of the malaria parasite (Ridley *et al.*, 1997).

The issue of haem disposal represents an "Achilles heel" for the parasite, leaving it susceptible to attack from chemotherapeutic agents, such as the 4-aminoquinolines. CQ has been shown to interact with FP by formation of a co-facial π-π stacking-type complex (Chou *et al.*, 1980) (Figure 1.6). It has been proposed that the quinoline moiety of CQ effectively intercalates two μ-oxo dimers of FP and also that the haem-quinoline complex is clearly non-covalent, as it can be diminished by extensive washing (O'Neill *et al.*, 1998; Sullivan *et al.*, 1996). This model predicts that the porphyrin plane can accommodate wide structural variations of the interacting species, leading to a weak specificity, consistent with the large variety of quinolines able to inhibit parasite growth. By binding to FP, CQ and the 4-aminoquinolines can inhibit the parasites method of crystallisation, resulting in higher concentrations of free haem, leading to parasite death (Slater *et al.*, 1992).

Complex with Haematin

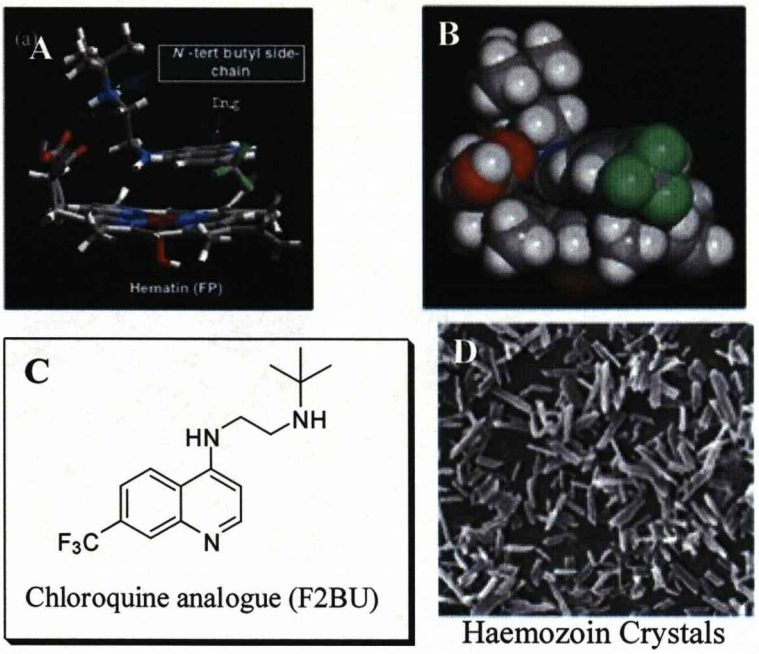

Figure 1.6 A-C Molecular representation of the complexation of chloroquine analogue, F2BU with FP and D Formation of haemozoin crystals

1.2.3 CQ Resistance of the Malaria Parasite

Resistance to CQ appeared in malaria parasites in the 1960s and since then has slowly but inexorably spread from South America and South East Asia and throughout Africa, the global heartland of malaria mortality and morbidity (Young *et al.*, 1961). The emergence of this resistance after so many years of widespread CQ use suggests that multiple mutations are required to produce the CQ resistance phenotype (O'Neill *et al.*, 1998). From a biochemical point of view, CQ-resistant isolates of *P. falciparum* accumulate less drug than their sensitive counterparts (Bray *et al.*, 1992; Bray *et al.*, 1998; Verdier *et al.*, 1985).

There are a number of possible theories for reduced CQ uptake including; altered pH gradients across the DV membrane or between the parasite cytosol and

the erythrocyte cytosol or altered membrane permeability or specificity of a permease or other transporter (Ridley, 1998).

Importantly, by making only very minor changes to the CQ structure, such as varying the amino-alkyl chain length by one carbon atom, compounds with good activity against the CQ-resistant strain of malaria can be produced (Bray *et al.*, 1998). This implies a high degree of structural specificity in the factors responsible for reduced CQ uptake. The major CQ resistance determinant has been found to be due to a membrane transporter known as *Plasmodium falciparum* chloroquine resistance transporter (PfCRT) (Wellems *et al.*, 1990). More recently it has been discovered that mutations in the gene coding for PfCRT are believed to confer CQ resistance by reducing the amount of CQ accumulated by the parasite (Bray *et al.*, 2005; Lakshmanan *et al.*, 2005).

1.2.4 The Development of Amodiaquine

Amodiaquine (AQ), a second member of the 4-aminoquinoline class of antimalarials, was initially synthesised by Burckhalter and co-workers in 1948 during a programme aimed at the discovery of effective 4-aminoquinoline compounds (Burckhalter *et al.*, 1948). At that time AQ was deemed to have an excellent activity/toxicity profile. AQ is closely related to CQ, differing only in the presence of a *p*-hydroxy-anilino aromatic ring in its side chain (Figure 1.5). Interestingly during *in vitro* tests, AQ was shown to be more active at inhibiting the growth of *P. falciparum* than CQ and has also been shown to be superior against CQ-resistant strains of *P. falciparum* (Hawley *et al.*, 1996b; Watkins *et al.*, 1984) (Table 1.2).

	IC_{50} (nM)		
Drug	3D7	HB3	K1
CQ	19.4 ± 1.9	14.9 ± 3.9	183.2 ± 11.1
AQ	11.2 ± 2.8	9.6 ± 3.7	15.5 ± 9.4

Table 1.2. ***In vitro*** **antimalarial activity of CQ and AQ.** *P. falciparum* strains 3D7 and HB3 are CQ-sensitive, K1 is CQ-resistant. IC_{50} values are expressed in nM.

AQ is accumulated within the parasite DV more efficiently than CQ which is unexpected on the basis of ion trapping as, despite being a diprotic weak base like CQ, its pKa values are lower (pK_{a1} = 8.1, pK_{a2} = 7.1) (Hawley *et al.*, 1996a). This increased uptake of AQ may be due to an enhanced affinity for an intra-parasitic binding site leading to a subsequent increase in drug accumulation and therefore greater activity against the malaria parasite (Hawley *et al.*, 1996b).

1.3 DRUG METABOLISM AND TOXICITY

1.3.1 Introduction to Drug Metabolism

Metabolism is a drug clearance process and knowledge of the metabolic pathways of a drug can help us understand the processes of elimination of that compound from the body. Humans and animals have evolved complex systems that detoxify foreign chemicals entering the body. Most of the substances entering the body are lipophilic and can be reabsorbed from the kidney tubule back into the bloodstream where they can go on to accumulate within tissues (Gram, 1980). In order for these chemicals to be efficiently eliminated they must undergo the process of biotransformation.

Metabolic processes are divided into phase I and phase II reactions which can occur sequentially. Phase I is the alteration of the original foreign molecule so as to add on a functional group which can then be conjugated during Phase II metabolism in order to undergo elimination (Timbrell, 2000).

1.3.1.1 Phase I Metabolism

Phase I reactions modify the structure of a xenobiotic so as to introduce a functional group which will increase the hydrophilicity of the molecule. The three main chemical reactions involved in this process are oxidation, reduction and hydrolysis (Table 1.3).

A series of enzymes, located in the endoplasmic reticulum, known as the cytochrome P450 microsomal mixed function oxidase (MFO) system, are particularly important in oxidation reactions (Gibson *et al.*, 1994).

Phase I	Phase II
Oxidation involving cytochrome P450	Glucuronidation/glucsidation
Oxidation - others	Sulfation
Reduction	Methylation
Hydrolysis	Acetylation
Hydration	Amino acid conjugation
Isomerisation	Glutathione conjugation
	Fatty acid conjugation
	Condensation

Table 1.3 Reactions classed as phase I or phase II metabolism

1.3.1.2 Phase II Metabolism

The conjugation reactions tabulated above, involve a diverse group of enzymes. They involve the addition of endogenous co-factors to the reactive moiety, leading to a progressive increase in polarity of the molecule. This increase in polarity means the compound will become more soluble in bile or urine and will consequently be excreted from the body, thus reducing the potential for toxicity (Pirmohamed *et al.*, 1996).

Glucuronidation is the most widespread, and the most important of the conjugation reactions, possibly due to the relative abundance of UDP-glucuronic acid, the co-factor required for the reaction which is present in all tissues of the body (Dutton, 1980) (Figure 1.7). Conjugation can occur with alcohols, phenols, hydroxylamines, carboxylic acids, amines, sulfonamides and thiols. The process involves nucleophilic attack of an oxygen, sulfur or nitrogen atom at C-1 of the glucuronic acid moiety. Drug-glucuronide conjugates are often excreted in bile and once in the intestine they have two possible fates. The first is that the drug will be excreted in faeces and the second is that it can be hydrolysed back to the parent compound by β–glucuronidase (present in gut bacteria). The free drug can then be absorbed through the gut wall and re-enter the liver *via* the hepatic portal vein and

the cyclic process can begin again. This re-circulation, known as enterohepatic circulation can occur for several cycles leading to retention and a substantially increased half-life of a drug (Dutton, 1980).

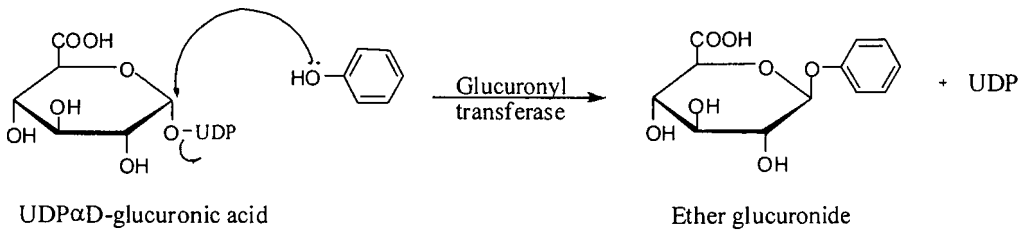

Figure 1.7 Formation of an ether glucuronide in the β-conformation.

Glutathione conjugation is recognised as a major defence system in deactivating toxic materials within the body (Gibson *et al.*, 1994). Glutathione exists as a tripeptide, composed of gluatamic acid, cysteine and glycine. Located in the cytosol of many cells, but primarily the liver, it can react with a vast range of structurally diverse electrophilic substrates such as epoxides, haloalkanes, nitroalkanes, alkenes, and aromatic compounds (Smith *et al.*, 2001; Timbrell, 2000). The presence of the cysteine residue provides a nucleophilic sulfydryl group and so the glutathione molecule is likely to react as the thiolate ion, GS^-. An important example of glutathione conjugation is the detoxification of the reactive metabolite formed from paracetamol, *N*-acetyl-*p*-benzoquinone imine (NAPQI) (Kitteringham *et al.*, 2003) (Figure 1.8). Paracetamol largely undergoes detoxification by the phase II processes glucuronidation and sulfation to form stable metabolites. Approximately 5-10 % of the dose undergoes P450 metabolism to form the toxic quinone imine metabolite, NAPQI, which can subsequently react with glutathione to form a conjugate (Newton *et al.*, 1986; Williams *et al.*, 2004). At overdose, the formation of toxic metabolites overloads the capacity of the conjugating system to inactivate

them. Toxicity occurs as a greater proportion of the drug undergoes bioactivation and binds covalently to proteins (Timbrell, 2000). This is an important process as it can be directly related to the metabolism of the antimalarial AQ (Chapter 1; Section 1.3.7).

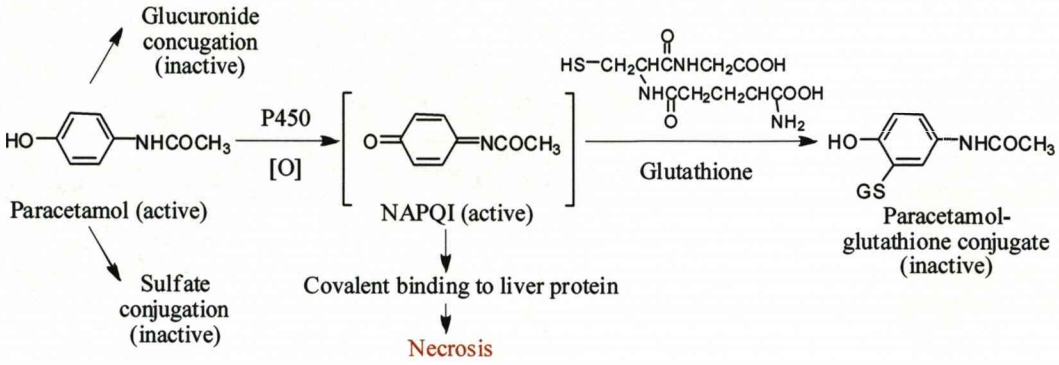

Figure 1.8 Proposed metabolic activation of paracetamol to a toxic, reactive intermediate (NAPQI). NAPQI can react with glutathione to form a conjugate. In the absence of GSH, such as paracetamol overdose, NAPQI can react with nucleophilic residues on proteins (e.g. SH of cysteine).

1.3.2 Metabolism of CQ

CQ has excellent oral bioavailability with almost complete absorption from the gastrointestinal tract (Gustafsson *et al.*, 1983). In man, CQ is found in the plasma and tissues mostly as the parent compound. It is metabolised mainly by the hepatic microsomal system by degradation of the alkyl side chain to form desethylchloroquine (desCQ) and also bisdesethylchloroquine (bisdesCQ) (Kim *et al.*, 2003) (Figure 1.9).

Excretion of CQ is slow, taking approximately 3-4 weeks for equilibrium to be reached between the tissue and plasma levels. Particularly high binding of CQ occurs within the tissues, especially those containing the pigment melanin (for

example the eyes and skin). Retinopathy is the most serious form of toxicity associated with long-term CQ usage in humans (Peters *et al.*, 1984).

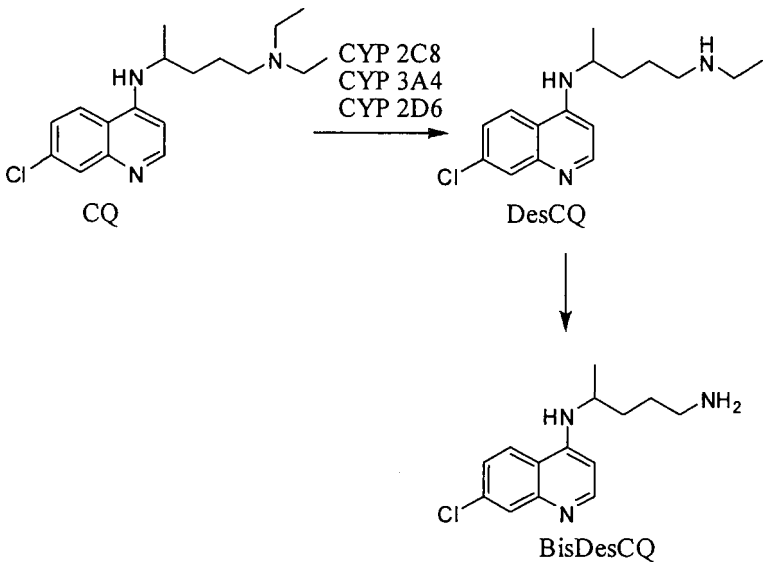

Figure 1.9 Chloroquine (CQ) and desethylchloroquine (desCQ) *N*-dealkylation pathways in humans (Projean *et al.*, 2003)

1.3.3 Drug Metabolism: Bioactivation *versus* Detoxication

On average, some 10,000 compounds undergo testing before one is found that can be marketed as a drug. Many compounds are dropped from the drug-discovery pipeline at different steps along the way, often due to toxicity. Therefore toxicity is a major barrier to drug development.

The toxicity profiles of some compounds can be related to chemical structures, and more specifically, to particular substructures, known as toxicophores (Hakimelahi *et al.*, 2005; Wang *et al.*, 1999).

By identifying chemical functionalities and acknowledging the conditions under which these functionalities could be changed, it may be possible to develop novel, more marketable drugs which carry less risk of causing adverse drug reactions (Guengerich, 2006).

A drug entering the systemic circulation may take one of three pathways, two of which can lead to various forms of toxicity.

Cellular accumulation of a drug can lead to direct toxicity. Accumulation is a major concern and can occur after administration of large doses of drug causing the excretion or metabolism processes to become saturated, hence decreasing the rate of elimination (Timbrell, 2000). It can also occur simply due to inefficient metabolism and excretion due to some property of the drug; for example the retinal toxicity observed with the long-term use of CQ. In some cases, cofactors or protective agents may be required and their concentration may become limited e.g. glutathione in paracetamol detoxification. Accumulation results in levels of drug higher than those required for therapeutic effect and thus the tissue cells experience chemical stress which can lead ultimately to cell death.

A drug may undergo bioactivation to give chemically more reactive metabolites. These reactive metabolites can bind to or interact with nucleic acids, protein receptors or enzyme transporter signalling pathways, to cause carcinogenicity, necrosis, apoptosis or hypersensitivity reactions.

Alternatively, the drug may undergo metabolism *via* phase I and II pathways, forming stable metabolites which can then be excreted.

It is an improved understanding of these processes that can allow us to better predict and therefore prevent adverse drug reactions.

1.3.4 Adverse Drug Reactions

Adverse drug reactions (ADRs) are significant drug toxicity problems that contribute to the morbidity and mortality of patients. An ADR has been defined as any noxious or unintended reaction to a drug that occurs when administered in standard doses by the appropriate route for the purpose of prophylaxis, diagnosis or

treatment (Vervloet *et al.*, 1998). ADRs can be classified into three types, A, B and C.

Type A (pharmacological) reactions encompass all those that are predictable from the known pharmacology of the drug (Davies, 1996). They account for over 80 % of all reactions and often represent an exaggeration of the pharmacological effect of the drug.

Type B (idiosyncratic) reactions are ones that are not predictable from knowledge of the basic pharmacology of a drug and exhibit marked inter-individual variation. The classic example of an idiosyncratic reaction is the toxicity of paracetamol (Figure 1.8). Whilst it cannot be classed as an adverse reaction *per se*, (the hepatoxicity is caused by inappropriate use of the drug), the hepatic injury resulting from paracetamol is a function of various host factors and not only dose. As with AQ toxicity, the quinone imine can bind to cellular macromolecules and initiate an idiosyncratic response. This explains why many drugs, that are not toxic in therapeutic doses, become toxic when higher doses are ingested or conjugation is impaired by depletion of cofactors.

Type C (chemical) reactions have biological characteristics which can either be predicted or rationalised in terms of chemical structure (Park *et al.*, 1998).

Tebuquine and halofantrine are two notable antimalarial drugs that have caused serious adverse reactions (Figure 1.10). Tebuquine reached pre-clinical toxicological trials on the basis of its antimalarial activity, however failed to reach man due to the presence of neutrophil toxicity in animals (Naisbitt *et al.*, 1998; Werbel *et al.*, 1986). In contrast, halofantrine is still in clinical use, however cases of cardiotoxicity have been reported and it is no longer used in patients with known

cardiac impairment (Bouchard *et al.*, 2002; Ker Keule *et al.*, 1993; Wesche *et al.*, 2000).

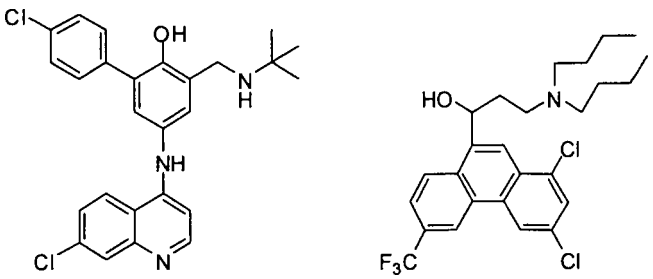

Tebuquine Halofantrine

Figure 1.10 Chemical structures of tebuquine and halofantrine.

1.3.5 Structural Alerts and the Prediction of Toxic Metabolites

It is important to know which chemical features, or toxicophores, of a drug are likely to cause an adverse reaction. An extensive list of structural alerts exist, these include (Kalgutkar *et al.*, 2005):

- aniline
- epoxide
- quinone
- quinone imine
- acyl halide
- hydroxylamine
- furan
- thiophene
- allylic alcohol
- acyl glucuronide
- 4-aminophenol

It is unfortunate that this list also encompasses a large number of pharmacophores, e.g. anilines and aromatic amines – which are particularly relevant to anti-infective agents (Figure 1.11). As highlighted with paracetamol, the presence of a structural alert does not guarantee toxicity.

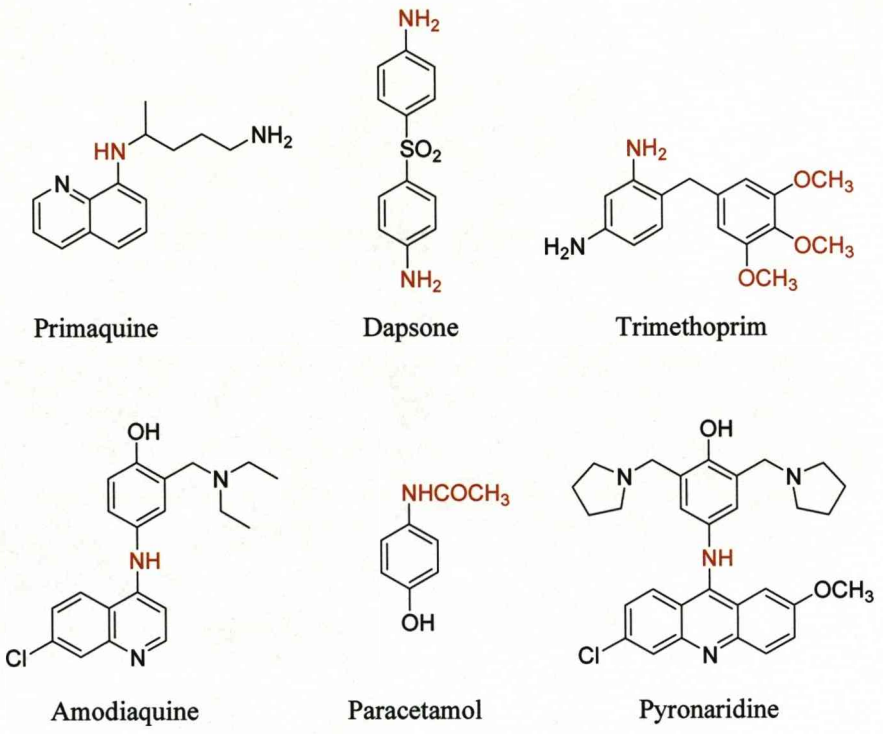

Figure 1.11 Structural alerts in anti-infective agents. Groups highlighted in red, such as the amine, methoxy and acetamido groups indicate the presence of structural alerts.

1.3.5.1 Computational Approaches to Predict Drug Toxicity

A new approach in the evaluation of drug toxicity, absorbtion, distribution, metabolism and excretion (ADME) and pharmacokinetics is the use of computational prediction. Many software packages are now available such as Meteor (Lhasa); (Boobis *et al.*, 2002) and MetaDrug™ (Genego); (Ekins *et al.*, 2000; Elkins *et al.*, 2006). These systems assess compounds for potential therapeutic indications and side effects by examining the compound's structure and making comparisons to large compound libraries and databases. MetaDrug™ in particular, will take a novel compound and split it into metabolites before running them through QSAR models and visualising them in the context of pathways, cell processes and toxic and disease networks disturbed by the compound's action. Although these programs have not yet been adequately validated and still require improvements, the emerging consensus is

that the predictions may provide an advantage to *in vitro* testing, as less investment in technology, resources and time are required. It is possible that in the future, these programs may provide a useful tool in the expedition of drug discovery.

1.3.6 CQ Toxicity

CQ toxicity is relatively uncommon, yet can be very serious, and is usually associated with long term usage and accumulation of the drug. Retinopathy and cardiac toxicity appear to be the main forms of toxicity related to the drug. CQ has been shown to have strong affinity for melanin granules and has been demonstrated to have a very high affinity for the retina in rhesus monkeys (Peters *et al.*, 1984). This retinal toxicity is likely to be due to non-specific accumulation owing to its long half-life and its weakly basic nature, resulting in its ability to enter any acidic cell type within the body *via* ion-trapping.

In patients undergoing CQ treatment for rheumatic diseases, several cases of cardiac damage, such as cardiomyopathy and conduction system disturbances, have been reported (Don Michael *et al.*, 1970). CQ is able to inhibit phospholipase activity and induce cytoplasmic inclusion body formation. It can also be accumulated within lysosomes, due to its basicity and can inhibit enzyme activity, increase lysosomal pH and cause inactivation of proteins (Teixeira *et al.*, 2002). It is these properties that have led to the described atrial and ventricular antiarrhythmic effects described.

1.3.7 The Metabolism and Toxicity of AQ

After oral dosing, in man, AQ is rapidly cleared from the plasma with a half-life of 5.2 ± 1.7 hours (Winstanley *et al.*, 1987). This is in contrast to CQ which has a half-life of 7-14 days, a factor which may contribute towards the increasing

resistance of malaria to CQ as the parasites may be seeing sub-therapeutic concentrations of drug for long periods of time (Watkins *et al.*, 1993).

In vivo, AQ is rapidly metabolised *via* the cytochrome P450 enzyme, CYP2C8 to form its equipotent desethyl analogue, desAQ which is responsible for most of the antimalarial activity. DesAQ achieves much higher concentrations than its parent drug meaning AQ can be regarded as a pro-drug (Figure 1.12) (Li *et al.*, 2002; Winstanley *et al.*, 1987; Winstanley *et al.*, 2004). The formation of desAQ is also seen in animal models (Winstanley, 1988) (Chapter 3).

However, due to cases of agranulocytosis and hepatoxicity, the clinical use of AQ has become severely limited (Neftel et al., 1986). The prevalence of these adverse effects has been estimated to be in the order of 1:2000 (Hatton *et al.*, 1986). AQ has a structural metabolic alert, as with paracetamol (Figure 1.11), and the toxic effects observed can be attributed to the formation of a toxic quinone imine metabolite (AQQI), which is also thought to be catalysed by myeloperoxidase (MPO) as well as cytochrome P450 (Figures 1.8 and 1.13) (Jewell *et al.*, 1995; Maggs *et al.*, 1987). This metabolite is thought to be of too low a molecular weight to be immunogenic itself, but when covalently bound to the thiol groups of a macromolecular carrier it could act as an antigen, as the detection of antidrug IgG antibodies suggests (Clarke *et al.*, 1991; Harrison *et al.*, 1992; Pirmohamed *et al.*, 1996).

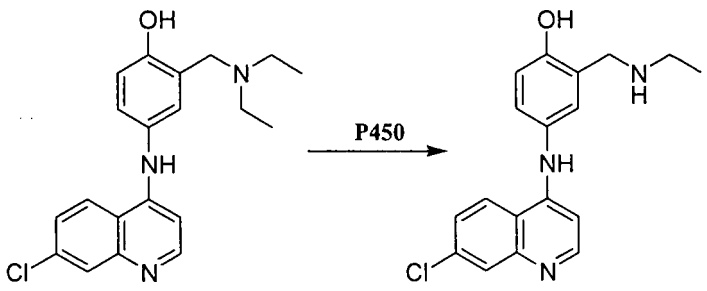

Figure 1.12 The cytochrome P450 mediated *N*-dealkylation of AQ to desAQ.

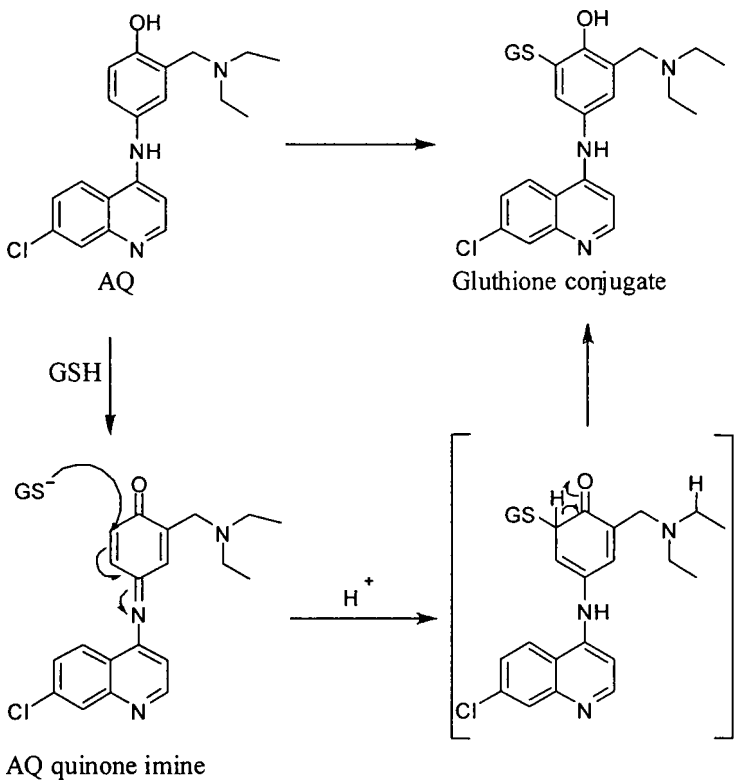

Figure 1.13 Possible mechanisms of AQ bioactivation and GSH conjugation.

1.4 RATIONAL APPROACHES TO DRUG DESIGN

1.4.1 Introduction

Chemical modification has long been used to dissociate the pharmacological activity of a drug from unwanted side effects. A lead compound with a desired pharmacological activity may have associated undesirable side effects, characteristics that limit its bioavailability or structural features which adversely influence its metabolism and excretion from the body.

The widespread application of the concept of isosterism to modify biological activity has given rise to the term bioisosterism (Patani *et al.*, 1996). Bioisosterism represents one approach that medicinal chemists use for the rational modification of old compounds towards the development of new, more effective drug molecules A number of classic bioisosteres exist such as fluorine, hydroxyl, amino and methyl group interchanges. In the case of AQ, two approaches have been used in order to attempt to prevent the occurrence of metabolic bioactivation:

i. Isomerisation of the 4'-hydroxyl group and the amino side chain leading to the production of isoquine (ISQ), a compound which does not undergo bioactivation to form the toxic quinone imine metabolite (O'Neill *et al.*, 2003).
ii. Halogen substitution of the 4'-hydroxyl group using fluorine or chlorine to increase the oxidation potential in comparison to AQ, thus preventing *in vivo* oxidation.

1.4.2 Interchange of the Amino and 4'-Hydroxyl Group of AQ

ISQ, the original lead compound, was prepared as part of a study to prepare a second generation of 4-aminoquinoline antimalarials (Figure 1.15). It was proposed that interchanging the 4' hydroxyl and the 3' Mannich side-chain of AQ would provide a new series of analogues unable to form toxic quinone imine metabolites *via* cytochrome P450-mediated metabolism (O'Neill *et al.*, 2003). The potent *in vitro* antimalarial activity of ISQ was translated into excellent oral *in vivo* ED_{50} activity of 1.6 and 3.7 mg/kg against the rodent malaria *P. yoelii* NS strain, compared to 7.9 and 7.4 mg/kg for AQ. Subsequent metabolism studies in the rat model demonstrated that ISQ does not undergo *in vivo* bioactivation, as evidenced by the complete lack of glutathione metabolites in bile. In sharp contrast to AQ, ISQ undergoes clearance by direct glucuronidation.

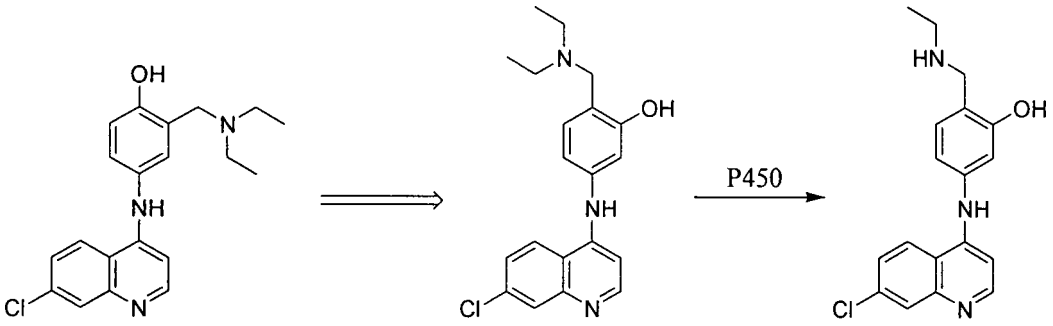

Figure 1.15 Isoquine, the isomeric analogue of AQ and its desethyl metabolite.

1.4.3 The Effect of Fluorine Substitution on AQ

The strategic substitution of fluorine into therapeutic agents can have a profound effect on the chemical properties, disposition and biological activity of drugs (Park *et al.*, 2001).

The inclusion of a fluorine atom into a drug molecule can influence both the disposition of the drug and interaction of the drug with its pharmacological target (Figure 1.16).

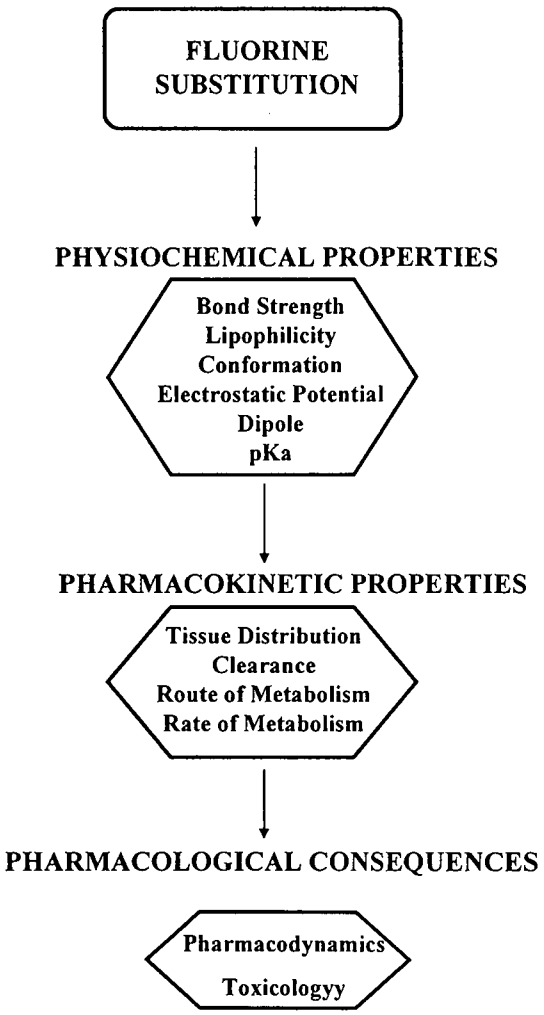

Figure 1.16 Flow diagram illustrating the effect of fluorine substitution on drug response. (Park *et al.*, 2001)

Fluorine substitution can also have a huge effect on drug disposition, in terms of distribution, drug clearance and drug metabolism. Such changes can be used constructively to improve both the safety and efficacy of a drug.

The isosteric replacement of a hydroxyl group is a commonly used strategy in medicinal chemistry. This substitution is based on the premise that fluorine is a

comparable hydrogen bond acceptor to a hydroxyl oxygen atom. Also, the higher electronegativity and lower polarizability of fluorine over oxygen has a major influence on the ability of fluorine to mimic a hydroxyl group (Dixon *et al.*, 1991).

The presence of fluorine can alter the oxidation potential of an aromatic system, and thus alter the rate of auto-oxidation and formation of quinones and quinone imines. This was demonstrated when the sequential introduction of fluorine atoms into the nucleus of paracetamol produced an increase in the oxidation potential of the molecule, as measured by cyclic voltammetry (Barnard *et al.*, 1993).

AQ and its desethyl analogue both have very low oxidation potentials, in comparison to paracetamol. This means that they can undergo facile chemical oxidation to their respective quinone imines. Studies have shown that by substituting the hydroxyl functionality with fluorine, the oxidation potential of AQ can be increased resulting in a more favourable balance between drug activation and detoxification whilst retaining antimalarial activity (Harrison, 1994; O'Neill *et al.*, 1994). On the basis of these findings it may be possible to design a novel and potent antimalarial which does not undergo bioactivation in the manner of AQ and is metabolically more stable than ISQ.

1.5 AIMS OF THESIS

The work presented in this thesis is aimed at determining whether it is possible to utilise rational drug design for the production of a novel, inexpensive antimalarial compound. The desired compound will exhibit similar efficacy to AQ against CQ-sensitive and CQ-resistant parasites, lack the ability to undergo bioactivation resulting in reactive metabolites and be unable to undergo non-specific accumulation within the body.

A safe and effective 4-aminoquinoline must have the following features:

- The correct structural features, which permit high-affinity binding in the parasite.
- No functional groups which allow metabolic conversion to products that have lower activity against resistant strains.
- No functionalities that can undergo bioactivation and subsequent binding to protein reactive nucleophiles.
- A functionality that allows metabolic clearance by conjugation, for example, glucuronidation, in order to prevent accumulation within the tissues leading to potential toxicity.

The strategies to be employed in order to achieve these specific requirements involve a combination of the following:

- Interchange of the 4'-hydroxyl group of AQ with the 3'-amino side chain to produce a compound that does not undergo oxidation to a quinone imine metabolite.

- Replacement of the diethyl amino side chain with a *tert* butyl group to increase the metabolic stability of the compound.
- Insertion of a fluorine or chlorine atom in place of the hydroxyl group to increase the oxidation potential of the drug.

Candidate compounds will undergo extensive dispositional and *in vivo* metabolic studies to determine the pathways of metabolism and clearance in rats. From these experiments we will determine the biodistribution of the drug in the body. Further analysis will reveal the possibility of retention and whether there is any accumulation or retention in the tissues over time. In addition, preliminary toxicity studies shall be performed and the results from these experiments will be compared to those from CQ and AQ.

1.6 REFERENCES

BARNARD, S., STORR, R., O'NEILL, P. & PARK, B. (1993). The effect of fluorine substitution on the physiochemical properties and the analgesic activity of paracetamol. *Journal of Pharmacy and Pharmacology*, **45,** 736-744.

BELL, D. & WINSTANLEY, P. (2004). Current issues in the treatment of uncomplicated malaria in Africa. *British Medical Bulletin*, **71,** 29-43.

BOHLE, D., DINNEBIER, R., MADSEN, S. & STEPHENS, P. (1997). Characterization of the products of the heme detoxification pathway in malarial late trophozoites by X-ray diffraction. *The Journal of Biological Chemistry*, **272,** 713-716.

BOOBIS, A., GUNDERT-REMY, U., KREMERS, P., MACHERAS, P. & PELKONEN, O. (2002). In silico prediction of ADME and pharmacokinetics. Report of an expert meeting organised by COST B15. *European Journal of Pharmaceutical Sciences*, **17,** 183-193.

BOUCHARD, O., BRUNEEL, F., SCHIEMANN, R., PEYTAVIN, G. & COULARD, J. (2002). Severe cardiac toxicity due to halofantrine: Importance of underlying heart disease. *Journal of Travel Medicine*, **9,** 214-215.

BRAY, P., HOWELLS, R. & WARD, S. (1992). Vacuolar acidification and chloroquine sensitivity in plasmodium falciparum. *Biochemical Pharmacology*, **43,** 1219-1227.

BRAY, P., MARTIN, R., TILLEY, L., WARD, S., KIRK, K. & FIDOCK, D. (2005). Defining the role of PfCRT in Plasmodium falciparum chloroquine resistance. *Molecular Microbiology*, **56,** 323-333.

BRAY, P., MUNGTHIN, M., RIDLEY, R. & WARD, S. (1998). Access to Hematin: the basis of chloroquine resistance. *The American Society for Pharmacology and Experimental Therapeutics*, **54,** 170-179.

BURCKHALTER, J., TENDWICK, J., JONES, F. & JONES, P. (1948). Aminoalkylphenols as antimalarials II (heterocyclic-amino)- alpha-amino-o-cresols: The synthesis of camoquine. *The Journal of the American Chemical Society*, **70,** 1363-1373.

CHOU, A., CHEVLI, R. & FITCH, C. (1980). Ferriprotoporphyrin IX fulfils the criteria for identification as the chloroquine receptor of malaria parasites. *Biochemistry*, **19,** 1543-1549.

CLARKE, J., NEFTEL, K., KITTERINGHAM, N. & PARK, B. (1991). Detection of antidrug IgG antibodies in patients with adverse drug reactions to amodiaquine. *Int. Arch. Allergy Appl. Immunol*, **95,** 369-375.

DAVIES, D. (1996). *Textbook of Adverse Drug Reactions*. Oxford, England: Oxford University Press.

DIXON, D. & SMART, B. (1991). Conformational energies of 2-fluoroethanol and 3-fluoroacetaldehyde enol-strength of the internal hydrogen-bond. *Journal of Physical Chemistry*, **95,** 1609-1612.

DON MICHAEL, T. & AIWAZZADEH, S. (1970). The effects of acute chloroquine poisoning with special reference to the heart. *American Journal of the Heart*, **79,** 831-42.

DUTTON, G. (1980). *Glucuronidation of Drugs and Other Compounds*. Florida: CRC Press, Inc.

EKINS, S. & OBACH, R. (2000). Three-dimensional quantitative structure activity relationship computational approaches for prediction of human in vitro intrinsic clearance. *The Journal of Pharmacology and Experimental Therapeutics*, **295,** 463-473.

ELKINS, S., ANDREYEV, S., RYABOV, A., KIRILLOV, E., RAKHMATULIN, E., SOROKINA, S., BUGRIM, A. & NIKOLSKAYA, T. (2006). A Combined approach to drug metabolism and toxicity assessment. *Drug Metabolism and Disposition*, **34,** 465-503.

FITCH, C. & KANJANANGGULPAN, P. (1987). The state of ferriprotoporphyrin IX in malaria pigment. *Journal of Biological Chemistry*, **262,** 15552-15555.

FOLEY, M. & TILLEY, L. (1998). Quinoline antimalarials: mechanisms of action and resistance and prospects for new agents. *Pharmacology and Therapeutics*, **79,** 55-87.

FRANCIS, S., SULLIVAN, D. & GOLDBERG, D. (1997). Hemoglobin metabolism in the malaria parasite plasmodium falciparum. *Annual Reviews of Microbiology*, **51,** 97-123.

GIBSON, G. & SKETT, P. (1994). *Introduction to Drug Metabolism*. Glasgow: Blackie Academic & Professional.

GRAM, T. (1980). *Extrahepatic Metabolism of drugs and other foreign compounds*. London: MTP Press Limited.

GUENGERICH, F. (2006). Cytochrome p450s and other enzymes in drug metabolism and toxicity. *The American Association of Pharmaceutical Scientists Journal*, **8,** E101-E111.

GUSTAFSSON, L., WALKER, O., ALVAN, G., BEERMANN, B., ESTEVEZ, F., GLEISNER, L., LINDSTROM, B. & SJOQVIST, F. (1983). Disposition of chloroquine in man after single intravenous and oral doses. *British Journal of Clinical Pharmacology*, **15,** 471-479.

HAKIMELAHI, G. & KHODARAHMI, G. (2005). The identification of toxicophores for the prediction of mutagenicity, hepatoxicity and cardiotoxicity. *Journal of the Iranian Chemical Society*, **2,** 244-267.

HARRISON, A. (1994). The effect of chemical modification on the metabolism of amodiaquine in the rat. In *Pharmacology and Therapeutics*. pp. 261. Liverpool: University of Liverpool.

HARRISON, A., KITTERINGHAM, N., CLARKE, J. & PARK, B. (1992). The mechanism of bioactivation and antigen formation of Amodiaquine in the rat. *Drug Metabolism and Dispostion*, **43,** 1421-1430.

HAWLEY, S., BRAY, P., MUNGTHIN, M., ATKINSON, J., O'NEILL, P. & WARD, S. (1998). Relationship between antimalarial drug activity, accumulation, and inhibition of heme polumerisation in plasmodium falciparum in vitro. *American Society for Microbiology*, **42,** 682-686.

HAWLEY, S., BRAY, P., O'NEILL, P., PARK, B. & WARD, S. (1996a). The role of drug accumulation in 4-aminoquinoline antimalarial potency - The influence of strucutural substitution and physiochemical properties. *Biochemical Pharmacology*, **52,** 723-733.

HAWLEY, S., BRAY, P., PARK, B. & WARD, S. (1996b). Amodiaquine accumulation in Plasmodium falciparum as a possible explanation for its superior antimalarial activity over chloroquine. *Molecular and Biochemical Parasitology*, **80,** 15-25.

JEWELL, H., MAGGS, J., HARRISON, A., O'NEILL, P., RUSCOE, J. & PARK, B. (1995). Role of hepatic metabolism in the bioactivation and detoxification of amodiaquine. *Xenobiotica*, **25,** 199-217.

JONES, M. & GOOD, M. (2006). Malaria parasites up close. *Nature Medicine*, **12,** 170-171.

KALGUTKAR, A., GARDNER, I., OBACH, R., SHAFFER, C., CALLEGARI, E., HENNE, K., MUTLIB, A., DALVIE, D., LEE, J., NAKAI, Y., O'DONNELL, J., BOER, J. & SHAWN, P. (2005). A comprehensive listing of bioactivation pathways of organic functional groups. *Current Drug Metabolism*, **6,** 161-225.

KER KEULE, F. & DOLAN, G. (1993). Halofantrine versus mefloquine. *Lancet*, **341,** 1044-1049.

KIM, K., PARK, J., LEE, J. & LIM, S. (2003). Cytochrome P450 2C8 and CYP3A4/5 are involved in chloroquine metabolism in human liver microsomes. *Archives of Pharmacal Research*, **26,** 631-637.

KITTERINGHAM, N., POWELL, H., JENKINS, R., HAMLETT, J., LOVATT, C., ELSBY, R., HENDERSON, C., WOLF, C., PENNINGTON, S. & PARK, B. (2003). Protein expression profiling of glutathione S-transferase pi null mice as a strategy to identify potential markers of resistance to paracetamol induced toxicity in the liver. *Proteomics*, **3,** 191-207.

LAKSHMANAN, V., BRAY, P., JOHNSON, D., HORROCKS, P., MUHLE, R., ALAKPA, G., HUGHES, R., WARD, S., KROGSTAD, D., SIDHU, A. & FIDOCK, D. (2005). A critical role of PfCRT K76T in Plasmodium falciparum verapamil-reversible chloroquine resistance. *The EMBO Journal*, **24,** 2294-2305.

LI, X.-Q., BJORKMAN, A., ANDERSON, T. & RIDDERSTROM, M. (2002). Amodiaquine clearance and its metabolism to N-desethylamodiaquine is mediated by CYP2C8: a new affinity and turnover enzyme-specific probe substrate. *Journal of Pharmacology and Experimental Therapeutics*, **300,** 399-407.

LOEB, R., CLARK, W. & COATNEY, G. (1946). Activity of a new antimalarial agent, Chloroquine (SN 7618). *The Journal of the American Medical Association*, **130,** 1069-1070.

MABASO, M., SHARP, B. & LENGELER, C. (2004). Historical review of malarial control in southern African with emphasis on the use of indoor residual house-spraying. *Tropical Medicine and International Health*, **9**, 846-856.

MACOMBER, P., O'BRIAN, R. & HAHN, F. (1966). Chloroquine: Physiological basis of drug resistance in plasmodium berghei. *Science*, **152**, 1374-1375.

MAGGS, J., KITTERINGHAM, N., AM, B. & PARK, B. (1987). Autooxidative formation of a chemically reactive from amodiaquine, a myelotoxin and hepatotoxin in man. *Biochemical Pharmacology*, **36**, 2061-2062.

MORGAN, M. & FIGUEROA-MUNOZ, J. (2005). Barriers to uptake and adherence with malaria prophylaxis by the African community in London, England: Focus group study. *Ethnicity and Health*, **10**, 355-372.

NAISBITT, D., WILLIAMS, D., O'NEILL, P., MAGGS, J., WILLCOCK, D. & PARK, B. (1998). Metabolism-dependant neutrophil cytoxicity of amodiaquine: A comparison with pyronaridine and related antimalarial drugs. *Chem. Res. Toxicol.*, **11**, 1586-1595.

NEFTEL, K., WOODTLY, W., SCHMID, M. & FRICK, P. (1986). Amodiaquine induced agranulocytosis and liver damage. *British Medical Journal*, **292**, 721-724.

NEWTON, J., HOEFLE, D., GEMBORYS, M., MUDGE, G. & HOOK, J. (1986). Metabolism and excretion of a glutathione conjugate of acetaminophen in the isolated perfused rat kidney. *Journal of Pharmacology and Experimental Therapeutics*, **237**, 519-524.

O'NEILL, P., BRAY, P., HAWLEY, S., WARD, S. & PARK, B. (1998). 4-Aminoquinolines - past, present, and future: A chemical perspective. *Pharmacology and Therapeutics*, **77**, 29-58.

O'NEILL, P., HARRISON, A., STORR, R., HAWLEY, S., WARD, S. & PARK, B. (1994). The effect of fluorine substitution on the metabolism and antimalarial activity of Amodiaquine. *The Journal of Medicinal Chemistry*, **37**, 1362-1370.

O'NEILL, P., MUKHTAR, A., STOCKS, P., RANDLE, L., HINDLEY, S., WARD, S., STORR, R., BICKLEY, J., O'NEIL, I., MAGGS, J., HUGHES, R., WINSTANLEY, P., BRAY, P. & PARK, B. (2003). Isoquine and related amodiaquine analogues: A new generation of improved 4-aminoquinoline antimalarials. *Journal of Medicinal Chemistry*, **46**, 4933-4945.

OAKS, J., SC, MITCHELL, V., PEARSON, G. & CARPENTOR, C. (1991). *Malaria: Obstacles and Opportunities*. Washington, D.C: National Academy Press.

OLLIARO, P., CATTANI, J. & WIRTH, D. (1996). Malaria, the submerged disease. *The Journal of the American Medical Association*, **275**, 230-233.

OLLIARO, P. & GOLDBERG, D. (1995). The plasmodium digestive vacuole: metabolic headquarters and choice of drug target. *Parasitology Today*, **11**, 294-297.

OLLIARO, P. & TAYLOR, W. (2003). Antimalarial compounds: from bench to bedside. *The Journal of Experimental Biology*, **206,** 3753-3759.

ORJIH, A., BANYAL, H., CHEVLI, R. & FITCH, C. (1981). Hemin Lyses Malaria Parasites. *Science*, **214,** 667-669.

PAGOLA, S., STEPHENS, P., BOHLE, D., KOSAR, A. & MADSEN, S. (2000). The structure of malaria pigment beta-haematin. *Nature*, **404,** 307-310.

PARK, B., KITTERINGHAM, N. & O'NEILL, P. (2001). Metabolism of fluorine-containing drugs. *Annual Review of Pharmacology and Toxicology*, **41,** 443-470.

PARK, B., PIRMOHAMED, M., BRECKENRIDGE, A. & KITTERINGHAM, N. (1998). Adverse drug reactions. *British Medical Journal*, **316,** 1295-1298.

PATANI, G. & LAVOIE, E. (1996). Bioisosterism: A rational approach in drug design. *Chemical Reviews*, **96,** 3147-3176.

PETERS, W. & RICHARDS, W. (1984). *Handbook of antimalarial drugs*. Berlin: Springer Verlag.

PIRMOHAMED, M., MADDEN, S. & PARK, B. (1996). Idiosyncratic drug reactions. Metabolic bioactiviation as a pathogenic mechanism. *Clinical Pharmacokinetics*, **31,** 215-230.

PROJEAN, D., BAUNE, B., FARINOTTI, R., FLINOIS, J.-P., BEAUNE, P., TABURET, A.-M. & DUCHARME, J. (2003). In vitro metabolism of chloroquine: Identification of CYP2C8, CYP3A4 and CYP2D6 ad the main isoforms catalysing N-desethylchloroquine formation. *Drug Metabolism and Disposition*, **31,** 748-754.

RANG, H., DALE, M. & RITTER, J. (1999). *Pharmacology*. Edinburgh: Churchill Livingstone.

RIDLEY, R. (1998). Malaria: Dissecting chloroquine resistance. *Current Biology*, **8,** R346-R349.

RIDLEY, R., DORN, A., VIPPAGUNTA, S. & VENNERSTROM, J. (1997). Haematin (haem) polymerization and its inhibition by quinoline antimalarials. *Annals of Tropical Medicine and Parasitology*, **91,** 559-566.

ROSENTHAL, P. (2001). *Antimalarial chemotherapy*. New Jersey: Humana Press.

SALIBA, K., FOLB, P. & SMITH, P. (1998). Role for the plasmodium falciparum digestive vacuole in Chloroquine resistance. *Biochemical Pharmacology*, **56,** 313-320.

SLATER, A. & CERAMI, A. (1992). Inhibition by chloroquine of a novel haem polymerase enzyme activity in malaria trophozoites. *Nature*, **355,** 167-169.

SMITH, D., VAN DE WATERBEEMD, H. & WALKER, D. (2001). *Pharmacokinetics and Metabolism in Drug Design*. Weinheim: Wiley-VCH.

SNOW, R., GUERRA, C., NOOR, A., MYINT, H. & HAY, S. (2005). The global distribution of clinical episodes of Plasmodium falciparum malaria. *Nature*, **434,** 214-217.

SULLIVAN, D., GLUZMAN, I., RUSSELL, D. & GOLDBERG, D. (1996). On the molecular mechanism of chloroquine's antimalarial action. *Proceedings of the National Academy of Sciences of the USA*, **93,** 11865-11870.

TEIXEIRA, R., FILHO, M., BENVENUTI, L., COSTA, R., PEDROSA, A. & NISHIOKA, S. (2002). Cardiac damage from chronic use of chloroquine. A case report and review of the literature. *Arquivos Brasileiros de Cardiologia*, **79.**

TIMBRELL, J. (2000). *Principles of biochemical toxicology.* London: Taylor & Francis Ltd.

VERDIER, F., LES BRAS, J., CLAVIER, F., HATIN, I. & BLAYO, M. (1985). Chloroquine uptake by Plasmodium falciparum-infected human erythrocytes during in vivo cell culture and its relationship to chloroquine resistance. *Antimicrobial Agents and Chemotherapy*, **27,** 561-564.

VERVLOET, D. & DURHAM, S. (1998). Adverse reactions to drugs. *British Medical Journal*, **316,** 1511-1513.

WANG, J. & RAMNARAYAN, K. (1999). Toward designing drug-like libraries: A novel computational approach for prediction of drug feasibility of compounds. *The Journal of Combinatorial Chemistry*, **1,** 524-533.

WATKINS, W. & MOBOSO, M. (1993). Treatment of plasmodium falciparum malaria with pyrimethamine-sulfadoxine-selective pressure for resistance is a function of long elimination half-life. *Transactions of the Royal Society of Tropical Medicine and Hygiene*, **87,** 75-78.

WATKINS, W., SIXSMITH, D. & SPENCER, H. (1984). Effectiveness of amodiaquine as treatment for chloroquine resistant plasmodium falciparum infections in Kenya. *Lancet*, **I.**

WELLEMS, T., PANTON, L., GLUZMAN, I., DO ROSARIO, V., GWADZ, R., WALKER-JONAH, A. & KROGSTAD, D. (1990). Chloroquine resistance not linked to mdr-genes in a Plasmodium falciparum cross. *Nature*, **345,** 253-255.

WERBEL, L., COOK, P., ELSLAGER, E., HUNG, J. & JOHNSON, J. (1986). Synthesis, antimalarial activity and quantitative structure actvity relationships of tebuquine and a series of related 5-[(7-chloro-4-quininyl)amino]-3-[(alkylamino)methyl][1,1'-biphenyl]-2-ols and N-oxides. *Journal of Medicinal Chemistry*, **29,** 924-939.

WESCHE, D., SCHUSTER, B., WANG, W.-X. & WOOSLEY, R. (2000). Mechanism of cardiotoxicity of halofantrine. *Clinical pharmacology and Therapeutics*, **67,** 521-529.

WHITE, N. (1992). Antimalarial drug resistance: the pace quickens. *Journal of Antimicrobial Chemotherapy*, **30,** 571-585.

WHITE, N. (1998). Drug resistance in malaria. *British Medical Bulletin*, **54,** 703-715.

WILLIAMS, D., GARCIA-ALLAN, C., HANTON, G., LENET, J., PROVOST, J., BRAIN, P., WALSH, R., JOHNSTON, G., SMITH, D. & PARK, B. (2004). Time course toxicogenomic profiles in CD-1 mice after nontoxic and nonleathal hepatotoxic paracetamol administration. *Chemical Research in Toxicology*, **17,** 1551-1561.

WINSTANLEY, P. (1988). Tissue distribution and excretion of amodiaquine in the rat. *Journal of Pharmacy and Pharmacology*, **40,** 343-349.

WINSTANLEY, P., EDWARDS, G., ORME, M. & BRECKENRIDGE, A. (1987). The disposition of amodiaquine in man after oral administration. *British Journal of Clinical Pharmacology*, **23,** 1-7.

WINSTANLEY, P., WARD, S., SNOW, R. & BRECKENRIDGE, A. (2004). Therapy of falciparum malaria in Sub-Saharan Africa: from molecule to policy. *Clinical Microbiology Reviews*, **17,** 612-637.

WWW.RBM.WHO.INT (2001-2010). Economic Costs of Malaria. Geneva 27, Switzerland: Rollback Malaria Partnership, World Health Organaisation.

YAYON, A., CABANTCHIK, Z. & GINSBURG, H. (1984). Identification of the acidic compartment of Plasmodium falciparum-infected human erythrocytes as the target of the antimalarial drug chloroquine. *The EMBO Journal*, **3,** 2695-2700.

YOUNG, M. & MOORE, D. (1961). Chloroquine resistance in Plasmodium falciparum. *American Journal of Tropical Medicine and Hygiene*, **10,** 317-320.

CHAPTER 2

CHEMICAL SYNTHESES OF THE 4-AMINOQUINOLINES AND CANDIDATE SELECTION

CONTENTS

2.1 INTRODUCTION

The main introduction to this thesis highlighted some of the key issues concerning the treatment of modern malaria and revealed how rational drug design involving structural change of current drugs can be used to design novel antimalarial agents. It is clear that a new 4-aminoquinoline drug is required to supersede amodiaquine (AQ) due to its ability to cause adverse reactions; this has prompted chemists to design a range of structural analogues.

This chapter is primarily concerned with the chemical syntheses of isoquine (ISQ) (**2c**), its desethyl and *tert*-butyl analogues (**3c** and **4c** respectively) and also AQ (**6c**) and its *tert*-butyl fluoro and chloro derivatives (**8d** and **11d** respectively) (Figure 2.1). The optimisation and eventual scale-up of these syntheses will then enable pharmacological evaluation leading to the selection of a suitable candidate for pre-clinical studies.

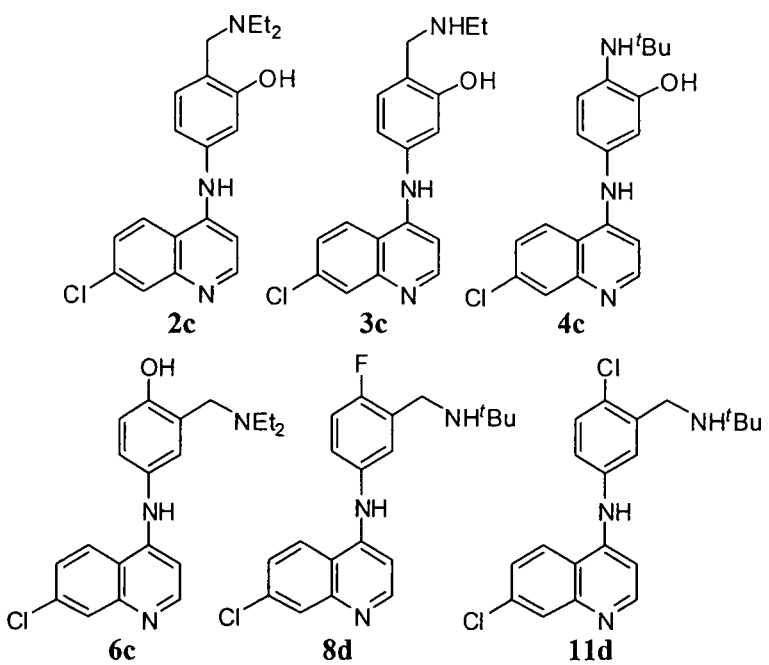

Figure 2.1 Compounds to be synthesised. Isoquine (ISQ) 2c, desethyl isoquine (desISQ) 3c, *N-tert*-butyl isoquine (NTBISQ) 4c, amodiaquine (AQ) 6c, *N-tert*-butyl fluoro amodiaquine (FAQ-4) 8d and *N-tert* butyl chloro amodiaquine (ClAQ-4) 11d.

2.1.1 Drug-Design Rationale

Previous structure-activity-relationship (SAR) work suggested that the presence of the 4'hydroxyl group within the aromatic ring imparted greater inherent antimalarial activity against CQ-resistant parasites than the corresponding deoxy analogues (O'Neill *et al.*, 1998; O'Neill *et al.*, 1997). However, as mentioned in chapter 1 (Section 1.4.2), interchange of the hydroxyl group with the amino side-chain of AQ provides a means of preventing oxidation to toxic metabolites whilst retaining the possible important bonding interactions of aromatic hydroxyl function (ISQ). ISQ has been noted to have poor oral bioavailability and undergoes extensive *N*-dealkylation to its desethyl form, desISQ (O'Neill *et al.*, 2003). It was postulated that incorporation of a *tert* butyl group as the amine side chain instead of a diethyl group would hopefully lend to the stability of the molecule (NTBISQ). The sterically hindered group is metabolically less labile than the *N*-ethyl group of AQ and ISQ and is not thought to be a substrate for CYP2C8 dealkylation. It was therefore proposed that we would not observe any major side chain loss in metabolism experiments.

An alternative method for avoiding the toxicity observed *in vivo* with AQ involves the substitution of the hydroxyl function with fluorine or chlorine. The introduction of a halogen atom can have a profound effect on the biological activity and the physiochemical parameters of some aromatic compounds. It has previously been shown with paracetamol that providing the oxidation potential of the fluoro derivative is sufficiently greater than that of the parent compound; fluorine substitution can block *in vivo* oxidation. Thus preventing formation of its quinone imine metabolite (Barnard *et al.*, 1993).

Previous studies on fluorinated analogues of AQ have shown that the critical balance between drug activation and the process of oxidative bioactivation can be altered, without any significant loss of activity against CQ-sensitive and CQ-resistant parasites (Madrid *et al.*, 2005). Studies within the group showed that interchange of the hydroxyl group of AQ with fluorine gave rise to a compound which did not undergo bioactivation to a reactive metabolite *in vivo* but had similar antimalarial activity to AQ (O'Neill *et al.*, 1994). Coupling this idea with the concept of a *tert* butyl group in place of the diethyl group will hopefully lead to two promising candidates for animal studies [FAQ-4 (**8d**) and ClAQ-4 (**11d**)]. FAQ-4 and ClAQ-4 should have greater *in vivo* stability than AQ and will be unable to form a toxic quinone imine metabolite.

Therefore, the aim of the work presented in this chapter was to develop a simple and efficient synthesis of three rationally designed lead compounds, NTBISQ, FAQ-4 and ClAQ-4, along side ISQ, desISQ and AQ. The compounds were to be synthesised in quantities sufficient enough to permit pharmacodynamic and pharmacokinetic analysis using standard methods.

2.2 MATERIALS AND METHODS

2.2.1 Materials

Unless otherwise noted, all solvents and reagents were obtained from commercial suppliers and were used without further purification. 3-Hydroxyacetanilide, 4-hydroxyacetanilide, and 2-fluoro, 5-nitrotoluene were purchased from Sigma Aldrich Chemical Co. (Poole, United Kingdom). [^{3}H]-4, 7 Dichloroquinoline (20 Ci/mmol; radiochemical purity by HPLC 99.9 %) was purchased from Morovek Biochemicals, Inc. (California, USA). ClAQ-4 (**11d**) was prepared by D. Stanford of the Department of Chemistry, University of Liverpool.

All compounds were purified by flash column chromatography, performed using a Merck 9385 Kieselgel 60 (230-400 mesh) silica gel, using hand bellows to apply pressure.

Analytical thin layer chromatography (TLC) was performed on aluminum backed sheets, pre-coated with a 0.25 mm layer of silica gel obtained from Merck. After elution, the plates were visualized using ultra-violet (254 nm).

Infrared (IR) spectra were recorded in the range of 4000-600 cm^{-1} using a Perkin-Elmer 298 infrared spectrometer. Solid samples were run as nujol mulls and liquids neat on sodium chloride discs.

^{1}H Nuclear Magnetic Resonance spectra were recorded using a Brucker instrument (400 MHz). ^{13}C spectra were recorded on a Varian Gemini 2000 instrument (100 Mhz). All spectra were recorded using deuterated chloroform or deuterated methanol as a solvent. Spectra are presented in the form: chemical shift in ppm (number of hydrogens, appearance of signal, coupling constant, assignment). The following symbols have been used in the description of spectra obtained:

δ = Chemical shift (in parts per million (ppm))

J = coupling constant (in Hz)

s = singlet

d = doublet

t = triplet

q = quartet

Mass spectra were performed by A. Mills of the Department of Chemistry, University of Liverpool and are given as accurate mass.

Microanalyses were performed in the microanalytical laboratory in the Department of Chemistry, University of Liverpool using a Carlo Erba elemental analyser.

Melting points (mp) were determined using a Gallemkamp melting point apparatus.

2.2.2 Methods – Chemical Synthesis

2.2.2.1 N-[4-(Diethylamino)methyl-3-hydroxyphenyl]-acetamide (2a)

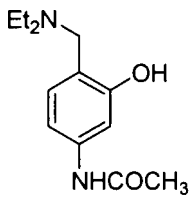

3-Hydroxyacetonilide **1** (4.00 g, 26.5 mmol) (Scheme 2.1) was dissolved in ethanol (20 mL) at room temperature to which aqueous formaldehyde (2.19 g, 2.5 eq) and diethylamine (2.13g, 1.1 eq) were then added and the solution was heated to

reflux for 16 h. The solvent was then removed under reduced pressure and the crude material was purified by silica gel flash column chromatography using 10 – 80 % MeOH/DCM as eluent. The product was afforded as a pale brown oily residue, **2a** (3.40 g, 54 %) ^{1}H-NMR (400 MHz, MeOD) δ 7.11 (dd, 1H, *J* = 8.2, 1.9 Hz Ar-*H*), 6.98 (d, 1H, *J* = 8.2 Hz, Ar-*H*), 6.87 (d, 1H, *J* = 1.9 Hz, Ar-*H*), (3.81 (s, 2H, C*H*$_2$), 2.72 (q, 4H, *J* = 7.2 Hz, NC*H*$_2$CH$_3$), 2.14 (s, 3H, C*H*$_3$), 1.09 (t, 6H, *J* = 7.2 Hz, NCH$_2$C*H*$_3$); ^{13}C-NMR (100 MHz) δ 168.9, 156.2, 138.4, 130.5, 118.5, 113.9, 106.1, 49.1, 22.9, 13.1; IR (neat): 3500-2800 (broad-OH band), 1650, 1612, 1548, 1417, 1348, 1256, 1152, 1138, 1016, 972, 870, 824, 754, 724 cm^{-1}; MS *m/z* calcd for $C_{13}H_{21}N_2O_2$ $[M+H]^+$ 237.16043 found 237.16042; Elemental analysis: C: 66.76, H: 8.42, N: 11.56 (required values; C: 66.10, H: 8.47, N:11.86).

2.2.2.2 N-[4-((Ethylamino)methyl)-3-hydroxyphenyl]-acetamide (3a)

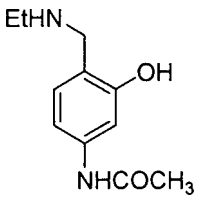

Compound **3a** was prepared in an identical manner to Mannich base **2a** but using ethylamine (1.89 mL), to afford the product as a brown, oily residue. (3.19 g, 58 %); ^{1}H-NMR (400 MHz, MeOD) δ 6.93 (d, 1H, *J* = 2.0 Hz, Ar-*H*), 6.81 (dd, 1H, *J* = 8.0, 1.9 Hz, Ar-*H*), 6.67 (d, 1H, *J* = 8.0 Hz, Ar-*H*), 3.49 (s, 2H, C*H*$_2$), 2.55 (q, 2H, NHC*H*$_2$CH$_3$), 1.89 (s, 3H, COC*H*$_3$), 1.01 (t, 3H, NHCH$_2$C*H*$_3$); ^{13}C-NMR (100 MHz) δ 168.9, 155.9, 138.2, 129.6, 119.2, 114.8, 105.4, 44.3, 44.0, 22.6, 15.8; IR (neat) 3500-2800 (broad-OH band), 1664, 1609, 1535, 1459, 1377, 1270, 1169, 1016, 968, 859, 722 cm^{-1}; MS *m/z* calcd for $C_{11}H_{16}N_2O_2$ $[M+H]^+$ 209.1291 found 209.1020;

Elemental analysis: C: 62.98, H: 7.32, N: 12.78 (required values; C: 63.40, H: 7.74, N:13.65).

2.2.2.3 N-[4-((tert-butylamino)methyl)-3-hydroxyphenyl]-acetamide (4a)

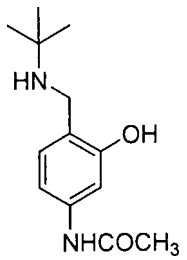

Compound **4a** was prepared in an identical manner to Mannich base **2a** using *tert* butylamine (2.1 mL) to give the product as an off-white solid (3.62 g, 72 %); ^{1}H-NMR (400 MHz, MeOD) δ 6.93 (d, 1H J = 8.2 Hz, Ar-*H*), 6.78 (dd, 1H, J = 8.2, 2.2 Hz, Ar-*H*), 6.53 (d, 1H, J = 2.2 Hz, Ar-*H*) 3.55 (s, 2H, CH_2), 1.59 (s, 3H, CH_3), 1.23 (s, 9H, ^{t}Bu); ^{13}C-NMR (100 MHz) δ 167.3, 154.2, 137.9, 129.6, 121.3, 114.6, 108.3, 54.6, 39.3, 31.0, 24.5; IR (Nujol) 3500-2800 (broad-OH band), 1732, 1682, 1614, 1548, 1489, 1462, 1377, 1322, 1274, 1213, 1171, 1148, 1114, 936, 866, 818, 790, 736 cm^{-1}; MS *m/z* calcd for $C_{13}H_{21}N_2O_2$ $[M+H]^+$ 237.16031 found 237.16042; Elemental analysis: C: 67.33, H: 8.12, N: 11.87 (required values; C: 66.07, H: 8.53, N:11.85).

2.2.2.4 N-[3-Diethylaminomethyl-4-hydroxy-phenyl]-acetamide (6a)

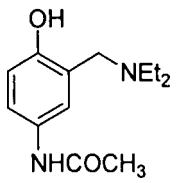

The AQ Mannich intermediate, **6a** was prepared in the same manner as the ISQ analogue **2a**, utilizing 4-hydroxyacetonilide as the precursor, to afford a brown, oily residue (4.01 g, 64 %); ^{1}H-NMR (400 MHz, MeOD) δ 7.07 (d, 1H, J = 8.6 Hz, Ar-*H*), 7.03 (dd, 1H, *J* = 8.6, 2.4 Hz, Ar-*H*), 6.49 (d, 1H, *J* = 8.6 Hz, Ar-*H*), 3.52 (s, 2H, C*H*$_2$), 2.50 (q, 4H, *J* = 7.2 Hz, NC*H*$_2$CH$_3$), 1.91 (s, 3H, COC*H*$_3$), 0.99 (t, 6H, *J* = 7.2 Hz, NCH$_2$C*H*$_3$); ^{13}C-NMR (100 MHz) δ 168.9, 151.6, 128.9, 123.4, 122.7, 121.7, 114.9, 49.1, 19.8, 13.6; IR (neat); 3500-2800 (broad-OH band), 1732, 1654, 1566, 1490, 1462, 1377, 1262, 1194, 1167, 1147, 1075, 1041, 982, 897, 859, 832, 768, 725, 688 cm^{-1}; MS *m/z* calcd for $C_{13}H_{21}N_2O_2$ $[M+H]^+$ 237.16038 found 237.16039; Elemental analysis: C: 67.23, H: 8.19, N: 11.91 (required values; C: 66.07, H: 8.53, N:11.85).

2.2.2.5 5-(7-Chloroquinolin-4-ylamino)-2-[(diethylamino)methyl]-phenol (2c)

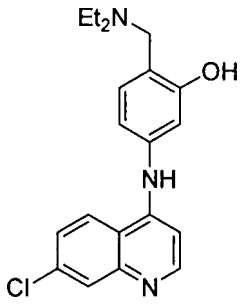

Aqueous HCl (20 %) (10 mL) was added to the amide, **2a,** (1.01 g, 4.2 mmol) and the solution heated to reflux for 5 h under an inert atmosphere. The solvent was

then removed *in vacuo* to give the resulting amine as its hydrochloric salt. 4, 7 Dichloroquinoline (0.97 g, 1.1 eq) and EtOH (20 mL) were added and the reaction heated to reflux for 16 h until completion (determined by TLC). The solvent was removed under reduced pressure and the crude product was purified by flash column chromatography using 10 - 80% MeOH/DCM as eluent to yield the product as a foamy, yellow solid, **2c** (1.02 g, 68 %): mp; 171.0-171.5 °C (decomposed); ^{1}H-NMR (400 MHz, MeOD) δ 8.65 (d, 1H, *J* = 5.2 Hz, quinoline-*H*), 8.01 (d, 1H, *J* = 2.2 Hz, quinoline-*H*), 7.72 (d, *J* = 8.9 Hz, quinoline-*H*), 7.43 (dd, 1H, *J* = 8.9, 2.2 Hz, quinoline-*H*), 6.75 (d, 1H, *J* = 5.2 Hz, quinoline-*H*), 6.49 (d, 1H, *J* = 8.0 Hz, Ar-*H*) 5.91 (dd, 1H, *J* = 8.0, 2.2 Hz, Ar-*H*) 5.81 (d, 1H, *J* = 2.2 Hz, Ar-*H*), 3.67 (s, 2H, C*H*$_2$), 2.46 (q, 4H, *J* = 7.1 Hz, NC*H*$_2$CH$_3$), 1.07 (t, 6H, *J* = 7.1 Hz, NCH$_2$C*H*$_3$); ^{13}C-NMR (100 MHz) δ 156.8, 151.4, 149.5, 148.2, 136.7, 131.2, 129.3, 127.4, 122.5, 118.9, 113.0, 112.8, 107.8, 100.7, 49.4, 49.2, 13.4; IR (Nujol) 2931, 2832, 1674, 1619, 1545, 1514, 1460, 1432, 1372, 1327, 1256, 1190, 1172, 1148, 1112, 1062, 992, 902, 873, 821, 812, 740 cm^{-1}; MS *m/z* calcd for $C_{20}H_{23}ClN_3O$ $[M+H]^+$ 356.15292 found 356.15287; Elemental analysis: C: 67.33, H: 6.12, N: 11.87 (required values; C: 67.5, H: 6.23, N:11.81).

2.2.2.6 5-(7-chloroquinolin-4-ylamino)-2-(ethylamino)methylphenol (3c)

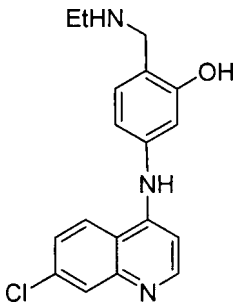

Compound **3c** was prepared in a similar way to ISQ affording a pale, brown solid (0.25 g, 16 %). mp 136.0-131.5 °C; ^{1}H-NMR (400 MHz, MeOD) δ 8.61 (d, 1H, *J* = 9.2 Hz, quinoline-*H*), 8.38 (d, 1H, *J* = 2.0 Hz, quinoline-*H*), 7.95 (dd, 1H, *J* = 7.1, 2.0 Hz, quinoline-*H*), 7.78 (d, 1H, *J* = 7.1 Hz, quinoline-*H*), 7.54 (d, 1H, *J* = 8.6 Hz, Ar-*H*), 7.41 (d, 1H, *J* = 9.1 Hz, quinoline-*H*), 7.14 (dd, 1H, *J* = 8.6, 2.6 Hz, Ar-*H*), 6.86 (d, 1H, *J* = 2.6 Hz, Ar-*H*), 4.25 (s, 2H, C*H*$_2$), 3.15 (q, 2H, *J* = 7.3 Hz, NHC*H*$_2$CH$_3$), 1.46 (t, 3H, J = 7.3 Hz, NHCH$_2$C*H*$_3$); ^{13}C-NMR (100 MHz) δ 156.8, 153.4, 148.7, 147.2, 142.8, 134.9, 130.5, 129.7, 127.3, 122.6, 120.1, 113.8, 113.1, 108.7, 100.6, 44.3, 44.0, 14.8; IR (Nujol) 3274, 1614, 1538, 1504, 1454, 1376, 1208, 109, 902, 821, 719 cm^{-1}; MS *m/z* calcd for $C_{18}H_{19}ClN_3O$ $[M+H]^+$ 329.63191 found 329.62969; Elemental analysis: C: 66.43, H: 6.17, N: 10.87 (required values; C: 65.95, H: 5.53, N:10.82).

2.2.2.7 2-[(tert-butylamino)methyl)-5-(7-chloroquinolin-4-ylamino]-phenol (4c)

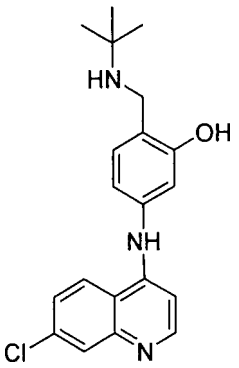

Compound **4c** was prepared using a similar procedure to **2c** providing the product as a pale yellow solid (1.17 g, 78 %); mp: 243.2–244.2 °C ^{1}H-NMR (400 MHz, MeOD) δ 8.26 (d, 1H, *J* = 5.7 Hz, quinoline-*H*), 8.16 (d, 1H, *J* = 9.1 Hz, quinoline-*H*), 7.75 (d, 1H, *J* = 2.2 Hz, quinoline-*H*), 7.40 (dd, 1H, *J* = 9.1, 2.2 Hz, quinoline-*H*), 7.06 (d, 1H, *J* = 7.9, Ar-*H*), 6.87 (d, 1H, *J* = 5.7 Hz, quinoline-*H*), 6.61 (d, 1H, *J* = 1.9 Hz, Ar-*H*), 6.58 (dd, 1H, *J* = 7.9, 2.1 Hz, Ar-*H*), 3.92 (s, 2H, C*H*$_2$), 1.12 (s, 9H, ^{t}Bu); ^{13}C-NMR (100 MHz, MeOD) δ 155.9, 150.8, 149.4, 147.6, 143.2, 136.5, 129.9, 129.1, 127.6, 122.6, 117.9, 113.5, 112.9, 105.3, 100.2, 48.7, 38.9, 31.0; IR (Nujol) 3473, 1606, 1587, 1537, 1459, 1377, 1238, 1165, 1125, 970, 908, 819, 778, 722 cm^{-1}; MS *m/z* calcd for $C_{20}H_{22}ClN_3O$ $[M+H]^+$ 356.15308 found 356.15306; Elemental analysis: C: 67.48, H: 6.42, N: 11.78 (required values; C: 67.50, H: 6.51, N:11.81).

2.2.2.8 4-[7-chloroquinolin-4-ylamino)-2-((diethylamino)methyl]-phenol (6c)

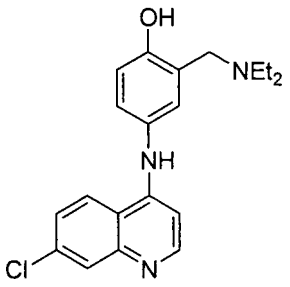

AQ was synthesized using a similar procedure to ISQ, **2c** to produce a pale, yellow solid, **6c** (1.14 g, 76 %). mp; 207.5-208.6 °C (decomposed); ^{1}H-NMR (400 MHz, MeOD) δ 8.61 (d, 1H, *J* = 9.2 Hz, quinoline-*H*), 8.37 (d, 1H, *J* = 7.2 Hz, quinoline-*H*), 7.98 (d, *J* = 1.9 Hz, quinoline-*H*), 7.78 (dd, 1H, *J* = 9.1, 1.9 Hz, quinoline-*H*), 7.53 (d, 1H, *J* = 2.6 Hz, quinoline-*H*), 7.41 (dd, 1H, *J* = 8.7, 2.6 Hz, Ar-*H*) 7.18 (d, 1H, *J* = 8.7 Hz, Ar-*H*) 6.82 (d, 1H, *J* = 7.2 Hz, Ar-*H*), 3.34 (s, 2H, CH_2), 2.46 (q, 4H, *J* = 7.1 Hz, NCH_2CH_3), 1.07 (t, 6H, *J* = 7.1 Hz, NCH_2CH_3); ^{13}C-NMR (100 MHz) δ 155.6, 143.4, 149.5, 130.8, 130.6, 129.2, 127.6, 125.4, 119.5, 117.6, 100.6, 49.4, 49.2, 9.4; IR (Nujol) 2891, 2842, 1663, 1619, 1565, 1513, 1460, 1432, 1384, 1331, 1246, 1197, 1173, 1152, 1109, 1062, 996, 912, 863, 820, 810, 738 cm^{-1}; MS *m/z* calcd for $C_{20}H_{23}ClN_3O$ $[M+H]^+$ 356.15292 found 356.15301; Elemental analysis: C: 67.43, H: 6.17, N: 11.77 (required values; C: 67.47, H: 6.23, N:11.81).

2.2.2.9 2-(bromomethyl)-1-fluoro-4-nitrobenzene (8a)

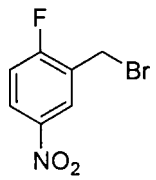

2-Fluoro-5-nitrotoluene, **7**, (1.90 g, 12.34 mmol) was dissolved in trifluoronitrotoluene (40 mL). To this, AIBN (0.20 g, 1.21 mmol) and NBS (3.00 g, 17.48 mmol) were added and the solution heated under nitrogen, at reflux for 24 h. The solution was cooled to 0°C and solids were filtered off before removal of the solvent *in vacuo* to give the bromo-substituted product, **8a**. The crude product was purified by flash column chromatography using 10 % EtOAc/Hexane as eluent to yield the product as a yellow oil. (1.32 g, 47 %): ^{1}H-NMR (400 MHz, $CDCl_3$) δ 8.78 (dd, 1H, *J* = 9.2 Hz (H-F), 2.8 Hz Ar-*H*), 8.22 (ddd, 1H, *J* = 16.36 (H-F), 9.1, 1.5 Hz, Ar-*H*), 7.27 (dd, 1H, *J* = 8.11 Hz (H-F), 1.0 Hz, Ar-*H*); 4.52 (s, 2H, CH_2); ^{13}C-NMR (100 MHz) δ 165.8, 143.7, 130.8, 127.6, 127.4, 118.7, 28.1; IR (neat): 1627, 1589, 1530, 1487, 1424,1349, 1325, 1254, 1078, 836, 745 cm^{-1}; MS *m/z* calcd for $C_7H_5NO_2F^{79}Br$ $[M+H]^+$ 234.0225 found 234.0293; Elemental analysis: C: 34.98, H: 2.14, N: 5.58 (required values; C: 35.93, H: 2.15, N: 5.99).

2.2.2.10 N-(2-fluoro-5-nitrobenzyl)-2-methylpropan-2-amine (8b)

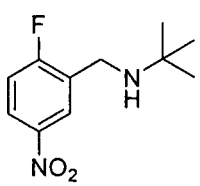

To a solution of **8a** (1.00g, 4.27 mmol) in acetonitrile, *tert*-butylamine (0.34g, 4.70 mmol) and potassium carbonate (0.65g, 4.70 mmol) were added and the mixture

was heated to reflux for 24 h. The solution was allowed to cool to room temperature before diluting with DCM and washing with distilled water. The organic layer was dried over $MgSO_4$, filtered and the solvent removed under reduced pressure to give the crude product. The crude product was then purified using flash column chromatography using 100 % DCM to give the product as an orange oil, **8b**. (0.59 g, 59 %): ^{1}H-NMR (400 MHz, MeOD) δ 8.57 (dd, 1H, *J* = 6.17, 3.26 Hz, Ar-*H*), 8.44 (ddd, 1H, *J* = 9.09, 8.91, 3.09 Hz, Ar-*H*), 7.53 (dd, 1H, *J* = 18.0, 8.91 Hz, Ar-*H*), 4.04 (s, 2H, C*H*$_2$), 1.48 (s, 9H, ^{t}Bu); ^{13}C-NMR (100 MHz) δ 158.7, 142.1, 130.6, 127.6, 127.4, 118.8, 49.8, 40.2, 29.1; IR (neat): cm^{-1} 3390, 2966, 2368, 2324, 1913, 1649, 1628, 1585, 1519, 1475, 1450, 1388, 1284, 1240, 1062, 812; MS *m/z* calcd for $C_{11}H_{15}N_2O_2F$ $[M+H]^+$ 227.1195 found 227.1189; Elemental analysis: C: 57.55, H: 6.39, N: 12.25 (required values; C: 58.40, H: 6.68, N: 12.38).

2.2.2.11 N-[3-((tert-butylamino)methyl)-4-fluorophenyl]-7-chloroquinolin-4-amine (8d)

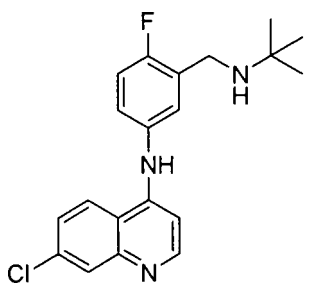

Concentrated HCl (5 mL) was added to the fluoronitrobenzylamine, **8b,** (1.01 g, 4.45 mmol). Tin granules (0.99 g, 8.32 mmol) were added and the solution was heated to reflux for 5 h. The solution was cooled and basified using NaOH solution (20 %) to pH 10 before extraction using DCM. After drying over potassium carbonate, the solution was filtered and the solvent removed *in vacuo* to give the

resulting amine as its hydrochloric salt. 4, 7 Dichloroquinoline (0.91 g, 4.90 mmol) and EtOH (20 mL) were added and the reaction heated at reflux for 16 h until completion (determined by TLC). The solvent was removed under reduced pressure and the crude product was purified by flash column chromatography using 0-20 % MeOH/DCM as eluent to yield the product as a light brown solid, **8d** (0.99 g, 66 %): mp; 181-183 °C (decomposed); ^{1}H-NMR (400 MHz, $CDCl_3$) δ 8.67 (d, 1H, *J* = 9.11 Hz, quinoline-*H*), 8.46 (d, 1H, *J* = 6.83 Hz, quinoline-*H*), 8.02 (d, 1H, *J* = 1.9 Hz, quinoline-*H*), 7.88 (dd, 1H, *J* = 6.08, 1.90 Hz, Ar-*H*), 7.82 (dd, 1H, *J* = 9.11, 1.9 Hz, quinoline-*H*), 7.65 (ddd, 1H, *J* = 15.75, 4.18, 1.9 Hz, Ar-*H*), 7.47 (dd, 1H, *J* = 18.03, 8.92, Ar-*H*), 7.02 (d, 1H, *J* = 6.83 Hz, quinoline-*H*); ^{13}C-NMR (100 MHz) δ 157.2, 145.6, 141.3, 140.8, 130.9, 130.1, 129.9, 127.6, 122.3, 120.8, 119.6, 117.6, 102.3, 59.2, 40.1, 26.7; IR (nujol): cm^{-1} 3361, 2967, 2324, 1610, 1585, 1540, 1502, 1475, 1448, 1378, 1340, 1213, 1101, 1062 MS *m/z* calcd for $C_{20}H_{21}ClFN_3$ $[M+H]^+$ 358.14862 found 358.14807.

2.2.2.12 Radiometric Synthesis of [^{3}H]–NTBISQ (4c)*

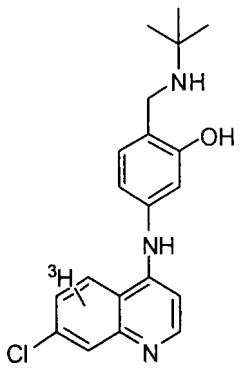

The radiolabelled compound **4c*** was prepared in a similar manner to non-labelled NTBISQ (**4c**) (Section 2.2.2.7). To the amine, **4b** (15 mg, 77.21 μmol), [^{3}H] – 4, 7 dichloroquinoline (1mCi/mL in 1 mL EtOH, 9.9 μg/mL) was carefully added

ensuring no droplets formed. EtOH (2 mL) was used to wash out the ampoule of radioactive material 4, 7 Dichloroquinoline (13 mg, 61.77 μmol) was added to the reaction mixture followed by HCl (2 μL) and the reaction was heated at reflux for 16 h until completion (determined by TLC). The solvent was allowed to evaporate in the fumehood and the crude product was purified by flash column chromatography using 10 - 80% MeOH/DCM as eluent to yield the product as a yellow solid, **4c*** (23.9 mg, 72 %). The radiolabelled product was analysed using LC-MS.

2.2.2.13 Radiometric Synthesis of [^{3}H]-FAQ-4 (8d)*

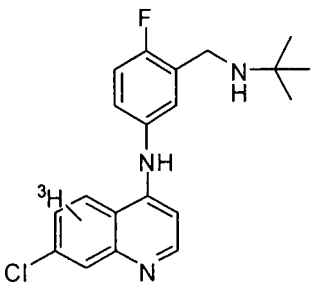

The radiolabeled compound **8d*** was prepared using the same method as **4c*** by addition of 4, 7 dichloroquinoline (8.1 mg, 41.12 μmol) to a solution of the amine side chain **8c** (10 mg, 51.28 μmol) and [^{3}H]-4, 7 dichloroquinoline (1mCi/mL in 1 mL EtOH, 9.9 μg/mL). A light brown solid, **8d***, was produced (7.2 mg, 39 %). The product was analysed by LC-MS.

2.2.2.14 Radiometric Synthesis of [^{3}H]-ClAQ-4 (11d)*

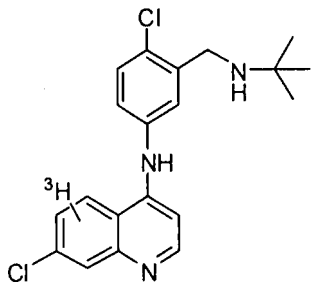

The radiolabeled compound **11d*** was prepared using the same method as **4c*** by addition of 4, 7 dichloroquinoline (28 mg, 142.13 μmol) to a solution of the chlorinated amine side chain (30 mg, 140.02 μmol) and [^{3}H]-4, 7 dichloroquinoline (1mCi/mL in 1 mL EtOH, 9.9 μg/mL). A light brown solid, **11d***, was produced (13.7 mg, 26 %). The product was analysed by LC-MS.

2.2.3 Methods – Pharmacological Evaluation

Antimalarial testing of the drugs used in this study was carried out using standard protocols at the Liverpool School of Tropical Medicine. The methods used are shown below (Berenbaum, 1978; Desjardins *et al.*, 1979; Lambros *et al.*, 1979; Trager *et al.*, 1976).

Four strains of *P. falciparum* were used in this study: The K1 and TM6 strains, which are known to be chloroquine resistant, and the HB3 and 3D7 strains which are sensitive to chloroquine. Parasites were maintained in continuous culture using the method of Jensen and Trager (Trager *et al.*, 1976). Cultures were grown in flasks containing human erythrocytes (2-5 %) with parasitaemia in the range of 1 % to 10 % suspended in RPMI 1640 medium supplemented with HEPES (25 mM), $NaHCO_3$ (32 mM), and 10 % human serum (complete medium). Cultures were gassed with a mixture of 3 % O_2, 4 % CO_2 and 93 % N_2.

Antimalarial activity was assessed using a sensitivity assay introduced by Desjardins, which involved incorporating [^{3}H]-hypoxanthine, the preferred form of purine required by the parasite for growth and development, into parasite nucleic acid as a marker to measure parasite growth (Asahi *et al.*, 1996; Desjardins *et al.*, 1979).

All compounds were prepared as the hydrochloride salt so that they were more soluble than their equivalent free-base. Stock drug solutions were prepared using DMSO (100 %) and diluted to the appropriate concentration using complete medium. The final solvent concentration was less than 0.1 % so parasite viability was unaffected. Assays were performed using 96-well micro titre plates. Each drug was tested in triplicate and parasite growth was compared to control wells (which constituted 100 % parasite growth). After 24 h incubation at 37 °C, 0.5 μCi [^{3}H]-hypoxanthine was added to each well. Cultures were incubated for a further 24 h before they were harvested onto glass filter-mats, dried for 1 h at room temperature, and counted using a Wallac 1450 Microbeta Trilux Liquid scintillation and luminescence counter. IC_{50} values were calculated by interpolation of the probit and transformation of the log dose – response curve.

2.3 RESULTS AND DISCUSSION

2.3.1 Chemistry

2.3.1.1 ISQ, DesISQ and NTBISQ

The preparation of ISQ and its analogues involved a three-step synthesis from inexpensive, commercially available starting materials based on a method originally utilized by Burckhalter and co-workers (Scheme 2.1) (Burckhalter *et al.*, 1948). The first step of the procedure involved a Mannich reaction of 3-hydroxyacetanilde, **1** to provide the Mannich intermediate in yields ranging from 54 % to 72 % (Table 2.1). The Mannich reaction involved condensation of the primary amine with formaldehyde to form a stable Schiff base. Electrophillic substitution by the imminium ion *ortho* to the hydroxyl group of 3-hydroxyacetanilide led to the formation of the Mannich intermediates in moderate to good yields (**2a, 3a** and **4a**) (Scheme 2.2) (Blicke, 1942). The next step involved an acid-catalysed hydrolysis of the amide function to give the corresponding Mannich-substituted 3-aminophenol in high yield (Table 2.1). The final stage of the synthesis involved coupling with 4, 7-dichloroquinoline to provide the target molecules required (**2c**, **3c** and **4c**) (Scheme 2.1). The compounds were obtained as their hydrochloride salts which proved to be more convenient for dosing in the subsequent animal studies performed (Chapters 3, 4 and 6).

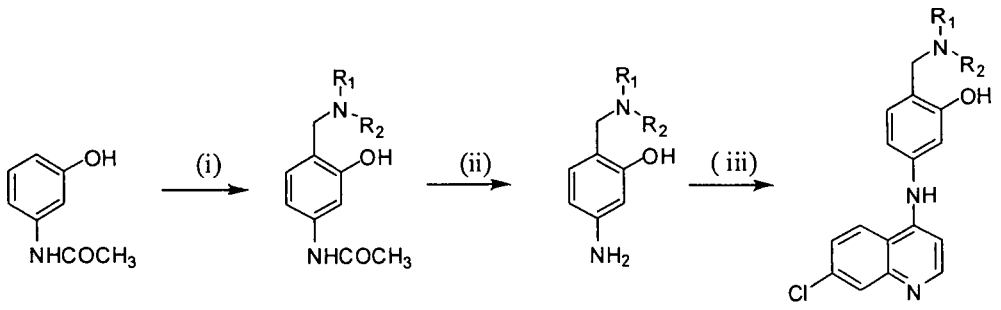

1 **2a, 3a, 4a** **2b, 3b, 4b** **2c, 3c, 4c**

(2) $R_1 + R_2 = (C_2H_5)_2$
(3) $R_1 = C_2H_5$, $R_2 = H$
(4) $R_1 = C(CH_3)_3$, $R_2 = H$

Scheme 2.1 Three step chemical syntheses of isoquine, ISQ (2c), desethyl isoquine, desISQ (3c) and *N-tert*-butyl isoquine, NTBISQ (4c). Reagents and conditions: (i) EtOH, formaldehyde (2.5 eq), (a) – $NHEt_2$, (b) – NH_2Et, (c) - $NH_2{}^tBu$ (1.1 eq), 80 °C, 16 h; (ii) conc. HCl, EtOH, 80 °C, 5 h; (iii) 4,7 dichloroquinoline (1.1 eq), EtOH, 80 °C, 16 h.

	% Yield		
Compound	(a)	(b)	(c)
ISQ, **2**	54	88	68
DesISQ, **3**	58	86	16
NTBISQ, **4**	72	92	78

Table 2.1 Percentage yields for each of the three steps of the synthesis for the isoquine analogues, ISQ, (2); desISQ, (3) and NTBISQ, (4).

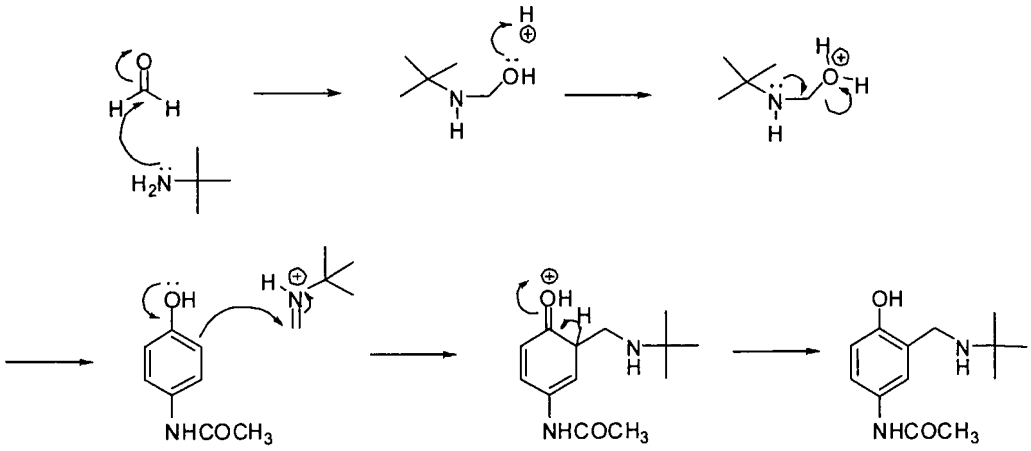

Scheme 2.2 Mechanism of the Mannich-type reaction: formation of intermediate 4a. Condensation of *tert* butylamine with formaldehyde forms the Schiff base.

2.3.1.2 The "Reverse Route" Synthesis

In an attempt to optimize the synthesis of the 4-aminoquinoline analogues, a second pathway for the synthesis of ISQ and its analogues was designed and termed the "reverse route". The reverse route involved only two steps, utilising inexpensive and commercially available materials. Direct coupling of 3-hydroxylamine with 4, 7-dichloroquinoline gave 3-(7-chloroquinolin-4-ylamino) phenol, **9**, in very high yields (Scheme 2.3). Indeed, it was possible to make **9** in multi-gram quantities and from this intermediate a divergent synthesis could be carried out. This was achieved by reacting **9** with the appropriate amine in a solution of ^{i}PrOH and *p*-formaldehyde. Unfortunately, the products formed from these reactions were obtained in low yield, and purification *via* flash column chromatography was deemed as unsuitable for industrial scale-up.

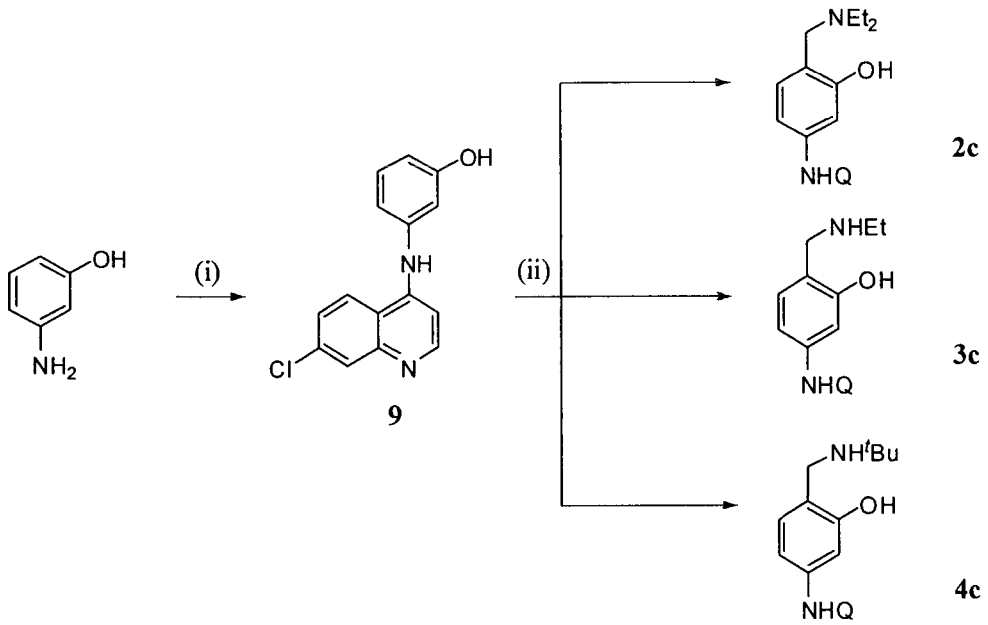

Scheme 2.3 "Reverse route" for the formation of isoquine analogues.
Reagents and conditions: (i) EtOH, 4,7- dichloroquinoline (1.2 eq), 80 °C, 16 h (90 %); (ii) $(CH_2O)n$ (1.1 eq), *i*PrOH, (**2c**) – $NHEt_2$ (39 %), (**3c**) – NH_2Et (17 %), (**4c**) - $NH_2{}^tBu$ (9.8 eq), 80 °C, 16 h. Yields obtained: (**2c**) (39 %), (**3c**) (17 %), (**4c**) (42 %).

2.3.1.3 Optimisation of Conditions – The "Reverse Route"

NTBISQ was initially prepared at GSK *via* the three-step "forward route" described previously (Chapter 2, section 2.3.1.1) (GlaxoSmithKline, 2006). However, the synthesis proved arduous to scale up to an industrial level due to poor selectivity of step two, resulting in low yields and poor purity coupled with instability of the drug substance under the processing conditions used. Therefore, GSK scientists used a computational-design approach in order to optimize the conditions used. The parameters chosen to be analysed by the "computational design of experiment" (DoE) screening programmes were:

- The number of Schiff base equivalents required
- The Schiff base addition time

- The reaction time
- The reaction temperature
- The volume of solvent

The factors favouring formation of product (NTBISQ) were first investigated by GSK (Figure 2.2).

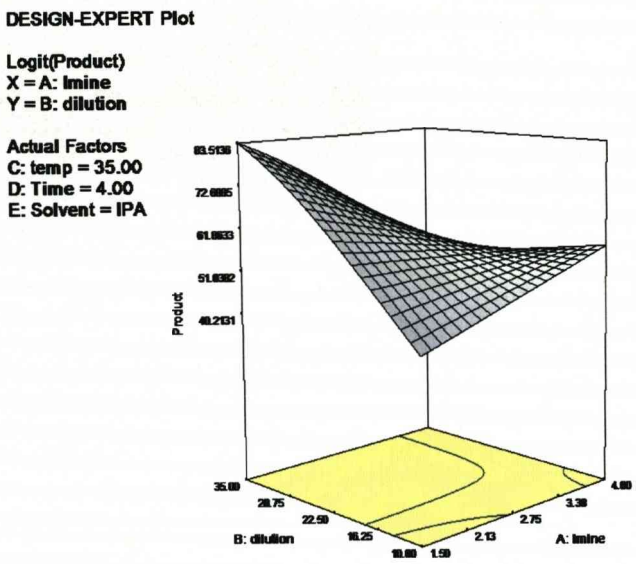

Figure 2.2 Example of a DoE plot showing the amount of NTBISQ formed with different volumes of solvent and different concentrations of imine. (Figure obtained from GlaxoSmithKline, Stevenage, UK (GlaxoSmithKline, 2006))

The results showed that product formation was favoured by high dilution, low temperature, low reaction time and lower concentrations of imine. Further plots were carried out exploring the factors required for maximum consumption of starting material and also minimal formation of side products. The overall predicted optimal reaction conditions from these experiments were four equivalents of imine, a dilution of twenty-four volumes, and a temperature of 35 °C over a time period of six hours. The use of *i*PrOH was found to be the ideal solvent for isolation of NTBISQ as it was found that the crystalline mono-Mannich product precipitated of solution whilst the bis-Mannich side-product remained in the solvent. This allowed for simple filtration

to isolate the desired material. The optimized synthesis identified a route similar to that of ours (the "reverse route", Scheme 2.3) (Scheme 2.4). Scientists reacted together compound **9** with *tert* butylamine in a solution of *i*PrOH and para-formaldehyde. The aim was to synthesise a large quantity of NTBISQ, however, instead of the recovery of NTBISQ; they instead observed the formation of a cyclic benzoxazine compound, **10.** This was a surprising result; however the target molecule was readily isolated by hydrolyis of **10** using HCl in ^{i}PrOH. The product was then purified by re-crystallisation, rather than flash column chromatography, resulting in a yield of 91 % (Scheme 2.4). This chemistry has been scaled up to 15 kg.

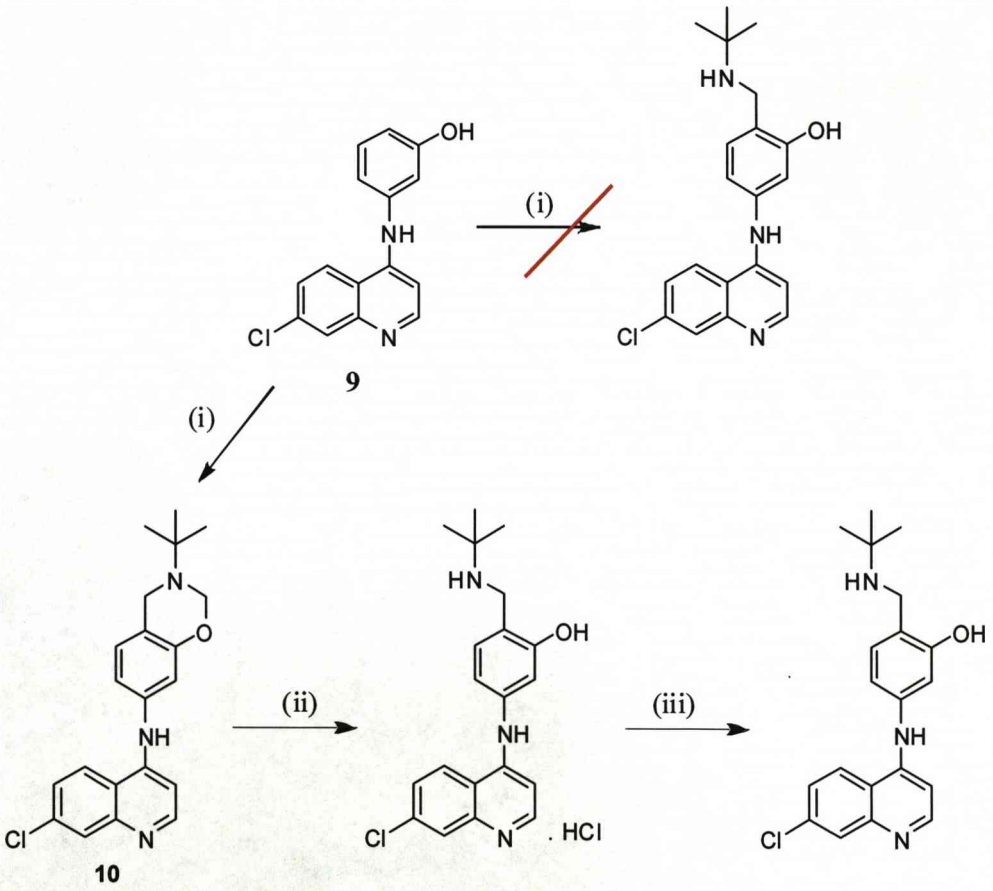

Scheme 2.4 GlaxoSmithKline optimised chemical synthesis of NTBISQ. Reagents and conditions: (i) $(CH_2O)n$ (5 eq), $NH_2{}^{t}Bu$ (5 eq), *i*PrOH (35 vol), 40 °C, 3 h (55 %); (ii) 20 % HCl, *i*PrOH (20 vol), RT, 2 h (96 %); (iii) 10 % KOH (ethanolic), *i*PrOH (15 vol), RT (91 %).

2.3.1.4 AQ and FAQ-4

AQ, **6c** was prepared, in good yield following the same synthetic pathway as ISQ and its analogues using 4-hydroxyacetanilde, **5** as the precursor (Scheme 2.5). Step one involved a Mannich reaction between the Schiff base formed from reaction of diethylamine and formaldehyde and the 4-hydroxyacetanilide, **5** to give the intermediate **6a**. Hydrolysis of **6a** using HCl in EtOH afforded the amine **6b** which could then be coupled with 4, 7 dichloroquinoline, completing the synthesis of AQ, **6c**.

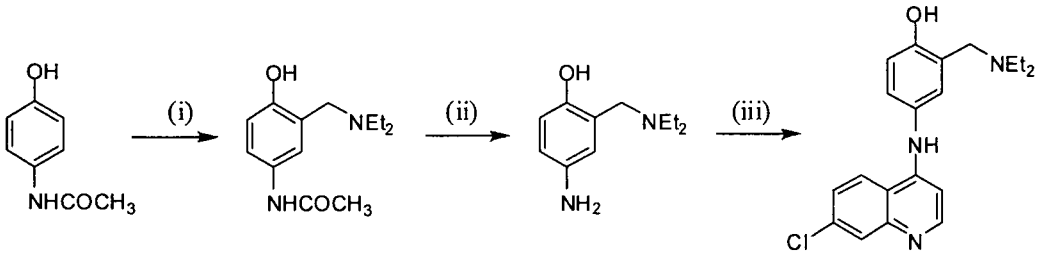

5 **6a** **6b** **6c**

Scheme 2.5 Three step chemical syntheses of amodiaquine, AQ (6c). Reagents and conditions: (i) EtOH, formaldehyde (2.5 eq), – $NHEt_2$, (1.1 eq), 80 °C, 16 h (64 %); (ii) conc. HCl, EtOH, 80 °C, 5 h (89 %); (iii) 4,7 dichloroquinoline (1.1 eq), EtOH, 80 °C, 16 h (76 %).

The synthesis of FAQ-4, **8d** involved four steps, commencing with a radical bromination of **7,** employing trifluoronitrotoluene as the solvent (Scheme 2.6).

AIBN was used as a radical initiator and *N*-bromosuccinamide as a source of bromine. Step two involved nucleophilic substitution at the C-Br bond of **8a** using *tert* butylamine in acetonitrile, in the presence of potassium carbonate to afford **8b** as an orange oil. The third step of the synthesis was a Sn/HCl reduction of the nitro group to the primary amine **8c**, and this was achieved in a good yield of 74 %. The final step involved coupling of the 4-aminophenol compound to 4, 7 dichloroquinoline in the presence of ethanol to yield the product, **8d**, in good yield.

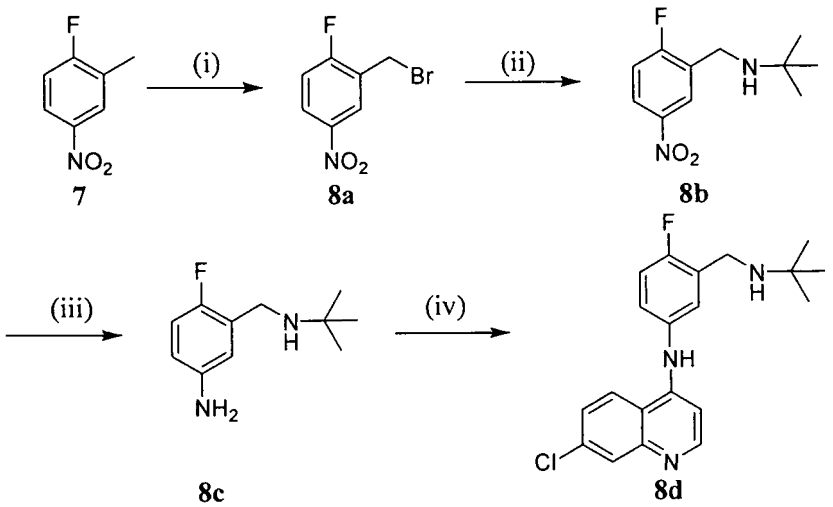

Scheme 2.6 Four step chemical synthesis of *N-tert*-butyl fluoro amodiaquine (FAQ-4), (8d). Reagents and conditions: (i) trifluoronitrotoluene, NBS (1.4 eq), AIBN (0.1 eq), 100 °C, 24 h (47 %); (ii) ACN, -$NH_2{}^tBu$ (1.1 eq), K_2CO_3 (1.1 eq), 83 °C, 24 h (59 %); (iii) conc. HCl, Sn (2eq), 100 °C, 5 h (74 %); (iii) 4,7 dichloroquinoline (1.1 eq), EtOH, 80 °C, 16 h (66 %).

2.1.3.5 Radiometric Syntheses of [^{3}H]-NTBISQ, [^{3}H]-FAQ-4 and [^{3}H]–ClAQ-4

NTBISQ (**4c***), FAQ-4 (**8d***) and ClAQ-4 (**11d***) were each radiolabelled using [^{3}H]-4, 7 dichloroquinoline (Scheme 2.7). The reaction involved the coupling of the relevant amino side-chain (**4b**, **8c** or **11c**) with tritium-labeled 4, 7 dichloroquinoline and non-radiolabeled 4, 7 dichloroquinoline. Only one step was required for this coupling reaction and so minimal loss of the radiolabel occurred during the synthesis. Each compound was analysed by radiometric HPLC and LC-MS using a mobile phase of acetonitrile (10-50 %, 30 min) and trifluoroacetic acid (TFA) (0.1 %) at a flow rate of 0.9 mL/min (Figure 2.3). NTBISQ was seen to elute at retention time (Rt) = 12.6 min, whilst the fluoro analogue eluted at Rt = 13.8 min and the chloro at Rt = 13.6 min. Radiochemical purity of each compound was observed to be greater than 97 %. LC-MS analysis located co-eluting pairs of chlorine isotope peaks in the positive-ion mass chromatograms for *m/z* 356 ([^{3}H]-NTBISQ $[M+1]^+$), *m/z* 358 ([^{3}H]-FAQ-4 $[M+1]^+$) and *m/z* 374 ([^{3}H]-ClAQ-4

$[M+1]^+$) (Figure 2.4). The parent compound was seen together with a fragment representing loss of the *tert* butylamino side-chain (-56 amu).

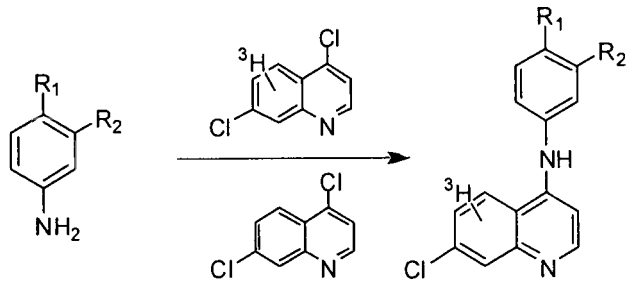

4b, 8c, 11c **4c*, 8d*, 11d***

4 $R_1 = CH_2NH(CH_3)_3$, $R_2 = OH$
8 $R_1 = F$, $R_2 = CH_2NH(CH_3)_3$
11 $R_1 = Cl$, $R_2 = CH_2NH(CH_3)_3$

Scheme 2.7 General scheme outlining the radiometric synthesis of [^{3}H]-NTBISQ, [^{3}H] -FAQ-4 and [^{3}H]-ClAQ-4. Reagents and conditions: **4b** (1 eq), **8c** (1 eq), **11c** (1 eq), 4,7 Dichloroquinoline (0.8 eq), [^{3}H] – 4, 7 dichloroquinoline (9.9.μg/mL, 20 Ci/mmol), EtOH, HCl (20 μL), 80 °C, 16 h.

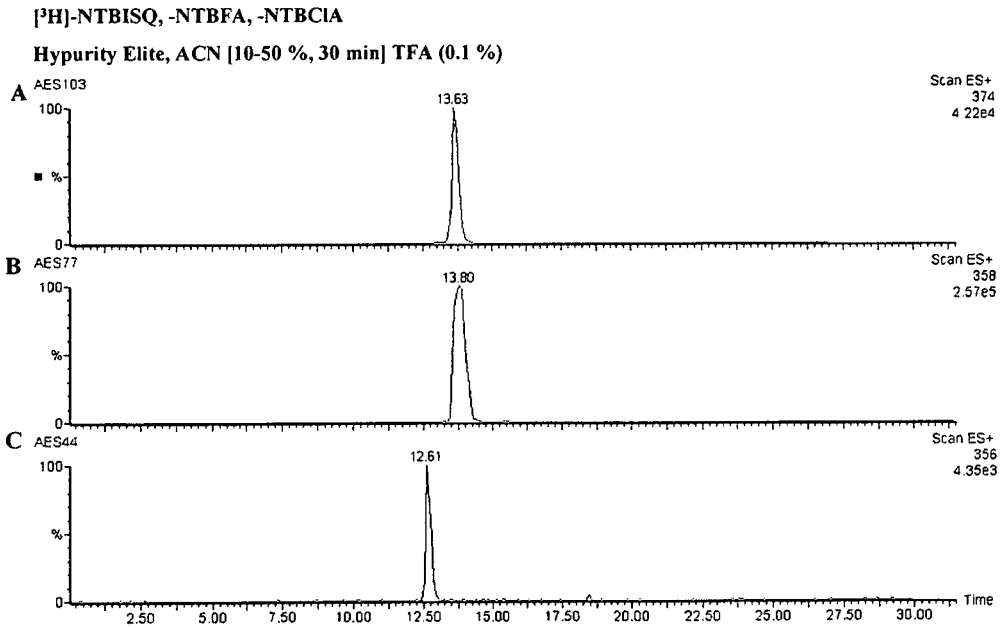

Figure 2.3 Positive-ion electrospray mass chromatograms corresponding to (A) [^{3}H]-ClAQ-4 (B) [^{3}H]-FAQ-4 and (C) [^{3}H]- NTBISQ.

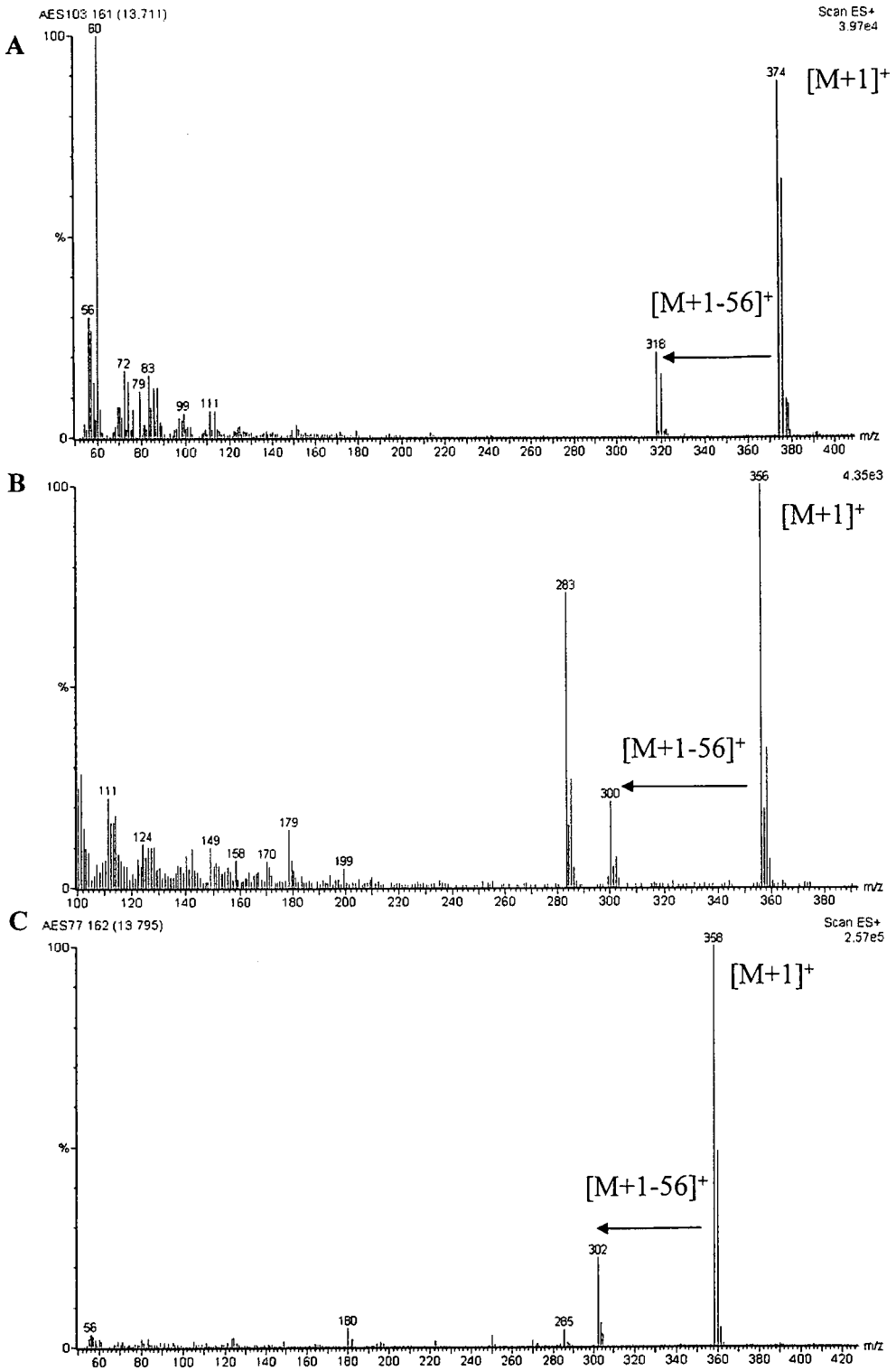

Figure 2.4 Positive-ion electrospray mass spectra showing the fragmentation of (A) [^{3}H]-ClAQ-4 (B) [^{3}H]-FAQ-4 and (C) [^{3}H]-NTBISQ

2.3.2 Pharmacodynamics of the 4-Aminoquinoline Series

2.3.2.1 In Vitro Antimalarial Activity

All of the compounds synthesized were evaluated by The School of Tropical Medicine, Liverpool using standard procedures (Berenbaum, 1978; Desjardins *et al.*, 1979; Lambros *et al.*, 1979; Trager *et al.*, 1976).

It was decided that the *in vitro* activities of NTBISQ, FAQ-4and ClAQ-4 should be evaluated along side the related 4-aminoquinolines CQ, AQ, ISQ and desISQ in order to define the activity range of an isoquine family. Four strains of *P. falciparum* were used; the CQ-resistant un-cloned K1 and CQ-resistant TM6 strains, and the CQ-sensitive HB3 and 3D7 strains (Table 1.4).

	IC_{50} nM			
Drug	K1	HB3	3D7	TM6
CQ	183.2 ± 11.1	14.9 ± 3.9	19.4 ± 1.9	75 ± 22.1
AQ	15.1 ± 9.4	9.6 ± 3.7	11.2 ± 1.4	7.2 ± 3.3
ISQ	17.6 ± 7.0	12.6 ± 4.7	11.6 ± 2.3	ND
DesISQ	6.0 ± 8.0	9.0 ± 4.1	9.2 ± 3.1	ND
NTBISQ	13.2 ± 3.2	12.6 ± 5.3	11.2 ± 2.2	ND
FAQ-4	20.2 ± 4.6	13.2 ± 3.4	11.2 ± 2.5	ND
ClAQ-4	ND	10.1 ± 3.2	ND	3.0 ± 2.2

Table 1.4 ***In vitro*** **antimalarial activities of CQ, AQ, ISQ, DesISQ, NTBISQ, FAQ-4 and ClAQ-4.** Data obtained from The School of Tropical Medicine, Liverpool. Values expressed as IC_{50} (nM) against four strains of the malaria parasite, *P. falciparum*: the CQ-resistant strains K1 and TM6 and the CQ-sensitive strains HB3 and 3D7. ND = No data.

All compounds showed good antimalarial activity against all three strains of *P. falciparum* tested. NTBISQ showed potent growth inhibition of both CQ-sensitive and CQ-resistant parasite strains, with IC_{50} values ranging between 11.2 and 13.2 nM respectively. NTBISQ exhibited similar activity to AQ against all three strains tested

It was anticipated that FAQ-4 and ClAQ-4 might be less active against malaria than their non-halogenated analogues due to the fact they are less basic. This reasoning was based on the fact that the 4-aminoquinolines cross the wall of the human red blood cell at pH 7.4 and enter the acidic compartment of the parasite along a concentration gradient. As the molecule passes along the gradient it becomes protonated and can no longer pass back through the wall of the erythrocyte, becoming "ion trapped". In doing so it accumulates inside the parasite DV to levels much higher than those in the circulating blood where it can then bind to free heme, preventing polymerisation to hematin (Chou *et al.*, 1980; Ferrari *et al.*, 1990; Sullivan *et al.*, 1996). Based on the mechanism of action of these compounds, the less basic the molecule, the less accumulation within the parasite DV might be expected (Ginsburg *et al.*, 1992). However, data obtained so far, clearly suggests that FAQ-4 and ClAQ-4 are as active as their non-halogenated counterparts.

Cross resistance is the subsequent resistance of the parasite to related antimalarials. The results in this section demonstrate a lack of cross-resistance between NTBISQ and CQ, as indicated by the similar IC_{50} values, in the nanomolar range, obtained across the three strains of malaria tested. This was in stark contrast to those obtained for CQ whereby it could be seen there was a marked difference between the IC_{50} values for the K1 strain versus the 3D7 and HB3 strains. The IC_{50} value for K1 was more than 9-fold higher than the values obtained against the 3D7 and HB3 strains. The lack of cross-resistance was found to be consistent for the other ISQ and AQ derivatives tested.

2.3.1.2 In Vitro Therapeutic Index

The compounds synthesized were subjected to a standard battery of *in vitro* cytotoxicity assays at GSK, Tres Cantos. The *in vitro* selectivity ratio was studied in terms of whole cell inhibition, comparing activity against *P falciparum* versus cytotoxicity in various mammalian cell lines such as hamster ovary cells, monkey kidney cells, human leukemia cells, human lung cells, mouse glial cells, rat liver cells and human hepatocytes (Table 1.5).

The potential cytotoxicity of NTBISQ was studied in immortalised cell lines derived from target organs for *in vivo* toxicity (Table 1.5). Mammalian cells were incubated with the compounds for twenty-four hours, and cell damage was determined using an oxidation-reduction marker as an indication of cell energy metabolism. Results were compared to the 4-aminoquinoline series as before. At present no data has been received for FAQ-4 or ClAQ-4.

Cell Line	Tox_{50} μM CQ	AQ	ISQ	desISQ	NTBISQ	Therapeutic Index NTBISQ
CHO (ovary, hamster)	>96.9	>70.2	113.2	71.1	84.3	7527
Cos-1 (kidney, monkey)	>96.9	>70.2	68.5	65.6	81.5	7276
HL-60 (promyelocytic leukemia, human)	>96.9	>70.2	61.8	48.8	50.7	4527
MRC5 (lung, human)	>96.9	>70.2	96.9	45.8	42.1	3759
Neuro 2 A (glial, mouse)	>96.9	>70.2	60.1	47.6	59	5268
MH1C1 (liver, rat)	>96.9	>70.2	45.2	<18.3	<16.9	<1509
Hep G2 (liver, human)	>96.9	>70.2	60.8	45.8	42.1	3759

Table 1.5 ***In vitro*** **cytotoxicity of NTBISQ and the 4-aminoquinoline series.** Data obtained from a pre-clinical, pharmacokinetics study at GlaxoSmithKline, Tres Cantos. Data are expressed as mean ± SD (n = 3). Maximum solubility in the assay conditions: AQ 70.2 μM, CQ 96.9 μM, ISQ 14.1 μM, desISQ >30.5 μM and NTBISQ 28.9 μM.

It can be seen immediately that the cytotoxicity values obtained for NTBISQ against the mammalian cell lines employed were at least 1500 times greater than values required to kill the malarial parasite (Table 5). NTBISQ was shown to have Tox_{50} values ranging from 1.1 - 5.7-fold lower than CQ. However, the fact remains that the *in vitro* therapeutic window for NTBISQ was still very high across all cell lines tested. These results illustrate that the concentration of NTBISQ required to kill the parasite is much higher than that required to kill each of the mammalian cell lines. This shows that not only is NTBISQ an extremely effective antimalarial *in vitro*, but it is also highly selective for the malaria parasite.

2.3.1 Pharmacokinetic Data

2.3.1.1 Oral Bioavailability

The term bioavailability is defined as the fraction of an ingested dose of a drug that gains access to the systemic circulation. It may be low if absorption is incomplete, or if the drug is metabolised in the gut wall or liver before reaching the systemic circulation (Rang *et al.*, 1999).

The oral bioavailabilities F (%) of ISQ, desISQ, NTBISQ and FAQ-4 were determined in a study, evaluating four species of animal, by GlaxoSmithKline. The data received indicated that less than 21 % of ISQ reached the systemic circulation after oral dosing (Table 1.6).

Species	ISQ F (%)	desISQ F (%)	NTBISQ F (%)	FAQ-4 F (%)
Mouse	21	100	100	37
Rat	17.0 ± 4.0	60 ± 26	89 ± 12	100
Dog	NQ	NE	92 ± 13	ND
Monkey	ND	40 ± 14	100	25 ± 5

Table 1.6 Oral bioavailability of ISQ, desISQ, NTBISQ, FAQ-4 in animals. Data obtained from a pre-clinical, pharmacokinetics study at GlaxoSmithKline, Tres Cantos, Spain. Data are expressed as mean ± SD (n=3). NE = Not estimated (emesis observed in oral leg may have resulted in decreased oral exposure). NQ = Not quantifiable. ND = no data.

As previously discussed (Chapter 1, section 1.5.2), ISQ is in fact, a pro-drug of desISQ, undergoing extensive P450-mediated dealkylation *via* the CYP2C8 enzyme (O'Neill *et al.*, 2003). DesISQ has been shown to have excellent bioavailability in the mouse and more moderate bioavailability across other species. Emesis in the dog study precluded an estimate of the oral bioavailability of this species.

The stand out candidate based on these sets of data was NTBISQ. The oral bioavailability of NTBISQ across all four species was greater than 89 % suggesting

that almost all of the drug would reach the systemic circulation after oral dosing. The implications of these tests revealed NTBISQ as the more favourable candidate to go forth into further clinical testing.

2.3.1.2 Blood Clearance

The levels of drug in blood are important in giving a composite picture of the disposition of a compound. A high clearance value may equate to a faster rate of metabolic degradation due to clearance being an expression of the amount of drug, in a volume of plasma that has been metabolised in unit time (Rang *et al.*, 1999).

The blood clearance values of ISQ, desISQ, NTBISQ and FAQ-4 are shown below (Table 1.7).

Species	Blood Clearance of ISQ (mL/min/kg)	Blood Clearance of desISQ (mL/min/kg)	Blood Clearance of NTBISQ (mL/min/kg)	Blood Clearance of FAQ-4 (mL/min/kg)
Mouse	21.9	43.5	17.2	40.4
Rat	89.2 ± 4.3	61.5 ± 21.6	25.9 ± 4.9	35 ± 4.2
Dog	151.4 ± 23.6	11.5 ± 2.6	6.39 ± 1.57	ND
Monkey	ND	49.4 ± 2.6	14.5 ± 0.7	17.9 ± 7.8

Table 1.7 Blood clearance of ISQ, desISQ, NTBISQ and FAQ-4 in animals. Data obtained from a pre-clinical, pharmacokinetics study at GlaxoSmithKline, Tres Cantos, Spain. Data are expressed as mean ± SD (n=3). For composite mouse studies, variability of parameters has not been estimated. ND = No data.

Clearance values of desISQ, NTBISQ and FAQ-4 were shown to be moderate across all four species. ISQ appeared to be cleared from the blood at a very high rate (exceeding that of blood flow in the liver) in the rat and dog with values close to that of CQ (140 mL/min/kg) (Augustijins *et al.*, 1992). This is consistent with the fact that ISQ is rapidly metabolised to desISQ *in vivo*.

DesISQ had substantially lower blood clearance compared to ISQ in the mouse and the rat. In the dog, blood clearance was about 2-fold higher than that of NTBISQ, the clearance of which was approximately 40 % of liver blood flow in all species.

2.3.1.3 Plasma Half-Life of NTBISQ

The plasma half-life of a drug can be defined as the time taken for the concentration of a drug in plasma to decrease by half from a given point. It reflects the rates at which the various dynamic processes, distribution, excretion and metabolism are taking place *in vivo* (Timbrell, 2000).

The half-life of NTBISQ was studied in mouse, rat and monkey (Table 1.8). The values obtained across all four species are moderate and it can be estimated that the half-life in humans may be approximately 9 hours.

Species	NTBISQ $T_{1/2}$ (h)
Mouse	3.3 ± 1.2
Rat	7.9 ± 4.3
Dog	14.2 ± 3.1
Monkey	9.0 ± 4.2
Human	N/A

Table 1.8 Half-life of NTBISQ in four different species of animals. Data obtained from a pre-clinical, pharmacokinetics study at GlaxoSmithKline, Tres Cantos, Spain. Data are expressed as mean ± SD (n=3).

The literature half-life values of AQ and CQ in humans are 5.2 ± 1.7 hours and 275.7 ± 110.8 hours respectively (Gustafsson *et al.*, 1983; Winstanley *et al.*, 1987). The long half-life of CQ must be noted as it has been suggested that a long terminal half-life is a considerable factor in drug-resistance. A long half-life means that the drug may be present in the body at sub-therapeutic concentrations for long

periods of time, allowing for the increase in selection pressure for resistant mutants (Watkins *et al.*, 1993).

2.3.2 Conclusions

This chapter clearly demonstrates the highly efficient chemical and radiochemical syntheses of a number of ISQ and AQ analogues. The pathways used were inexpensive, facile and led to generally good yields of product. In the case of the ISQ analogues, in particular NTBISQ, a second route was investigated, and was further optimized by our industrial partners GlaxoSmithKline. This resulted in the ultimate large-scale formation of 15 kg of NTBISQ.

The efficient synthesis of these compounds has led to a preliminary comparison of four promising antimalarial drugs and their possibility for further development. Each compound was assessed for antimalarial activity against both CQ-sensitive and CQ-resistant parasites. All showed excellent activity against all three strains of malaria, notably against the CQ-resistant strain, K1 with no signs of cross-resistance, as with CQ.

The 4-aminoquinoline compounds were analysed against various mammalian cell lines for toxicity. Whilst the Tox_{50} values for NTBISQ were lower than that of CQ, the *in vitro* therapeutic index remained greater than 1500 showing that NTBISQ was selective for the malaria parasite over mammalian cell lines.

The oral bioavailability of NTBISQ was shown to be highly impressive across all four species, with an average value of 95 %. FAQ-4 showed 100 % bioavailability in the rat; however the results were lower in the mouse and monkey.

These studies have generated vital data that validated the selection of NTBISQ as a lead compound for progression into rigorous metabolism and definitive

safety assessment studies. FAQ-4 and ClAQ-4 were selected as back-up compounds, and investigation into their metabolism has also been carried out.

The forthcoming chapters of this thesis will present an in depth study of the *in vivo* metabolic fate of NTBISQ, FAQ-4 and ClAQ-4, with comparisons made to CQ, AQ and ISQ.

2.4 REFERENCES

ASAHI, H., KANAZAWA, T., KAJIHARA, Y., TAKAHASHI, K. & TAKAHASHI, T. (1996). Hypoxanthine: a low molecular weight factor essential for growth of erthyrocytic Plasmodium falciparum in a serum-free medium. *Parasitology*, **113,** 19-23.

AUGUSTIJINS, P., GEUSSENS, P. & VERBEKE, N. (1992). Chloroquine levels in blood during chronic treatment of patients with rheumatoid arthritis. *European Journal of Clinical Pharmacology*, **42,** 429-433.

BARNARD, S., STORR, R., O'NEILL, P. & PARK, B. (1993). The effect of fluorine substitution on the physiochemical properties and the analgesic activity of paracetamol. *Journal of Pharmacy and Pharmacology*, **45,** 736-744.

BERENBAUM, M. (1978). A method for testing synergy with any number of agents. *Journal of Infectious Diseases*, **137,** 122-130.

BLICKE, F. (1942). *Organic Reactions. The Mannich Reaction (Chapter 10).* New York: John Wiley & Sons, INC.

BURCKHALTER, J., TENDWICK, J., JONES, F. & JONES, P. (1948). Aminoalkylphenols as antimalarials II (heterocyclic-amino)- alpha-amino-o-cresols: The synthesis of camoquine. *The Journal of the American Chemical Society*, **70,** 1363-1373.

CHOU, A., CHEVLI, R. & FITCH, C. (1980). Ferriprotoporphyrin IX fulfils the criteria for identification as the chloroquine receptor of malaria parasites. *Biochemistry*, **19,** 1543-1549.

DESJARDINS, R., CANFIELD, C., HAYNES, J. & CHULAY, J. (1979). Quantitative assessment of antimalarial activity in vitro by a semiautomated microdilution technique. *Antimicrobial Agents and Chemotherapy*, **16,** 710-718.

FERRARI, V. & CUTLER, D. (1990). Uptake of chloroquine by human erythrocytes. *Biochemical Pharmacology*, **39,** 753-762.

GINSBURG, H. & KRUGLIAK, M. (1992). Quinoline containing antimalarials: Mode of action, drug-resistance and its reversal. An update with unresolved puzzles. *Biochemical Pharmacology*, **43,** 63-70.

GLAXOSMITHKLINE (2006). GSK369796A - New route development work: initial focus on amide reduction approach. ed. Shone, A. Stevenage, Hertfordshire, UK: GlaxoSmithKline.

GUSTAFSSON, L., WALKER, O., ALVAN, G., BEERMANN, B., ESTEVEZ, F., GLEISNER, L., LINDSTROM, B. & SJOQVIST, F. (1983). Disposition of chloroquine in man after single intravenous and oral doses. *British Journal of Clinical Pharmacology*, **15,** 471-479.

LAMBROS, C. & VANDERBERG, J. (1979). Synchronisation of Plasmodium falcuparum erythrocyte stages in culture. *Journal of Parasitology*, **65,** 418-420.

MADRID, P., SHERRILL, J., LIOU, A., WEISMAN, J., DERISI, J. & GUY, R. (2005). Synthesis of ring-substituted 4-aminoquinolines and evaluation of their antimalarial activities. *Bioorganic Medicinal Chemistry Letters*, **15,** 1015-1018.

O'NEILL, P., BRAY, P., HAWLEY, S., WARD, S. & PARK, B. (1998). 4-Aminoquinolines - past, present, and future: A chemical perspective. *Pharmacology and Therapeutics*, **77,** 29-58.

O'NEILL, P., HARRISON, A., STORR, R., HAWLEY, S., WARD, S. & PARK, B. (1994). The effect of fluorine substitution on the metabolism and antimalarial activity of Amodiaquine. *The Journal of Medicinal Chemistry*, **37,** 1362-1370.

O'NEILL, P., MUKHTAR, A., STOCKS, P., RANDLE, L., HINDLEY, S., WARD, S., STORR, R., BICKLEY, J., O'NEIL, I., MAGGS, J., HUGHES, R., WINSTANLEY, P., BRAY, P. & PARK, B. (2003). Isoquine and related amodiaquine analogues: A new generation of improved 4-aminoquinoline antimalarials. *Journal of Medicinal Chemistry*, **46,** 4933-4945.

O'NEILL, P., WILLCOCK, D., HAWLEY, S., BRAY, P., STORR, R., WARD, S. & PARK, B. (1997). Synthesis, antimalarial activity and molecular modeling of tebuquine analogues. *Journal of Medicinal Chemistry*, **40,** 437-448.

RANG, H., DALE, M. & RITTER, J. (1999). *Pharmacology*. Edinburgh: Churchill Livingstone.

SULLIVAN, D., GLUZMAN, I., RUSSELL, D. & GOLDBERG, D. (1996). On the molecular mechanism of chloroquine's antimalarial action. *Proceedings of the National Academy of Sciences of the USA*, **93,** 11865-11870.

TIMBRELL, J. (2000). *Principles of biochemical toxicology*. London: Taylor & Francis Ltd.

TRAGER, W. & JENSON, J. (1976). Human malaria parasites in continuous culture. *Science*, **193,** 673-675.

WATKINS, W. & MOBOSO, M. (1993). Treatment of plasmodium falciparum malaria with pyrimethamine-sulfadoxine-selective pressure for resistance is a function of long elimination half-life. *Transactions of the Royal Society of Tropical Medicine and Hygiene*, **87,** 75-78.

WINSTANLEY, P., EDWARDS, G., ORME, M. & BRECKENRIDGE, A. (1987). The disposition of amodiaquine in man after oral administration. *British Journal of Clinical Pharmacology*, **23,** 1-7.

CHAPTER 3

THE *IN VIVO* METABOLISM AND DISTRIBUTION OF CHLOROQUINE AND AMODIAQUINE IN RATS

CONTENTS

3.1 INTRODUCTION

Chloroquine (CQ) has been used in the treatment of malaria for over 50 years and its disposition in man has been well documented. As discussed in the introduction to this thesis, there is increasing resistance to CQ by malaria parasites, and this is driving an ever increasing urgency to find new antimalarials.

In man, CQ is rapidly and completely absorbed from the gastrointestinal tract after oral administration with peak plasma levels being attained 1 – 3 hours after a single oral dose (Gustafsson *et al.*, 1983). CQ is found mainly as the parent compound in the tissues and plasma of humans, but the major route of metabolism is cleavage of the alkyl groups to its desethyl (desCQ) and bisdesethyl (bisCQ) analogues (Figure 3.1) (Ademowo *et al.*, 2000; Gustafsson *et al.*, 1983; Hellgren *et al.*, 1989; McChesney *et al.*, 1967; Projean *et al.*, 2003). This dealkylation process does not result in loss of antimalarial activity as the main metabolite, desCQ, has appreciable antimalarial activity against CQ-sensitive strains and has been shown to have an additive effect on the antimalarial action of CQ (Aderounmu, 1984).

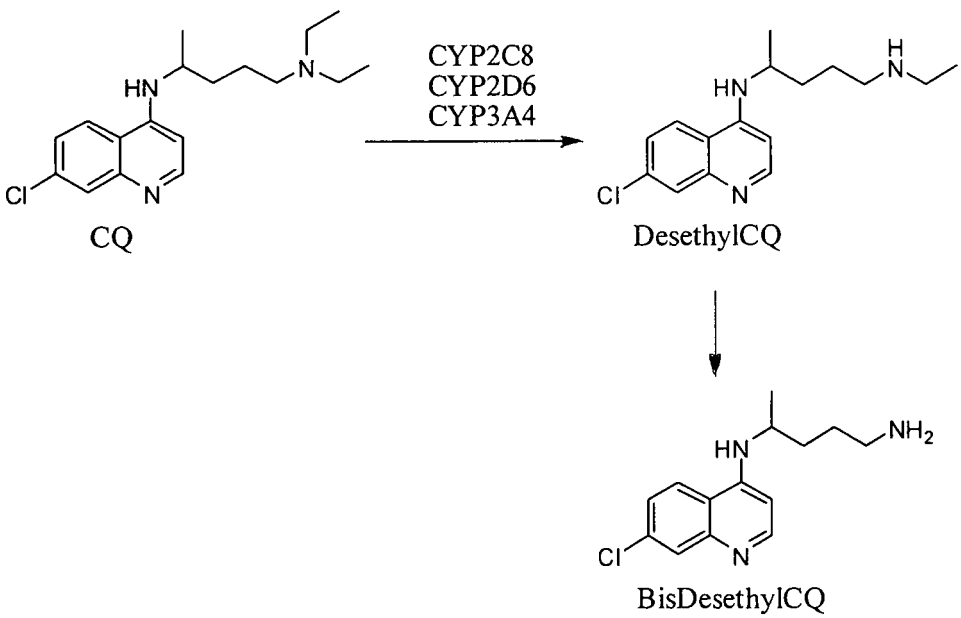

Figure 3.1 Chloroquine (CQ) and desethyl chloroquine *N*-dealkylation pathways in humans (Minzi *et al.*, 2003).

Although CQ is thought to be relatively well tolerated in the treatment of malaria; several cases of ocular toxicity and have been noted with the long-term usage of the drug, for example in patients being treated for rheumatism (Santaella *et al.*, 2007). The basis for this toxicity lies with CQ having a distinct affinity for melanin-containing tissues in pigmented animals such as the iris, skin and hair which can lead to accumulation (Kasuya *et al.*, 1976; Lindquist *et al.*, 1972; Tanaka *et al.*, 2004).

In addition to the ocular toxicity linked to the long-term use of CQ, phospholipidosis is also a concern. Phospholipidosis is a generalised condition in humans and animals that is characterised by the intracellular accumulation of phospholipids and the concurrent development of concentric lamellar bodies (Reasor *et al.*, 2001). There are an abundance of data providing mechanisms for the induction of phospholipidosis; however, the process is likely to be complex and may differ from one drug to another (Hostetler, 1984; Martin *et al.*, 1989; Reasor *et al.*, 2006). Many drugs containing a cationic lipophilic structure are capable of inducing phopholipidosis in cells during *in vivo* administration (Figure 3.2). Drugs with this kind of structure typically contain a hydrophobic moiety, such as an aromatic and/or aliphatic ring structure, which may be halogen substituted and a hydrophilic domain comprising of an amine group (Figure 3.2). CQ and the other 4-aminoquinolines in this study can clearly be seen to have a structural alert, common to that of the drugs shown which are known to induce phospholipidosis, and therefore have potential to cause the disorder (Figure 3.2) (Figure 3.3). Indeed, evidence for of CQ-induced phospholipidosis in the liver has previously been reported in the literature (Harder *et al.*, 1980; Shaikh *et al.*, 1987).

The functional consequences of this biochemical disorder for cellular and tissue function are not yet fully understood and the general consensus is that the condition is an adaptive response rather than a toxicological manifestation; however additional studies are needed. Until this is issue is resolved, concerns about phospholipidosis will continue to exist at regulatory agencies (Reasor *et al.*, 2006).

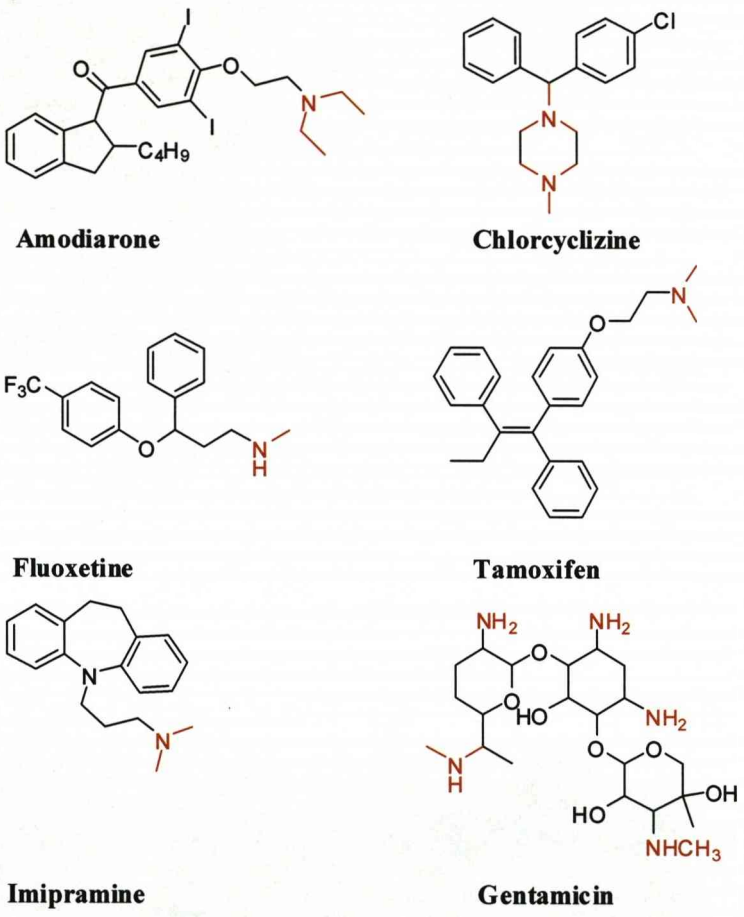

Figure 3.2 Structures of representative drugs that can induce phospholipidosis *in vivo*. The hydrophilic moiety of each molecule has been highlighted in red.

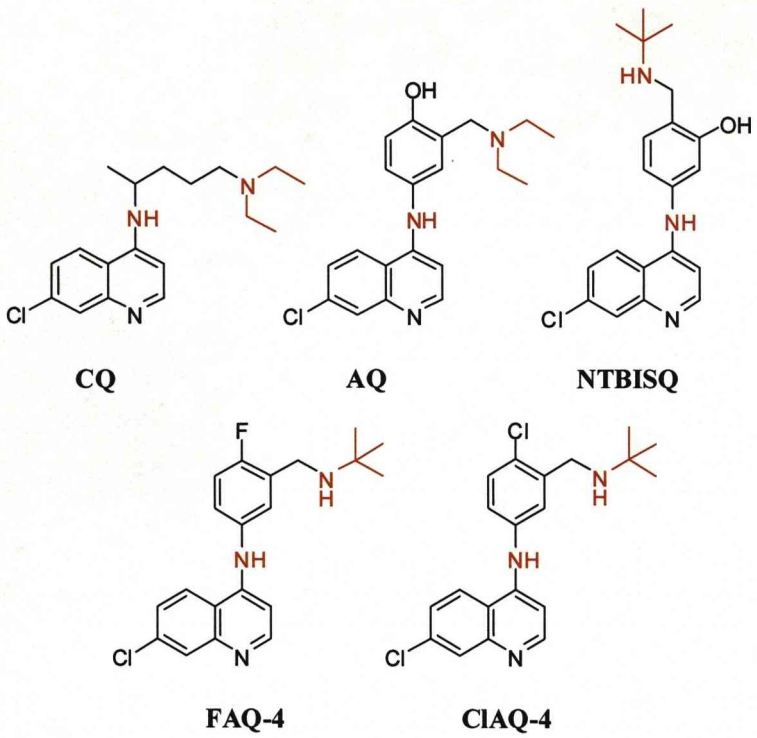

Figure 3.3 Structures of chloroquine (CQ), amodiaquine (AQ), *N-tert* butyl isoquine (NTBISQ), *N-tert* butyl fluoro amodiaquine (FAQ-4) and *N-tert* butyl chloro amodiaquine (ClAQ-4). Structural analogues of chloroquine share the same metabolic alert for potential induction of phospholipidosis.

There has been a great deal of work regarding the *in vivo* metabolic fate of CQ in humans, however relatively little work in rats has been published. We wished to make a direct comparison of the chemical aspects of the metabolism and distribution of AQ and CQ. Therefore the work presented in this chapter is an investigation of the metabolism and distribution of [^{14}C]-CQ in the rat. The results could then be related directly to previous work on the metabolism of [^{3}H]-AQ in rats using exactly the same experimental model (Randle, 2001). In addition it is of interest to compare the metabolic pathways in the rat and man. The rat and human models can then be compared directly in order to assess the validity of the rat model for *in vivo* studies. This work also shows a comparative study of the cytotoxicity of CQ and AQ in rat hepatocytes.

3.2 MATERIALS AND METHODS

3.2.1 Materials

[^{14}C] – CQ (54 mCi/mmol; radiochemical purity by HPLC 98.9 %) was a gift, generously donated by GlaxoSmithkline, (Stevenage, UK). Tissue solubilizer–450 (0.5 N quaternary ammonium hydroxide in toluene) was purchased from Beckmann Chemicals, (Bremen, Germany). Ultima Flo and Ultima Gold scintillant were from Packard Bioscience BV, (Groningen, Netherlands). HPLC grade solvents were products of Fisher Scientific, (Loughborough, Leicestershire, UK). All other chemicals were purchased from Sigma Aldrich Co. (Poole, United Kingdom).

Adult male Wistar rats (200-400 g) were obtained from Charles River (Margate, UK). The protocols described were undertaken in accordance with criteria outlined in a licence granted under the Animals (Scientific Procedures) Act 1986 and approved by the University of Liverpool Animal Ethics Committee.

3.2.2 Methods

3.2.2.1 In Vivo Metabolism of [^{14}C]-CQ in the Rat (5 h)

Adult male Wistar rats (250 -400 g n = 4) were anaesthetised with urethane (1.4 g/mL in isotonic saline; 1 mL/kg, i.p.). Polyethylene cannulae were inserted into the trachea, femoral vein and common bile duct and the penis was ligated. Drug-blank bile was collected for approximately 20 minutes before treatment. [^{14}C]-CQ (54 μmol/kg; 20 μCi/rat) was dissolved in saline (0.5–1 mL depending on animal weight) and was injected over 10 min (*i.v.*). Bile was collected hourly for a time period of 5 h into pre-weighed eppendorfs. Samples were weighed after collection to determine the extent of biliary secretion and stored at –30 °C until analysis by LC-MS.

After 5 h, urine was aspirated from the bladder and transferred to a pre-weighed eppendorf tube and a cardiac puncture was performed. The blood was centrifuged (1000 g, 6 min) and the plasma transferred to a separate tube. The plasma from each experiment was pooled together and then proteins were removed *via* the exhaustive addition of MeOH (5 eq vv) followed by centrifugation (1200 g, 10 min). The supernatant was removed and concentrated by evaporation before re-dissolving it in MeOH (200 μL). The plasma and urine samples were stored at –30 °C until analysis by LC-MS.

Aliquots of bile and urine (30 μL) were mixed with scintillant (4 mL) for determination of radioactivity.

3.2.2.2 LC-MS Analysis of Bile, Urine and Plasma Samples

Aliquots of bile, urine and plasma (100 μL) were analysed at room temperature on a Hypersil 5-μm HyPurity Elite C-18 column (150 × 4.6 mm; Thermo Hypersil-Keystone, Runcorn, Cheshire, UK) with a gradient of acetonitrile (5-40 % over 30 min) in trifluoroacetic acid (0.1 %, v/v). The LC system consisted of two Jasco PU980 pumps (Jasco UK, Great Dunmow, Essex, UK) and a Jasco HG-980-30 mixing module. The flow rate was 0.9 mL/min. Eluate split-flow to the LC-MS interface was ca. 40 μL/min. A Quattro II mass spectrometer (Micromass MS Technologies, Manchester, UK) fitted with the standard co-axial electrospray source was used in the positive-ion mode. Nitrogen was used as the nebulizing and drying gas. The interface temperature was 80 °C; the capillary voltage, 3.9 kV. Spectra were acquired between m/z 100-1050 over a scan duration of 5 s. Fragmentation of analyte ions was achieved at a cone voltage of 50-70 V. Data were processed with MassLynx 3.5 software (Micromass). Radiolabelled analytes in the remainder of the

eluate were detected with a Radiomatic A250 flow detector (Packard, Pangbourne, Berkshire, UK). Eluate was mixed with Ultima-Flo AP scintillant (Packard Bioscience BV, Groningen, Netherlands) at 1 mL/min.

3.2.2.3 In Vivo Retention Studies of [^{14}C]-CQ in the Rat (24 h)

Adult male Wistar rats (200-400 g, n=4) were administered a solution of [^{14}C]–CQ (54 mol/kg; 20 μCi/rat) dissolved in saline (0.5–1 mL; *i.p.*). The animals were then transferred to individual metabolism cages equipped with a well for collecting urine and faeces. The rats were allowed full access to food and drink for a 24 h period before administration of a lethal dose of pentabarbitone.

Aliquots of urine (30 μL) were collected and mixed with scintillant for determination of radioactivity. The collected faeces were weighed and dissolved in distilled water for a period of 16 h before determination of radioactivity using the same method as described earlier (Chapter 3, Section 3.2.2.6). The major organs were then removed and assessed for radioactivity.

3.2.2.4 In Vivo Retention Studies of [^{14}C]-CQ in the Rat (48 h)

Adult male Wistar rats (n = 4) were administered a solution of [^{14}C]–CQ (54 mol/kg; 20 μCi/rat) dissolved in saline (0.5 – 1 mL; *i.p.*). The animals were kept in a normal animal cage for a period of 24 h before they were transferred to individual metabolism cages equipped with a well for collecting urine and faeces. The rats remained in the metabolism cages for a further 24 h, with full access to food and drink, before administration of a lethal dose of pentabarbitone.

Aliquots of urine (30 μL) were collected and mixed with scintillant for determination of radioactivity. The collected faeces were weighed and dissolved in

distilled water for a period of 16 h before determination of radioactivity using the same method as described (Chapter 3, Section 3.2.2.6). The major organs were then removed and assessed for radioactivity.

3.2.2.5 In Vivo Retention Studies of [^{14}C]-CQ in the Rat (168 h)

Adult male Wistar rats (n = 4) were administered a solution of [^{14}C]–CQ (54 mol/kg; 20 μCi/rat) dissolved in saline (0.5 – 1 mL; *i.p.*). The animals were kept in a normal animal cage for a period of 168 h with full access to food and drink before administration of a lethal dose of pentabarbitone. The major organs were then removed and assessed for radioactivity.

3.2.2.6 Tissue Distribution of [^{14}C]–CQ in the Rat

At the end of the relevant time-point (5 h, 24 h, 48 h or 168 h) the animals were sacrificed by a lethal dose of pentabarbitone and the major organs were excised (brain, eyes, heart, lungs, liver, kidneys, spleen, testes and skin) and stored at –30 °C.

Duplicate portions (50–100 mg) of the tissues were weighed and solubilized in tissue solubilizer (0.75 mL) at 50 °C for 16 h. The solutions were decolourised with hydrogen peroxide (200 μL) over 1 h and then neutralised using glacial acetic acid (30 μL) before leaving in the darkness for 16 h to prevent chemoluminescence. Ultima Gold scintillant (10 mL) was added before the radioactivity was determined by scintillation counting.

3.2.2.7 Cytotoxicity of [^{14}C]–CQ in Isolated Rat Hepatocytes

Male Wistar rats (200 - 250g) (n = 3) were terminally anaesthetised with pentobarbitone sodium (90mg/kg in isotonic saline *i.p.*). Hepatocytes were isolated using a two-step collagenase perfusion method adapted from that of Guguen-Guillouzo *et al* (Guguen-Guillouzo *et al.*, 1986). The abdomen was opened and the liver cannulated through the portal vein using a gauge catheter. Before perfusion, the heart was removed to allow free loss of perfusion buffers. The liver was washed with calcium-free HEPES buffer for 10 mins at a flow rate of 40ml/min. The liver was then perfused with digestion buffer, a mixture of wash buffer with 5 % $CaCl_2$ solution, for 6 – 10 mins. The digested tissue was then excised and placed in a Petri dish containing wash buffer and DNAase (0.1 % w/v). The tissue was anchored and the Glison's capsule was disrupted and disturbed to release the cells. The cell suspension was filtered through gauze to eliminate cell debris, blood and sinusoidal cells. The cells were washed three times in DNAase wash buffer before re-suspending in incubation buffer (HEPES buffer and $MgSO_4.7H_20$ (0.25 % w/v)). Cell viability was then assessed microscopically using the trypan blue exclusion test.

The cells were then incubated with various concentrations of either CQ or AQ for a period of 6 hours before determining cell viability in the presence of test compound using the trypan blue exclusion test.

3.2.2.8 Statistical Analysis

All results are expressed as mean ± standard error of the mean (SEM). Values to be compared were analysed for non-normality using a Shapiro-Wilk test. Student t-tests were used when normality was indicated. A Mann-Whitney U test was used for non-parametric data. For analysis of sets of data with variance, a 1-way

analysis of variance (ANOVA) test was used for parametric data and a Kruskell-Wallis test was used for non-parametric data. All calculations were performed using StatsDirect statistical software, results were considered to be significant when $P < 0.05$.

3.3 RESULTS AND DISCUSSION

3.3.1. LC-MS Analysis of *In Vivo* Metabolites of [^{14}C]-CQ in the Rat

Following *i.v.* administration of [^{14}C]-CQ (54 μmol/kg, 20 μCi), the recovery over 0 – 5 h in bile was 1.84 ± 0.26 % and in urine 6.99 ± 1.43 % of the dose.

[^{14}C]-CQ was excreted mainly as the parent compound, **II,** in urine [retention time (Rt) 14.14 min] and comprised 74.63 ± 1.33 % of the total radioactive metabolites produced during urinary excretion (Figure 3.4).

Two other urinary metabolites were identified by LC-MS analysis, which located co-eluting pairs of chlorine isotope peaks in the positive-ion mass chromatograms for *m/z* 292 and 336 [metabolites **I** (Rt 12.52 min) and **III** (Rt 16.77 min) respectively] (Figures 3.5 and 3.6). It was deduced that metabolite **I** was the desethyl analogue of CQ comprising 5.97 ± 2.67 % of the metabolites eliminated (Figure 3.5A). Metabolite **III** was found to be an oxygenated version of the parent compound ($[M+1+16]^+$) comprising 19.40 ± 3.29 % of the total metabolites eliminated. Inspection of the fragmentation pattern of **III** revealed that oxygenation had occurred within the quinoline ring, rather than the amine side chain, leading to the assumption that the *N*-oxide had been formed (Figure 3.6B) (Figure 3.11).

A common fragment seen in all spectra was loss of the amine side-chain, represented by loss of 73 atomic mass units (amu) (Figure 3.6).

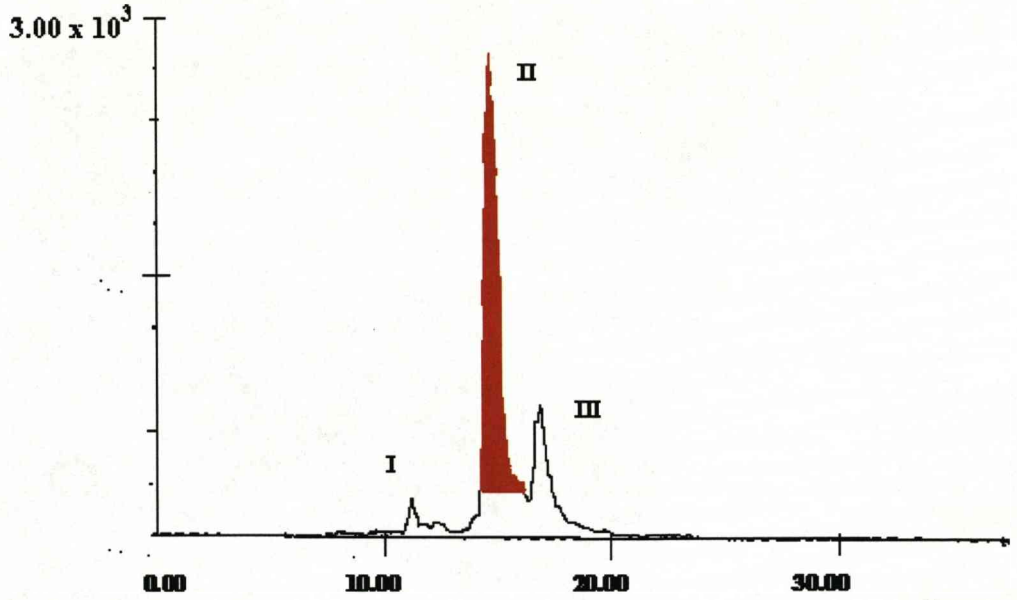

Figure 3.4 HPLC radiochromatogram of the urinary metabolites of [^{14}C]-CQ (54 µmol/kg, 20 µCi; 1 h collection) where **I** represents an unknown minor metabolite, possibly desethylCQ, the shaded peak, **II** represents the parent compound and **III** represents CQ *N*-oxide.

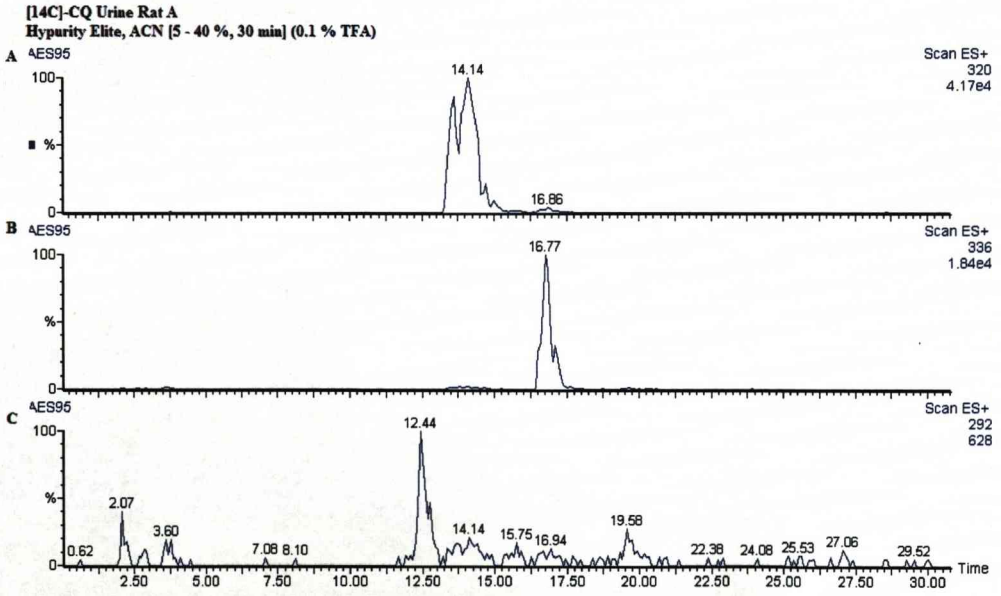

Figure 3.5 Positive-ion electrospray mass chromatograms corresponding to (A) *m/z* 320[^{14}C]-CQ (parent compound) *m/z* 292**, (B)** *m/z* 336, [^{14}C]-CQ-*N*-oxide and **(C)** [^{14}C]-desethylCQ excreted in the urine of male Wistar rats 5 h after dosing *i.v.* with [^{14}C]-CQ (54 µmol/kg, 20 µCi).

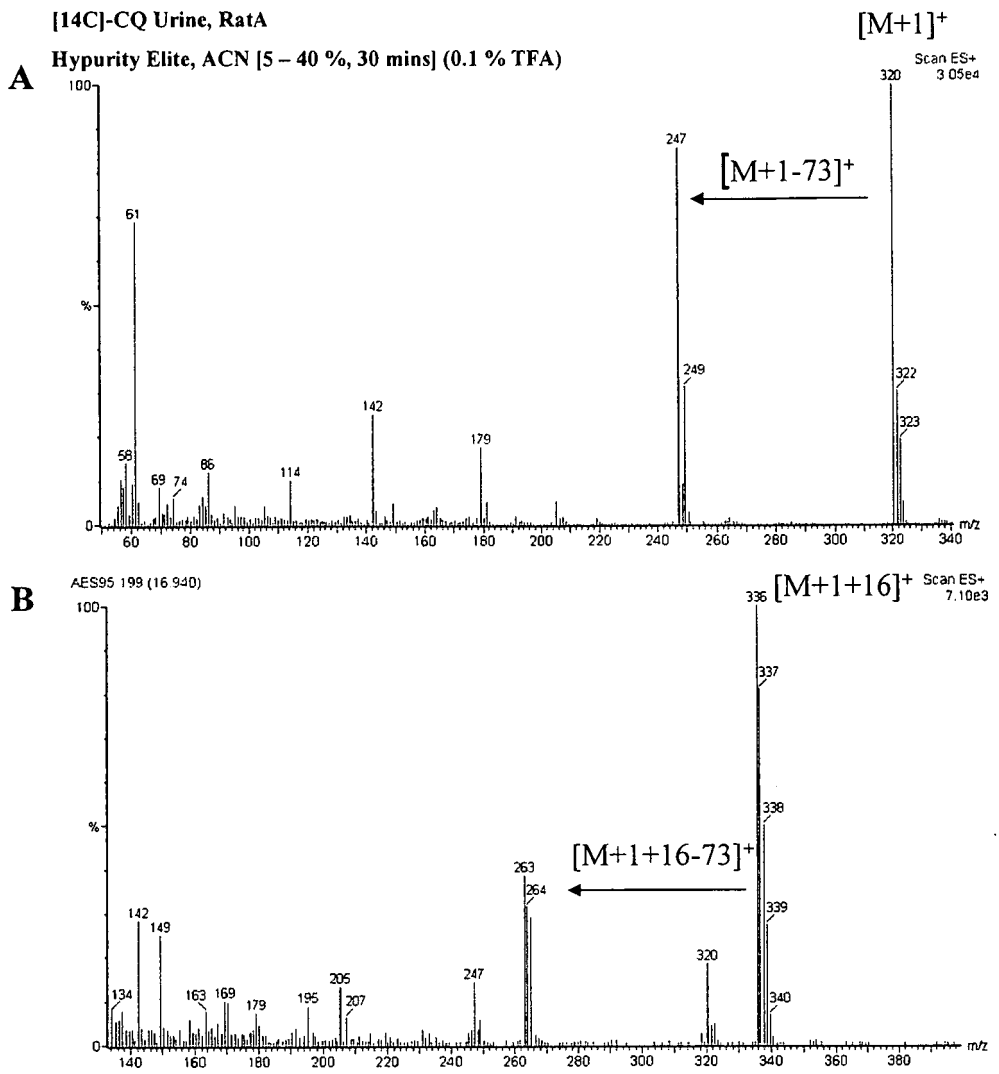

Figure 3.6 Positive-ion electrospray mass spectra showing the fragmentation of (A) [^{14}C]-CQ eluted as parent compound and **(B)** [^{14}C]-CQ as its *N*-oxide excreted in the urine of male, Wistar rats 5 h after dosing *i.v.* with [14C]-CQ (54 μmol/kg, 20 μCi).

In the bile, two major metabolites and one minor metabolite were resolved by HPLC (Figure 3.7). The major metabolites were determined by LC-MS analysis. Co-eluting pairs of chlorine isotope peaks in the positive-ion mass chromatograms for *m/z* 320 and *m/z* 336 were identified. The peak of *m/z* 320, metabolite **II** was identified as parent compound (CQ, Rt 17.62 min) (Figure 3.8B). This was seen together with the fragment *m/z* 247 which represented loss of the diethylamino side-

chain (Figure 3.9A). Metabolite **III** (Rt 19.41 min) was found to be common to both bile and urine and was an oxygenated metabolite of CQ of *m/z* 336 (Figure 3.8A). The fragmentation pattern of the oxygenated species **III** indicated that the *N*-oxide had been formed as loss of the amino side-chain did not result in the tandem loss of oxygen (Figure 3.8B). The minor metabolite **IV** could not be identified as it was not sufficiently abundant to yield diagnostic fragments by cone-voltage fragmentation in the source of the mass spectrometer. The main route of elimination in bile was *N*-oxidation with metabolite **III** being observed to make up 67.94 ± 10.56 % of the total radioactive products. The parent compound **II** was found to comprise 30.33 ± 6.23 % of the total metabolites formed whilst the unknown, **IV**, comprised less than 2 % of the dose eliminated (Table 3.1).

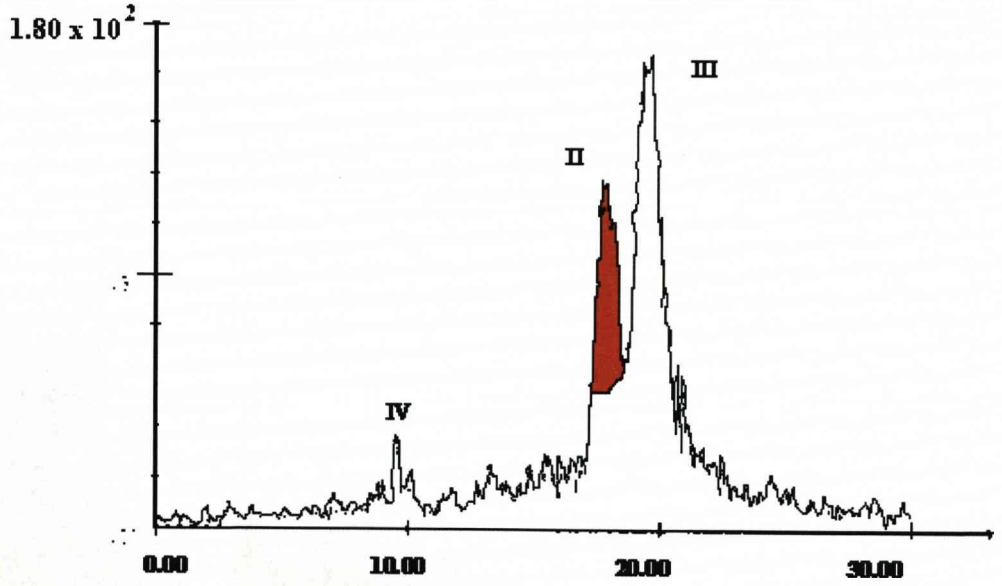

Figure 3.7 HPLC radiochromatogram of the biliary metabolites of [^{14}C]-CQ (54 µmol/kg, 20 µCi; 1 h collection) where II represents the parent compound, III represents CQ *N*-oxide and IV represents an unknown minor metabolite.

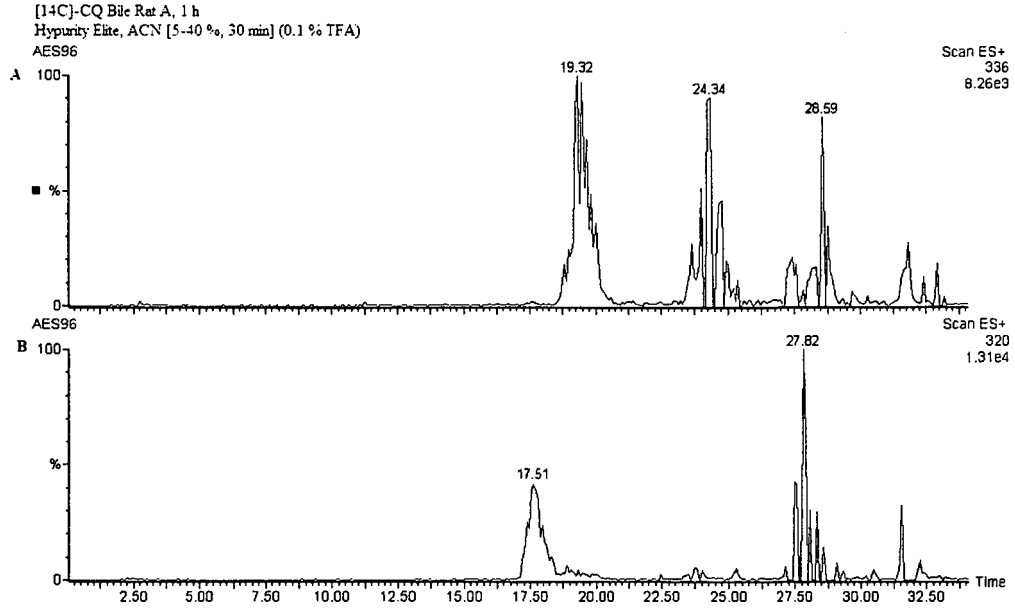

Figure 3.8 Positive-ion electrospray mass chromatograms corresponding to (A) *m/z* 336, [^{14}C]-CQ-*N*-oxide metabolite and (B) *m/z* 320 [^{14}C]-CQ (parent compound) excreted in the bile of male Wistar rats dosed *i.v.* with [^{14}C]-CQ (54 µmol/kg, 20 µCi).

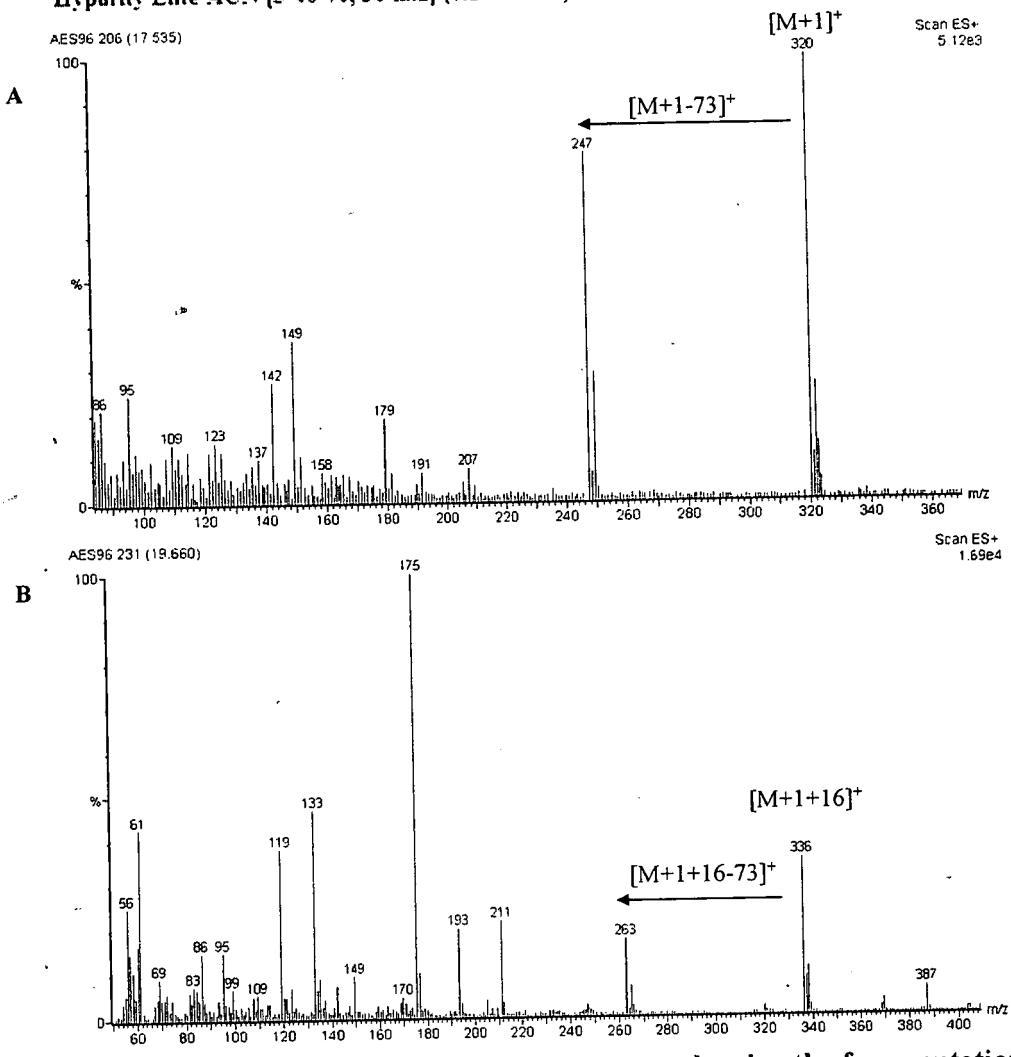

Figure 3.9 Positive-ion electrospray mass spectra showing the fragmentation of (A) [^{14}C]-CQ eluted as parent compound and (B) [^{14}C]-CQ as its *N*-oxide excreted in the bile of male, Wistar rats dosed *i.v.* with [^{14}C]-CQ (54 µmol/kg, 20 µCi, 1 h).

A notable feature of the chromatograms of the metabolites produced in bile was the later retention times in relation to analogous peaks eluted in urine and also that of the chromatogram produced for the [^{14}C]-CQ standard (Figures 3.10A-C) (Table 3.1). For example, CQ eluted at around 14 minutes in urine, however in bile it eluted at a retention time of almost 18 minutes. This shift in retention time could

not be explained and it was assumed that some form of interaction between the metabolites of CQ and the endogenous components of bile had occurred

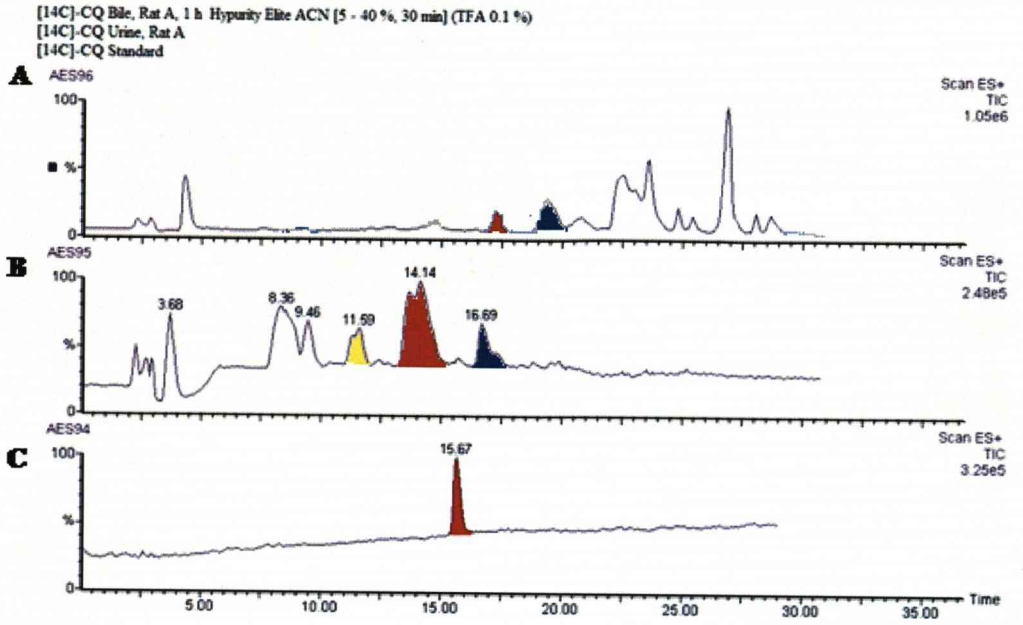

Figure 3.10 Positive-ion electrospray mass chromatograms showing the total ion current for (A) peak-shifted metabolites in bile, (B) metabolites in urine excreted by the male, Wistar rats dosed i.v. with [^{14}C]-CQ (54 µmol/kg, 20 µCi) and (C) parent compound eluting at 15.67 minutes. The red colour represents [^{14}C]-CQ, blue represents [^{14}C]-CQ *N*-oxide, whilst yellow represents desethylCQ.

As previously described (Section 3.1), CQ is metabolised in humans by the *N*-dealkylation pathway, to desethyl CQ and bisdesethyl CQ by cytochrome P450. The major constitutive P450 isoforms involved in the dealkylation process are CYP2C8, CYP3A4/5 and CYP2D6 (Kim *et al.*, 2003; Li *et al.*, 2003; Projean *et al.*, 2003). Rats, however, do not share all of these same isoforms. For example, in rats six isoforms of CYP2D have been identified by genomic analysis CYP2D1, CYP2D2, CYP2D3, CYP2D4, CYP2D5,CYP2D18 but not CYP2D6 (Gonzalez, 1996; Nelson *et al.*, 1996). This may explain why we tend to see *N*-oxidation rather than dealkylation as the major metabolic pathway in rats.

Peak	Retention Time (min)	*m/z*	Metabolite Identity	Metabolite proportion (% of radiolabeled metabolites, 0-1 h)
I	12.52	292	desethylCQ	5.97 ± 2.67 %
II	14.14 (urine), 17.62 (bile)	320	CQ	74.63 ± 1.33 %, 30.33 ± 6.23 %
III	16.77 (urine), 19.41 (bile)	336	CQ-*N*-oxide	19.40 ± 3.21 %, 67.94 ± 10.96 %
IV	9.75	ND	ND	1.73 ± 0.26 %

Table 3.1 Peak numbers of metabolites correspond to the radiochromatographic analysis of bile and urine from rats dosed *i.v.* with [^{14}C]-CQ (54 µmol/kg, 20 µCi). Metabolites were characterised by LC-MS. ND = No data.

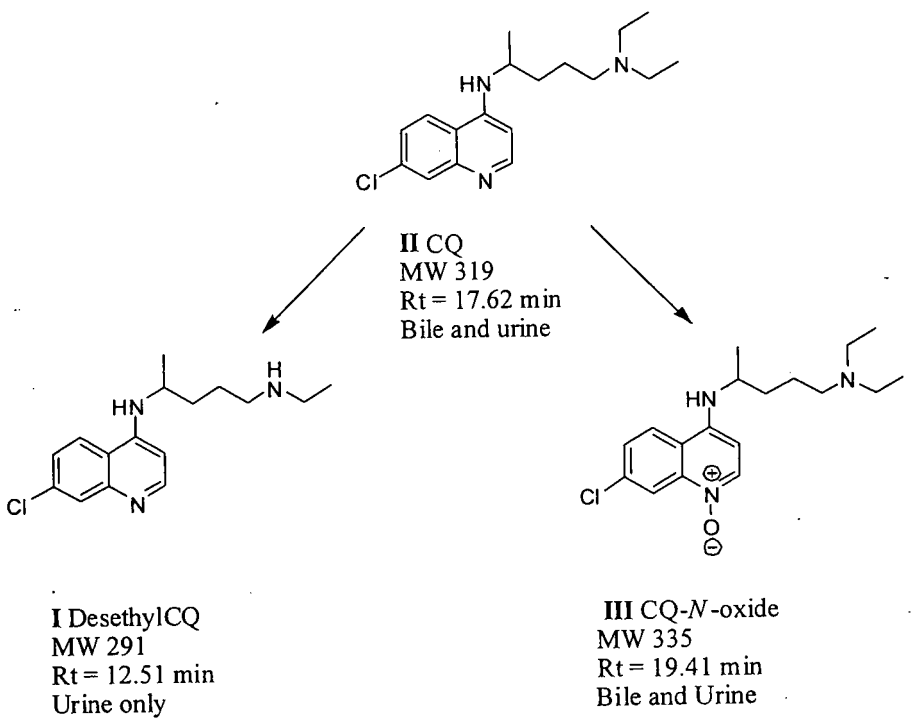

Figure 3.11 Urinary and biliary metabolites excreted by the male, Wistar rat after dosing with [^{14}C]-CQ (54 µmol/kg, 20 µCi).

Similarly to CQ, AQ is metabolised mainly to its desethyl analogue in humans. However, in contrast it also undergoes bioactivation to a quinone imine metabolite which is detoxified *via* glutathione conjugation (Harrison *et al.*, 1992;

Ruscoe *et al.*, 1994). Previous studies in the group, using an identical experimental protocol to that used here, have generated data on the metabolism of AQ in rats (Randle, 2001).

After dosing male, Wistar rats with [^{3}H]-AQ (54 μmol/kg, 5 μCi/rat) over 5 hours, four peaks could be seen in the radiochromatogram representing the metabolic composition of urine. These peaks represented the formation of four metabolites (Figure 3.12). The major metabolite present in urine was the parent compound (*m/z* 356) (78.05 ± 12.01 % of the radioactive metabolites) which was seen together with the fragment *m/z* 283 representing loss of the side-chain. A small amount of desethylAQ (*m/z* 328) was also recovered in urine (6.34 ± 2.11 %) as well as a benzoic acid analogue (*m/z* 317; 14.63 ± 2.31 % of metabolites excreted in urine). Finally, a small amount of a mercapturate analogue of desthylAQ was found (m/z 489, 0.98 ± 0.11 %).

In bile, only one metabolite could be resolved, the glutathione conjugate of AQ (*m/z* 661) (Figure 3.12).

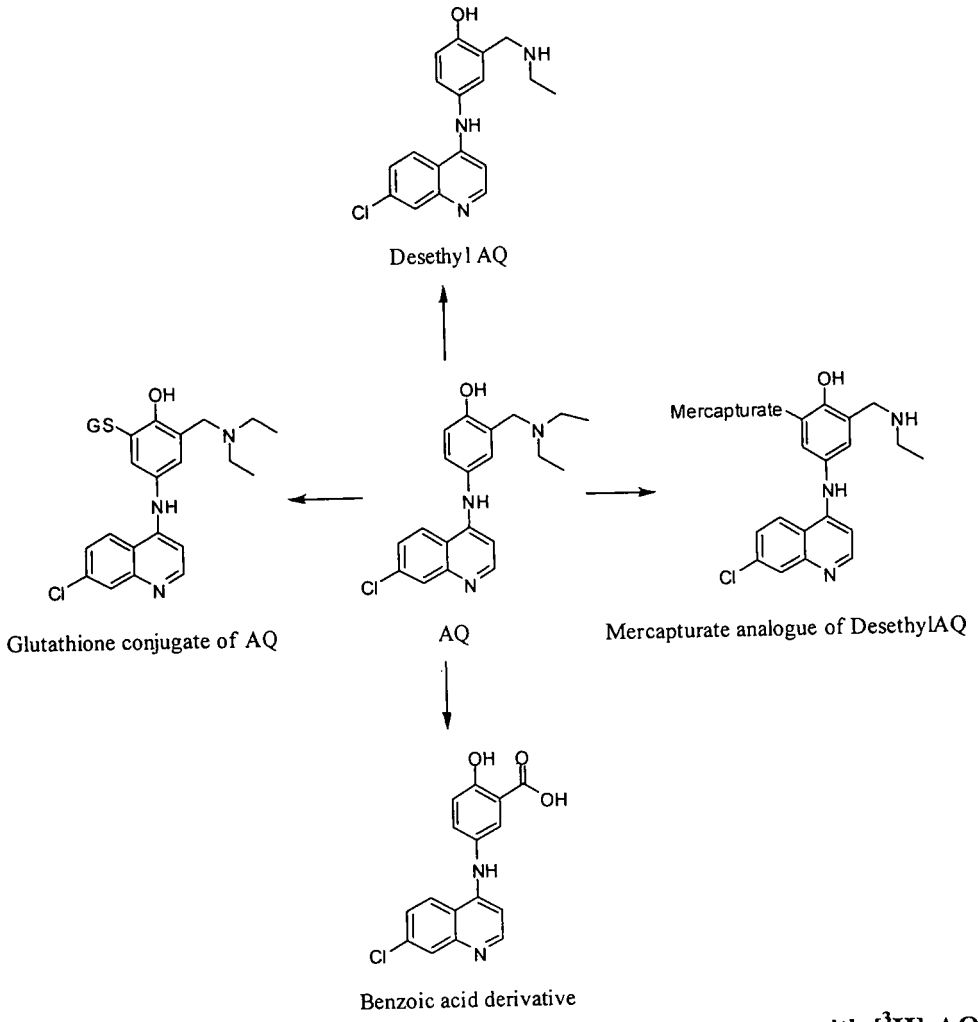

Figure 3.12 Metabolic Scheme for AQ, 5 h after dosing rats with [^{3}H]-AQ (54 µmol/kg, 5 µCi/rat), with suggested metabolites as proposed by a study performed at the University of Liverpool (Randle, 2001).

3.3.1.1 Conclusions

The metabolic profile of [^{14}C]-CQ in rats was deduced. The route of metabolism proved to be fairly simple, with CQ being excreted mainly as the parent compound in the urine. The main route of metabolism of [^{14}C]-CQ was been found to be *N*-oxidation, as recovered in both bile and urine. There was a small amount of dealkylated metabolite in the urine, and potentially in the bile also, however, the spectrum proved to be too poorly resolved in order to determine the accuracy of this statement. Not only was the resolution of the biliary spectrum extremely poor, the

retention times of the peaks representing the metabolites were shifted to higher time-points. We can only assume that the endogenous components of bile were causing this change in retention time.

Introduction of a phenyl ring system into the CQ structure, (AQ), led to a more complex metabolic profile in rats. A small amount of desethylAQ was recovered in the urine; however this was not the major route of metabolism as in humans. The major metabolite after dosing with AQ was a glutathione conjugate, which is thought to be the detoxified adduct of AQ quinone imine in humans (Naisbitt *et al.*, 1996). It appeared that the phenyl ring of AQ leads to a compound much more susceptible to undergo chemical reactions inside the body. Rather than simple dealkylation or oxidation as with CQ, we have also seen conjugation reactions involving glutathione and mercapturic acid.

CQ is mainly excreted as the parent compound in humans; this was mirrored in our studies in the rat. However, in man, the main route of metabolism of CQ is dealkylation (as mentioned Section 4.1), whereas in rat we saw mainly *N*-oxidation and only a small amount of de-ethylation.

3.3.2 Tissue Distribution of [^{14}C]-CQ and [^{3}H]-AQ in the Rat

Five hours after administration of a single dose of [^{14}C]-CQ to cannulated rats 46.99 ± 4.45 % of the dose could be accounted for in the organs, bile and urine (Figure 3.13). Of this, 35.64 ± 2.47 % was found in the organs alone. The largest proportion of this dose was found to be in the liver (19.25 ± 1.27 %), followed by the skin (9.03 ± 0.84 %) and the kidneys (4.42 ± 1.31 %). Minor levels of radioactivity were detected in the brain, heart, lungs, spleen and testis (less than 1.54 %). More than 50 % of the radioactive dose was unaccounted for after 5 h. Under acidic

conditions, CQ can become protonated to its membrane-impermeable form and is then unable to cross the gut wall. This lends to the possibility that the majority of the unaccounted dose remained in the gastro-intestinal tract due to accumulation.

On comparison with the results generated 5 hours after dosing with [^{3}H]-AQ, a similar pattern of distribution in the tissues was observed (Figure 3.14). The amount of radioactivity retained in the kidneys was significantly greater in rats dosed with [^{3}H]-AQ than in those dosed with [^{14}C]-CQ (4.42 ± 1.31 % versus 9.45 ± 1.31 % respectively) ($p = 0.046$). This was also true when comparing the excretion of drug in bile, whereby significantly more drug was excreted 5 hours after administration after dosing with [^{3}H]-AQ than [^{14}C]-CQ (16.13 ± 1.97 % versus 1.87 ± 0.26 % respectively) ($p = 0.017$).

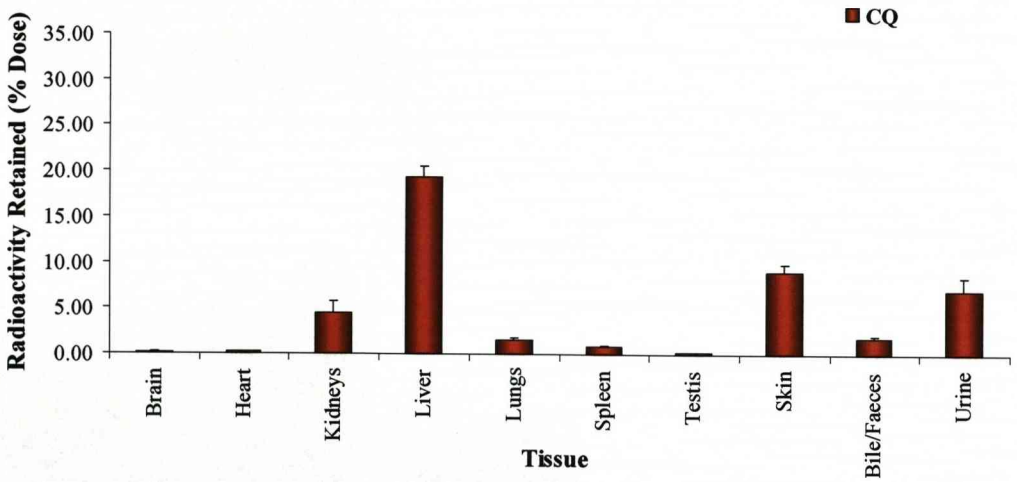

Figure 3.13 Percentage of radioactive dose recovered in tissues 5 h, after administration of [^{14}C]–CQ (54 µmol/kg, 20 µCi/rat) to male Wistar rats (n = 4). Results are expressed as mean percentage of dose ± SEM.

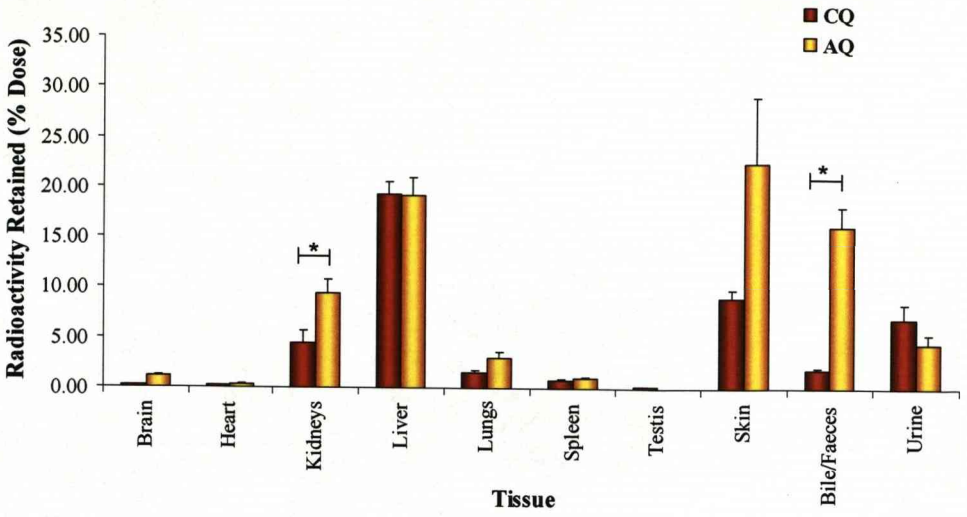

Figure 3.14 Percentage of radioactive dose recovered in tissues 5 h, after administration of [^{14}C]-CQ and [^{3}H]-AQ (54 µmol/kg, 20 µCi/rat) to male Wistar rats (n = 4). Results are expressed as mean percentage of dose ± SEM. Statistics were performed using a one way ANOVA test for parametric data and Kruskal Wallis test for non-parametric data. *P<0.05, **P<0.01, ***P<0.001

In order to investigate the possibility of accumulation of [^{14}C]-CQ in the rat after a single dose, the experimental time-point was increase to 24 h and beyond (Figures 3.15 and 3.16).

Twenty-four hours after dosing with [^{14}C]-CQ the total dose accounted for was 61.46 ± 6.71 % with very little retention of radioactivity detected in any of the major organs (Figure 3.15). There still remained a typical pattern of distribution, with the largest proportion of radioactivity located in the liver (5.45 ± 0.71 %), however excretion of radiolabelled material by both biliary and urinary routes increased significantly ($p = 0.0286$ and $p = 0.0105$ respectively). In all, excretion by these routes was greater than 56 % of the total dose (biliary 34.40 ± 9.05 %; urinary 22.45 ± 3.97 %). The distribution in tissues after dosing with [^{3}H]-AQ was highly comparative with that after dosing with [^{14}C]-CQ (Figure 3.15). The only significant difference lay with the percentage of radioactivity retained in the skin, whereby 1.81

± 0.21 % of the dose remained in the skin of rats dosed with [^{14}C]-CQ and 6.34 ± 1.40 % remained in rats dosed with [^{3}H]-AQ (p = 0.0464).

Forty-eight hours after administration of [^{14}C]-CQ to rats, the radioactivity in all major organs was negligible aside from the liver and skin which retained only 2.95 ± 0.11 % and 1.39 ± 0.22 % of the dose respectively (Figure 3.16). The total amount of radioactivity retained in the organs was 5.16 ± 0.42 % of the dose. More than 45 % of the dose was eliminated in the faeces (47.55 ± 0.53 %) with renal elimination containing 27.33 ± 0.52 % of the total administrated dose.

After seven days, the amount of [^{14}C]-CQ remaining in the tissues was negligible and there were no signs of retention of the drug.

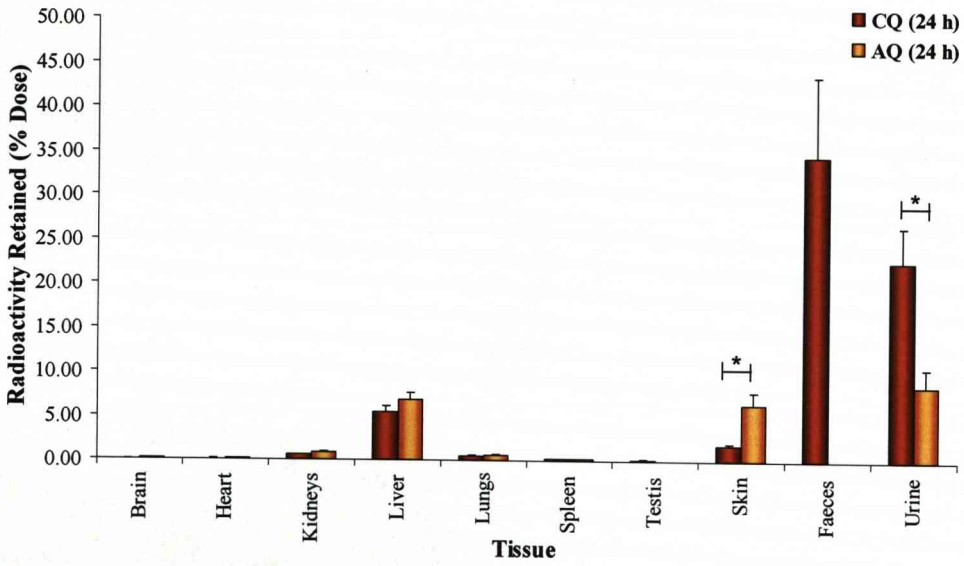

Figure 3.15 The percentage of radioactive dose recovered in tissues 24 h, after administration of [^{14}C]–CQ and [^{3}H]-AQ (54 µmol/kg, 20 µCi/rat) to male Wistar rats (n = 4). Results are expressed as mean percentage of dose ± SEM. Unpaired t-test for parametric data and Mann-Whitney test for non-parametric data. *P<0.05, **P<0.01, ***P<0.001

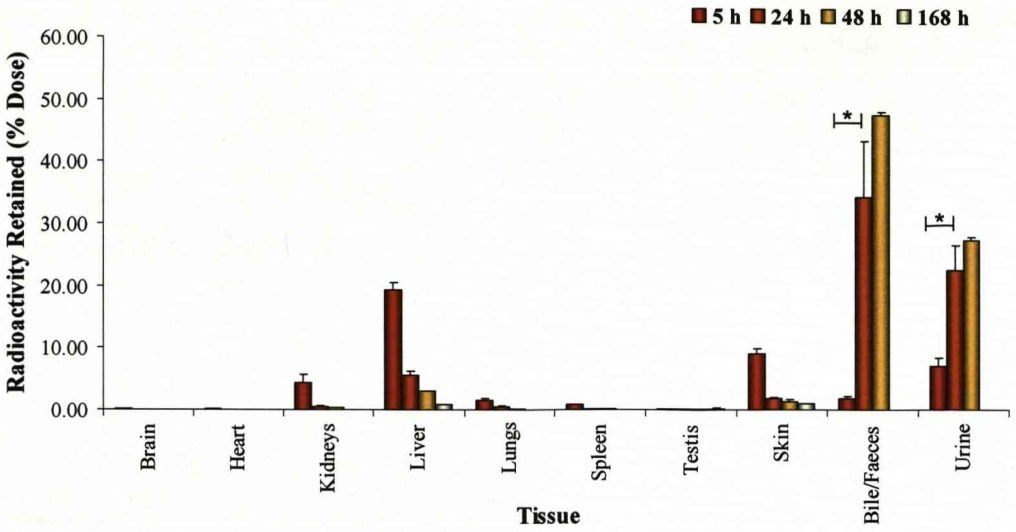

Figure 3.16 The percentage of radioactive dose recovered in tissues, 5 h, 24 h, 48 h and 168 h, after administration of [^{14}C] – CQ (54 μmol/kg, 20 μCi/rat) to male Wistar rats (n = 4). Results are expressed as mean percentage of dose ± SEM. Unpaired t-test for parametric data and Mann-Whitney test for non-parametric data. *P<0.05, **P<0.01, ***P<0.001

3.3.2.1 Conclusions

After dosing with [^{14}C]-CQ (54 μmol/kg, 20 μCi) the majority of drug was found to be in liver and skin of rats. This was not an unexpected result solely on the basis of tissue size and the role of the liver in drug metabolism. There appeared to be relatively little excretion in urine and bile after 5 hours, although this increased to almost 75 % of the dose after 48 h. After 7 days less than 2.5 % remained in the body.

The results showed that the incorporation of a phenyl ring into the CQ side-chain made little difference to the pattern of distribution of the drug in the rat after administration of an identical dose. In general, the pattern of distribution tended to be identical in animals dosed with CQ and AQ, despite the fact they had radically different routes of metabolic clearance. It appeared that the two compounds enter the same tissues of the body regardless of any structural differences. The rate of clearance of total products was also seen to be similar for both CQ and AQ. There

was, however, significantly more radioactivity distributed in the kidneys after dosing with AQ and also a significant difference in the amount of biliary excretion (more than 8 times the amount of radioactivity was excreted in the bile of rats dosed with AQ than those dosed with CQ).

3.3.3 Cytotoxicity of CQ and AQ in Isolated Rat Hepatocytes

Rat hepatocytes, isolated using a two-step collagen digestion method (Section 3.2.2.7) were incubated with CQ or AQ at concentrations of 0, 20, 50, 100, 200 and 500 μM (Figure 3.17) Results were expressed as the percentage of viable cells, measured microscopically, using a trypan blue exclusion test (as a percentage of the control). After incubation with CQ, it can clearly be seen that there was no effect on cell viability until the concentration of drug reached 200 μM, whereby there was a 30 % decrease in cell viability. This was in contrast to the results shown with AQ, a drug known to cause hepatoxicity in humans. After incubation with AQ the results showed a marked decrease in cell viability at 100 μM (30.72 ± 21.49 %) and saw that at 200 μM only 12.77 ± 10.75 % of the cells remained viable. The results for CQ and AQ, at 200 μM, were shown to be significant ($p = 0.0046$). After incubation with 500 μM of CQ and AQ, there was a highly significant difference between the effect of the two drugs on the liver cells ($p = 0.0002$). Of the cells treated with CQ, 40.57 ± 0.18 % of the cells remained viable, compared with complete cell death after incubation with AQ.

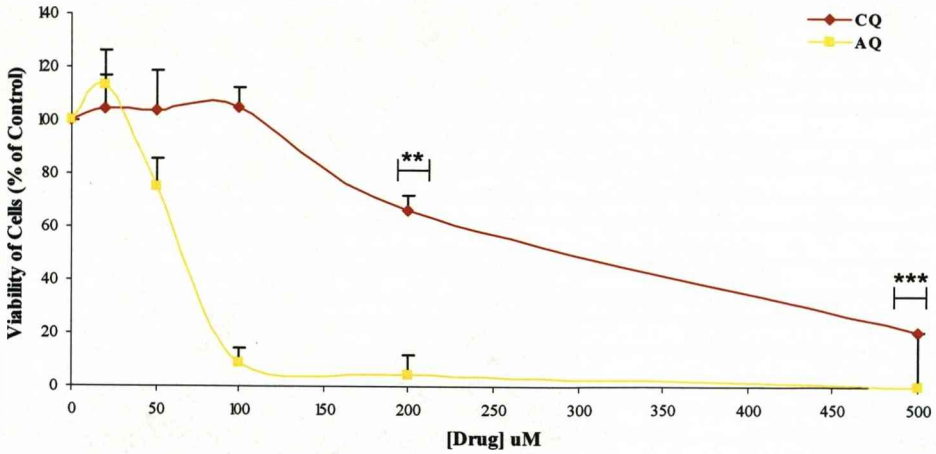

Figure 3.17 Viability of male, Wistar rat hepatocytes, incubated for 6 h with various concentrations of CQ and AQ, and stained with Trypan blue dye as an indicator for cell death. Results are expressed as mean percentage of dose ± SEM. Statistics were performed using a one way ANOVA test. *P<0.05, **P<0.01, ***P<0.001

3.3.3.1 Conclusions

This study showed unequivocally that CQ was less toxic in rat hepatocytes than AQ, a known causative agent of hepatoxicity in man, at concentrations ranging from 0 – 500 μM. The 4-aminophenol structure of AQ has led to decrease of Tox_{50} from greater than 300 μM with CQ to 70 μM. Combined with the knowledge of the presence of a glutathione conjugate excreted in bile, it is possible that this toxicity, as in man, is due to the electrophilic AQ quinone imine.

These findings suggest that this could be a useful study to compare the relative toxicities of novel compounds in the 4-aminoquinoline series (Chapters 4 and 5).

3.3.4 Conclusion

The full metabolic and distributional profile of [^{14}C]-CQ in rats has been defined, with the main route of metabolism being identified as *N*-oxidation and the main areas of accumulation being the liver and skin.

The results of this work have provided data that can be used to begin to build an overall structure metabolism relationship profile for the 4-aminoquinolines antimalarials.

In addition to this, we will now be able to directly compare the information generated in this chapter with that from *N-tert* butyl isoquine (NTBISQ), *N-tertiary* butyl fluoro amodiaquine (FAQ-4) and *N-tert* butyl chloro amodiaquine (ClAQ-4) in the forthcoming chapters (Chapters 4 and 5). This will lead to a full investigation on how structural alteration of these molecules affects the pathway of metabolism inside the rat and also the distribution and rate of clearance.

3.4 REFERENCES

ADEMOWO, O., SODEINE, O. & WALKER, O. (2000). The disposition of chloroquine and its main metabolite desethylchloroquine in volunteers with and without chloroquine-induced pruritus: Evidence for decreased chloroquine metabolism in volunteers with pruritis. *Clinical Pharmacology and Therapeutics*, **67,** 237-241.

ADEROUNMU, A. (1984). In vitro assessment of the antimalarial activity of chloroquine and its major metabolites. *Annals of Tropical Medicine and Parasitology*, **78,** 581-585.

GUGUEN-GUILLOUZO, C. & GUILLOUZO, A. (1986). *Methods for preparation of adult and fetal hepatocytes, isolated and cultured hepatocytes*. Paris: INSERM and John Libbey Eurotext.

GUSTAFSSON, L., WALKER, O., ALVAN, G., BEERMANN, B., ESTEVEZ, F., GLEISNER, L., LINDSTROM, B. & SJOQVIST, F. (1983). Disposition of chloroquine in man after single intravenous and oral doses. *British Journal of Clinical Pharmacology*, **15,** 471-479.

HARDER, A., KOVATCHEV, S. & DEBUCH, H. (1980). Interactions of chloroquine with different glycerophospholipids. *Hoppe-Seyler's Zeitschrift fur Physiologie Chemie*, **361,** 1847-1850.

HARRISON, A., KITTERINGHAM, N., CLARKE, J. & PARK, B. (1992). The mechanism of bioactivation and antigen formation of Amodiaquine in the rat. *Drug Metabolism and Dispostion*, **43,** 1421-1430.

HELLGREN, U., KIHAMIA, C., MAHIKWANO, L., BJORKMAN, A., ERIKSSON, O. & ROMBO, L. (1989). Response of Plasmodiaum falciparum to chloroquine treatment: relation to whole blood concentrations of chloroquine and desethylchloroquine. *Bulletin of the World Health Organisation*, **87,** 197-202.

HOSTETLER, K. (1984). Molecular studies of the induction of cellular phospholipidosis by cationic amphiphilic drugs. *Federation proceedings: official publication of the Federation of American Societies for Experimental Biology*, **43,** 2582-2585.

KASUYA, Y., MIYATA, H. & WATANABE, M. (1976). Toxicoloical studies on the chloroquine-melanin affinity in vivo and in vitro in relation to the chloroquine retinopathy. *Journal of Toxicological Science*, **1**.

LINDQUIST, N. & ULLBERG, S. (1972). The melanin affinity of chloroquine and chlorpromazine studies by whole body auto-radiography. *Acta Pharmacologica et Toxicologica*, **31 (suppl. II),** 3-32.

MARTIN, W., KACHEL, D., VILEN, T. & NATARAJAN, V. (1989). Mechanism of phospholipidosis in amiodarone pulmonary toxicity. *Journal of Pharmacology and Experimental Therapeutics*, **251,** 272-8.

MCCHESNEY, E., FASCO, M. & BANKS, W. (1967). The metabolism of chloroquine in man during and after repeated oral dosage. *Journal of Pharmacology and Experimental Therapeutics*, **158,** 323-331.

MINZI, O., RAIS, M., SVENSSON, J., GUSTAFSSON, L. & ERICSSON, O. (2003). High-performance liquid chromatographic method for determination of amodiaquine, chloroquine and their monodesethyl metabolites in biological samples. *Journal of Chromatography B*, **783,** 473-480.

NAISBITT, D., RUSCOE, J., WILLIAMS, D., O'NEILL, P., PIRMOHAMED, M. & PARK, B. (1996). Disposition of amodiaquine and related antimalarial agents in human neutrophils: Implications for drug design. *The Journal of Pharmacology and Experimental Therapeutics*, **280,** 884-893.

PROJEAN, D., BAUNE, B., FARINOTTI, R., FLINOIS, J.-P., BEAUNE, P., TABURET, A.-M. & DUCHARME, J. (2003). In vitro metabolism of chloroquine: Identification of CYP2C8, CYP3A4 and CYP2D6 ad the main isoforms catalysing N-desethylchloroquine formation. *Drug Metabolism and Disposition*, **31,** 748-754.

RANDLE, L. (2001). The metabolism of isoquine, a new 4-aminoquinoline antimalarial. In *Pharmacology and Thereapeutics*. pp. 46. Liverpool: University of Liverpool.

REASOR, M., HASTINGS, K. & ROGER, G. (2006). Drug-induced phospholipidosis: issues and future directions. *Expert Opinion on Drug Safety*, **5,** 567-583.

REASOR, M. & KACEW, S. (2001). Drug-induced phospholipidosis: Are there functional consequences? *Experimental Biology and Medicine*, **226,** 825-830.

RUSCOE, J., JEWELL, H., MAGGS, J., O'NEILL, P., STORR, R., WARD, S. & PARK, B. (1994). The effect of chemical substitution on the metabolic activation, metabolic detoxication, and pharmacological activity of amodiaquine in the mouse. *The Journal of Pharmacology and Experimental Therapeutics*, **273,** 393-404.

SANTAELLA, R. & FRAUNFELDER, F. (2007). Ocular adverse effects associated with systemic medications. *Drugs*, **67,** 75-93.

SHAIKH, N., DOWNER, E. & BUTANY, J. (1987). Amiodarone - an inhibitor of phospholipase activity: a comparartive study of the inhibitory effects of amiodarone, chloroquine and chlorpromazine. *Molecular and Cellular Biochemistry*, **76,** 163-172.

TANAKA, M., TAKASHINA, H. & TSUTSUMI, S. (2004). Comparative assessment of ocular tissue distribution of drug-related radioactivity after chronic oral administration of 14C-levofloxacin and 14C-chloroquine in pigmented rats. *Journal of Pharmacy and Pharmacology*, **56,** 977-983.

CHAPTER 4

THE METABOLISM AND DISTRIBUTION OF THE NOVEL 4-AMINOQUINOLINE - *N-TERT* BUTYL ISOQUINE

CONTENTS

4.1 INTRODUCTION

This chapter describes a formal study on the metabolism and distribution of *N*-tert butyl isoquine (NTBISQ), a rationally designed novel 4- aminoquinoline.

As discussed in Chapter 1, the universal utility of the 4-aminoquinoline drugs chloroquine (CQ) and amodiaquine (AQ) has been eroded to the point of therapeutic uselessness due to resistance and toxicity (Hatton *et al.*, 1986; Macomber *et al.*, 1966; Neftel *et al.*, 1986).

Drug-design studies have led to the formation of regioisomers of AQ, e.g. isoquine (ISQ), where interchange of the amino side-chain and the hydroxyl group have created a more stable amino phenol template (O'Neill *et al.*, 2003). Substitution of the diethyl group of ISQ with a *tert* butyl gives the potentially, metabolically more stable analogue, NTBISQ. NTBISQ has been selected as the lead candidate to go forward for further pre-clinical studies. This selection was based on the cost-effective and facile chemical synthesis of the compound, as well as its potent antimalarial properties (IC_{50} 13.2 ± 3.2 nM against the K1 CQ–resistant strain of *P. falciparum*) and promising pharmacokinetic data (Table 4.1) (Chapter 2). NTBISQ was noted to have excellent activity against all strains of malaria tested with no evidence of cross-resistance between sub-species of parasite. Its half-life ($T_{1/2}$) was found to be less than 15 h across all four species tested. This compared favourably to that of CQ, the half-life of which has been noted to be approximately 275 hours, which could be a contributing factor to the development of resistance by malaria parasites (Gustafsson *et al.*, 1983). This shorter half-life may offer a significant advantage in terms of the opportunity to combine with an artemisinin-based drug. The oral bioavailability (F %) of NTBISQ across all species tested was greater than 89 % indicating that almost all of the drug can enter the systemic circulation after

oral dosing. Blood clearance levels of NTBISQ were found to be moderate across all species.

Species	$T_{1/2}$ (h)	F (%)	Blood Clearance (mL/min/kg)
Mouse	3.3 ± 1.2	100	17.2
Rat	7.9 ± 4.3	89 ± 12	25.9 ±4.9
Dog	14.2 ± 3.1	92 ± 13	6.39 ± 1.57
Monkey	9.0 ± 4.2	100	14.5 ± 0.7

Table 4.1 Summary of pharmacokinetic data of NTBISQ in animals. Data was obtained from pre-clinical, pharmacokinetic studies at GlaxoSmithKline, Tres Cantos, Spain. Data are expressed as mean ± SD (n = 3).

The original lead compound ISQ was shown to be excreted mainly as the parent compound in the urine of rats. In bile, the main metabolite was found to be a glucuronide of the carboxylic acid (Scheme 4.2). In a similar way to AQ, ISQ was observed to undergo dealkylation, however; it is incapable of forming the toxic quinone imine adduct (Scheme 4.1). ISQ also undergoes glucuronidation and oxidation to its carboxylic acid *in vivo*, in rats. The absence of an ISQ-glutathione conjugate indicates that the bioactivation seen with AQ has been blocked (O'Neill et al., 2003).

It was proposed that the *N-tert* butyl analogue, NTBISQ will share this enhanced metabolic stability of ISQ and will not undergo bioactivation to form the toxic quinone imine metabolite seen with AQ. The aim of this work was to explore the metabolism and distribution of NTBISQ and to compare the results with ISQ and AQ. Of particular interest was the potential impact of the N-*tert* butyl group on simplifying the metabolic profile of the original lead compound, ISQ. Previous work has demonstrated that this molecule undergoes multiple routes of metabolism as depicted in scheme 4.2. The susceptibility of the *N*-diethylamino group to metabolic cleavage is partly responsible for the poor bioavailability of ISQ (Chapter 1).

This chapter examines the metabolic fate of chemically synthesised [^{3}H]-NTBISQ *in vivo*, in the rat (chemical and radiochemical syntheses described in Chapter 2). In addition to this, the distribution of [^{3}H]-NTBISQ in the rat was investigated, and the effects of time and dose were explored. The results of this work were compared to those of [^{3}H]-ISQ from a previous study which utilised exactly the same experimental model (Randle, 2001)).

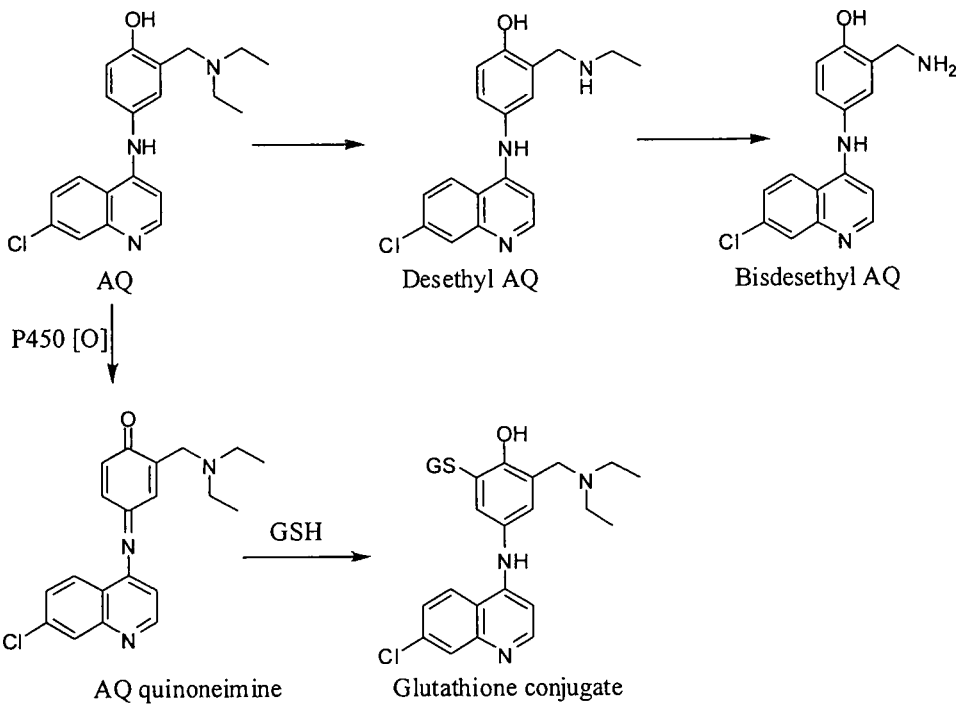

Scheme 4.1 AQ *N*-dealkylation pathways and the P450 oxidation of AQ to the toxic quinone imine, followed by conjugation to glutathione in humans. (Hombhanje et al., 2004; O'Neill et al., 1998)

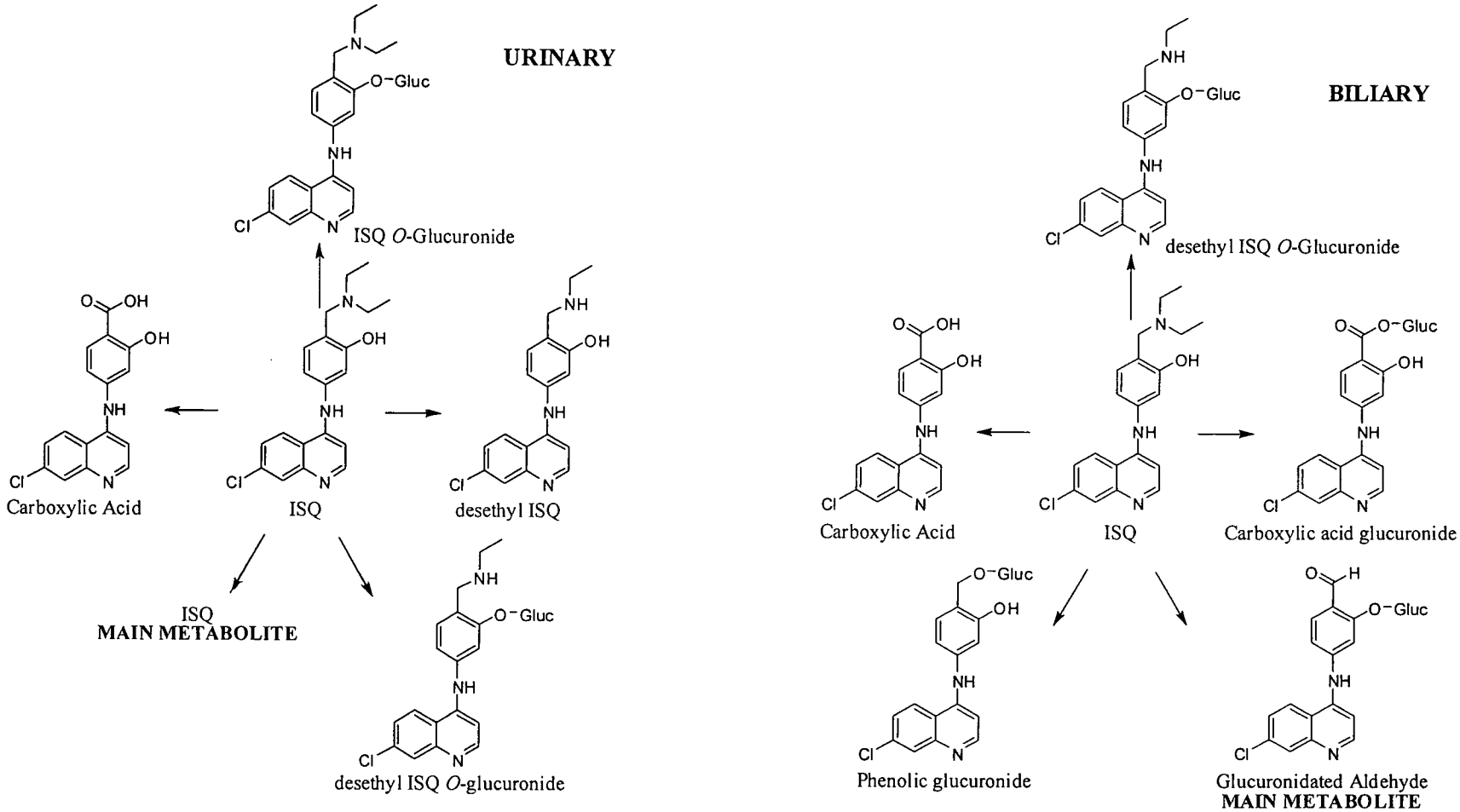

Scheme 4.2 The urinary and biliary metabolites of ISQ in the rat (O'Neill *et al.*, 2003)

4.2 MATERIALS AND METHODS

4.2.1 Materials

[^{3}H]-NTBISQ (4.6 μCi/mmol; radiochemical purity by HPLC greater than 98 %) was prepared via a 1-step synthesis described previously, (Chapter 2, Section 2.2.2.12). Tissue solubilizer–450 (0.5 N quaternary ammonium hydroxide in toluene) was purchased from Beckmann Chemicals, (Bremen, Germany). Ultima Flo and Ultima Gold scintillant were from Packard Bioscience BV, (Groningen, Netherlands). HPLC grade solvents were products of Fisher Scientific, (Loughborough, Leicestershire, UK). All other chemicals were purchased from Sigma Aldrich Co. (Poole, United Kingdom).

All data for ISQ was taken from a study by LE Randle, (Department of Pharmacology, The University of Liverpool) (Randle, 2001) (O'Neill *et al.*, 2003).

Adult male Wistar rats (200-400 g) were obtained from Charles River (Margate, U.K.). The protocols described were undertaken in accordance with criteria outlined in a licence granted under the Animals (Scientific Procedures) Act 1986 and approved by the University of Liverpool Animal Ethics Committee.

4.2.2 Methods

4.2.2.1 In Vivo Metabolism of [^{3}H]-NTBISQ in the Rat (5 h)

Adult male Wistar rats (250 - 400 g n = 4) were anaesthetised with urethane (1.4 g/mL in isotonic saline; 1 mL/kg, i.p.). Polyethylene cannulae were inserted into the trachea, femoral vein and common bile duct and the penis was ligated. Drug-blank bile was collected for approximately 20 minutes before treatment. [^{3}H]-NTBISQ (54 μmol/kg; 20 μCi/rat or 216 μmol/kg; 20 μCi/rat) was dissolved in saline (0.5–1 mL depending on animal weight and dose) and was injected over 10 min

(*i.v.*). Bile was collected hourly for a time period of 5 h into pre-weighed Eppendorf tubes. Samples were weighed after collection to determine the extent of biliary secretion and stored at –30 °C until analysis by LC-MS.

After 5 h, urine was aspirated from the bladder and transferred to a pre-weighed Eppendorf tube and a cardiac puncture was performed. The blood was centrifuged (1000 g, 6 min) and the plasma transferred to a separate tube. The plasma from each experiment was pooled together and then blood proteins were removed by the exhaustive addition of MeOH (5 eq vv) followed by centrifugation (1200 g, 10 min). The supernatant was removed and concentrated by evaporation before re-dissolving it in MeOH (200 μL). The plasma and urine samples were stored at –30 °C until analysis by LC-MS.

Aliquots of bile and urine (30 μL) were mixed with scintillant (4 mL) for determination of radioactivity.

4.2.2.2 LC-MS Analysis of Bile, Urine and Plasma Samples

Aliquots of bile, urine and plasma (100 μL) were analysed at room temperature on a Hypersil 5-μm HyPurity Elite C-18 column (150 × 4.6 mm; Thermo Hypersil-Keystone, Runcorn, Cheshire, UK) with a gradient of acetonitrile (10-50 % over 30 min) in trifluoroacetic acid (0.1 %, v/v). The LC system consisted of two Jasco PU980 pumps (Jasco UK, Great Dunmow, Essex, UK) and a Jasco HG-980-30 mixing module. The flow rate was 0.9 mL/min. Eluate split-flow to the LC-MS interface was ca. 40 μL/min. A Quattro II mass spectrometer (Micromass MS Technologies, Manchester, UK) fitted with the standard co-axial electrospray source was used in the positive-ion mode. Nitrogen was used as the nebulizing and drying gas. The interface temperature was 80 °C; the capillary voltage, 3.9 kV. Spectra

were acquired between m/z 100 - 1050 over a scan duration of 5 s. Fragmentation of analyte ions was achieved at a cone voltage of 50-70 V. Data were processed with MassLynx 3.5 software (Micromass). Radiolabelled analytes in the remainder of the eluate were detected with a Radiomatic A250 flow detector (Packard, Pangbourne, Berkshire, UK). Eluate was mixed with Ultima-Flo AP scintillant (Packard Bioscience BV, Groningen, Netherlands) at 1 mL/min.

4.2.2.3 Tissue Distribution of [^{3}H]–NTBISQ in the Rat

At the end of the relevant time-point (5 h, 24 h, 48 h, 168 h or 240 h) the animals were killed by a lethal dose of pentabarbitone and the major organs were excised (brain, eyes, heart, lungs, liver, kidneys, spleen, testes and skin) and stored at –30 °C.

Duplicate portions (50 – 100 mg) of the tissues were weighed and solubilized in tissue solubilizer (0.75 mL) at 50 °C for 16 h. The solutions were decolourised with hydrogen peroxide (200 µL) over 1 h and then neutralised using glacial acetic acid (30 µL) before leaving in the darkness for 16 h to prevent chemoluminescence. Ultima Gold scintillant (10 mL) was added before the radioactivity was determined by scintillation counting.

4.2.2.4 In Vivo Retention Studies of [^{3}H]-NTBISQ in the Rat (24 h)

Adult male Wistar rats (200 - 400 g, n = 4) were administered a solution of [^{3}H]–NTBISQ (54 µmol/kg; 20 µCi/rat) dissolved in saline (0.5 – 1 mL; *i.p.*). The animals were then transferred to individual metabolism cages equipped with a well for collecting urine and faeces. The rats were allowed food and drink *ad libitum* for a 24 h period before administration of a lethal dose of pentabarbitone.

Aliquots of urine (30 μL) were collected and mixed with scintillant for determination of radioactivity. The collected faeces were weighed and dissolved in distilled water for a period of 16 h before determination of radioactivity using the same method as described earlier (Chapter 4, Section 4.2.2.3). The major organs were then removed and assessed for radioactivity.

4.2.2.5 In Vivo Retention Studies of [^{3}H]-NTBISQ in the Rat (48 h)

Adult male Wistar rats (n = 4) were administered a solution of [^{3}H]–NTBISQ (54 μmol/kg; 20 μCi/rat) dissolved in saline (0.5 – 1 mL; *i.p.*). The animals were kept in a normal animal cage for a period of 24 h before they were transferred to individual metabolism cages equipped with a well for collecting urine and faeces. The rats remained in the metabolism cages for a further 24 h, with full access to food and drink, before overdose using pentabarbitone.

Aliquots of urine (30 μL) were collected and mixed with scintillant for determination of radioactivity. The collected faeces were weighed and dissolved in distilled water for a period of 16 h before determination of radioactivity using the same method as described earlier (Chapter 4, Section 4.2.2.3). The major organs were then removed and assessed for radioactivity.

4.2.2.6 In Vivo Retention Studies of [^{3}H]-NTBISQ in the Rat (168 h and 240 h)

Adult male Wistar rats (n = 4) were administered a solution of [^{3}H]–NTBISQ (54 μmol/kg; 20 μCi/rat) dissolved in saline (0.5 – 1 mL; *i.p.*). The animals were kept in a normal animal cage for a period of 168 h or 240 h with full access to food and drink before administration of a lethal dose of pentabarbitone. The major organs were then removed and assessed for radioactivity.

4.2.2.7 Cytotoxicity of NTBISQ and ISQ in Isolated Rat Hepatocytes

Male Wistar rats (200 - 250g) (n = 3) were terminally anaesthetised with pentobarbitone sodium (90mg/kg in isotonic saline *i.p.*). Hepatocytes were isolated using a two-step collagenase perfusion method adapted from that of Guguen-Guillouzo *et al* (Guguen-Guillouzo *et al.*, 1986). The abdomen was opened and the liver cannulated through the portal vein using a gauge catheter. Before perfusion, the heart was removed to allow free loss of perfusion buffers. The liver was washed with calcium-free HEPES buffer for 10 mins at a flow rate of 40ml/min. The liver was then perfused with digestion buffer, a mixture of wash buffer with 5 % $CaCl_2$ solution, for 6 – 10 mins. The digested tissue was then excised and placed in a Petri dish containing wash buffer and DNAase (0.1 % w/v). The tissue was anchored and the Glison's capsule was disrupted and disturbed to release the cells. The cell suspension was filtered through gauze to eliminate cell debris, blood and sinusoidal cells. The cells were washed three times in DNAase wash buffer before re-suspending in incubation buffer (HEPES buffer and $MgSO_4.7H_20$ (0.25 % w/v)). Cell viability was then assessed microscopically using the trypan blue exclusion test.

The cells were then incubated with various concentrations of either NTBISQ or ISQ for a period of 6 hours before determining cell viability in the presence of test compound using the trypan blue exclusion test.

4.2.2.8 Statistical Analysis

All results are expressed as mean ± standard error of the mean (SEM). Values to be compared were analysed for non-normality using a Shapiro-Wilk test. Student t-tests were used when normality was indicated. A Mann-Whitney U test was used for non-parametric data. For analysis of sets of data with variance, a 1-way

analysis of variance (ANOVA) test was used for parametric data and a Kruskell-Wallis test was used for non-parametric data. All calculations were performed using StatsDirect statistical software, results were considered to be significant when $P < 0.05$.

4.3 RESULTS AND DISCUSSION

4.3.1. LC-MS Analysis of *In Vivo* Metabolites of [^{3}H]-NTBISQ in the Rat

Following *i.v.* administration of [^{3}H]-NTBISQ (54 μmol/kg, 20 μCi) to rats the total recovery of radioactivity in urine was 2.77 ± 0.32 % of the dose administered. Only one peak was resolved by HPLC (Figure 4.1). This was identified by LC-MS analysis, which located co-eluting pairs of chlorine isotope peaks in the positive-ion mass chromatogram for *m/z* 356 (**I**, parent compound) (Figure 4.2B). The parent compound eluted at Rt = 13.03 mins, viewed together with *m/z* 300 (loss of the *tert* butyl group) and appeared to be the only detectable metabolite in urine (Figures 4.2A and 4.3).

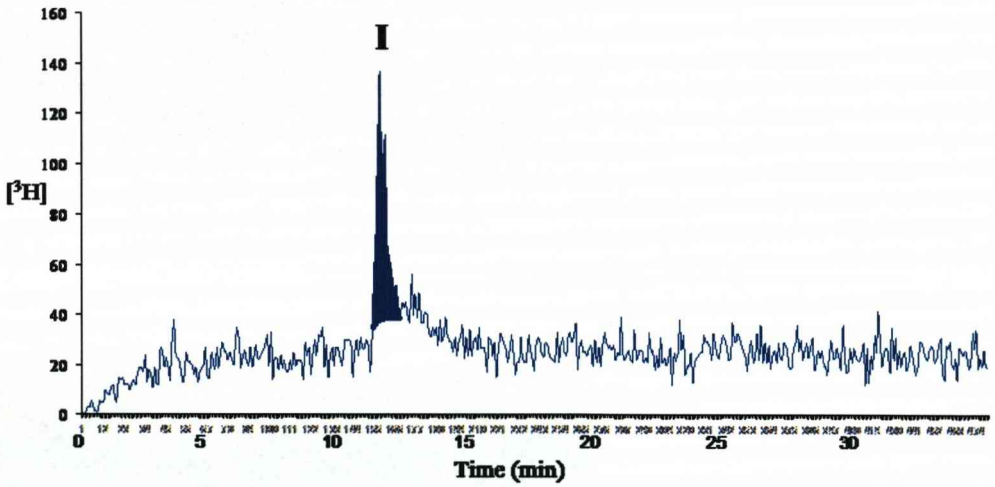

Figure 4.1 HPLC radiochromatogram of the urinary metabolite of found in male Wistar rats, after dosing with [^{3}H]-NTBISQ (54 μmol/kg, 20 μCi). The shaded peak **I** represents the parent compound.

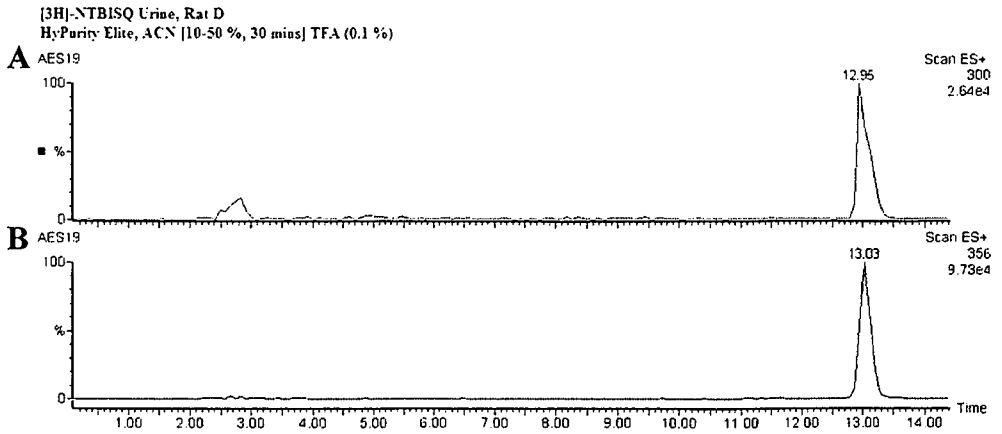

Figure 4.2 Positive-ion electrospray mass chromatograms corresponding to [^{3}H]-NTBISQ. (**A**) representation of the fragmentation of the *tert* butyl side-chain (*m/z* 300), (**B**) *m/z* 356 (parent compound) excreted in the urine of male Wistar rats 5 h after dosing *i.v.* with [^{3}H]-NTBISQ (54 μmol/kg, 20 μCi).

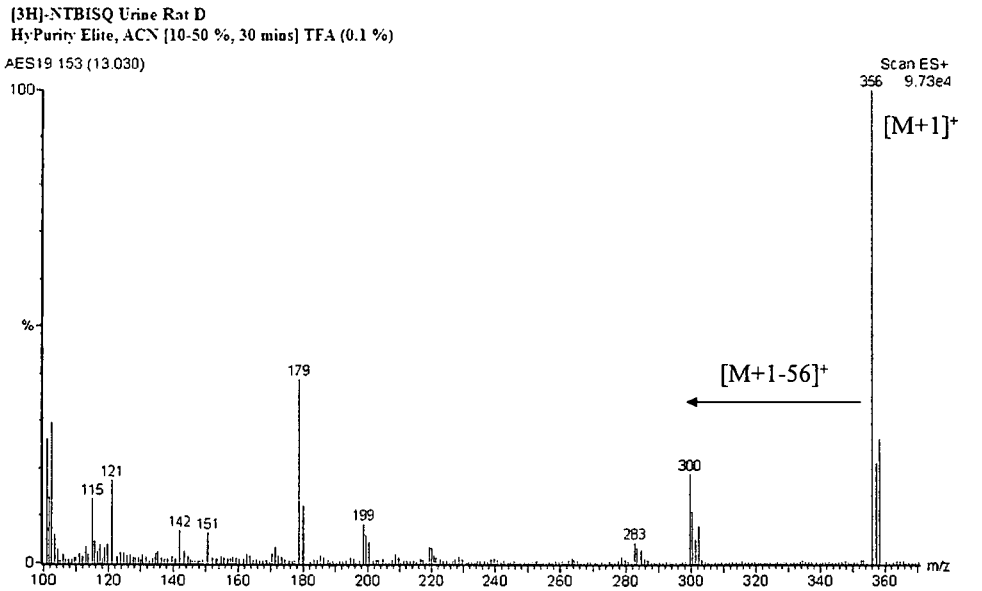

Figure 4.3 Positive-ion electrospray mass spectrum showing the fragmentation of [^{3}H]-NTBISQ excreted in the urine of male, Wistar rats, as parent compound, 5 h after dosing *i.v.* with [^{3}H]-NTBISQ (54 μmol/kg, 20 μCi).

In bile, one peak was observed by HPLC following *i.v.* administration of [^{3}H]-NTBISQ (54 μmol/kg, 20 μCi) (Figure 4.4). The *O*-glucuronide of NTBISQ was identified by LC-MS analysis which located co-eluting pairs of chlorine isotopes in the positive-ion mass chromatogram for *m/z* 532 (**II**) (Figure 4.5). The metabolite recognized as $[M+1+176]^+$ (Figure 4.6) eluted at Rt = 10.74 mins. The metabolite comprised 89.88 ± 2.31 % of the metabolites formed and it was thought that conjugation of glucuronic acid had occurred with the phenolic group of NTBISQ (Scheme 4.3). The glucuronide metabolite was not present in drug-free bile.

A small peak eluting at Rt = 13.03 mins was also observed in the HPLC trace for rat bile. This was in too small quantities to be located in the LC-MS trace; however it was thought to be representative of the parent compound.

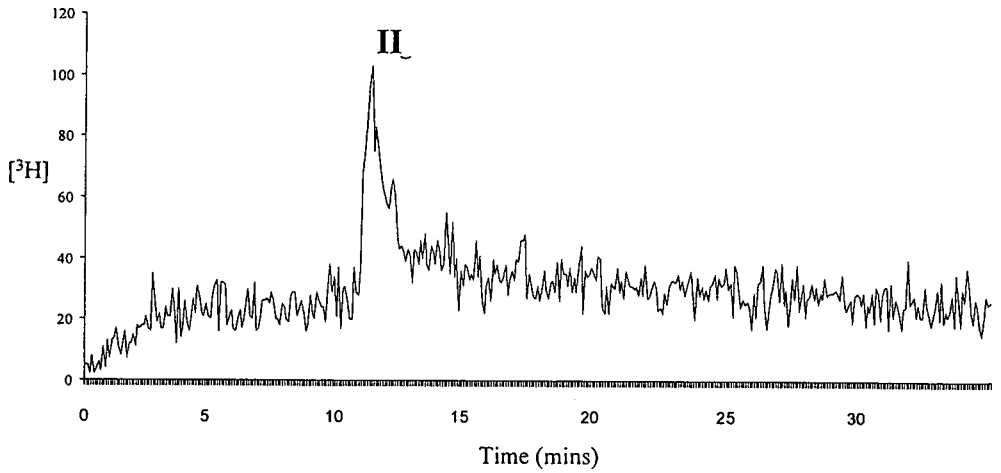

Figure 4.4 HPLC radiochromatogram of the biliary metabolite found in male Wistar rats, after dosing with [^{3}H]-NTBISQ (54 μmol/kg, 20 μCi, 2 h collection). II represents a phenolic glucuronide of the parent compound.

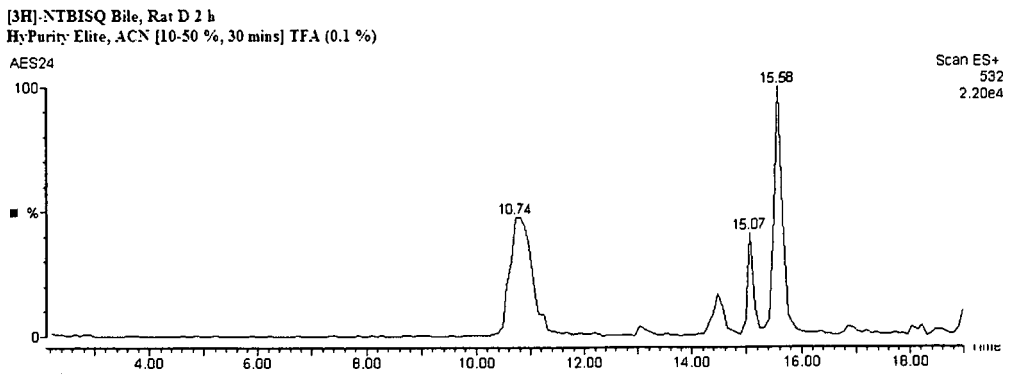

Figure 4.5 Positive-ion electrospray mass chromatogram corresponding to [^{3}H]-NTBISQ-*O*-glucuronide (m/z 532) excreted in the bile of male Wistar rats after dosing *i.v.* with [^{3}H]-NTBISQ (54 μmol/kg, 20 μCi, 2 h collection).

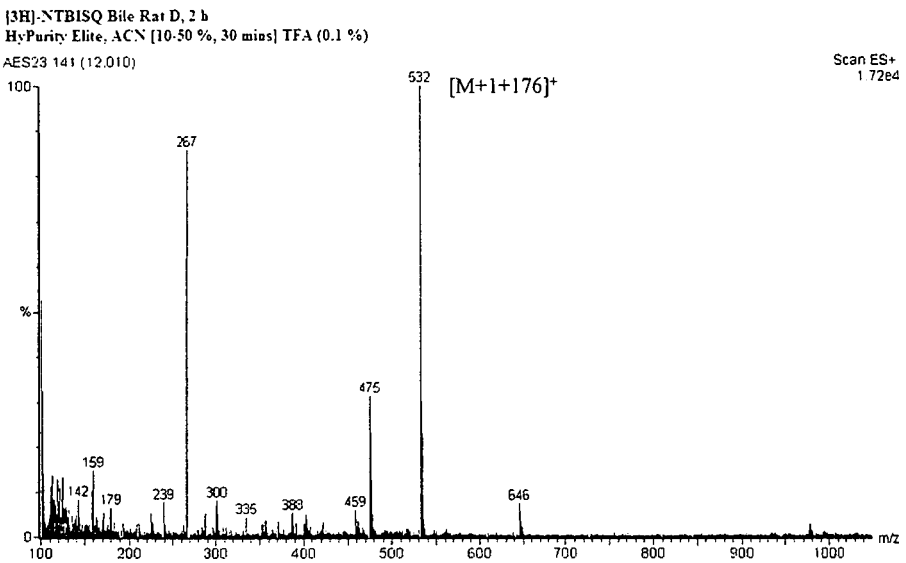

Figure 4.6 Positive-ion electrospray mass spectrum showing the fragmentation of [^{3}H]-NTBISQ-*O*-glucuronide excreted in the bile (2 h collection) of male, Wistar rats, 5 h after dosing *i.v.* with [^{3}H]-NTBISQ (54 μmol/kg, 20 μCi).

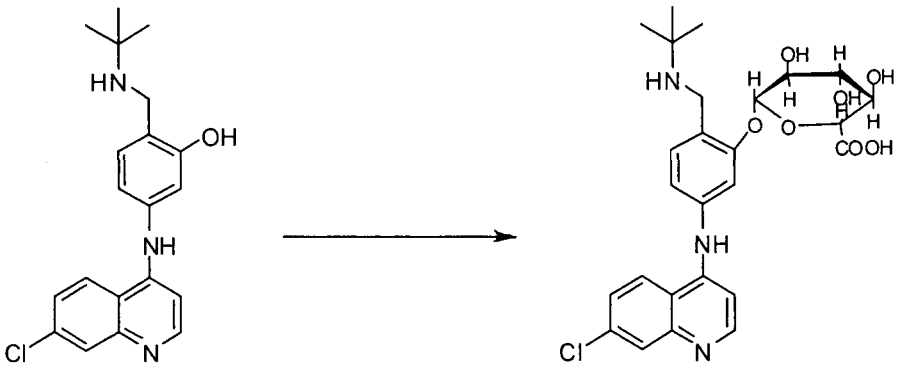

NTBISQ (I)
MW = 355
Rt = 12.95 mins
Urine

NTBISQ-*O*-glucuronide (II)
MW = 531
Rt - 10.74 mins
Bile

Scheme 4.3 Metabolites found in urine and bile of male, Wistar rats after dosing with [^{3}H]-NTBISQ (54 μmol/kg, 20 μCi).

In sharp contrast to AQ, which undergoes phase II conjugation with glutathione *in vivo*, NTBISQ was observed to undergo direct glucuronidation in rats. In order to investigate the chemical basis of why one molecule form is more likely to undergo direct glucuronidation over the other, a molecular modelling study was carried out by an associate of the group, Dr. Nick Greeves. This study investigated the various energy conformations of the 3'hydroxy *tert*-butyl substituted compound *versus* the 4'hydroxy *tert*-butyl substituted compound (*N-tert* butyl isoquine versus *N- tert* butyl amodiaquine) at neutral and acidic pH.

The results of this study showed that at neutral pH, the 3'hydroxy derivative was more nucleophilic than the 4'hydroxy compound implying that the nucleophilic attack that occurs between the hydroxyl group and glucuronic acid was more liable to occur with NTBISQ than the AQ analogue.

4.3.2 *In Vitro* Drug Metabolic Profile of NTBISQ

The *in vitro* disposition of NTBISQ was investigated at GlaxoSmithKline using animal and human hepatocytes and liver microsomes. GSK scientists incubated NTBISQ with liver microsomes and hepatocytes from mouse, rat, dog, monkey and human and in plasma, blood and urine samples of mouse and rat following *i.v.* and oral administration of NTBISQ. NTBISQ was observed to undergo metabolism in microsomes and hepatocytes by multiple, common pathways *in vitro,* including mono-oxygenation, ketone formation, oxidative deamination to the aldehyde and also glucuronidation (Figure 4.7). These metabolites were also detected in mouse plasma and urine and rat plasma and blood. Loss of the *tert* butyl side chain was observed in mouse urine and to a small extent in mouse plasma. The rate of *in vitro* metabolism was found to be low to moderate for NTBISQ in liver microsomes and isolated hepatocytes from pre-clinical species and human.

It was deduced that incorporation of the *tert*-butyl group on the nitrogen, a part of the molecule susceptible to oxidative metabolism, significantly reduced metabolism at this site in both *in vitro* and *in vivo* models as compared with ISQ.

Further more, there was no evidence for glutathione conjugation or reactive metabolism *via* the quinone imine pathway associated with AQ.

These results indicated that the pathway of metabolism of NTBISQ could involve more than just simple glucuronidation, however they fully supported our own findings at The University of Liverpool.

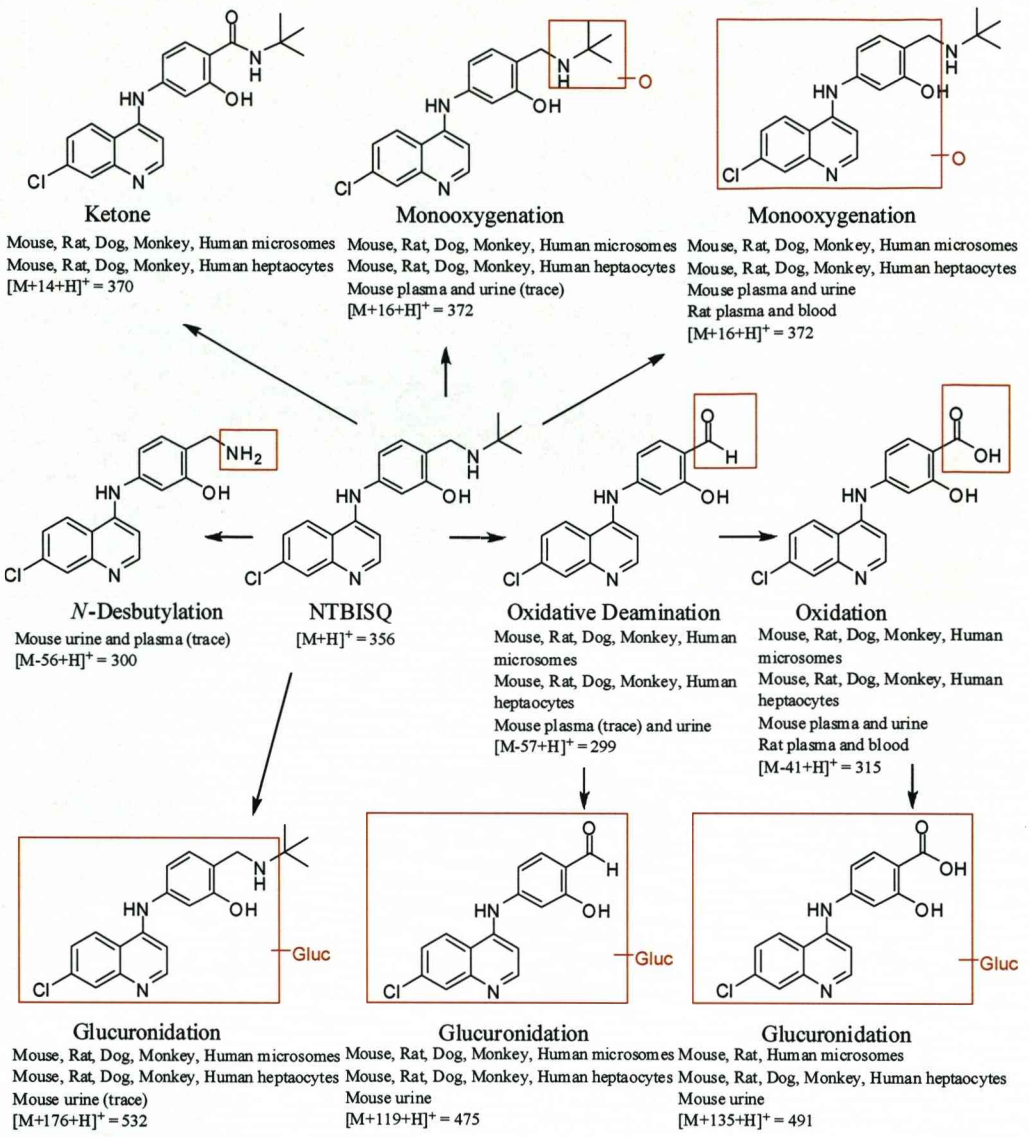

Figure 4.7 Metabolic pathway for NTBISQ in mouse, rat, dog, monkey in human liver microsomes and hepatocytes as proposed by GlaxoSmithKline (Bates, 2005)

4.3.2.1 Conclusions

After 5 h, NTBISQ was excreted solely as the parent compound in urine and underwent direct glucuronidation in bile from rats given an *i.v.* dose of 54 μmol/kg, 20 μCi. With the absence of any form of glutathione conjugate in the metabolic profile (c.f. AQ), it is clear that, as with ISQ, we have created a means of metabolic

escape by isomerisation of the phenol moiety with the amino side-chain. Furthermore, incorporation of the *tert* butylamine group in place of the diethylamine group of ISQ has simplified the metabolic profile and a distinct lack of dealkylation has been observed, resulting in a metabolically more stable compound.

The potential of the ISQ derivatives to undergo P450 hydroxylation to the aromatic ring still remains. Such hydroxylation could lead to the formation of a quinone imine. In all studies carried out no such hydroxylation was observed. These findings were further corroborated by an *in vitro* study carried out at GlaxoSmithKline where they too saw glucuronidation as a major pathway of metabolism of NTBISQ, along with mono-oxygenation and deamination. No evidence of bioactivation was observed in any of the studies conducted at either Liverpool or GlaxoSmithKline.

4.3.3 Tissue Distribution of [^{3}H]-NTBISQ and [^{3}H]-ISQ in the Rat

Five hours after administration of a single dose of [^{3}H]-NTBISQ (54 μmol/kg, 20 μCi) to cannulated rats, 51.78 ± 5.52 % of the dose was accounted for in the organs, bile and urine (Figure 4.8). Of this, 41.34 ± 4.90 % was found in the organs alone. Similarly to CQ and AQ, (Chapter 3), the largest proportion of the dose could be found in the liver (25.84 ± 2.25 %) and also the skin (8.87 ± 1.15 %). LC-MS investigation of homogenised liver samples deduced that the drug was present in this organ as the parent compound.

The brain and heart retained very minor amounts of radioactivity after 5 h, reducing any fears of cardiotoxicity or neurotoxicity as a consequence of drug accumulation. Biliary and urinary excretion was minimal with only 3.65 ± 0.30 % of the dose found in bile and 2.77 ± 0.32 % found in urine after 5 h. Again, as with CQ

and AQ, the full radioactive dose could not be accounted for, suggesting that there was another area of accumulation within the rat. A strong possibility remains that this radioactivity could be within the gastrointestinal tract.

Plasma radioactivity fell below background-activity within 0.5 h of completion of the injection, making meaningful comparisons of drug levels in plasma and tissues impossible. Issues of extraction of NTBISQ from blood were also encountered at GlaxoSmithKline, possibly due to extensive haem-binding.

On comparison with the tissue distribution of [^{3}H]-ISQ in rats (54 μmol/kg, 20 μCi) it can be seen that a similar pattern of distribution of drug existed. The majority of the radioactivity also was found in the liver (32.93 ± 2.95 %) followed by the skin (21.45 ± 1.90 %) (Figure 4.9). The total amount of radioactivity accounted for was 70.92 ± 8.02 %). The amount of radioactivity found in the skin 5 h after dosing was almost 2.5-fold higher than that after dosing with [^{3}H]-NTBISQ, this was found to be statistically significant with $p = 0.011$. The distribution of radioactivity in the kidneys also showed high statistical significance with almost twice the amount of radiolabeled compound retained after dosing with [^{3}H]-ISQ than [^{3}H]-NTBISQ ($p = 0.0006$). In addition to this, excretion in bile after dosing with [^{3}H]-ISQ was significantly higher than that in the bile of rats dosed with [^{3}H]-NTBISQ (12.73 ± 0.47 % versus 3.65 ± 0.30 %) ($p = 0.0061$). These significant changes in distribution and routes of clearance could be attributed to the structural differences between the two molecules, i.e. the diethylamino side-chain of ISQ versus the *tert* butylamino side-chain of NTBISQ.

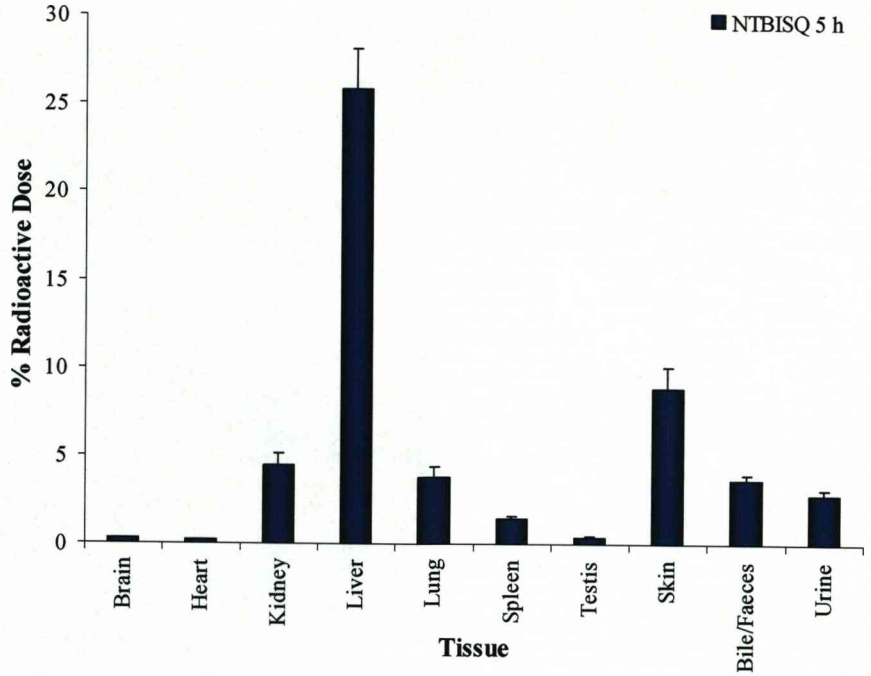

Figure 4.8 Percentage of radioactive dose recovered in tissues 5 h, after administration of [^{3}H]–NTBISQ (54 µmol/kg, 20 µCi/rat) to male Wistar rats (n = 4). Results are expressed as mean percentage of dose ± SEM.

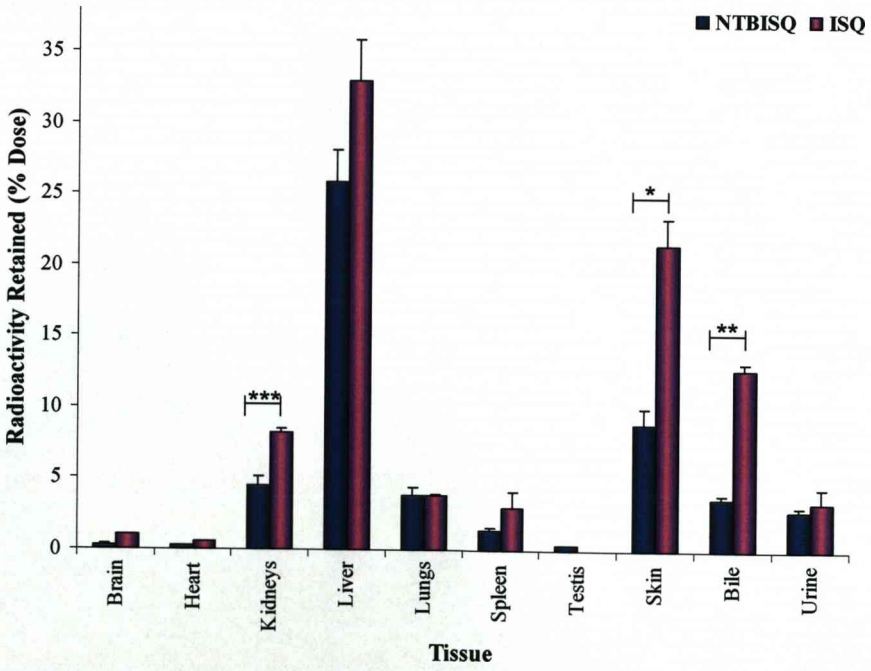

Figure 4.9 The percentage of radioactive dose recovered in tissues 5 h, after administration of [^{3}H]–NTBISQ and [^{3}H]-ISQ (54 µmol/kg, 20 µCi/rat) to male Wistar rats (n = 4). Results are expressed as mean percentage of dose ± SEM. Statistics were performed using a one way ANOVA test for parametric data and Kruskal Wallis test for non-parametric data. *P<0.05, **P<0.01, ***P<0.001

In order to obtain a more clearly resolved mass spectrum for bile and urine analysis, a higher dose was used (216 μmol/kg, 20 μCi). A dose comparison study was set up to investigate the effects increased dose on the distribution of [^{3}H]-NTBISQ in the rat (Figure 4.10). The pattern of distribution and also the levels of radioactivity remained similar between both high dose and low dose rats and no statistical significance were found between sets of data, indicating that accumulation of [^{3}H]-NTBISQ in the rat was not dose-dependent.

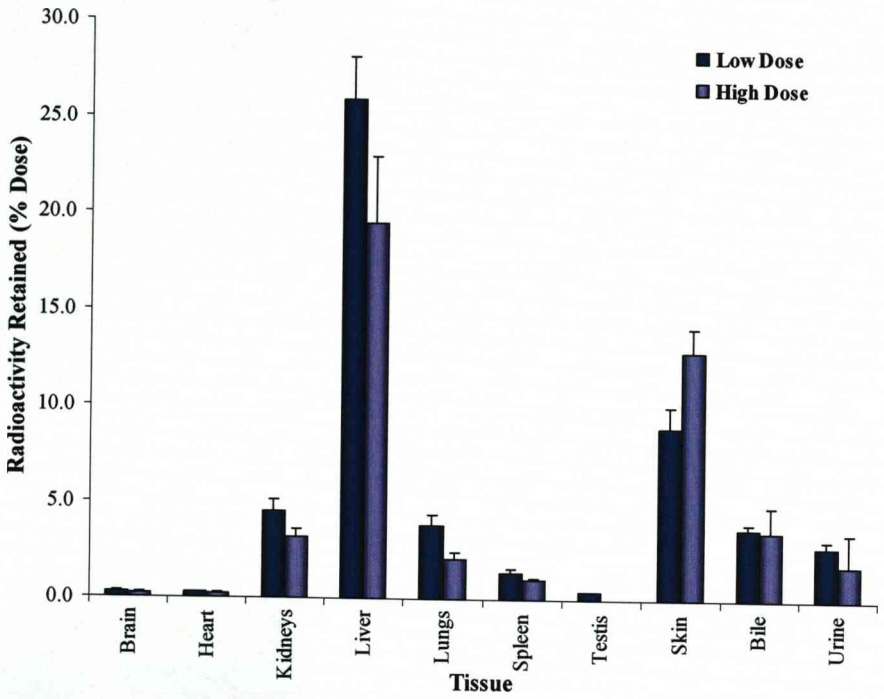

Figure 4.10 The percentage of radioactive dose recovered in tissues, 5 h after administration of [^{3}H] – NTBISQ (54 μmol/kg, 20 μCi/rat or 216 μmol/kg, 20 μCi/rat) to male Wistar rats (n = 4). Results are expressed as mean percentage of dose ± SEM. Statistics were performed using the unpaired t-test for parametric data and Mann-Whitney test for non-parametric data *P<0.05, **P<0.01, ***P<0.001.

Following on from the retention/accumulation studies carried out with [^{14}C]-CQ; experiments were set up using longer time-points from 24 h to 240 h (Figures 4.11 and 4.12). The aim of these experiments was to assess how long [^{3}H]-NTBISQ

remained inside the rat and to investigate whether the compound underwent retention which could potentially lead to toxicity.

Twenty-four hours after dosing with [^{3}H]-NTBISQ, the total dose accounted for was 39.17 ± 5.57 %. The data obtained from [^{3}H]-ISQ was incomplete, with missing data of the amount of radioactivity excreted in urine and faeces over a 24 h period. Only one experiment was carried out and so statistics could not be performed and direct comparisons must be treated with caution.

The distribution of radioactivity appeared to be very similar after dosing with [^{3}H]-NTBISQ and [^{3}H]-ISQ, with the highest proportion of dose, again, being retained in the liver and skin. In the case of rats dosed with [^{3}H]-NTBISQ, biliary output rose significantly from 5 h to 24 h from 3.65 ± 0.30 % to 13.70 ± 1.96 % ($p = 0.0068$), and even more so from 5 h to 48 h ($p = 0.0002$)) (3.65 ± 0.30 % to 23.30 ± 0.54 % indicating the effective excretion of the drug. Elimination of [^{3}H]-NTBISQ was noted to be mainly biliary, in the form of the *O*-glucuronide, from 24 h onwards.

After 48 h, the amount of biliary and urinary excretion totalled 35.80 ± 1.32 %, much less than that of [^{14}C]-CQ (74.88 ± 1.05 %) (Chapter 3) implying there may be a greater degree of retention of [^{3}H]-NTBISQ within the tissues.

After 168 h, 3.64 ± 1.15% of the radioactive dose still remained in the tissues of the rat, mainly in the liver and skin (Figure 4.12). This prompted us to increase the experimental time-point to 10 days (240 h). After this time less than 2 % of the dose remained in the rat, 0.90 ± 0.45 % in the liver and 0.70 ± 0.25 % in the skin.

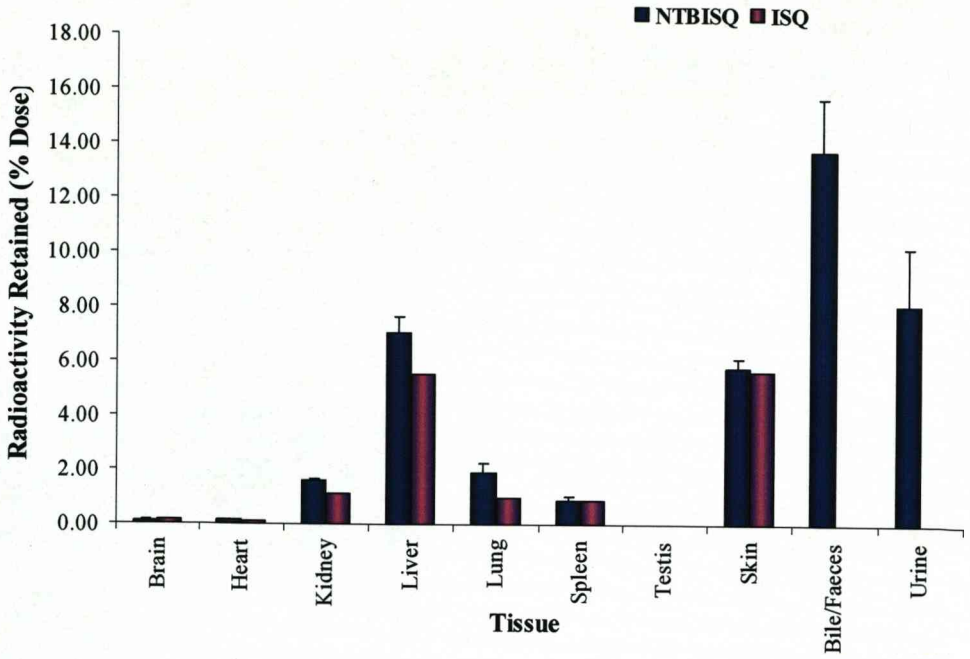

Figure 4.11 Percentage of radioactive dose recovered in tissues 24 h, after administration of [^{3}H]–NTBISQ (n = 4).or [^{3}H]-ISQ (n = 1) (54 µmol/kg, 20 µCi/rat) to male Wistar rats. Results for [^{3}H]–NTBISQ are expressed as mean percentage of dose ± SEM. Statistics could not be performed.

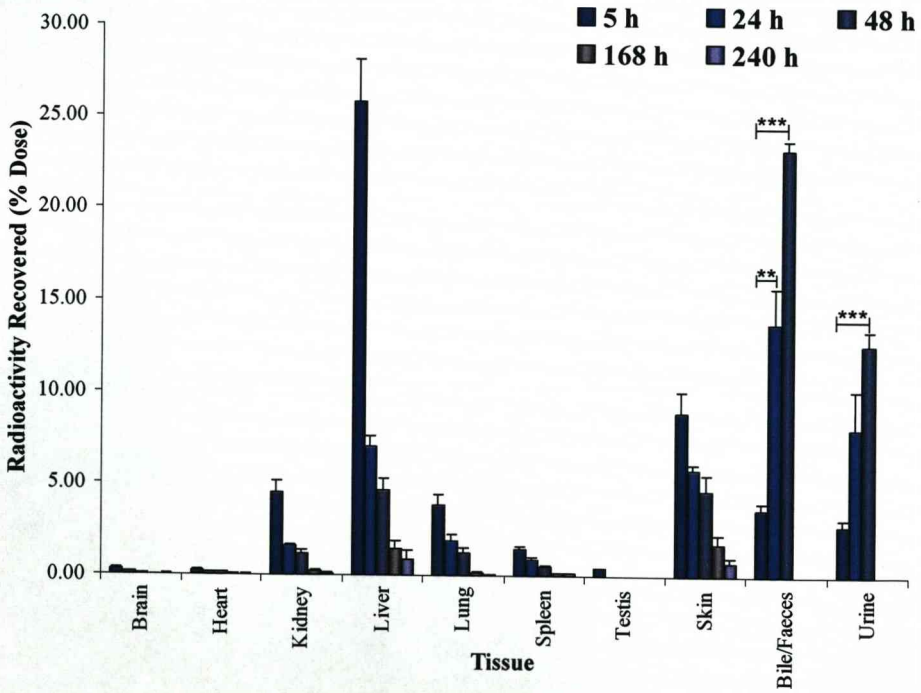

Figure 4.12 Percentage of radioactive dose recovered in tissues, 5 h, 24 h, 48 h, 168 h and 240 h after administration of [^{3}H]–NTBISQ (54 µmol/kg, 20 µCi/rat) to male Wistar rats (n = 4). Results are expressed as mean percentage of dose ± SEM. Unpaired t-test for parametric data and Mann-Whitney test for non-parametric data. *P<0.05, **P<0.01, ***P<0.001

4.3.3.1 Conclusions

Administration of [^{3}H]-NTBISQ and [^{3}H]-ISQ to rats led to the majority of the dose being retained in the liver and skin. As with [^{14}C]-CQ, this was not entirely unexpected due to these organs being, by far, the largest in size in the body and also the liver is residence to the greatest number of metabolizing enzymes.

After examining two different doses of [^{3}H]-NTBISQ in the rat, (54 μmol/kg versus 216 μmol/kg), no significant differences in distribution of compound could be seen, suggesting that any accumulation observed was not likely to be dose-dependant.

Previous work has shown that [^{3}H]-ISQ has a far more complex metabolic pathway than [^{3}H]-NTBISQ (Schemes 4.2 and 4.3), and yet the pattern of distribution remained very similar (Figure 4.9). The only areas in the rat showing significantly altered accumulation between the two compounds were the kidneys and skin, whereby [^{3}H]-ISQ was observed to accumulate to a greater extent than [^{3}H]-NTBISQ.

Further investigation into the clearance of NTBISQ by measurement of blood levels proved impossible due to the inextractability of NTBISQ from blood. Radioactivity in plasma was observed to be much lower than that of background level.

Due to the poor total recovery of [^{3}H]-NTBISQ after 5 h, it seemed highly probable that there was another area of accumulation within the rat and a strong possibility remains that this was the gastrointestinal tract.

4.3.4 Toxicology of NTBISQ

4.3.4.1 Cytotoxicity of NTBISQ in Isolated Rat Hepatocytes

Rat hepatocytes, isolated using a two-step collagen digestion method (Section 4.2.2.8) were incubated with CQ, AQ or NTBISQ at concentrations of 0, 20, 50, 100, 200 and 500 μM for 6 hours (Figure 4.13) Results were expressed as the percentage of viable cells, measured microscopically, using a trypan blue exclusion test (as a percentage of the control).

NTBISQ was shown to exhibit similar levels of toxicity in rat hepatocytes as AQ (Tox_{50} (NTBISQ) 40 ± 10 μM, Tox_{50} (AQ) 65 ± 15 μM). When comparing the Tox_{50} value of NTBISQ in rat hepatocytes with the IC_{50} value of NTBISQ against the 3D7 CQ-sensitive strain of malaria (11.2 ± 2.2 nM), the therapeutic index can be calculated as 3571. Therefore, the amount of drug required to damage the cells is more than 3500-fold that required to kill the parasite.

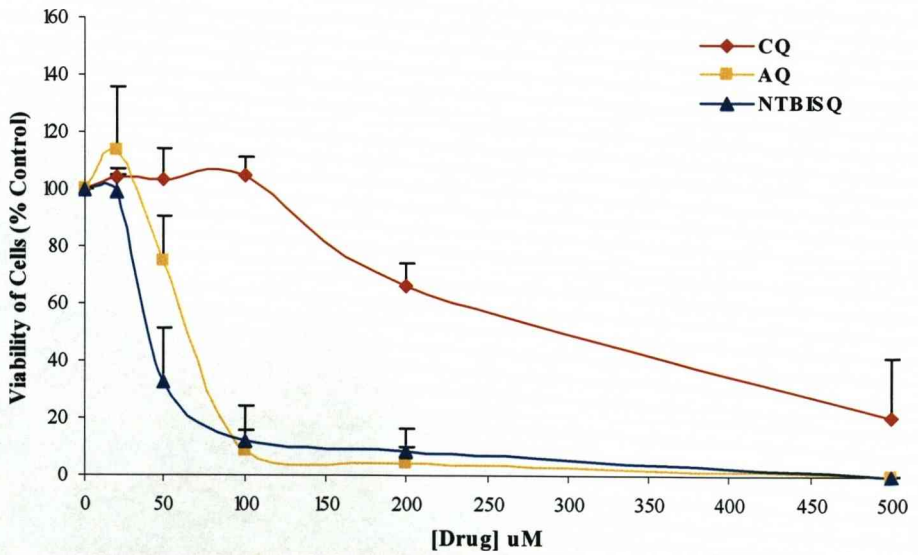

Figure 4.13 Viability of male, Wistar rat hepatocytes, incubated for 6 h with various concentrations of CQ and AQ, and stained with Trypan blue dye as an indicator for cell death. Results are expressed as mean percentage of dose ± SEM. Statistics were performed using a one way ANOVA test. *P<0.05, **P<0.01, ***P<0.001

A complementary toxicological study of NTBISQ was carried out at the Worldwide Development division of GlaxoSmithKline, Tres Cantos, Spain. The systemic toxicity of NTBISQ was evaluated in mice, rats, dogs and monkeys in order to assess its safety as a drug (GlaxoSmithKline, 2005).

4.3.4.2 Central Nervous System

Central nervous system (CNS) effects were observed in acute and short-term dosing studies in all species tested. Single doses of 100 mg/kg or more resulted in severe adverse reactions in dogs, such as laboured breathing, tremors and convulsions. In monkeys, doses above 180 mg/kg led to multiple episodes of emesis along with slight tremors and decreased activity.

In repeat dose studies in rats, CNS effects were evident after four daily doses of 150 mg/kg/day. These effects were presented as reduced activity, partially closed eyelids, hunched posture, abnormal gait and pilo-erection. Similar adverse signs were seen in mice also, after four days of receiving a dose of 300 mg/kg/day.

In a 14 day study in monkeys, using a dose of 75 mg/kg/day, persistent and non-tolerable adverse side effects were observed, but on reducing the dose to 35 mg/kg/day these effects became tolerable and recoverable. These findings were consistent across the 4-aminoquinoline class with CQ and AQ.

4.3.4.3 Phospholipidosis

Chapter 3 of this thesis began a brief introduction to phospholipidosis. As described, phospholipidosis is a well documented class effect of the 4-aminoquinoline family of antimalarials (Glaumann *et al.*, 1992; Halliwell, 1997; Shaikh *et al.*, 1987).

After dosing with NTBISQ, in almost all of the tissues evaluated, foamy macrophages were present, consistent with the occurrence of phospholipidosis. However, after a four week period without drug, there was a complete recovery in all tissues tested. In comparative studies both CQ and AQ showed a similar profile of phospholipidosis.

4.3.4.4 Primary Target Organs

A fourteen-day toxicology study in rats showed that the primary targets of NTBISQ were the heart, skeletal muscle and the liver.

After dosing male rats with NTBISQ (10 mg/kg/day) an increase in the incidence of focal myocardial degeneration/necrosis occurred. In addition to this, focal myofibre degeneration was observed in skeletal muscle of both male and female rats. Again, after four weeks without dose there was complete recovery of skeletal muscle damage and evidence of repair of the cardiac lesion.

Secondary to the hepatic phospholipidosis, hepatocyte apoptosis was also observed and transaminase levels in the blood were noted to be elevated after dosing with NTBISQ (50 mg/kg/day) indicating damage to the cells of the liver. This finding may explain our results, which showed higher levels of cytotoxicity of NTBISQ in rat hepatocytes (when compared to CQ) (Section 4.3.3).

These findings were all replicated in comparison studies with CQ and AQ. Not only this, but reports in the literature describe a similar pathology in rat skeletal muscle after dosing with CQ (Kumamoto *et al.*, 1989).

4.3.4.5 Conclusions

The findings from these toxicology studies showed that NTBISQ was consistent with and comparable to CQ and AQ, except for the additional adverse hepatic effects AQ is known to cause.

The heart, skeletal muscle and liver were all primary targets after dosing with NTBISQ in rats. Importantly, all effects observed were at a dose much higher than that of the targeted therapeutic dose. All of the unwanted effects observed were deemed to be reversible and could be clinically monitored.

4.3.5 Conclusion

In a recent study by Lin and co-workers they described the potential for ISQ and its derivatives to undergo a similar oxidation reaction as AQ *in vivo* to form an *O*-quinone methide (Scheme 4.4) (Miroshnikova *et al.*, 2006). The studies in this chapter show implicitly this not to be the case and that isomerisation of AQ to ISQ has in fact resulted in the successful elimination of bioactivation, in the rat to any form of toxic quinone imine metabolite. This was notable by the lack of glutathione conjugates in the bile and urine of rats treated with [^{3}H]-ISQ, thus proving that this route of bioisosterism has provided a route of metabolic escape.

By making further structural changes by incorporating a *tert* butyl group in place of the diethyl group of ISQ, we have not only successfully blocked bioactivation, but also produced a molecule with a simple metabolic route by virtue of the enhanced stability of the *N-tert* butyl side-chain. Importantly, no P450 hydroxylation of the aromatic ring was observed. Indeed, NTBISQ was found to mainly undergo direct glucuronidation *in vivo* in rats.

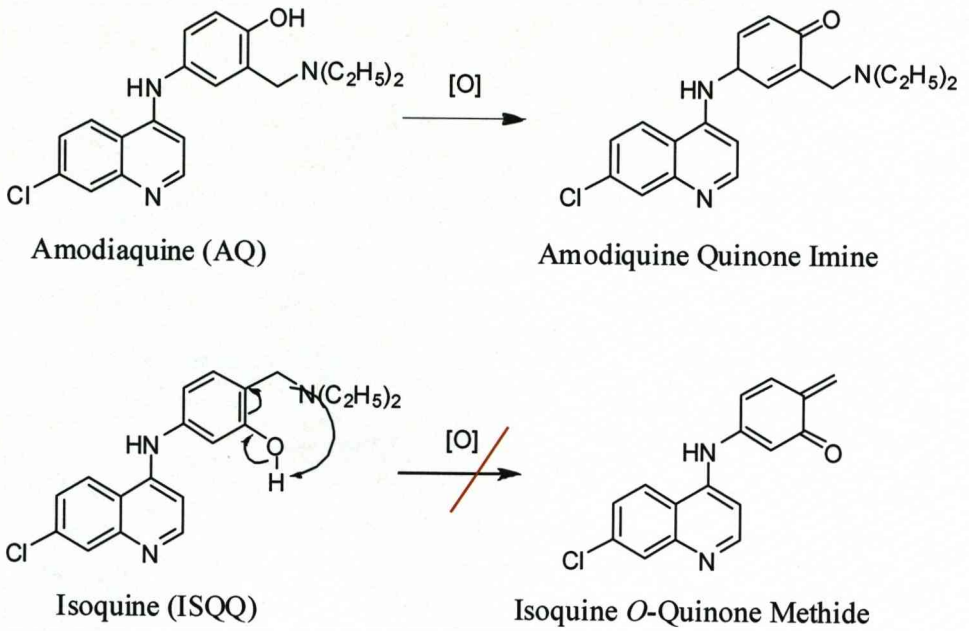

Scheme 4.4 Oxidation of AQ to a the toxic quinone imine metabolite and potential pathway of isoquine *O*-quinone methide formation according to Lin and co-workers (Miroshnikova *et al.*, 2006).

Toxicological studies of NTBISQ have revealed that the compound can affect the heart, liver and skeletal muscle of rats at high doses. Toxicity of this kind with the 4-aminoquinoline class of antimalarials is not unknown. Cardiotoxicity has previously been reported with the use of CQ and hydroxylCQ in patients undergoing treatment for connective tissue disorders or lupus. Chronic dosing of these drugs has led to instances of heart conduction disorders and also retinopathy (Roos *et al.*, 2002; Tanaka *et al.*, 2004).

The toxic effects observed with NTBISQ were also seen with CQ and AQ in an identical study. Importantly, the effects were only observed at very high concentrations and with repeated dosage. The adverse effects were deemed to be reversible and also species specific as they were not seen in the monkey or mouse, therefore they are unlikely to occur at therapeutic doses in clinic.

Dispositional studies after a single dose of NTBISQ showed accumulation in the liver. However, this was seen to diminish over time and did not lead to concerns over direct toxicity due to retention. No such accumulation was seen in the heart or muscle in these studies.

The data in this chapter reports the initial findings of an extremely promising novel compound. We have clearly demonstrated that NTBISQ has a desirable ADME profile, with no bioactivation observed in rats *in vivo* or *in vitro* and a simple metabolic profile. This, coupled with its excellent antimalarial and pharmacokinetic properties gives rise to a novel 4-aminoquinoline with great potential for use in the battle against malaria.

4.4 REFERENCES

BATES, M. (2005). Technical Evidence Candidate Selection - N-tert butyl isoqine. ed. O'Neill, P., Park, B. & Ward, S.

GLAUMANN, H., MOTAKEFI, A. & JANSSON, H. (1992). Intracellular distribution and effect of the antimalarial drug mefloquine on lysosomes of rat liver. *Liver*, **12,** 183-190.

GLAXOSMITHKLINE (2005). GSK369796 Investigator's Brochure. ed. O'Neill, P., Park, B. & Ward, S. Tres Cantos.

GUGUEN-GUILLOUZO, C. & GUILLOUZO, A. (1986). *Methods for preparation of adult and fetal hepatocytes, isolated and cultured hepatocytes.* Paris: INSERM and John Libbey Eurotext.

GUSTAFSSON, L., WALKER, O., ALVAN, G., BEERMANN, B., ESTEVEZ, F., GLEISNER, L., LINDSTROM, B. & SJOQVIST, F. (1983). Disposition of chloroquine in man after single intravenous and oral doses. *British Journal of Clinical Pharmacology*, **15,** 471-479.

HALLIWELL, W. (1997). Cationic amphiphilic drug-induced phospholipidosis. *Toxicologic Pathology*, **25,** 53-60.

HATTON, C., PETO, T., BUNCH, C. & PASVOL, G. (1986). Frequency of severe neutropenia associated with amodiaquine prophylaxis against malaria. *The Lancet*, 411-414.

HOMBHANJE, F., HWAIHWANJE, L., TSUKAHARA, T., SARAWATRI, M., NAKAGAWA, M., OSAWA, H. & PANIU, M. (2004). The disposition of oral amodiaquine in Papua New Guinean children with falciparum malaria. *British Journal of Clinical Pharmacology*, **59,** 298-301.

KUMAMOTO, T., ARAKI, S., WATANABE, S., IKEBE, N. & FUKUHARA, N. (1989). Experimental chloroquine myopathy: morphological and biochemical studies. *European Neurology*, **29,** 202-207.

MACOMBER, P., O'BRIAN, R. & HAHN, F. (1966). Chloroquine: Physiological basis of drug resistance in plasmodium berghei. *Science*, **152,** 1374-1375.

MIROSHNIKOVA, O., HUDSON, T., GERENA, L., KYLE, D. & LIN, A. (2006). Synthesis and antimalarial activity of new isotebuquine analogues. *Journal of Medicinal Chemistry*, **50,** 889-896.

NEFTEL, K., WOODTLY, W., SCHMID, M. & FRICK, P. (1986). Amodiaquine induced agranulocytosis and liver damage. *British Medical Journal*, **292,** 721-724.

O'NEILL, P., BRAY, P., HAWLEY, S., WARD, S. & PARK, B. (1998). 4-Aminoquinolines - past, present, and future: A chemical perspective. *Pharmacology and Therapeutics*, 77, 29-58.

O'NEILL, P., MUKHTAR, A., STOCKS, P., RANDLE, L., HINDLEY, S., WARD, S., STORR, R., BICKLEY, J., O'NEIL, I., MAGGS, J., HUGHES, R., WINSTANLEY, P., BRAY, P. & PARK, B. (2003). Isoquine and related amodiaquine analogues: A new generation of improved 4-aminoquinoline antimalarials. *Journal of Medicinal Chemistry*, **46,** 4933-4945.

RANDLE, L. (2001). The metabolism of isoquine, a new 4-aminoquinoline antimalarial. In *Pharmacology and Thereapeutics.* pp. 46. Liverpool: University of Liverpool.

ROOS, J., AUBRY, M. & EDWARDS, W. (2002). Chloroquine cardiotoxicity. Clinicopathologic features in patients and comparison with three patients with Fabry disease. *Cardiovascular Pathology*, **11,** 277-283.

SHAIKH, N., DOWNER, E. & BUTANY, J. (1987). Amiodarone - an inhibitor of phospholipase activity: a comparartive study of the inhibitory effects of amiodarone, chloroquine and chlorpromazine. *Molecular and Cellular Biochemistry*, **76,** 163-172.

TANAKA, M., TAKASHINA, H. & TSUTSUMI, S. (2004). Comparative assessment of ocular tissue distribution of drug-related radioactivity after chronic oral administration of 14C-levofloxacin and 14C-chloroquine in pigmented rats. *Journal of Pharmacy and Pharmacology*, **56,** 977-983.

CHAPTER 5

STRUCTURE-ACTIVITY-RELATIONSHIPS OF THE 4-AMINOQUINOLINE ANTIMALARIALS – A GLOBAL PERSPECTIVE

CONTENTS

5.1 INTRODUCTION

The haemoglobin degradation pathway in *Plasmodium falciparum* has been successfully exploited as the therapeutic target of chloroquine (CQ) (**1a**) and other 4-aminoquinolines. As the parasite catabolizes human haemoglobin, the haematin bi-product (**1c**) is detoxified by crystallisation to haemazoin (Francis *et al.*, 1997). CQ interacts with the porphyrin ring of haematin by a π-π stacking interaction of the quinoline ring. Accumulation of the haem:drug complex within the erythrocyte ultimately poisons the parasite. Resistance to this mechanism of action has proven difficult to induce and has developed relatively slowly and only after considerable human exposure. CQ resistance is the result of point mutations in a parasite transporter known as PfCRT (Bray *et al.*, 2005).

Amodiaquine (AQ) (**1b**) is active against CQ-resistant strains of *P. falciparum*. However, its use has been severely restricted by hepatotoxicity and agranulocytosis in humans (Hatton *et al.*, 1986; Neftel *et al.*, 1986). This appears to be the result of bioactivation to form a reactive quinone imine metabolite that can bind irreversibly to cellular macromolecules and may lead to direct toxicity as well as immune-mediated hypersensitivity reactions. IgG antibodies have been detected in patients with adverse reactions to AQ (Christie *et al.*, 1989; Rouveix *et al.*, 1989).

In order to enhance the metabolic stability of AQ we demonstrated that introduction of fluorine into the 4-hydroxyanilino nucleus increases the oxidation potential of the molecule and reduces the *in vivo* oxidation of the molecule to a cytotoxic quinone imine. From this earlier work, we demonstrated that the 4'-hydroxyl group could be replaced with a 4'-fluorine atom to produce an AQ analogue, fluoro-AQ (**2d**), with antimalarial activity in the low nanomolar range.

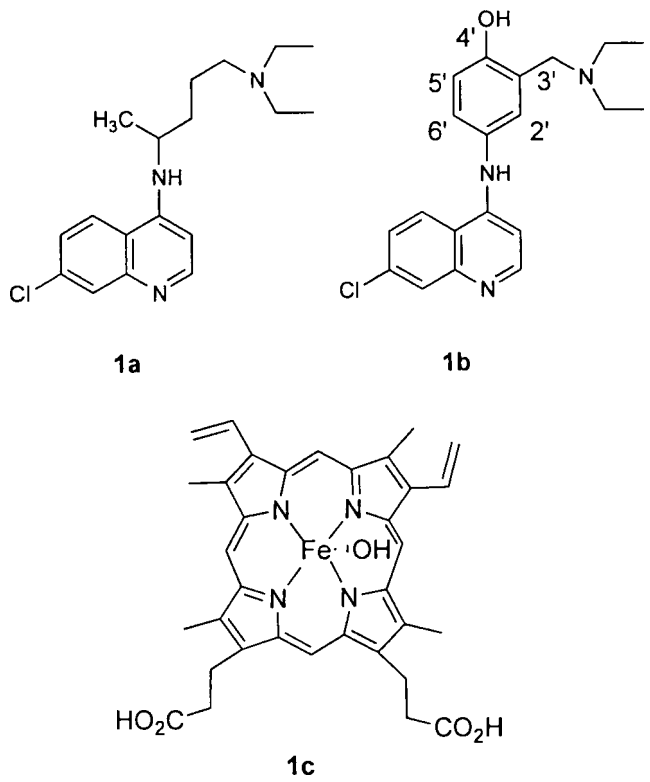

Figure 5.1 Structures of CQ (1a), AQ (1b) and Drug Target Haematin (1c)

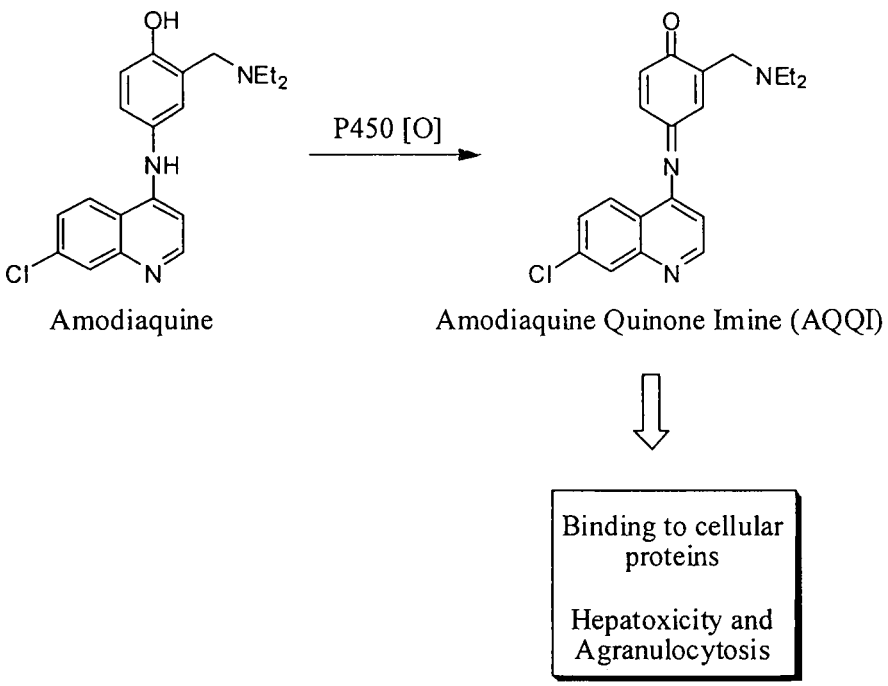

Scheme 5.1 Oxidation of AQ to a reactive quinone imine metabolite

An alternative approach to circumvent the facile oxidation of AQ involves isomerisation of the 3' and 4' groups. It was proposed that interchange of the 3'-hydroxyl and the 4'- Mannich side-chain function of AQ would provide a new series of analogues that cannot form toxic quinone imine metabolites *via* cytochrome P450-mediated metabolism. Isomeric AQ analogues were prepared using a simple two-step procedure, and then tested against K1 (CQ-resistant) and HB3 (CQ-sensitive) strains of *P. falciparum in vitro*. While several analogues displayed potent antimalarial activity against both strains, isoquine (ISQ) (**1d**), the direct isomer of AQ, was selected for *in vivo* antimalarial assessment. The potent *in vitro* antimalarial activity of ISQ was translated into excellent oral *in vivo* ED50 activity of 1.6 and 3.7 mg/kg against the *P. yoelii* NS strain compared to 7.9 and 7.4 mg/kg for AQ. Subsequent metabolism studies in the rat model demonstrated that ISQ does not undergo *in vivo* bioactivation, as evidenced by the complete lack of glutathione metabolites in bile. A drawback with **1d** is the low oral bioavailability in animal models and this was demonstrated to be on account of extensive metabolism of the *N*-diethylamino Mannich side-chain. Further studies in this area have revealed that the *N-tert* butyl analogue (**1e**) (Figure 5.2) has superior pharmacokinetic and pharmacodynamic profiles to ISQ in four animal species, including primates. This compound is undergoing further advanced pre-clinical evaluation with GlaxoSmithKline pharmaceuticals.

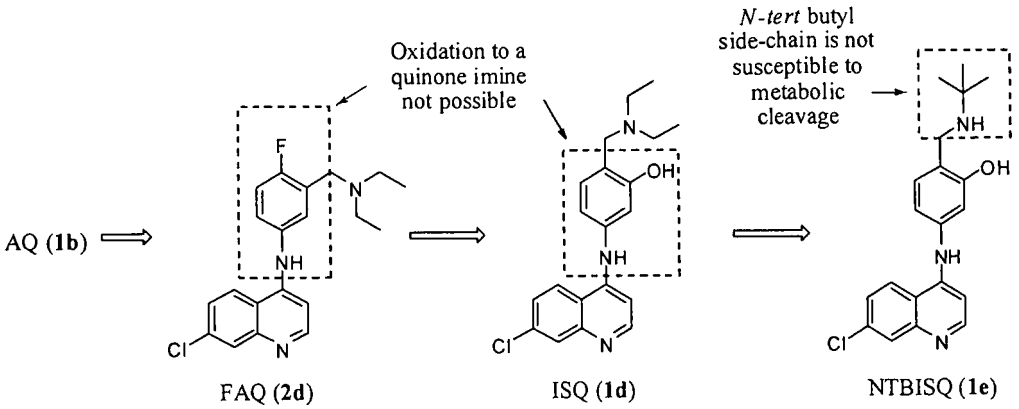

Figure 5.2 Rational drug-design of AQ analogues based on metabolism/toxicity considerations. The *N-tert* butyl analogue **1e** has an exceptional pharmacodynamic and pharmacokinetic profile.

Recent independent studies by the Sergheraert and the Lin groups have utilized the aryl anilino quinoline core as a template for the design of additional isomers of AQ and tebuquine (TBQ) (Delarue *et al.*, 2001; Miroshnikova *et al.*, 2006). The latter 4-aminoquinoline is a biaryl analogue of AQ with potent antimalarial activity but was not developed further due to toxicity. Our own studies with TBQ and other 4-hydroxyanilino containing antimalarials such as cycloquine and pyronaridine have confirmed that these molecules readily produce metabolism dependent neutrophil toxicity. For TBQ, we obtained evidence for the formation of a glutathione adduct derived by a novel chemical mechanism where the Mannich side-chain is replaced with glutathione.

The aim of this research was to investigate two series of AQ analogues where the 4'-hydroxyl function of AQ is replaced by either fluorine or chlorine; the intention, as in previous work, was to produce analogues incapable of producing quinone imine metabolites by P450 oxidation. The array of target molecules is highlighted in Figure 5.3. For comparison purposes, we have also examined the

antimalarial profile of two 4'-dehydroxy analogues of AQ. Following completion of the syntheses, appropriate antimalarial assessment and pre-clinical pharmacological assessment, we aimed to select suitable back-up compounds to (**1d**) with appropriate properties suitable for drug development.

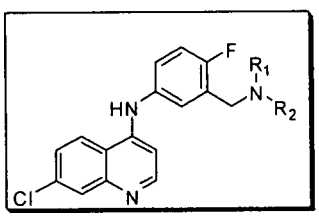

2d: R_1, R_2 = Et
2e: R_1, R_2 = $(CH_2)_4$
2f: R_1, R_2 = $(CH_2)_5$
2g: R_1, R_2 = $(CH_2)_2N(Me)(CH_2)_2$
2h: R_1, R_2 = nPr
2i: R_1, R_2 = nBu
2j: R_1, R_2 = $(CH_2)_2O(CH_2)_2$
2k: R_1, = H, R_2 = tBu

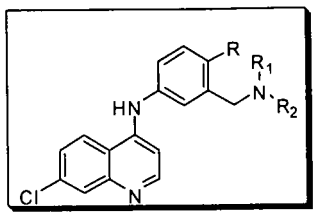

3d: R = Cl, R_1, R_2 = Et
3e: R = Cl, R_1, R_2 = $(CH_2)_4$
3f: R = Cl, R_1, R_2 = $(CH_2)_5$
3g: R = Cl, R_1, R_2 = $(CH_2)_2N(Me)(CH_2)_2$
3h: R = Cl, R_1, R_2 = nPr
3i: R = Cl, R_1, R_2 = nBu
3j: R = Cl, R_1, R_2 = $(CH_2)_2N(Et)(CH_2)_2$
3k: R = Cl, R_1, R_2 = $(CH_2)_2N(iPr)(CH_2)_2$
3l: R = Cl, R_1, R_2 = $(CH_2)N(2\text{-pyridyl})(CH_2)_2$
3m: R = Cl, R_1, R_2 = 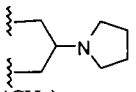
3n: R = Cl, R_1, R_2 = $(CH_2)_6$
3o: R = Cl, R_1 = H, R_2 = ^{t}Bu
4d: R = H, R_1 = H, R_2 = ^{t}Bu

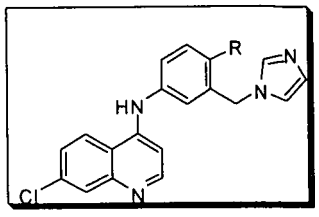

2l: R = F
3p: R = Cl
4e: R = H

Figure 5.3 Structures of 4'chloro and 4' fluoro analogues of AQ

5.2 RESULTS AND DISCUSSION

5.2.1 Chemistry

Although the original reported route to fluoro-AQ was relatively efficient we reasoned that shortening the number of synthetic steps and developing a route where a point of diversity appears in the penultimate step of the synthesis could achieve a significant improvement to the synthesis of target molecules in Figure 5.3. The alternative route adopted for the synthesis of 4'-chloro and 4'-fluoro analogues is shown in Scheme 5.2.

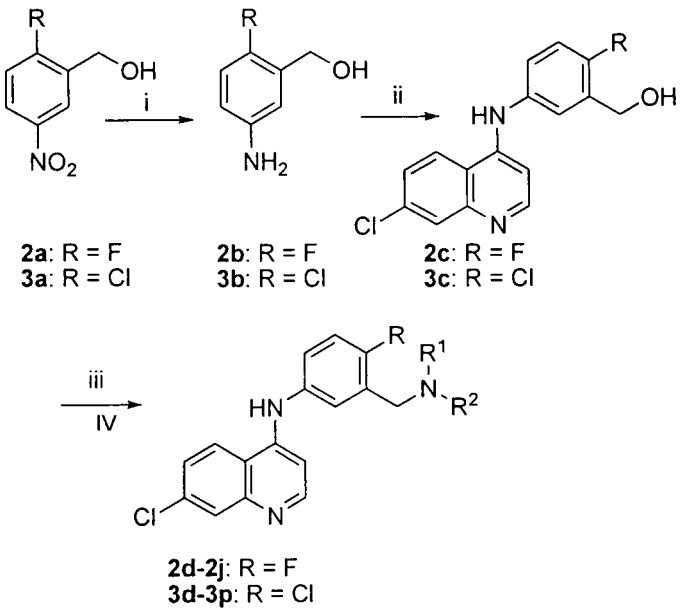

Reagents and conditions (i) $Fe/HCl/H_2O$, reflux; (ii) 4,7-dichloro quinoline, EtOH, reflux, (iii) DIEA, CH_2Cl_2, DMF, MnO_2; (iv) amine then $NaHB(OAc)_3$.

Scheme 5.2 Synthesis of 4'fluoro and 4'chloro analogues by reductive amination of aldehydes, 2c and 3c.

For the synthesis of 4'-chloro analogues nitro reduction of **3a** was easily achieved using iron powder and HCl in reluxing aqueous ethanol. The resulting amine **3b** was then allowed to react with 4, 7-dichloroquinoline to provide **3c** in excellent yield as a yellow powder following standard work-up. Quinoline **3c** proved

to be quite insoluble in dichloromethane, so a combination of dichloromethane, DMF and a small amount of diisopropylethyl amine were used as solvents to dissolve the alcohol for MnO_2-mediated oxidation. After 18h reflux, precipitates derived from the oxidant MnO_2 were filtered off with celite. In many runs, significant losses occurred at this stage and a more satisfactory work-up procedure involved the use of a pre-column with ethyl acetate prior to flash column chromatography using methanol/dichloromethane as eluent. The key aldehyde was obtained in moderate to good yields following flash column chromatography. The final step involved reductive amination of the aldehyde **3c** with a variety of different amines to produce a small array of target molecules depicted in Figure 5.3. In all cases the reductive amination procedure worked well and flash column chromatography gave the products **3d-3p** in good yields. (Table 5.1)

Scheme 5.2 also depicts the synthesis of the fluorinated series of analogues and the approach used is essentially the same as that discussed. The only exception to this was alternative conditions were explored for the reduction of the nitro group of **2a** and the oxidation of the benzylic alcohol **2c** to the corresponding aldehyde. Disappointingly, the use of powdered iron/ HCl gave the desired amine **2b** in low yields following basification and work-up. Alternative reducing conditions using methanol, ammonium chloride and zinc dust or granulated tin and concentrated hydrochloric acid provided the product **2b** in good yield, following addition of sodium hydroxide solution to the amine in the work-up phase of the reaction. The synthesis of **2c** from **2b** proceeded in high yields without event. In contrast to the 4'-chloro series, oxidation of **2c** with MnO_2 gave the desired aldehyde in poor yields, possibly due to the insolubility of the quinoline aldehyde. An alternative method based on chromium (VI) was explored which provided the aldehyde in moderate

yield. Reductive amination and work-up provided the desired compound as a dark brown solid. NMR analysis of the products prior to chromatography indicated complex formation (very broad peaks in the aromatic and aliphatic region); the nature of this complexation remains undefined. Acidification using HCl and basification using sodium bicarbonate provided the free bases which were pure by NMR and microanalysis following flash column chromatography. Although the new route provided target molecules in acceptable yields for the 4'-chloro series, the final reductive amination step in the 4'-fluoro series requires optimisation (Tables 5.1 A and B). For this reason, the previously used linear approach was employed for selected analogues as shown Scheme 5.3. The first step in the sequence involved free radical bromination of 2-fluoro-5-nitrotoluene (or 2-chloro-5-nitrotoluene) using NBS/AIBN to give the benzylic bromide as a crystalline solid in good yield.

A Fluoro Series

Aldehyde	Amine	Product	Yield (%)
2c	diethylamine	**2d**	24
2c	pyrrolidine	**2e**	20
2c	piperidine	**2f**	31
2c	N-methylpiperazine	**2g**	31
2c	dipropylamine	**2h**	27
2c	dibutylamine	**2i**	42
2c	morpholine	**2j**	23

B Chloro Series

Aldehyde	Amine	Product	Yield (%)
3c	diethylamine	**3d**	74
3c	pyrrolidine	**3e**	61
3c	piperidine	**3f**	92
3c	N-methylpiperazine	**3g**	89
3c	dipropylamine	**3h**	85
3c	dibutylamine	**3i**	24
3c	N-ethyl piperazine	**3j**	63
3c	N-isopropylpiperazine	**3k**	62
3c	1-(2-pyridyl)-piperazine	**3l**	98
3c	4-(-pyrrolidinyl)-piperazine	**3m**	56
3c	hexamethylene imine	**3n**	35

Tables 5.1A and B Yields for reductive amination of aldehydes 2c and 3c

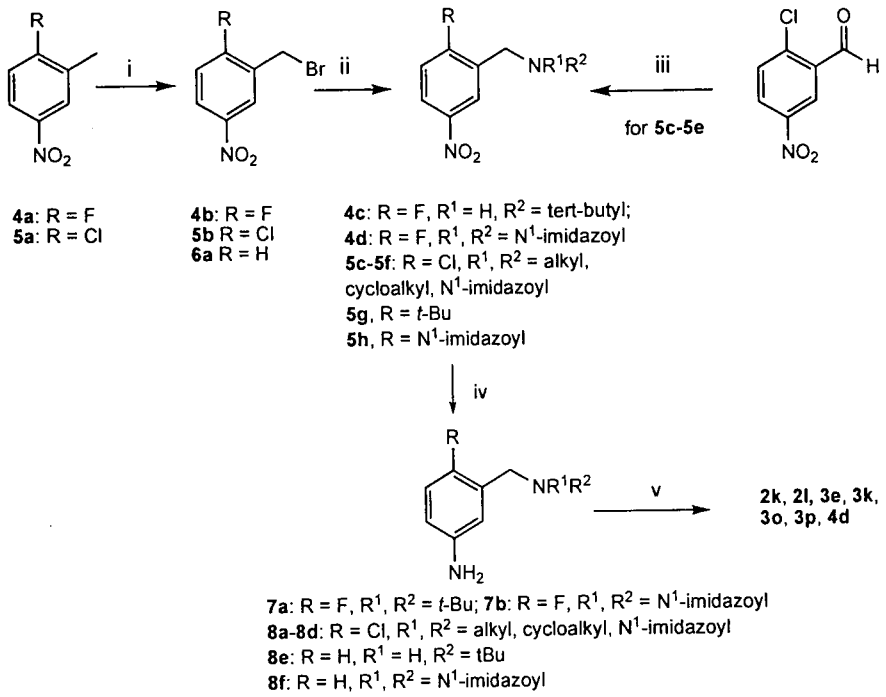

Reagents and conditions: (i) NBS, AIBN, reflux; (ii) amine, K_2CO_3, CH_3CN, reflux; (iii) MeOH, RT then 0°C, $NaHB(OAc)_3$; (iv) Sn/HCl, H_2O, reflux; (v) 4,7-dichloroquinoline, EtOH, HCl, reflux

Scheme 5.3 Synthesis of 4-dehydroxy, 4'chloro and 4'fluoro analogues of AQ.

The resulting benzyl bromide **4b** was then allowed to react with the appropriate amine to provide intermediates (**4c**, **4d**, and **5c-5f**) that were reduced and coupled with 4, 7-dichloroquinoline as shown. Benzyl bromides **4b**, **5b** and **6a** were also allowed to react with imidazole and this enabled the synthesis of novel weak base imidazole derivatives **7b**, **8d** and **8f**. For intermediates **5c-5e** 2-chloro 5-nitro benzaldehyde was also used as starting material in a reductive amination approach as shown (Scheme 5.3).

5.2.2 Biology

5.2.2.1 In Vitro Antimalarial Activity versus Plasmodium falciparum

Initial testing was carried out using a CQ-sensitive strain of *P. falciparum* (Table 5.2). In the 4'-fluoro series, the weak base morpholine analogue **2j** and analogues **2h** and **2i** expressed relatively poor antimalarial activity versus the 3D7 strain. The *N-tert* butyl analogue **2k** was the most potent in this series with activity equivalent to CQ (**1a**) and ISQ (**1d**). The 4'-chloro analogues tested were all active around 30 nM with the exception of **3h** and in line with the 4'-fluoro series, the 4'-chloro *N-tert* butyl analogue **3o** expressed the highest antimalarial activity. Interestingly, within these two templates, the side-chain alkyl amine or cyclic amine groups can be replaced with imidazole to produce analogues **2l** and **3p** which both showed antimalarial activity in the low nanomolar region.

Table 5.3 lists activity for the 4'-chloro series versus a CQ-resistant TM6 and sensitive HB3 strain. The IC_{50}s were lower against these two strains and the most potent analogue was the *N-tert* butyl analogue **3o**. Analogues **3e**, **3f**, **3j** and **3k** also expressed excellent activities against these two strains. For the 4'-chloro series as a whole, there is a clear lack of cross-resistance.

Compound	IC_{50} (nM) 3D7	Compound	IC_{50} (nM) 3D7
2d	27.3 (3) ± 11.5	**3d**	30.4 (3) ± 15.2
2e	29.7 (3) ± 11.1	**3f**	25.7 (3) ± 10.6
2f	33.2 (3) ± 15.2	**3g**	86.8 (3) ± 43.1
2g	35.1 (3) ± 8.7	**3h**	277.3 (3) ± 34.6
2h	85.2 (3) ± 18.1	**3j**	39.7 (3) ± 9.3
2i	95.2 (3) ± 30.2	**3l**	27.2 (3) ± 18.1
2j	550.7 (3) ± 90.4	**3n**	14.5 (3) ± 2.2
2k	12.1 (3) ± 5.3	**3o**	7.8 (6) ±3.2
2l	27.2 (3) ± 3.4		
CQ (**1a**)	9.1 (3) ± 4.9	AQ (**1b**)	4.7 (3) ± 2.9
ISQ (**1d**)	7.8 (6) ± 2.2	NTBISQ (**1e**)	6.0 (6) ± 4.0

Table 5.2 ***In vitro*** **antimalarial activities of the chloro and fluoro series versus CQ-sensitive 3D7 strain of** ***Plasmodium falciparum.*** [a]AQ and NTBISQ (**1e**) were tested as the hydrochloride salt. CQ was tested as the diphosphate. All other compounds were all tested as free bases.

Compound	IC_{50} (nM) TM6	IC_{50} (nM) HB3
3d	10.2 ± 5.3	12.3 ± 5.1
3e	4.2 ± 1.3	15.2 ± 3.7
3f	9.4 ± 6.7	12.3 ± 3.2
3g	24.4 ± 4.8	54.5 ± 8.3
3i	66.3 ± 11.3	144.3 ±12.8
3j	10.3 ± 4.3	9.6 ± 3.4
3k	6.4 ± 2.3	9.1 ± 2.1
3l	500 ± 22.4	485 ± 14.1
3m	360.3 ± 13.3	760 ± 23.3
3n	7.0 ± 1.2	16.1 ± 7.2
3o	4.5 ± 3.2	8.1 ± 3.2
4d	5.0 ± 2.2	10.1 ± 3.2
CQ	75 ± 22.1	20.2 ± 10.1
AQ	7.2 ± 3.3	5.5 ± 3.2

Table 5.3 ***In vitro*** **antimalarial activities of 4-chloro series versus CQ-sensitive HB3 Strain and TM6 CQ-Resistant of** ***Plasmodium falciparum.*** TM6 is a CQ-resistant strain of *P. falciparum*, HB3 and 3D7 are CQ-sensitive strains of *P. falciparum.*

As this project progressed, the excellent profiles displayed by the ISQ analogue **1d,** and in particular the metabolic advantages provided by the *N-tert* butyl side-chain led to the selection of **2k** for further biological assessment against eight additional strains of *P. falciparum.* In the expanded testing contained in Table 5.3, data is also included for the pyrrolidino analogue **2e**.

Strain	CQ	AQ	**2k**	**2e**
TM6	212.0 ± 30.1	6.9 ± 3.2	21.9 ± 5.4	60.8 ± 8.9
K1	170.6 ± 22.3	20.0 ± 2.3	22.0 ± 3.4	45.9 ± 12.2
HB3	16.0 ± 3.4	8.5 ± 3.4	14.6 ± 5.4	63.7 ± 11.2
PH3	30.8 ± 12.3	15.2 ± 4.4	25.8 ± 6.7	25.0 ± 8.2
TM4	112.8 ± 22.2	15.1 ± 3.3	17.3 ±4.9	46.9 ± 18.1
DD2	59.3 ± 11.1	9.5 ± 1.4	22.4 ± 1.6	36.9 ± 4.9
V1S	154.0 ± 17.3	8.9 ± 4.6	26.1 ± 7.6	52.5 ± 9.5
J164	133.5 ± 14.5	18.5 ± 4.2	29.2 ± 4.5	34.7 ± 8.3

Table 5.4 Expanded *in vitro* antimalarial activities of 2k and 2e versus a panel of *P. falciparum* Isolates. [a]TM6, K1, TM4, V1S, J164 are all CQ- resistant strains of *P. falciparum.* The strains HB3, PH3, DD2 are CQ-sensitive.

The data indicates that **2k** is superior to the pyrrolidino analogue **2e** against all of the strains examined. It is also clear that *N-tert* butyl analogue **2k** is potent against CQ-resistant strains, though it is not quite as active as AQ against both CQ-sensitive and resistant parasites. Based on the activity presented in Table 5.4, the **2k** was selected for further studies in the mouse model of malaria.

5.2.2.2 In Vivo Antimalarial Activity Against Plasmodium Berghei ANKA

The therapeutic efficacy of **2k** and selected 4-aminoquinolines was evaluated in a standard '4-day test' in CD1 mice infected intravenously with the murine pathogen *P berghei* ANKA at GlaxoSmithKline, Tres Cantos, Spain.

Compound	ED_{50} (mg/kg)	95 % Confidence Interval	ED_{90} (mg/kg)	95 % Confidence Interval
AQ	2.1	2.0 to 2.2	3.2	2.0 to 2.2
ISQ	3.7	3.4 to 3.9	5.3	3.4 to 3.9
desISQ	5.3	4.1 to 6.8	7.3	4.1 to 6.8
NTBISQ (**1e**)	2.8	3.3 to 4.3	4.7	4.8 to 6.1
(**2k**)	5.3	4.1 to 6.8	12.4	4.1 to 6.8

Table 5.5 Therapeutic efficacy of 2k, NTBISQ (1e) and the ISQ series against *P. berghei* ANKA infection in mice. Standard 4-day Test assay[a]. [a]
Groups of five mice were inoculated *i.v.* with 10^7 infected erythrocytes/mice. The compound was administered orally once a day for four days starting one hour after infection. Seven drug doses were used ranging from 40 to 0.31 mg/kg to determine ED_{50} and ED_{90} values. Parasitaemia after treatment was measured in peripheral blood by flow cytometry 24 hours after the administration of the 4th dose. The results obtained are shown in Table 5.4.

ISQ showed *in vivo* therapeutic efficacy against *P. berghei* ANKA with ED_{50} and ED_{90} in the same range as that of AQ. Analogue **2k** was also potent in this *in vivo* assay with an ED_{50} value of 5.3 mg/kg. In conclusion, both **2k** and NTBISQ showed good therapeutic efficacy against murine parasites (*P. berghei*), in the same range as AQ and other ISQ series compounds.

The therapeutic efficacy of **2k**, ISQ, desISQ and the two control compounds, AQ and CQ were also evaluated in the standard '4-day test' against the murine pathogen *P. yoelii* 17X. Mice were infected with 6.4 x 10^6 parasitized erythrocytes/mouse *i.v.* and treatments were started 1 hour after infection. The products were administered once a day *p.o.* in saline. Parasitaemia in peripheral blood were measured 96 hours after infection (day 4) and then, every 2-3 days until day 23 in order to assess recrudescence after treatment. The results (ED_{50}, ED_{90}, and non-recrudescence level) are shown in Table 5.6.

Compound	Test	Parameter	Mean (mg/kg)	IC 95 %[1] (mg/kg)
CQ	4-day	ED_{50}[2]	3.3	2.8 to 3.7
		ED_{90}	4.4	4.0 to 4.9
		NRL[3]	>40[4]	NA[5]
AQ	4-day	ED_{50}	2.6	2.1 to 3.2
		ED_{90}	3.7	3.3 to 4.1
		NRL	>40[4]	NA
ISQ	4-day	ED_{50}	5.2	4.6 to 5.8
		ED_{90}	7.6	6.9 to 8.3
		NRL	>40[4]	NA
DesISQ	4-day	ED_{50}	5.5	5.1 to 5.9
		ED_{90}	8	7.6 to 8.5
		NRL	>40[4]	NA
2k	4-day	ED_{50}	7.7	6.7 to 8.9
		ED_{90}	10.6	9.4 to 11.8
		NRL	>40[4]	NA

Table 5.6 Therapeutic efficacy of 2k and ISQ derivatives against *P. yoelii* 17X infection in mice. Standard 4-day Test assay. CQ and AQ were included as control compounds.

(1) Interval of confidence of the mean

(2) Dose at which a 50 % of reduction of parasitaemia in peripheral blood is achieved at day 4 after infection

(3) Non recrudescence level (NRL) is defined as the minimum dose at which no recrudescence is observed. Highest dose deployed in this study was 40 mg/kg.

(4) NRL level is only defined for treatments which make parasitaemia undetectable by flow cytometry at day 4 in the '4-day test'. At the highest dose deployed CQ, AQ, ISQ, desethylISQ and **2k** (40 mg/kg) were unable to render parasitaemia undetectable, therefore it is not possible to evaluate NRL level for these compounds properly, although actually it is higher than 40 mg/kg

(5) Not applicable

5.2.3 Mechanism of Action - Hematin Binding Studies

Recent efforts have centred on developing titration methods to determine accurate equilibrium constants and binding stoichiometries for the most widely used quinoline antimalarials. We have applied a UV-Visible spectroscopic method for determining accurate binding equilibrium constants for several clinically used antimalarials and compared the results with fluoro analogue **2k**. Initially, the titrations were carried out in a mixed aqueous/organic solvent to minimize porphyrin

aggregation effects and m-oxo dimer formation. Buffered 40% DMSO was used to provide a strictly monomeric haem species in solution.

The mode of action for haem binding was investigated. The potential binding processes one and two (Scheme 5.4) were mathematically modelled and examined as possible best fits for the titrations. In model one there is a step-wise bonding of two equivalents of drug to one molecule of haem. In model two there is a step-wise addition of two additions of haem to one equivalent of drug.

The UV-Visible spectra obtained after each titrated addition was analyzed and stacked against the corresponding absorbances. The data was transferred for analysis using the Pro-Fit non-linear curve fitting program licensed from Quansoft. The data was fitted to achieve chi^2 at minima to produce K_1 and K_2 fitted parameters for both models. This was initially done at one wavelength and then simultaneously at 10-15 wavelengths to give a more unbiased approach to fitting and more accurate values in comparison to fitting at just a single wavelength. Table 5.7 below shows the K_1 and K_2 values obtained from this method for CQ, AQ, quinine, **2k** and mefloquine, with the best fitted model shown.

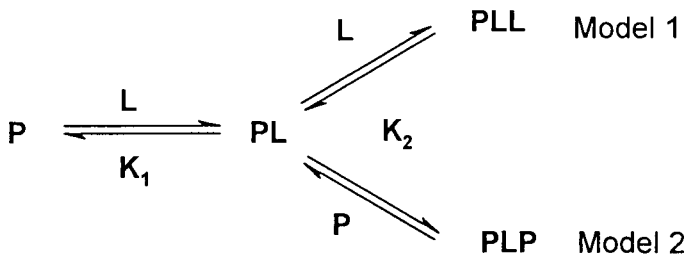

Scheme 5.4 Potential binding interactions for drug (L) with haem (P). After the first association of porphyrin with drug, there are two distinct binding events in which either another drug or porphyrin molecule coordinate to the intermediate adduct.

An important observation indicated from the resulting fits is that the binding stoichiometries for the quinoline-methanol antimalarials, quinine and mefloquine are different from the 4-aminoquinolines included in this work. The second binding event in the CQ titrations involves the addition of another molecule of haem whereas the second binding to the quinine-haem adduct involves a second molecule of ligand. This is in line with earlier studies derived from NMR experiments suggesting that the binding modes of 4-aminoquinoline antimalarials, such as CQ and AQ and quinoline-methanol antimalarials, such as quinine and mefloquine, are different.

Compound	Solvent	Log K_1	Log K_2	Best fit Model
CQ	40% DMSO	4.60(±0.1)	6.70(±0.1)	2
AQ	40% DMSO	4.40(±0.1)	6.20(±0.1)	2
Quinine	40% DMSO	4.40(±0.1)	4.10(±0.1)	1
Mefloquine	40% DMSO	3.84(±0.1)	3.17(±0.1)	1
2k	40% DMSO	5.45(±0.1)	5.68(±0.1)	2

Table 5.7 Equilibrium constants for the binding of antimalarials with haem in DMSO solutions

The data measured are in quite good agreement with the literature and demonstrate that the fluoro analogue **2k** can form a 2:1 complex in solution with clearly defined association constants. Selected analogues from the new series of 4-aminoquinolines were also examined for their ability to inhibit β-haematin formation.

All of the compounds tested had excellent activity in this assay including the imidazole containing analogues **2p**, **3p** and **4e**. These molecules are interesting in the sense that in addition to π-π stacking over the porphyrin ring system of haematin, these agents may also have the capacity to interfere with haematin dimerisation or

crystallisation by binding to iron by axial ligation. Both the **2k** and chloro variant **3o** had super-imposable activity in the assay.

In an assay to determine the concentration of drug to inhibit β-haematin formation all compounds tested were shown to be equally as potent as CQ with the exception of **4e** (Table 5.8). This compound was a deshydroxyl analogue of AQ indicating the importance of the hydroxyl group in binding to the porphyrin nucleus.

Compounds	IC_{50} Drug: haemin molar ratio[1]
2k	1.66
2l	1.78
3p[a]	1.58
3j	1.66
4d	1.65
4e	2.65
AQ[b]	0.85
CQ	1.78

Table 5.8 Results of the BHIA assay (inhibition of β-haematin formation). [1]The drug concentration required to inhibit β-haematin formation by 50% (IC_{50}) was determined for each compound. The results are the mean IC_{50} of two different experiments performed in duplicate. [a] Compounds not completely dissolved. (Parapini *et al.*, 2000)

5.2.4 Conclusion

The aim of this study was to investigate the antimalarial activity of two series of AQ analogues where the 4'-hydroxyl function of AQ was replaced by either fluorine or chlorine. The intention of this was to block formation of a toxic quinone imine metabolite *in vivo* whilst retaining an electronegative function capable of intramolecular hydrogen bonding. In addition to this, interest was paid to the interaction of target compounds with haem.

The study introduced a divergent synthesis which proved successful for the preparation of the chloro series, producing a number of analogues in high yield. The linear approach was preferred for the synthesis of the fluoro series due to low yields obtained following the divergent route.

Fluoro analogues were tested against the CQ-sensitive 3D7 strain of *P. falciparum* malaria whilst chloro analogues were tested against three *falciparum* strains, the CQ-sensitive 3D7 and HB3 strains and the CQ-resistant TM6 strain. A significant conclusion derived from these studies has been that the majority of the fluoro analogues were active around 30 nM. The exceptions to this were the dipropyl, dibutyl and morpholine side-chain analogues. After calculating the lipophilicity of these compounds using computational prediction software (VCCLAB, 2005) it was observed that molecules with very high lipophilicity tend to be less potent as antimalarials (Table 5.9).

Previous studies in the group have reported the importance of a *tert* butyl function for optimal activity (O'Neill *et al.*, 1997). This was mirrored in the results of this chapter as the highest activities were observed with molecules containing a *tert* butylamino group in the side-chain (**2k** and **3o**).

Further screenings of molecule **2k** (known as FAQ-4) against a number of CQ-sensitive and CQ-resistant strains of *P. falciparum* malaria showed there was no evidence of cross resistance with this drug.

Compound	IC_{50} (nM)	LogP
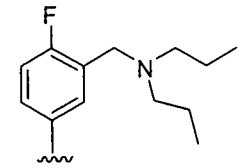 **2h**	85.2 ± 18.1	5.98 ± 1.0
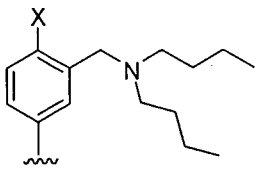 **2i/3h**	95.2 ± 30.2 (X = F) 277.3 ± 34.6 (X = Cl)	6.97 ± 1.3 (X = F) 7.40 ± 0.9 (X = Cl)
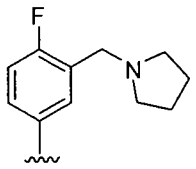 **2j**	550.7 ± 90.4	5.36 ± 0.4
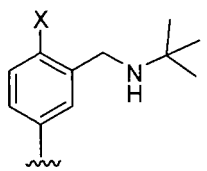 **2k/3o**	12.1 ± 5.3 (X = F) 7.8 ±3.2 (X = Cl)	5.14 ± 0.5 (X = F) 5.51 ± 0.7 (X = Cl)
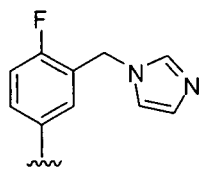 **2l**	27.2 ± 3.4	4.68 ± 0.41

Table 5.9 Comparison of the *in vitro* activity and lipophilicity of the most and least potent chloro and fluoro analogues (against the 3D7 strain of *P. falciparum*).

Studies have shown that the mechanism of action of quinoline antimalarial drugs such as CQ relies strongly on the inhibition of the crystallisation process of haem to β-haematin (Chou *et al.*, 1980; Slater *et al.*, 1992; Sullivan *et al.*, 1996). The mode of bonding between the drug and haem is believed to be by a π-π stacking interaction between aromatic groups in the drug and haem (Constantinidis *et al.*, 1988). Egan and co-workers have described the binding of quinoline antimalarial

drugs to haem in a 40 % DMSO solution (Egan *et al.*, 1997). According to Egan, the best-fit model for the binding of CQ to haem gives a stoichiometry of 1:1. Our study contradicts this result in that we found we could model a 2:1 interaction of CQ:haem. This model predicts a two-stage interaction between the drug and haem, whereby the drug can bind to haem with binding constant K_1 before a second equivalent binds with binding constant K_2. These results are significant since mefloquine and quinine do not form a 2:1 complex with haem but form a 1:1 complex.

5.3 REFERENCES

BRAY, P., MARTIN, R., TILLEY, L., WARD, S., KIRK, K. & FIDOCK, D. (2005). Defining the role of PfCRT in Plasmodium falciparum chloroquine resistance. *Molecular Microbiology*, **56,** 323-333.

CHOU, A., CHEVLI, R. & FITCH, C. (1980). Ferriprotoporphyrin IX fulfils the criteria for identification as the chloroquine receptor of malaria parasites. *Biochemistry*, **19,** 1543-1549.

CHRISTIE, G., BRECKENRIDGE, A. & PARK, B. (1989). Drug protein conjugates.18. detection of antibodies towards the antimalarial amodiaquine and its quinone imine metabolite in man and the rat. *Biochemical Pharmacology*, **38,** 1451-1458.

CONSTANTINIDIS, I. & SATTERLEE, J. (1988). UV-Visable and carbon NMR-studies of chloroquine binding to urohemin-1 chloride and uroporphyrin-1 in aqueoue-solutions. *Journal of the American Chemical Society*, **110,** 4391-4395.

DELARUE, S., GIRAULT, S., MAES, L., DEBREU-FONTAINE, M., LABAEID, M., GRELLIER, P. & SERGHERAERT, C. (2001). Synthesis and in vitro and in vivo antimalarial acitvity of new 4-anilinoquinolines. *Journal of Medicinal Chemistry*, **44,** 2827-2833.

EGAN, T., MAVUSO, W., ROSS, D. & MARQUES, H. (1997). Thermodynamic factors controlling the interaction of quinoline antimalarial drugs with ferriprotoporphyrin IX. *Journal of Inoorganic Biochemistry*, **68,** 137-145.

FRANCIS, S., SULLIVAN, D. & GOLDBERG, D. (1997). Hemoglobin metabolism in the malaria parasite plasmodium falciparum. *Annual Reviews of Microbiology*, **51,** 97-123.

HATTON, C., PETO, T., BUNCH, C. & PASVOL, G. (1986). Frequency of severe neutropenia associated with amodiaquine prophylaxis against malaria. *The Lancet*, 411-414.

MIROSHNIKOVA, O., HUDSON, T., GERENA, L., KYLE, D. & LIN, A. (2006). Synthesis and antimalarial activity of new isotebuquine analogues. *Journal of Medicinal Chemistry*, **50,** 889-896.

NEFTEL, K., WOODTLY, W., SCHMID, M. & FRICK, P. (1986). Amodiaquine induced agranulocytosis and liver damage. *British Medical Journal*, **292,** 721-724.

O'NEILL, P., WILLCOCK, D., HAWLEY, S., BRAY, P., STORR, R., WARD, S. & PARK, B. (1997). Synthesis, antimalarial activity and molecular modeling of tebuquine analogues. *Journal of Medicinal Chemistry*, **40,** 437-448.

PARAPINI, S., BASILICO, N., PASINI, E., EGAN, T., OLLIARO, P., TARAMELLI, D. & MONTI, D. (2000). Standardization of the physicochemical parameters to assess in vitro the beta-hematin inhibitory activity of antimalarial drugs. *Experimental Parasitology*, **96,** 249-256.

ROUVEIX, B., COULOMBEL, L., AYMARD, J., CHAU, F. & ABEL, L. (1989). Amodiaquine-induced immune agranulocytosis. *British Journal of Haematology*, **71,** 7-11.

SLATER, A. & CERAMI, A. (1992). Inhibition by chloroquine of a novel haem polymerase enzyme activity in malaria trophozoites. *Nature*, **355,** 167-169.

SULLIVAN, D., GLUZMAN, I., RUSSELL, D. & GOLDBERG, D. (1996). On the molecular mechanism of chloroquine's antimalarial action. *Proceedings of the National Academy of Sciences of the USA*, **93,** 11865-11870.

VCCLAB (2005). Virtual computational chemistry laboratory. pp. http://www.vcclab.org.

CHAPTER 6

THE EFFECT OF HALOGEN SUBSTITUTION ON THE METABOLISM AND DISTRIBUTION OF TWO NOVEL 4-AMINOQUINOLINES

CONTENTS

6.1 INTRODUCTION

This chapter explores a second route of potential metabolic escape by the substitution of the 4'-hydroxyl group of amodiaquine (AQ) with a halogen atom.

In 1993 Barnard *et al.* investigated the effects of the introduction of fluorine to the aromatic nucleus of paracetamol (Barnard *et al.*, 1993). They found that substitution of fluorine led to an increase in oxidation potential of the drug, thereby blocking the *in vivo* formation of a cytotoxic quinone imine (discussed in Chapter 1, Section 1.3.1.1). In a further study, undertaken at The University of Liverpool, this was effect was also noted with AQ. The systematic fluorine substitution of the aminophenol ring was investigated in order to try and increase the oxidative stability of the ring system and also to reduce the *in vivo* oxidation to amodiaquine quinone imine (AQQI) (O'Neill *et al.*, 1994) (Chapter 1, Section 1.4.5). Isosteric replacement of the hydroxyl group provided an analogue with significantly raised oxidation potential and reduced bioactivation *in vivo*. In contrast to the reduction in biological activity observed in the fluorinated paracetamol series, fluorinated analogues of AQ retained pharmacological activity, which suggested that oxidation to quinone imine metabolites is not required for antimalarial activity.

These studies present a strong case for the use of fluorine as a means to prevent the oxidation of AQ to AQQI. In addition to this, it is thought that chlorine substitution may also have a similar effect. Combining this with a *tert* butylamino side-chain in place of the diethylamino side-chain of AQ to increase metabolic stability, two back-up compounds have been rationally designed and synthesized. These compounds are *N-tert* butyl fluoro amodiaquine (FAQ-4) and *N-tert* butyl chloro amodiaquine (ClAQ-4) (Figure 6.1). The chemical and radiochemical syntheses of these compounds were described in Chapter 2.

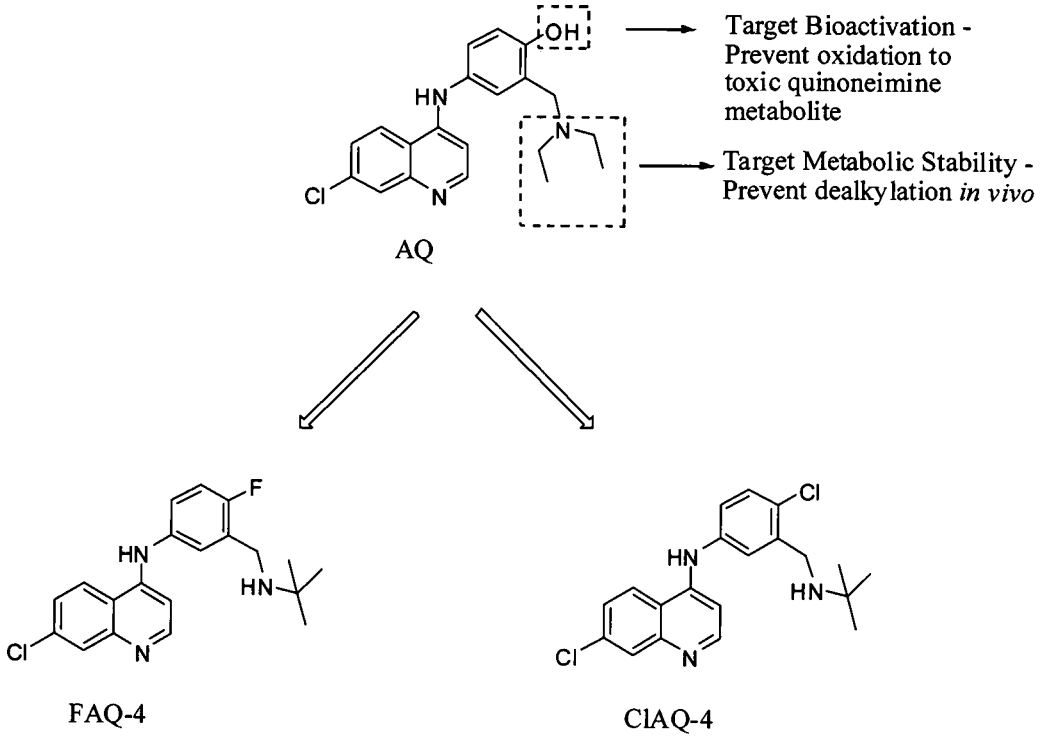

Figure 6.1 Structures of two novel 4-aminoquinolines, FAQ-4 and ClAQ-4 to be used as back-up candidates.

These particular compounds were chosen to go forward as candidates in this study due their exceptional antimalarial properties *in vitro* (Table 6.1). Each compound was active against both chloroquine-sensitive and -resistant strains of parasite in the nanomolar range. In addition to this, FAQ-4 was observed to be almost as active as AQ *in vivo* in mice against the *P. berghei* rodent strain of malaria (see comprehensive SAR in Chapter 5).

Preliminary pharmacokinetic studies have been initiated with FAQ-4. Results to date show that whilst the oral bioavailability could not match *N-tert* butyl isoquine (NTBISQ) (Chapter 4) across all species, it was shown to be 100 % in the rat and better than that of isoquine (ISQ) in other species (Table 6.1). Data for ClAQ-4 has not yet been generated.

Species	ISQ F%	desISQ F %	NTBISQ F %	FAQ-4 F %
Mouse	21	100	100	37
Rat	17.0 ± 4.0	60 ± 26	89 ± 12	100
Dog	NQ	NE	92 ± 13	ND
Monkey	ND	40 ± 14	100	25 ± 5

Table 6.1 Oral bioavailability of FAQ-4 in animals compared to other compounds of the same class. Data obtained from a pre-clinical, pharmacokinetics study at GlaxoSmithKline, Tres Cantos, Spain. Data are expressed as mean ± SD (n=3). NE = Not estimated (emesis observed in oral leg may have resulted in decreased oral exposure). NQ = Not quantifiable. ND = no data.

The aim of this chapter was to investigate the metabolism and distribution of two new series of AQ analogues where the 4'-hydroxyl function of AQ is replaced by either a 4'-fluorine or 4'-chlorine atom. This approach provides analogues that are resistant to aromatic hydroxylation whilst retaining full activity against malaria parasites. In addition, these halogenated ring systems cannot form potentially toxic electrophilic quinone imine metabolites (c.f. AQ).

6.2 MATERIALS AND METHODS

6.2.1 Materials

[^{3}H]-FAQ-4 (24.08 Ci/mmol; radiochemical purity by HPLC greater than 97 %) and [^{3}H]-ClAQ-4 (46.50 Ci/mmol; radiochemical purity by HPLC greater than 98 %) were prepared *via* a 1-step synthesis described previously, (Chapter 2, Sections 2.2.2.12 and 2.2.2.14). Tissue solubilizer–450 (0.5 N quaternary ammonium hydroxide in toluene) was purchased from Beckmann Chemicals, (Bremen, Germany). Ultima Flo and Ultima Gold scintillant were from Packard Bioscience BV, (Groningen, Netherlands). HPLC grade solvents were products of Fisher Scientific, (Loughborough, Leicestershire, UK).

Adult male Wistar rats (200-400 g) were obtained from Charles River (Margate, U.K.). The protocols described were undertaken in accordance with criteria outlined in a licence granted under the Animals (Scientific Procedures) Act 1986 and approved by the University of Liverpool Animal Ethics Committee.

5.2.2 Methods

6.2.2.1 In Vivo Metabolism of [^{3}H]-FAQ-4 and [^{3}H]-ClAQ-4 in the Rat (5 h)

Adult male Wistar rats (250 - 400 g n = 4) were anaesthetised with urethane (1.4 g/mL in isotonic saline; 1 mL/kg, i.p.). Polyethylene cannulae were inserted into the trachea, femoral vein and common bile duct and the penis was ligated. Drug-blank bile was collected for approximately 20 minutes before treatment. [^{3}H]-FAQ-4 or [^{3}H]-ClAQ-4 (54 μmol/kg; 20 μCi/rat) was dissolved in saline (0.5–1 mL depending on animal weight) and was injected over 10 min (*i.v.*). Bile was collected hourly for a time period of 5 h into pre-weighed eppendorf tubes. Samples were

weighed after collection to determine the extent of biliary secretion and stored at –30 °C until analysis by LC-MS.

After 5 h, urine was aspirated from the bladder and transferred to a pre-weighed Eppendorf tube and a cardiac puncture was performed. The blood was centrifuged (1000 g, 6 min) and the plasma transferred to a separate tube. The plasma from each experiment was pooled together and then blood proteins were removed by the exhaustive addition of MeOH (5 eq vv) followed by centrifugation (1200 g, 10 min). The supernatant was removed and concentrated by evaporation before re-dissolving it in MeOH (200 μL). The plasma and urine samples were stored at –30 °C until analysis by LC-MS.

Aliquots of bile and urine (30 μL) were mixed with scintillant (4 mL) for determination of radioactivity.

6.2.2.2 LC-MS Analysis of Bile, Urine and Plasma Samples

Aliquots of bile, urine and plasma (100 μL) were analysed at room temperature on a Hypersil 5-μm HyPurity Elite C-18 column (150 × 4.6 mm; Thermo Hypersil-Keystone, Runcorn, Cheshire, UK) with a gradient of acetonitrile (10-50 % over 30 min (FAQ-4), 20-50 % over 30 min (ClAQ-4)) in trifluoroacetic acid (0.1 %, v/v). The LC system consisted of two Jasco PU980 pumps (Jasco UK, Great Dunmow, Essex, UK) and a Jasco HG-980-30 mixing module. The flow rate was 0.9 mL/min. Eluate split-flow to the LC-MS interface was ca. 40 μL/min. A Quattro II mass spectrometer (Micromass MS Technologies, Manchester, UK) fitted with the standard co-axial electrospray source was used in the positive-ion mode. Nitrogen was used as the nebulizing and drying gas. The interface temperature was 80 °C; the capillary voltage, 3.9 kV. Spectra were acquired between m/z 100 - 1050

over a scan duration of 5 s. Fragmentation of analyte ions was achieved at a cone voltage of 50-70 V. Data were processed with MassLynx 3.5 software (Micromass). Radiolabelled analytes in the remainder of the eluate were detected with a Radiomatic A250 flow detector (Packard, Pangbourne, Berkshire, UK). Eluate was mixed with Ultima-Flo AP scintillant (Packard Bioscience BV, Groningen, Netherlands) at 1 mL/min.

6.2.2.3 In Vivo Retention Studies of [^{3}H]-FAQ-4 and [^{3}H]-ClAQ-4 in the Rat

Adult male Wistar rats (200 - 400 g, n = 4) were administered a solution of [^{3}H]–FAQ-4 or [^{3}H]-ClAQ-4 (54 μmol/kg; 20 μCi/rat) dissolved in saline (0.5 – 1 mL; *i.p.*). The animals were then transferred to individual metabolism cages equipped with a well for collecting urine and faeces. The rats were allowed food and drink *ad libitum* for a 24 h period before administration of a lethal dose of pentabarbitone.

Aliquots of urine (30 μL) were collected and mixed with scintillant for determination of radioactivity. The collected faeces were weighed and dissolved in distilled water for a period of 16 h before determination of radioactivity using the method described (Section 6.2.2.6). The major organs were then removed and assessed for radioactivity.

6.2.2.4 In Vivo Retention Studies of [^{3}H]-FAQ-4 and -ClAQ-4 in the Rat (48 h)

Adult male Wistar rats (n = 4) were administered a solution of either [^{3}H]–FAQ-4 or [^{3}H]-ClAQ-4 (54 μmol/kg; 20 μCi/rat) dissolved in saline (0.5 – 1 mL; *i.p.*). The animals were kept in a normal animal cage for a period of 24 h before they were transferred to individual metabolism cages equipped with a well for collecting

urine and faeces. The rats remained in the metabolism cages for a further 24 h, with full access to food and drink, before overdose using pentabarbitone.

Aliquots of urine (30 μL) were collected and mixed with scintillant for determination of radioactivity. The collected faeces were weighed and dissolved in distilled water for a period of 16 h before determination of radioactivity using the same method as described earlier (Chapter 6, Section 6.2.2.4). The major organs were then removed and assessed for radioactivity.

6.2.2.5 In Vivo Retention Studies of [^{3}H]- FAQ-4 and [^{3}H]-ClAQ-4 in the Rat (168-240 h)

Adult male Wistar rats (n = 4) were administered a solution of [^{3}H]–FAQ-4 or [^{3}H]-ClAQ-4 (54 μmol/kg; 20 μCi/rat) dissolved in saline (0.5 – 1 mL; *i.p.*). The animals were kept in a normal animal cage for a period of 168 h or 240 h with full access to food and drink before administration of a lethal dose of pentabarbitone. The major organs were then removed and assessed for radioactivity.

6.2.2.6 Tissue Distribution of [^{3}H]–FAQ-4 and [^{3}H]-ClAQ-4 in the Rat

At the end of the relevant time-point (5 h, 24 h, 48 h, 168 h or 240 h) the animals were killed by a lethal dose of pentabarbitone and the major organs were excised (brain, eyes, heart, lungs, liver, kidneys, spleen, testes and skin) and stored at –30 °C.

Duplicate portions (50 – 100 mg) of the tissues were weighed and solubilized in tissue solubilizer (0.75 mL) at 50 °C for 16 h. The solutions were decolourised with hydrogen peroxide (200 μL) over 1 h and then neutralised using glacial acetic acid (30 μL) before leaving in the darkness for 16 h to prevent chemoluminescence.

Ultima Gold scintillant (10 mL) was added before the radioactivity was determined by scintillation counting.

6.2.2.7 Cytotoxicity of FAQ-4 and ClAQ-4 in Isolated Rat Hepatocytes

Male Wistar rats (200 - 250g) (n = 3) were terminally anaesthetised with pentobarbitone sodium (90mg/kg in isotonic saline *i.p.*). Hepatocytes were isolated using a two-step collagenase perfusion method adapted from that of Guguen-Guillouzo *et al* (Guguen-Guillouzo *et al.*, 1986). The abdomen was opened and the liver cannulated through the portal vein using a gauge catheter. Before perfusion, the heart was removed to allow free loss of perfusion buffers. The liver was washed with calcium-free HEPES buffer for 10 mins at a flow rate of 40ml/min. The liver was then perfused with digestion buffer, a mixture of wash buffer with 5 % $CaCl_2$ solution, for 6 – 10 mins. The digested tissue was then excised and placed in a Petri dish containing wash buffer and DNAase (0.1 % w/v). The tissue was anchored and the Glison's capsule was disrupted and disturbed to release the cells. The cell suspension was filtered through gauze to eliminate cell debris, blood and sinusoidal cells. The cells were washed three times in DNAase wash buffer before re-suspending in incubation buffer (HEPES buffer and $MgSO_4.7H_20$ (0.25 % w/v)). Cell viability was then assessed microscopically using the trypan blue exclusion test.

The cells were then incubated with various concentrations of the relevant compound for a period of 6 hours before determining cell viability in the presence of test compound using the trypan blue exclusion test.

6.2.2.8 Statistical Analysis

All results are expressed as mean ± standard error of the mean (SEM). Values to be compared were analysed for non-normality using a Shapiro-Wilk test. Student t-tests were used when normality was indicated. A Mann-Whitney U test was used for non-parametric data. For analysis of sets of data with variance, a 1-way analysis of variance (ANOVA) test was used for parametric data and a Kruskell-Wallis test was used for non-parametric data. All calculations were performed using StatsDirect statistical software, results were considered to be significant when $P < 0.05$.

6.3 RESULTS AND DISCUSSION

6.3.1 LC-MS Analysis of *In Vivo* Metabolites of [^{3}H]-FAQ-4 in the Rat

Following administration of [^{3}H]-FAQ-4 (54 μmol/kg, 20 μCi) to male, Wistar rats, the total recovery of radioactivity in the bile was 9.76 ± 2.34 % of the given dose. This was in the form of six different metabolites (Figure 6.2). Metabolites **I**, **II** and **III** were very minor, comprising less than 11 % of the total metabolites present, and could not be identified. Metabolite **IV**, retention time (Rt) 8.36 min, was found to be the most abundant radioactive component in bile and comprised 62.50 ± 9.37 % of the total metabolites present. LC-MS analysis identified the characteristic eluting pairs of chlorine isotopes in the positive-ion mass chromatogram for *m/z* 469 (Figure 6.3B). This molecular weight could not be attributed to any known simple metabolite and the addition of 111 amu to the parent compound did not correspond to any recognised conjugate. The absence of **IV** in drug-blank bile proved the unknown compound to be a product of metabolism and not an endogenous component of bile (Figure 6.5). This was further proved by comparison of the mass spectrum of *m/z* 469 with that of the parent compound (*m/z* 358) which showed many of the same molecular fragmentation (Figure 6.4). Metabolite **IV** appeared to show the diagnostic loss of 129 amu on the mass spectrum to a peak of *m/z* 340. This also was unassigned. In an attempt to try and ascertain the identity of **IV** and other unknown metabolites, pooled bile was concentrated *via* the exhaustive addition of water and methanol using a Sep-Pak® cartridge. This served only to concentrate the endogenous components of bile at the expense of the drug metabolites. In addition to this, pooled bile samples were fractionated using HPLC in order to isolate the unknown metabolite **IV**. The isolated fractions were then analysed using LC-MS, however resolution could not be

improved and no further information on the unknown metabolites could be determined. It is possible that the unknown metabolite of *m/z* 469 could be a result of multiple transformations *in vivo*, or that [^{3}H]-FAQ-4 has formed some type of complex from interaction with endogenous bile acids.

The parent compound **V** eluted at Rt = 12.36 (Figure 6.2, represented by the shaded area). Only 5.35 ± 2.22 % of the radioactive dose was parent compound. Again, LC-MS analysis detected co-eluting pairs of chlorine isotopes for *m/z* 358 ([M+1]$^+$) and the familiar fragmentation pattern of loss of the *tert* butyl side-chain (-56 amu) could be clearly seen (Figures 6.3 and 6.4A). A sixth metabolite **VI** (Rt = 17.02 min) was also shown on the HPLC trace; however this too could not be identified using LC-MS.

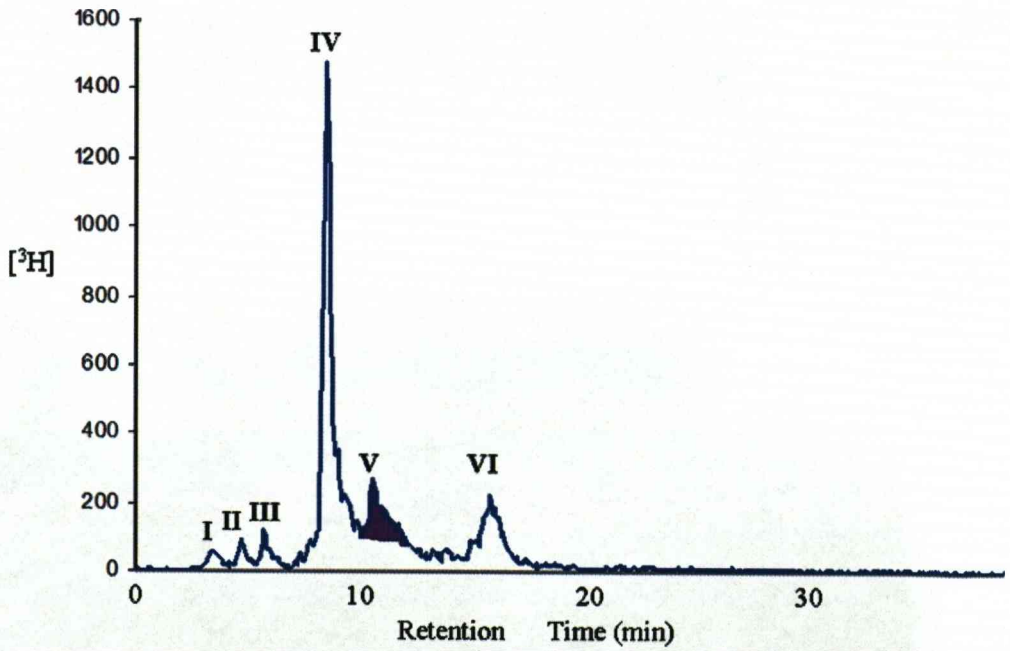

Figure 6.2 HPLC radiochromatogram of the biliary metabolites of [^{3}H]-FAQ-4 (54 µmol/kg, 20 µCi; 1 h collection). I, II and **III** represent unknown minor metabolites, **IV** represents a major metabolite of *m/z* 469, **V** represents the parent compound [^{3}H]-FAQ-4, **VI** represents a fourth unidentifiable metabolite.

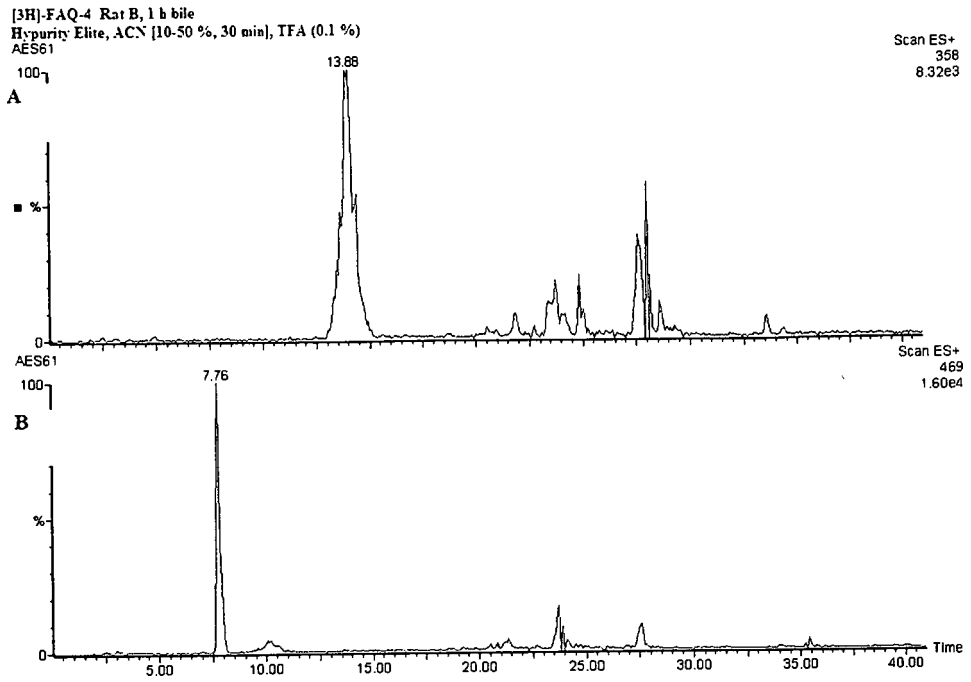

Figure 6.3 Positive-ion electrospray mass chromatograms corresponding to (A) *m/z* 358, [^{3}H]-FAQ-4 and (B) *m/z* 469, an unknown metabolite excreted in the bile of male Wistar rats 5 h after dosing *i.v.* with [^{3}H]-FAQ-4 (54 µmol/kg, 20 µCi).

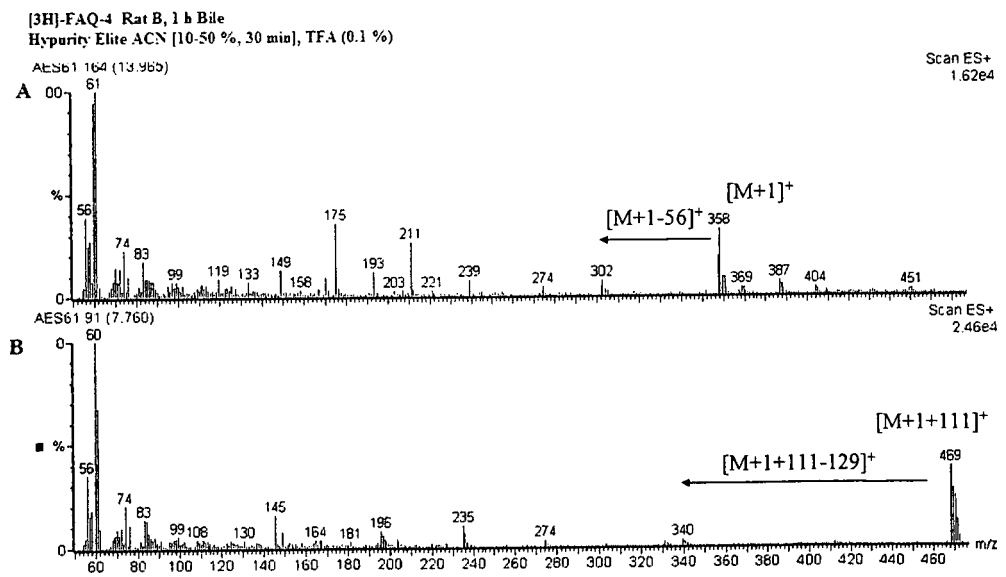

Figure 6.4 Positive-ion electrospray mass spectrum showing the fragmentation of an unknown metabolite of [^{3}H]-FAQ-4, with m/z 469, excreted in the bile of male, Wistar rats dosed *i.v.* with [^{3}H]-FAQ-4 (54 µmol/kg, 20 µCi, 1 h).

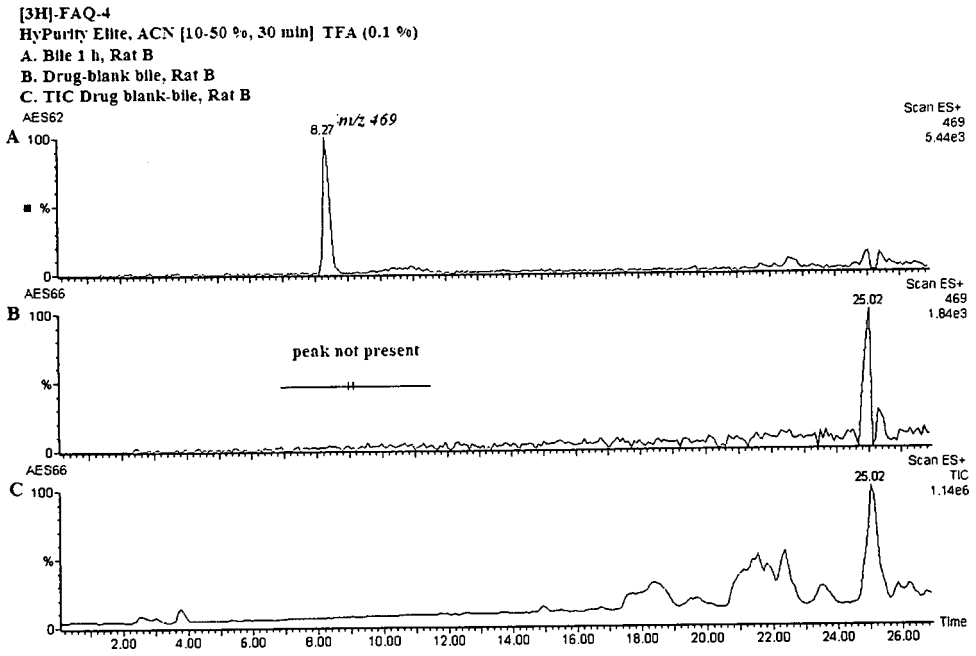

Figure 6.5 Positive-ion electrospray mass chromatograms corresponding to (A) *m/z* 469, the unknown, major metabolite excreted in rat bile after dosing *i.v.* with and [^{3}H]-FAQ-4 (54 μmol/kg, 20 μCi); **(B)** Drug-blank bile indicating the absence of the unknown prior to dosing in male, Wistar rats and **(C)** Total-ion current for drug-blank bile.

The metabolic profile of [^{3}H]-FAQ-4 in the urine of male, Wistar rats proved to be more straightforward to deduce than that in bile. Following administration of the drug, 7.69 ± 1.14 % was recovered in urine. The HPLC radio-chromatogram showed six metabolites (Figure 6.6). Metabolites **I** and **III** were also seen in bile and were present only in minor quantities, too low to be identified by LC-MS. Metabolites **VII**, **V**, **VIII** and **IX** were determined by LC-MS which identified pairs of chlorine isotopes in the positive-ion mass chromatogram for *m/z* 388, 358, 374 and 564 (Figure 6.7). Metabolite **VII** (*m/z* 388) eluted at Rt = 10.91 min, comprising 14.22 ± 2.21 % of the total radioactive metabolites and was identified as the side-chain carboxylic acid (Scheme 6.1). The corresponding glucuronide (*m/z* 564, **IX**) was observed at Rt = 15.75 min (9.95 ± 3.11 %), the identity of which was confirmed

by the diagnostic elimination of dehydroglucuronic acid (-176 amu). Metabolite **V** (*m/z* 358, $[M+1]^+$) was quite clearly the parent compound. It eluted at Rt = 12.36 min and was the major metabolite found in urine (67.53 ± 9.22 %). Metabolite **VIII** (*m/z* 374) was identified as the *N*-oxide of [^{3}H]-FAQ-4 ($[M+1+16]^+$). Analysis of the fragmentation pattern of *m/z* 374 showed the diagnostic loss of 56 amu to *m/z* 318, indicating that the oxygen was most certainly not part of the amino side-chain and was instead part of the quinoline ring system (*N*-oxide) (Figure 6.8).

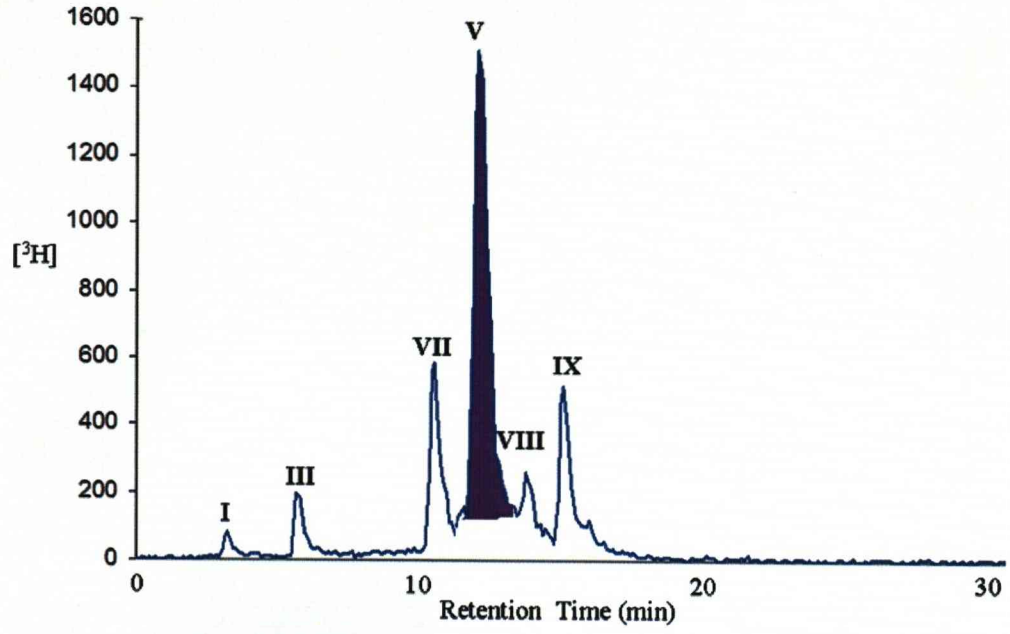

Figure 6.6 HPLC radiochromatogram of the urinary metabolites of [^{3}H]-FAQ-4 (54 µmol/kg, 20 µCi). **I** and **III** represent unknown metabolites, **V** represents the parent compound, [^{3}H]-FAQ-4, **VII** represents a derivative of [^{3}H]-FAQ-4 with a carboxylic acid within the *tert* butyl side-chain, **VIII** represents a mono-oxygenated species – likely to be [^{3}H]-FAQ-4-*N*-oxide and **IX** represents a glucuronide of metabolite **VII**.

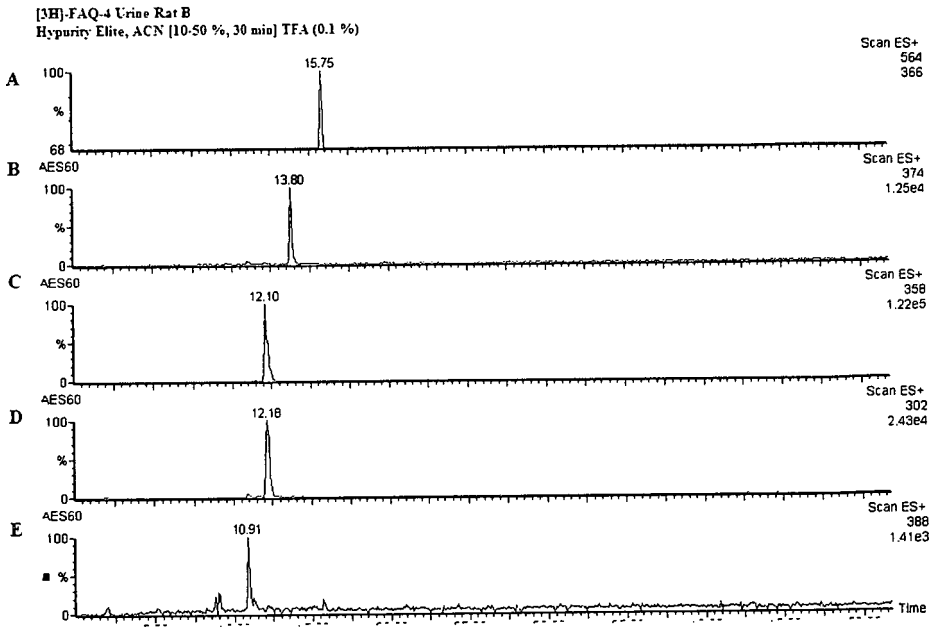

Figure 6.7 Positive-ion electrospray mass chromatograms corresponding to (A) *m/z* 564 **(IX)**, the glucuronide of metabolite **VII**; **(B)** *m/z 374*, **(VIII)** [^{3}H]-FAQ-4-*N*-oxide; **(C)** *m/z* 358 **(V)**, parent compound - [^{3}H]-FAQ-4; **(D)** *m/z 302*, the characteristic loss of side-chain observed with [^{3}H]-FAQ-4; **(E)** *m/z* 388 **(VII)**, [^{3}H]-FAQ-4 with a carboxylic acid incorporated into the amino side-chain excreted in the urine of male Wistar rats, 5 h after dosing *i.v.* with [^{3}H]-FAQ-4 (54 μmol/kg, 20 μCi).

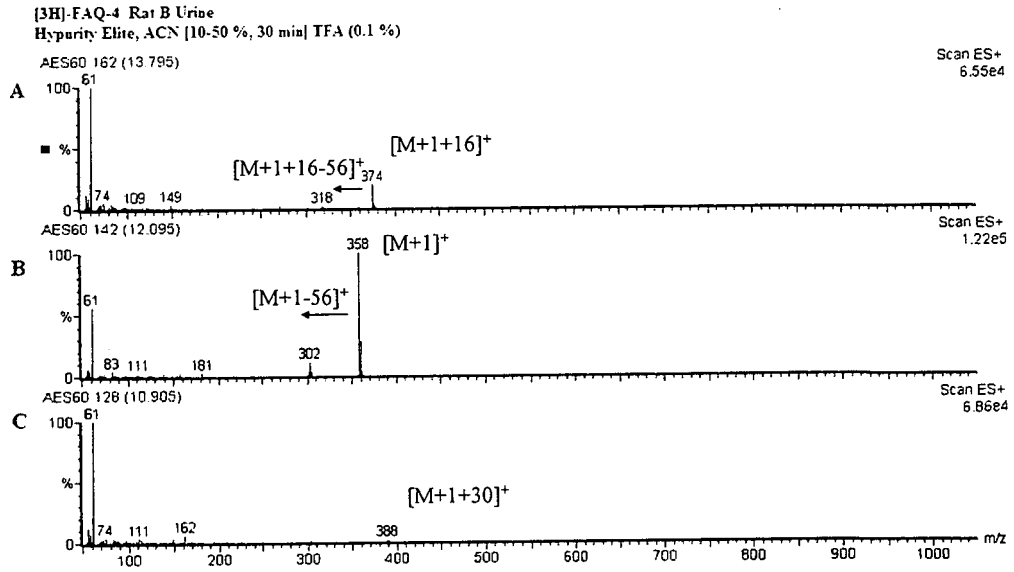

Figure 6.8 Positive-ion electrospray mass spectrum showing the fragmentation of (A) *m/z* 374, [^{3}H]-FAQ-4-*N*-oxide **VIII; (B)** *m/z 358*, parent compound, [^{3}H]-FAQ-4 **V; (C)** *m/z* 388, carboxylic acid side-chain derivative of [^{3}H]-FAQ-4 **VII,** excreted in the urine of male, Wistar rats dosed *i.v.* with [^{3}H]-FAQ-4 (54 μmol/kg, 20 μCi).

6.3.1.1 Conclusion

[^{3}H]-FAQ-4 has been shown to undergo metabolism to a total of nine metabolites in rats, *in vivo* (Table 6.2). Of these, four have been identified and the structures elucidated (Scheme 6.1). The major biliary metabolite of [^{3}H]-FAQ-4 was thought to be *m/z* 469; however, a corresponding structure could not be assigned. In urine [^{3}H]-FAQ-4 was excreted mainly as the parent compound. Importantly, no glutathione conjugates were identified indicating that the incorporation of fluorine into the AQ backbone has eliminated the possibility of the formation of a toxic quinone imine metabolite.

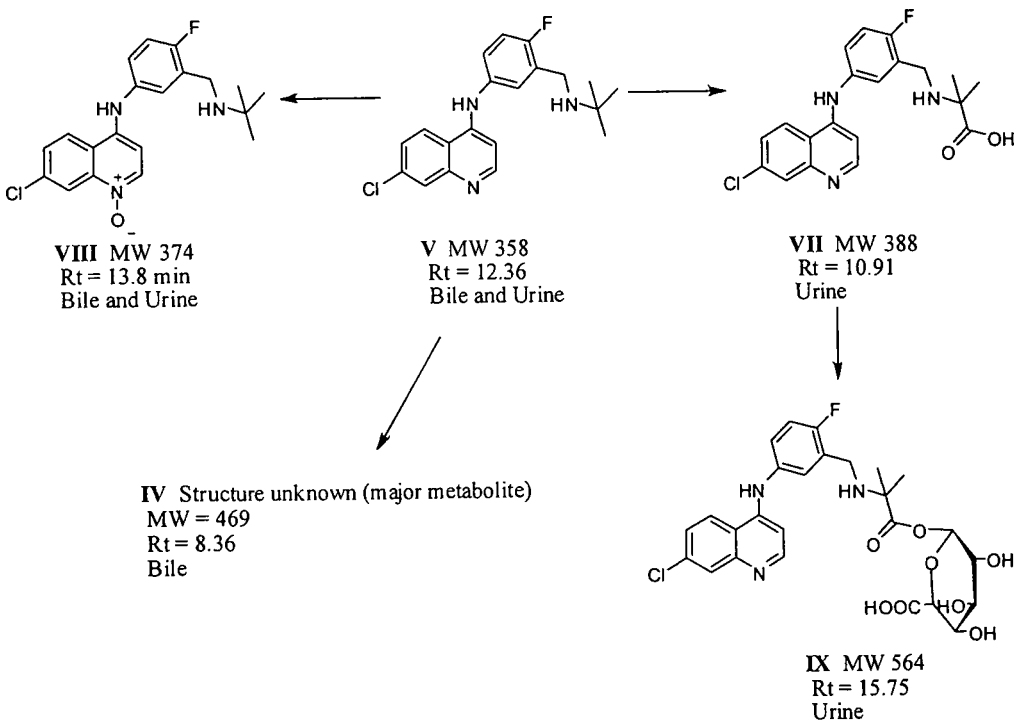

Scheme 6.1 Structures of the metabolites identified in the bile and urine of male, Wistar rats dosed *i.v.* with [^{3}H]-FAQ-4 (54 μmol/kg, 20 μCi).

Peak	Retention Time (min)	*m/z*	Metabolite Identity	Metabolite proportion (% of radiolabeled metabolites, 0-5 h)	Present in Bile/Urine
I - III	3.60, 3.80, 6.26	ND	ND	2.43 ± 0.21, 0.47 ± 0.03, 3.57 ± 2.31	Bile and Urine
IV	8.36	469	ND	62.5 ± 9.37	Bile
V	12.36	358	FAQ-4	5.35 ± 2.22, 67.53 ± 9.22	Bile and Urine
VI	16.26	ND	ND	19.0 ± 3.49	Bile
VII	10.91	388	Carboxylic acid in side-chain of FAQ-4	14.22 ± 2.21	Urine
VIII	13.8	374	FAQ-4-*N*-oxide	3.55 ± 0.21	Urine
IX	15.75	564	Glucuronide of carboxylic acid side-chain derivative	9.95 ± 3.11	Urine

Table 6.2 A summary of the metabolites produced in the bile and urine of male, Wistar rats after dosing with [^{3}H]-FAQ-4 (54 µmol/kg, 20 µCi). Metabolites were characterised by LC-MS. ND = No data.

6.3.2 LC-MS Analysis of *In Vivo* Metabolites of [^{3}H]-ClAQ-4 in the Rat

Administration of the novel 4-aminoquinoline, [^{3}H]-ClAQ-4 to male, Wistar rats (54 µmol/kg, 20 µCi, *i.v.*) led to the formation of a total of six metabolites in bile (Figure 6.9). Metabolites **I** and **II** were very minor and comprised less than 3 % of the total metabolites excreted. Metabolite **III** eluted at Rt = 13.29 min (4.52 ± 0.03 %) and was characterized using LC-MS which identified co-eluting pairs of chlorine isotopes in the positive-ion electrospray mass chromatogram for *m/z* 390 (Figure 5.10). This corresponded to a mono-oxygenated species, the fragmentation pattern of which indicated that the oxygen atom was located within the quinoline ring system and not the amine side-chain (Figure 6.11). This led us to deduce that the *N*-oxide

had been formed. The major metabolite produced in bile was a side-chain carboxylic acid derivative of [^{3}H]-ClAQ-4 **IV** (Figure 6.9 and Scheme 6.2). **IV** eluted at Rt = 14.74 min and represented 60.76 ± 2.34 % of the metabolites present in bile. LC-MS analysis located co-eluting pairs of chlorine isotopes for *m/z* 404 in the positive-ion mass spectrum. The acyl glucuronide of this metabolite was not located in the bile. Metabolites **V** and **VI** could not be assigned. The eluted at 16.09 and 18.09 min and represented 12.48 ± 2.94% and 19.53 ± 6.82 % of the biliary metabolites respectively.

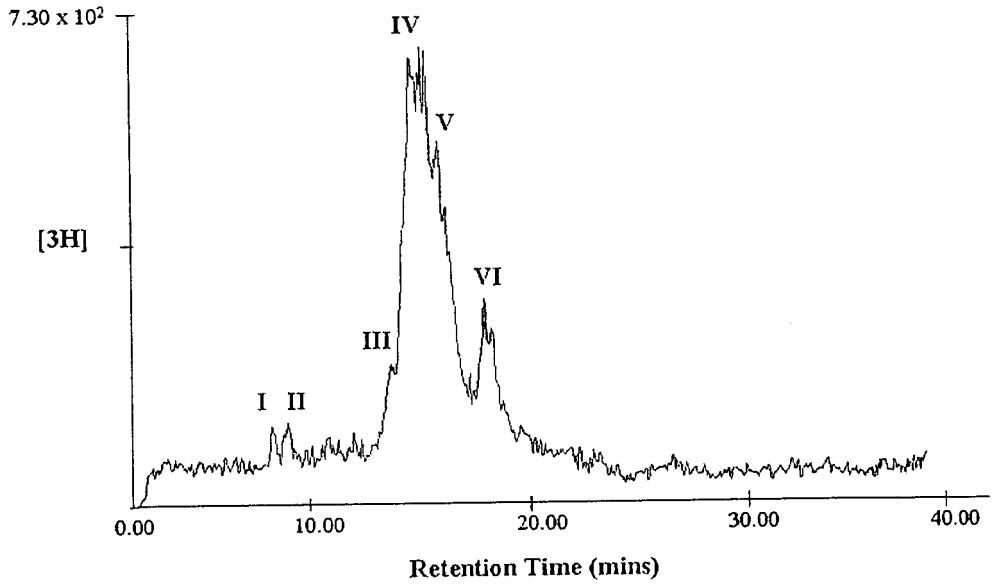

Figure 6.9 HPLC radiochromatogram of the biliary metabolites of [^{3}H]-ClAQ-4 (54 µmol/kg, 20 µCi; 3 h collection). I, II represent unknown minor metabolites; III represents [^{3}H]-ClAQ-4-*N*-oxide (*m/z* 390); **IV** represents a [^{3}H]-ClAQ-4 derivative with a carboxylic acid group situated within the amino side-chain (*m/z* 404); **V and VI** represent further unidentified metabolites.

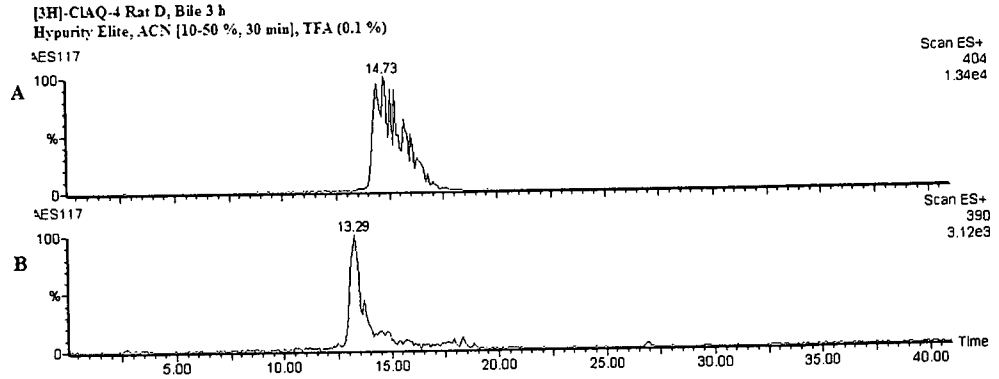

Figure 6.10 Positive-ion electrospray mass chromatograms corresponding to (A) *m/z* 404 **(IV)** a carboxylic acid-derivative of [^{3}H]-ClAQ-4 and **(B)** *m/z* 390 **(III)** [^{3}H]-ClAQ-4-*N*-oxide found in the bile of male, Wistar rats, dosed i.v. with [^{3}H]-ClAQ-4 (54 μmol/kg, 20 μCi, 3 hour collection).

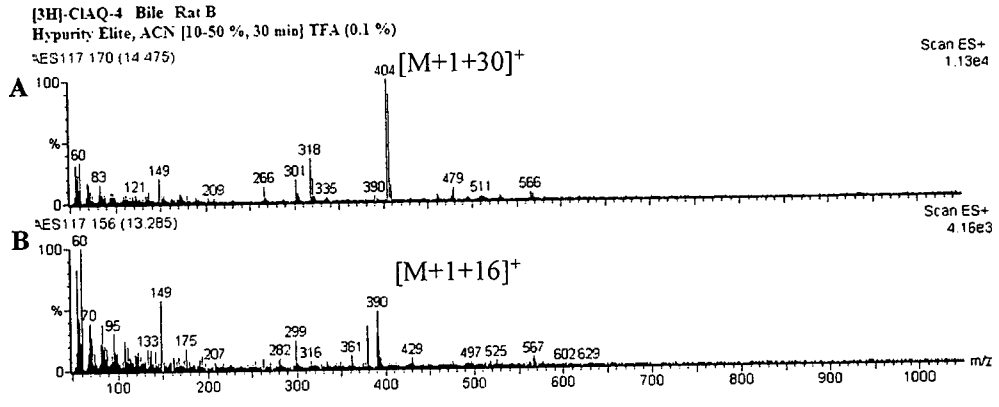

Figure 6.11 Positive-ion electrospray mass spectrum showing the fragmentation of (A) *m/z* 404 carboxylic acid side-chain derivative of [^{3}H]-ClAQ-4 **IV** and **(B)** *m/z* 390, [^{3}H]-ClAQ-4-*N*-oxide **III** excreted in the bile of male, Wistar rats dosed *i.v.* with [^{3}H]-ClAQ-4 (54 μmol/kg, 20 μCi, Rat B 3 h collection).

As with [^{3}H]-FAQ-4, the metabolic profile of [^{3}H]-ClAQ-4 in urine proved to be much clearer and easier to deduce than in bile. Four metabolites were shown in the radio-chromatogram (Figure 6.12). LC-MS analysis located co-eluting pairs of chlorine isotopes for *m/z* 404, 374, 390 and 333 (Figure 6.13). The first metabolite to be resolved eluted at Rt = 11.93 min and represented 28.48 ± 3.33 % of the total metabolites observed (**IV**). This metabolite was common to both bile and urine and was found to be the side-chain carboxylic acid derivative, *m/z* 404 (Figure 6.13,

Scheme 6.2). Figure 6.14 shows the characteristic loss of the amine side-chain and a similar fragmentation pattern to that of the parent compound. The major component of urine was shown to be the parent compound, [^{3}H]-ClAQ-4 **VII** (Figure 6.12, shaded peak Rt = 13.46 min; 55.70 ± 6.31 %). The *N*-oxide of [^{3}H]-ClAQ-4 (*m/z* 390, **III**), observed in bile was also found in urine to a much greater extent (34.73 ± 1.67 %). This again was characterized using LC-MS and a similar fragmentation pattern was observed (Figure 6.14). The final metabolite to be found in urine was *m/z* 333. This corresponded to the benzyl acid derivative of [^{3}H]-ClAQ-4 (Scheme 6.2) and eluted at Rt = 16.52 min and was 11.39 ± 2.99 % of the metabolites present in urine.

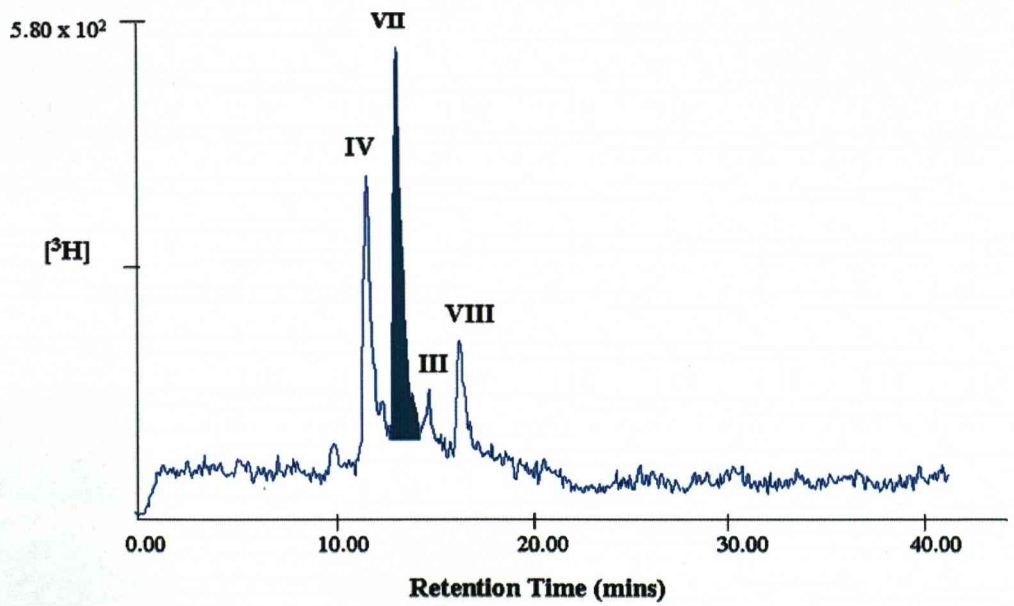

Figure 6.12 HPLC radiochromatogram of the urinary metabolites of [^{3}H]-ClAQ-4 (54 µmol/kg, 20 µCi; 3 h collection). **IV** represents a metabolite of *m/z* 404, the carboxylic acid (situated within the *tert* butyl side-chain), the shaded peak, **VI**, represents the parent compound, [^{3}H]-ClAQ-4, **III** represents [^{3}H]-ClAQ-4-*N*-oxide and **VIII** represents a benzoic acid derivative of [^{3}H]-ClAQ-4.

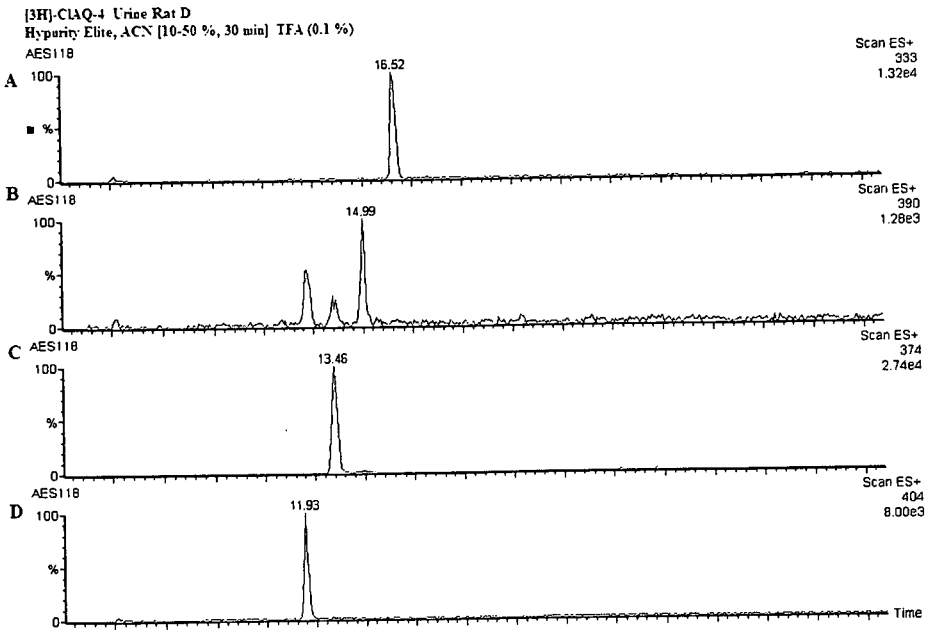

Figure 6.13 Positive-ion electrospray mass chromatograms corresponding to (A) *m/z* 333 **(VIII)** a benzoic acid-derivative of [^{3}H]-ClAQ-4; **(B)** *m/z* 390 **(III)** [^{3}H]-ClAQ-4-*N*-oxide; (C) *m/z* 374 **(VII)** parent compound; (D) *m/z* 404 **(IV)**,derivative of [^{3}H]-ClAQ-4 with carboxylic acid group found in amino side-chain. Metabolites were found in the urine of male, Wistar rats, dosed *i.v.* with [^{3}H]-ClAQ-4 (54 μmol/kg, 20 μCi).

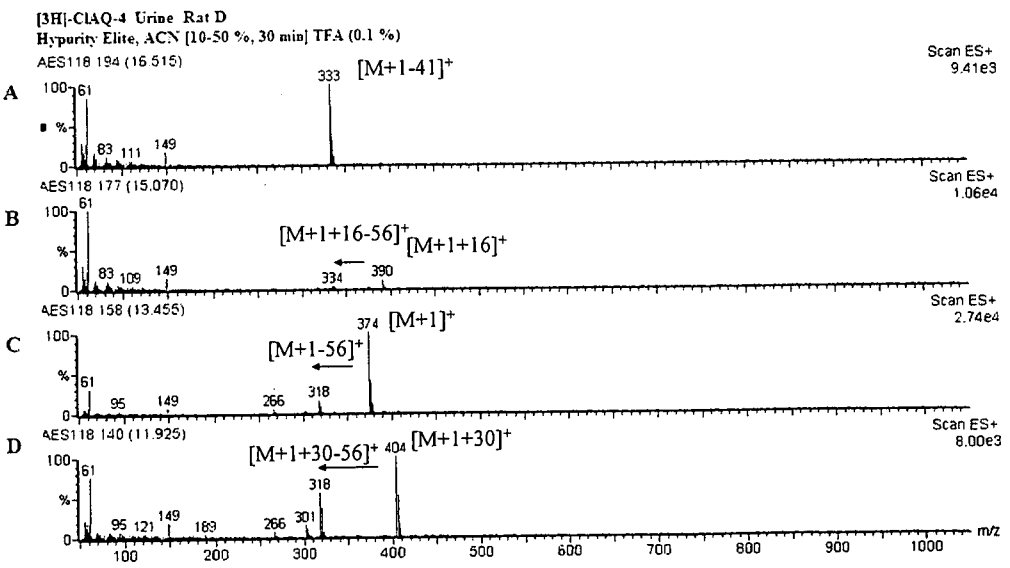

Figure 6.14 Positive-ion electrospray mass spectrum showing the fragmentation of (A) *m/z* 333, benzoic acid derivative of [^{3}H]-ClAQ-4 **VIII**; **(B)** *m/z* 390, [^{3}H]-ClAQ-4-*N*-oxide **III**; **(C)** *m/z* 374, parent compound **(VII)** and **(D)** *m/z* 404, carboxylic acid side-chain derivative of [^{3}H]-ClAQ-4 excreted in the urine of male, Wistar rats dosed *i.v.* with [^{3}H]-ClAQ-4 (54 μmol/kg, 20 μCi, h).

6.3.2.1 Conclusion

The metabolic profile of [^{3}H]-ClAQ-4 in rats has been deduced. All major metabolites were structurally assigned (Scheme 6.2, Table 6.3). The major route of metabolism appeared to be oxidation to the side-chain carboxylic acid **IV** (Scheme 6.2). Oxygenation of the nitrogen of the quinoline ring to form the *N*-oxide **III** was also observed. No evidence of bioactivation of [^{3}H]-ClAQ-4 was observed, as indicated by the lack of glutathione conjugate formation.

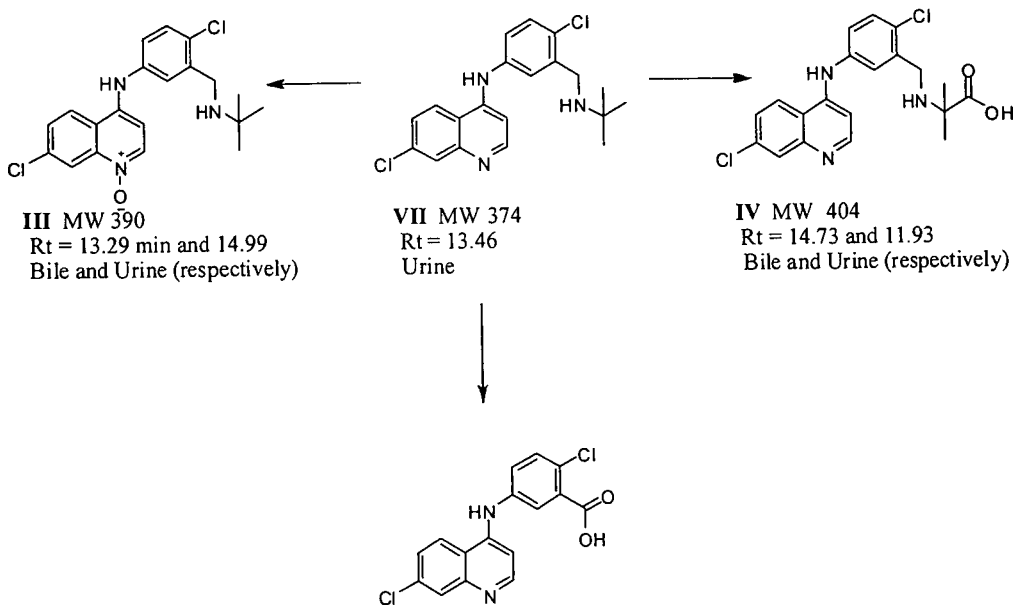

Scheme 6.2 Structures of the metabolites identified in the bile and urine of male, Wistar rats dosed *i.v.* with [^{3}H]-ClAQ-4 (54 μmol/kg, 20 μCi).

Peak	Retention Time (min)	*m/z*	Metabolite Identity	Metabolite proportion (% of radiolabeled metabolites, 0-5 h)	Present in Bile/Urine
I, II, V and VI	7.30, 8.02, 16.09, 18.09	ND	ND	1.08 ± 0.21, 1.63 ± 0.26, 12.48 ± 2.94, 19.53 ± 6.82	Bile
III	13.29, 14.99	390	ClAQ-4-*N*-oxide	4.52 ± 0.03, 34.43 ± 1.67	Bile and Urine
IV	14.73, 11.93	404	Carboxylic acid side-chain derivative of ClAQ-4	60.76 ± 2.34 28.48 ± 3.33	Bile and Urine
VII	13.46	374	ClAQ-4	55.70 ± 6. 31	Urine
VIII	16.52	333	Benzoic acid derivative of ClAQ-4	11.39 ± 2. 99	Urine

Table 6.3 A summary of the metabolites produced in the bile and urine of male, Wistar rats after dosing with [^{3}H]-ClAQ-4 (54 μmol/kg, 20 μCi). Metabolites were characterised by LC-MS. ND = No data.

6.3.3 Tissue Distribution of [^{3}H]-FAQ-4 and [^{3}H]-ClAQ-4 in the Rat

Five hours after administration of a single dose of [^{3}H]-FAQ-4 to cannulated rats 55.94 ± 5.82 % of the dose could be accounted for in the organs, bile and urine (Figure 6.15). The pattern of distribution followed that seen previously with CQ, AQ, NTBISQ and ISQ with the majority of the dose being retained in the liver (17.49 ± 0.82 %) and skin 12.44 ± 1.76 %). Elimination of the drug seemed to be favoured neither by biliary or urinary excretion systems with 9.16 ± 1.29 % of the dose being excreted in bile and 8.06 ± 1.12 % being excreted in the urine.

As might be expected, the pattern of distribution of [^{3}H]-ClAQ-4 in the tissues of male, Wistar rats followed the same pattern as the other 4-aminoquinoline compounds tested. Slightly less radioactivity than [^{3}H]-FAQ-4 was recovered in the tissues, bile and urine, 47.35 ± 4.77 %, the majority of which being found in the liver (12.41 ± 0.29 %). Significant differences in areas of accumulation were seen with

the kidneys, liver and biliary and urinary output. Five hours after dosing with [^{3}H]-ClAQ-4 there was significantly more radioactivity found in the kidneys than observed with [^{3}H]-FAQ-4, 5.43 ± 0.28 % versus 3.97 ± 0.13 % ($p = 0.0054$). In the liver, there was significantly less [^{3}H]-ClAQ-4 than [^{3}H]-FAQ-4 ($p = 0.0209$). This was followed by a significant increase in biliary excretion after dosing with [^{3}H]-ClAQ-4 (14.88 ± 0.83 %, $p = 0.0052$). The increased biliary excretion of [^{3}H]-ClAQ-4 could be attributed to increased lipophilicity.

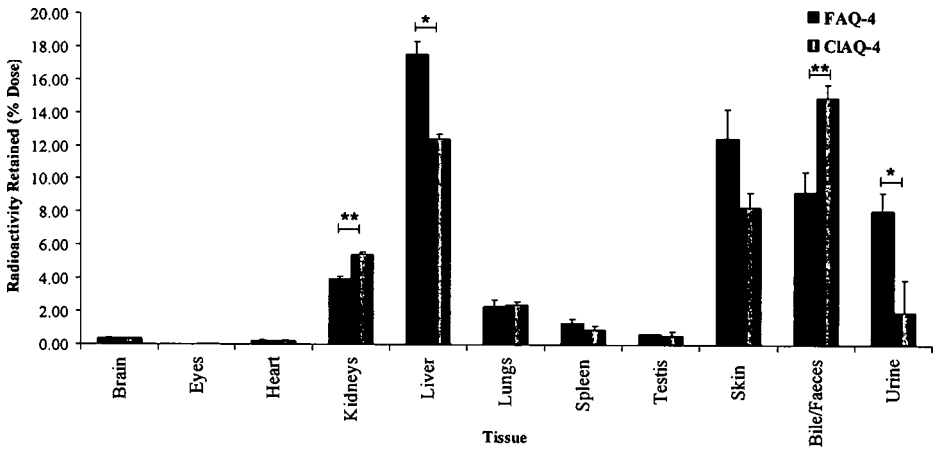

Figure 6.15 Percentage of radioactive dose recovered in tissues 5 h, after administration of [^{3}H]-FAQ-4 and [^{3}H]-ClAQ-4 (54 µmol/kg, 20 µCi/rat) to male Wistar rats (n = 4). Results are expressed as mean percentage of dose ± SEM. Statistics were performed using a one way ANOVA test for parametric data and Kruskal Wallis test for non-parametric data. *P<0.05, **P<0.01, ***P<0.001

On comparison of the tissue distribution of the two novel compounds with AQ, 5 h after administration it can be observed that at an equivalent dose, the halogenated analogues appear to accumulate in the major organs to a much lesser extent than AQ (Figure 6.16). In the brain, kidneys, liver and skin it can be seen that there was significantly less retention with the halogenated analogues of AQ.

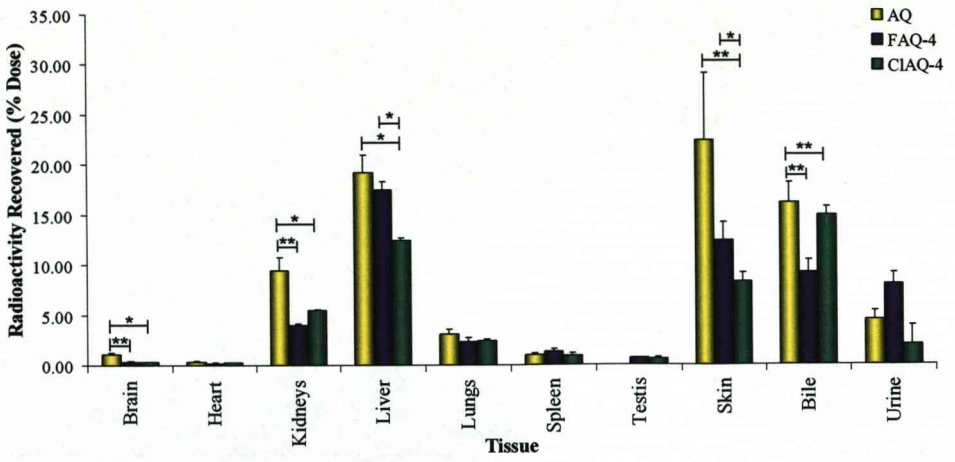

Figure 6.16 Percentage of radioactive dose recovered in tissues 5 h, after administration of [^{3}H]-AQ, [^{3}H]-FAQ-4 and [^{3}H]-ClAQ-4 (54 µmol/kg, 20 µCi/rat) to male Wistar rats (n = 4). Results are expressed as mean percentage of dose ± SEM. Statistics were performed using a one way ANOVA test for parametric data and Kruskal Wallis test for non-parametric data. *P<0.05, **P<0.01, ***P<0.001

Animals were dosed with either [^{3}H]-FAQ or [^{3}H]-ClAQ-4 and kept in metabolism cages for a period of 24 hours in order to see if the drugs were effectively eliminated or if they would accumulate in the tissues over time (Figure 6.17). Results showed that both drugs were effectively eliminated after 24 hours with the total amount of radioactivity recovered with [^{3}H]-FAQ-4 and [^{3}H]-ClAQ-4 being 51.36 ± 8.68 % and 61.00 ±.93 % respectively. In the kidneys, almost 2-fold more drug was found in rats dosed with [^{3}H]-FAQ-4 than those dosed with [^{3}H]-ClAQ-41.48 ± 0.11 % versus 0.31 ± 0.07 %, this was found to be highly significant ($p < 0.0001$). The same was seen on comparison of the radioactivity retained in the liver 24 hours after dosing. After dosing with [^{3}H]-FAQ-4 6.57 ± 0.27 % of the dose remained in the liver, whilst after dosing with the chloro analogue only 1.87 ± 0.21 % remained (3.5 fold less). This showed great mathematical significance with $p < 0.0001$. The lungs were another example where the choice of halogen substitute appeared to make a great difference to the retention of the drug. After dosing with

[^{3}H]-FAQ-4 1.17 ± 0.06 % of the dose remained, in comparison, after dosing with [^{3}H]-ClAQ-4 only 0.25 ± 0.08 % remained, a decrease of almost 5-fold ($p < 0.0001$).

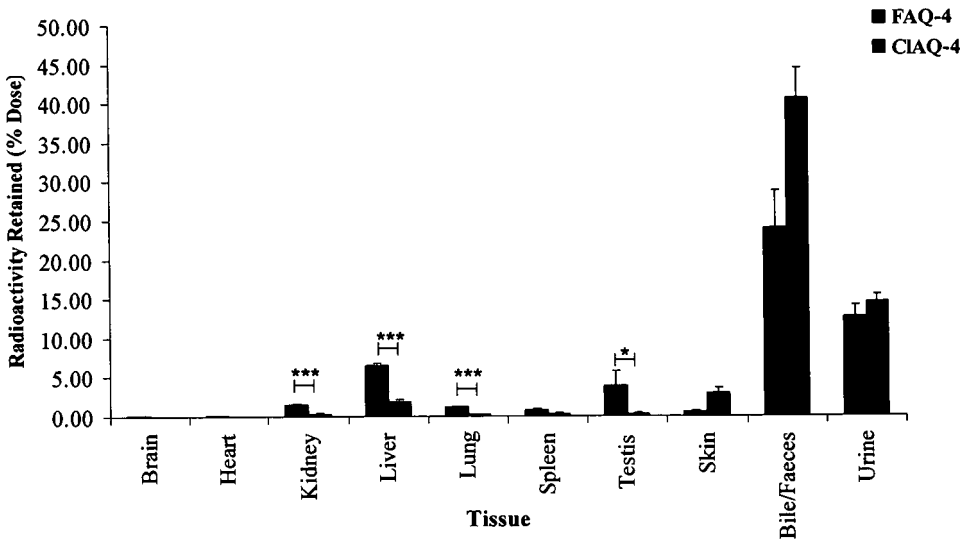

Figure 6.17 Percentage of radioactive dose recovered in tissues 24 h, after administration of [^{3}H]-FAQ-4 and [^{3}H]-ClAQ-4 (54 µmol/kg, 20 µCi/rat) to male Wistar rats (n = 4). Results are expressed as mean percentage of dose ± SEM. Statistics were performed using a one way ANOVA test for parametric data and Kruskal Wallis test for non-parametric data. *P<0.05, **P<0.01, ***P<0.001.

Although the amount of [^{3}H]-FAQ-4 remaining in the rat after 24 hours was relatively low (14.76 ± 2.47) (as compared to 38.54 ± 3.41% after 5 h), and significantly lower in the liver and skin ($p = 0.0286$ and $p = 0.0011$ respectively), it was deemed appropriate to investigate to further time-points (Figure 6.18). After 48 hours 72.79 ± 2.56 % of the dose could be accounted for in tissues, faeces and urine. Of this, less than 8 % remained in the tissues; the remainder had been excreted, mainly by biliary excretion. After one week (168 h) very little radioactivity remained inside the rat (1.22 ± 0.24 %). After 10 days (240 h) radioactivity was negligible in the tissues of the rat indicating a lack of accumulation and the effective clearance of [^{3}H]-FAQ-4 after a single dose of 54 µmol/kg.

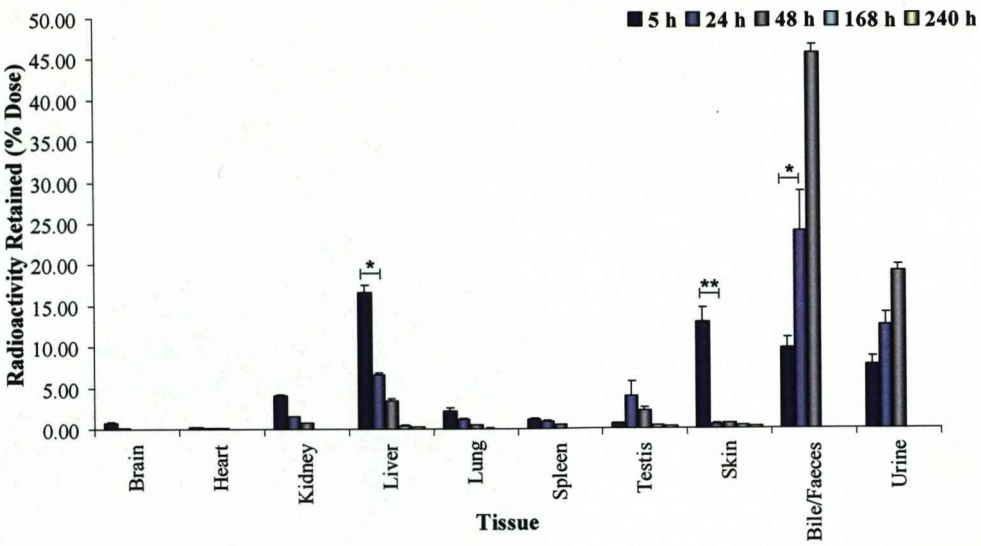

Figure 6.18 Percentage of radioactive dose recovered in tissues 5 h, 24 h, 48 h, 168 h and 240 h after administration of [^{3}H]-FAQ-4 (54 µmol/kg, 20 µCi/rat) to male Wistar rats (n = 4). Results are expressed as mean percentage of dose ± SEM. Statistics were performed using a one way ANOVA test for parametric data and Kruskal Wallis test for non-parametric data. *P<0.05, **P<0.01, ***P<0.001

6.3.3.1 Conclusion

In vivo studies in rats to assess the distribution and potential accumulation/retention of two novel compounds have been carried out. The results show that both drugs show a similar pattern of distribution to other 4-aminoquinolines of the same class, with the majority of the dose being found in the liver and skin. Incorporation of a halogen appears to reduce the retention within the tissues as compared to AQ, however the choice halogen is important as the chloro analogue appears to have significantly less retention and was cleared much more effectively by biliary excretion. After carrying out studies for up to 10 days it has been shown that [^{3}H]-FAQ-4 was effectively cleared from the rat and there were no issues of retention.

6.3.4 *In Vitro* Cytotoxicity of FAQ-4 and ClAQ-4 in Rat Hepatocytes

Rat hepatocytes, isolated using a two-step collagen digestion method (Section 3.2.2.8) were incubated with AQ, FAQ-4 or ClAQ-4 at concentrations of 0, 20, 50, 100, 200 and 500 μM (Figure 6.19) Results were expressed as the percentage of viable cells, measured microscopically, using a trypan blue exclusion test (as a percentage of the control). The results from this study show that the most profound difference in toxicity of rat hepatocytes was observed with FAQ-4 (Figure 6.19). By replacing the hydroxyl group of AQ with fluorine and incorporating a *tert* butyl group into the amine side-chain the Tox_{50} increases from 78 μM to 385 μM, a 5-fold difference. ClAQ-4 also showed less toxicity than AQ after incubation with rat hepatocytes, although to a lesser extent than FAQ-4 (Tox_{50} 120 μM). The *in vitro* therapeutic index of both FAQ-4 and ClAQ-4 was observed to be very high at 29167 and 11881 respectively showing that the amount of compound required to kill the parasite is much lower than that that will cause toxicity to hepatocytes.

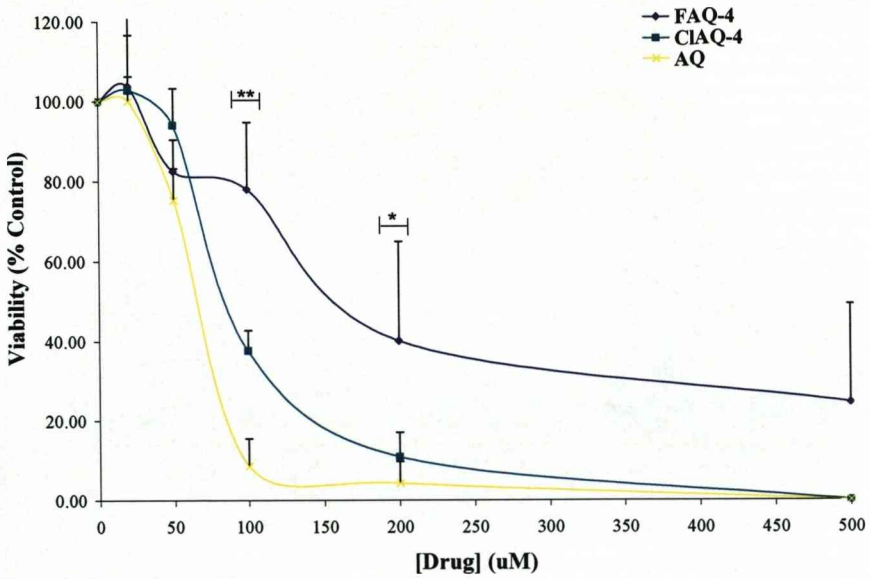

Figure 6.19 Viability of male, Wistar rat hepatocytes, incubated for 6 h with various concentrations of FAQ-4 or ClAQ-4, and stained with Trypan blue dye as an indicator for cell death. Results are expressed as mean percentage of dose ± SEM. Statistics were performed using a one way ANOVA test for parametric data and Kruskal Wallis test for non-parametric data. *P<0.05, **P<0.01, ***P<0.001

Compound	IC_{50} HB3 Strain (nM)	Tox_{50} Rat Hepatocytes (μM)	*In Vitro* Therapeutic Index
AQ	9.6 ± 3.7	78 ± 2.35	8125
FAQ-4	13.2 ± 3.4	385 ± 25.66	29167
ClAQ-4	10.1 ± 3.2	120 ± 14.56	11881

Table 6.6 The *in vitro* therapeutic index of AQ, FAQ-4 and ClAQ-4 as a measure of the cytotoxicity in male, Wistar rat hepatocytes

6.3.6 Conclusion

The metabolism and distribution of two novel 4-aminoquinolines antimalarial compounds, FAQ-4 and ClAQ-4 has been investigated. Both compounds were shown to follow a similar pattern of distribution, typical of that seen with other members of the 4-aminoquinoline class investigated. Accumulation occurred mainly in the liver and skin of rats. This was observed more so with the fluoro analogue but diminished with time, ruling out any concerns of retention.

The metabolic profile of FAQ-4 was partially determined; however one major metabolite remained unidentified. It was thought that this metabolite was of molecular weight 468 but the structure could not be assigned and the possibility remains that there was an undefined complex with endogenous biliary components. Further analysis employing the use of more sensitive LC-MS equipment is imperative.

The metabolic profile of ClAQ-4 was more easily defined and all major metabolites were characterized, with the main pathway of metabolism being formation of the side-chain carboxylic acid analogue (also observed in the metabolic profile of FAQ-4). ClAQ-4 underwent more extensive metabolism by this route than FAQ-4. It is possible that the increased lipophilicity of ClAQ-4 (logP = 5.50) may have an impact on bioavailability as the drug may undergo extensive first-pass metabolism.

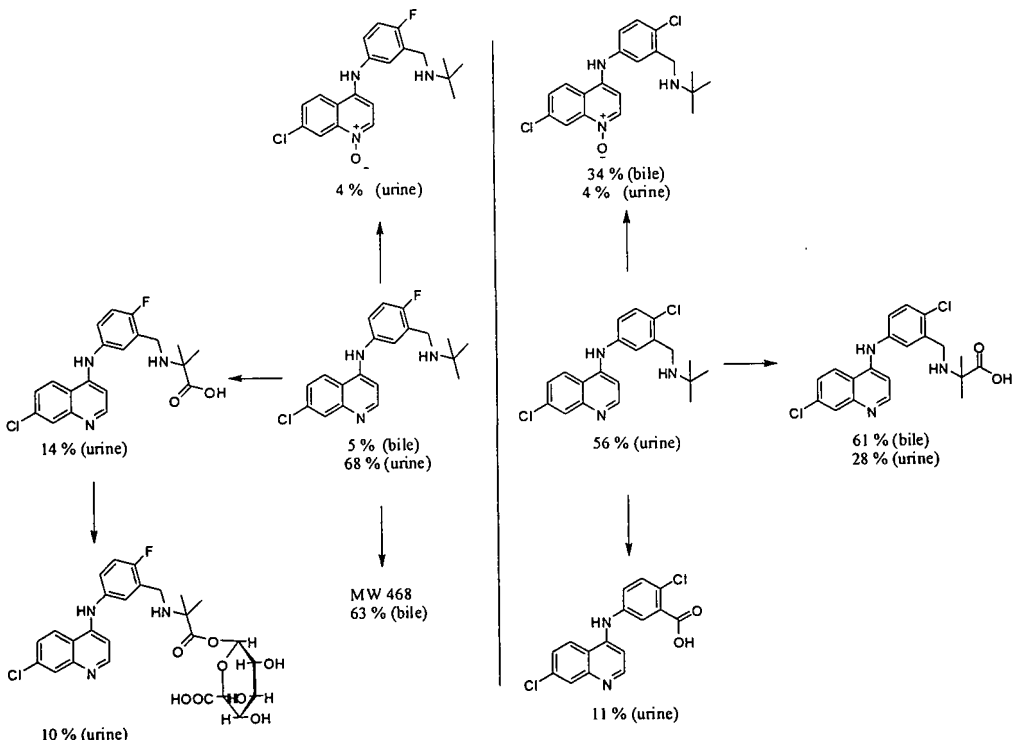

Scheme 6.3 Metabolic profiles of FAQ-4 and ClAQ-4 compared.

Importantly, no glutathione conjugation was observed with either halogenated compound.

In addition to the metabolism studies of these compounds, research into the potential toxicity was also carried out. Cytotoxicity studies revealed that incorporation of a halogen in place of the hydroxyl group of amodiaquine greatly decreased the toxicity of these compounds in rat hepatocytes. The choice of halogen atom appeared to be important as the fluoro analogue proved to be much less toxic than the chloro analogue.

Combined with the excellent antiparasitic properties of FAQ-4 and ClAQ-4, the results of this study reveal two candidates worthy of being considered back-up compounds to *N-tert* butyl isoquine (NTBISQ) in the search for a novel 4-aminoquinoline antimalarial.

6.4 REFERENCES

ADEDOYIN, A., FRYE, R., MAURO, K. & BRANCH, R. (1998). Chloroquine modulation of specific metabolizing enzyme activities:investigation with selctive five drug cocktail. *British Journal of Clinical Pharmacology*, **46,** 215-219.

BARNARD, S., STORR, R., O'NEILL, P. & PARK, B. (1993). The effect of fluorine substitution on the physiochemical properties and the analgesic activity of paracetamol. *Journal of Pharmacy and Pharmacology*, **45,** 736-744.

GUGUEN-GUILLOUZO, C. & GUILLOUZO, A. (1986). *Methods for preparation of adult and fetal hepatocytes, isolated and cultured hepatocytes.* Paris: INSERM and John Libbey Eurotext.

HASLER, J., JOHANSSON, I. & MASIMIREMBWA, C. (1995). Inhibitory effects of antiparasitic drugs on cytochrome P450 2D6. *European Journal of Clinical Pharmacology*, **48,** 35-38.

O'NEILL, P., HARRISON, A., STORR, R., HAWLEY, S., WARD, S. & PARK, B. (1994). The effect of fluorine substitution on the metabolism and antimalarial activity of Amodiaquine. *The Journal of Medicinal Chemistry*, **37,** 1362-1370.

SEDGEWICK, S., HO, C. & WOODGATE, R. (1991). Mutogenic DNA repair in enterobacteria. *Journal of Bacteriology*, **173,** 5604-5611.

SIMOOYA, O., SIJUMBIL, G., LENNARD, M. & TUCKER, G. (1998). Halofantrine and chloroquine inhibit CYP2D6 activity in healthy Zambians. *British Journal of Clinical Pharmacology*, **45,** 315-317.

WENNERHOLM, A., NORDMARK, A., PIHLSGARD, M., MAHINDI, M., BERTILSSON, L. & GUSTAFSSON, L. (2006). Amodiaquine, its desethyl metabolite, or both, inhibit the metabolism of debrisoquine (CYP2D6) and losartan (CYP2C9) in vivo. *European Journal of Clinical Pharmacology*, **62,** 539-546.

CHAPTER 7

FINAL DISCUSSION

CONTENTS

7.1 DISCUSSION

The necessity for a new 4-aminoquinoline antimalarial to supersede chloroquine (CQ) and amodiaquine (AQ) is apparent. The PfCRT-mediated resistance to CQ and the toxicity of AQ have prompted a re-examination of the pharmacology of new and existing antimalarials. Novel antimalarials are required that are both safe and effective. It is therefore important to produce new compounds which are active against CQ-resistant strains of malaria and do not undergo metabolic activation *in vivo*.

Piperaquine (PQ), a bisquinoline compound (Figure 7.1) is currently undergoing phase III trials in combination with dihydroartemisinin (DHA) (Davis *et al.*, 2005; Myint *et al.*, 2007). PQ was introduced as a monotherapy for the treatment of malaria in the 1960s. It was considered at least as effective as CQ against *P. falciparum* and *vivax* malaria and better tolerated. Its use declined in the 1980s due to the emergence of PQ-resistant strains of *P falciparum* and the appearance of artemisinin derivatives. In the 1990s, a group of Chinese scientists re-discovered PQ as one of the components of short-course artemisinin-based combination therapies to achieve a high cure-rate without significant adverse effects (Hien *et al.*, 2004). A number of clinical trials carried out by White *et al.* describe DHA-PQ as a highly efficacious and well tolerated combination therapy for the treatment of malaria (Myint *et al.*, 2007). Concerns with this combination lie in the fact that the calculated terminal half-life for PQ is around 543 hours (Chen *et al.*, 1979). Compared to that of DHA (approximately 0.5 hours), the development of resistance could be a possibility due to prolonged exposure of PQ at sub-therapeutic levels. Of equal concern is that the long half-life of PQ may lead to toxicity through accumulation as has been observed for CQ. PQ does not, however, contain any

obvious structural alert for metabolic activation. It is therefore of great importance to design a drug that has a half-life shorter than that of both CQ and PQ.

In terms of research of AQ analogues, a number of different groups have developed routes to potent 4-aminoquinoline AQ derivatives. For example, Sergheraert and co-workers in France have synthesised a series of novel 4-aminoquinolines whose design retains the aromatic ring of AQ but lacks the 4'-hydroxyl group responsible for the transformation to the toxic quinone imine formation *in vivo* (Figure 7.1) (Delarue *et al.*, 2001). The strategy of the Sergheraert group involved the incorporation of a basic side-chain in both the 3' and 4' positions of the aromatic nucleus to prevent nucleophilic addition of proteins during metabolism. The results of this work revealed several compounds with high antimalarial activity, with no cross-resistance *in vitro* and low cytotoxicity in tests using a human lung cell line (Delarue *et al.*, 2001).

More recently, studies utilising structural changes to tebuquine have been reported. These investigations described a series of isotebuquine analogues with a hydroxy group *meta* rather than *para* position to the amino group of the aniline moiety (Figure 7.1). These structural alterations meant the analogues would be unable to produce the toxic quinone imine metabolite *in vivo*. *In vitro* testing of these novel isotebuquine analogues against CQ-sensitive and CQ-resistant parasites showed them to exhibit activity similar to that of tebuquine (Miroshnikova *et al.*, 2006). However, during *in vivo* analysis the new isotebuquine analogues showed only marginal antimalarial activity, possibly due to poor solubility in vehicle and water.

Pyronaridine, an acridine-type Mannich base was first synthesised in the early 1970s by members of the Zheng laboratory and has been used for nearly twenty

years as a monotherapy to treat malaria in China (Figure 7.1). In line with the World Health Organisation initiative regarding artemisinin-based combination therapies (ACTs), MMV are funding a project to develop a low-cost, fixed-ratio combination of pyronaridine and artesunate for the treatment of acute uncomplicated malaria. The ACT is currently undergoing phase III clinical trials (Shao, 1990). Concerns have been raised in regard to pyronaridine having a similar structural alert to AQ and paracetamol for hepatoxicity (Lee *et al.*, 2004; Naisbitt *et al.*, 1998). However, in contrast to AQ, which contains a single Mannich amino side-chain at the 3' position, pyronaridine contains amino side-chains at both the 3' and 5' positions of the aminophenol ring system. Thus, although metabolic oxidation to a quinone imine can occur with this drug (Lee *et al.*, 2004), the presence of the additional substituent at the 5' position might prevent electrophilic attack of the quinone imine with sulfur-containing proteins. Like tebuquine however, the quinone imine metabolite of pyronaridine has potential to recycle intracellular glutathione leading to its depletion which in turn can lead to oxidative stress (Scheme 7.1) (Naisbitt *et al.*, 1998).

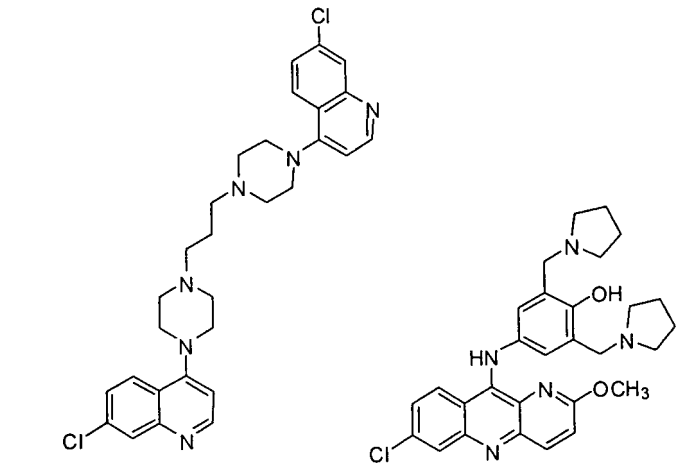

Piperaquine

Pyronaridine

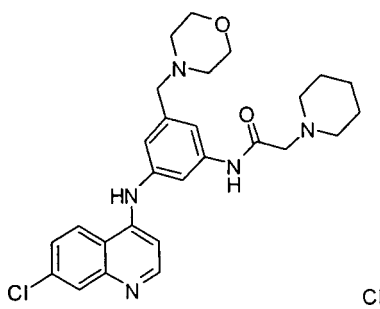

Sergheraert's 4-anilinoquinoline **49**

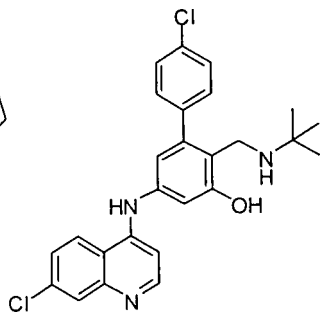

Isotebuquine analogue **1a**

Figure 7.1 4-Aminoquinoline derivatives: piperaquine, pyronaridine, a novel 4-aminoquinoline from the Sergheraert group and an isotebuquine analogue synthesised by Lin *et al* (Miroshnikova et al., 2006).

Glutathione Depletion

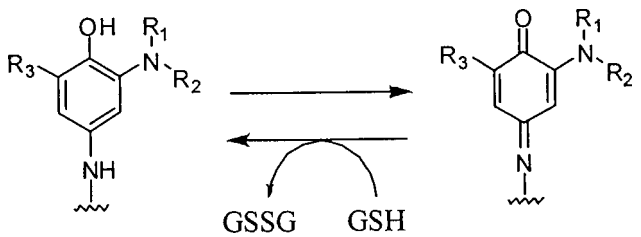

Tebuquine R_3 = *p*Cl-Ph
R_1 = H
R_2 = ^{t}Bu

Pyronaridine R_3 = H_2C-N

R_1, R_2 = $(CH_2)_4$

Scheme 7.1 Redox depletion of glutathione by tebuquine and pyronaridine

Our studies have shown the development of two distinct routes in the production of a novel 4-aminoquinoline antimalarial.

The first strategy involved the interchange of the hydroxyl group of AQ with the amino side-chain thus preventing the quinone imine metabolite from being able to form. This led initially to isoquine (ISQ), a candidate with unacceptably poor oral bioavailability due to multiple routes of metabolism for the *N*-diethylamino side-chain. Replacement of the diethylamino side chain with the more stable *tert* butylamino moiety led to *N-tert* butyl isoquine [(NTBISQ) Chapter 4] a drug candidate with almost 100 % oral bioavailability across four animal species.

The second strategy involves the introduction of a halogen atom in place of the hydroxyl group of AQ. Substitution of AQ with fluorine has been shown to completely abolish the intracellular depletion of glutathione associated with formation of the toxic quinone imine metabolite of AQ and also prevents activation within granulocytes (O'Neill et al., 1994; Tingle et al., 1995). Combining this line of reasoning with the increased metabolic stability of a *tert* butylamino side-chain led us to the compounds *N-tert* butyl fluoro amodiaquine and *N-tert* butyl chloro amodiaquine [(FAQ-4 and ClAQ-4) Chapter 5]. Figure 7.2 highlights the pathway of development of the lead compound, NTBISQ and the back-up compounds, FAQ-4 and ClAQ-4 from CQ.

We have presented extensive metabolic and dispositional studies on NTBISQ, FAQ-4, and ClAQ-4, making direct comparisons to CQ, AQ and ISQ. Each compound was synthesised *via* highly efficient and inexpensive routes, allowing for in depth *in vitro* and *in vivo* pharmacological testing to be performed. This chapter presents an overview of all the major findings of this thesis and will directly compare the results generated by each of the three novel compounds.

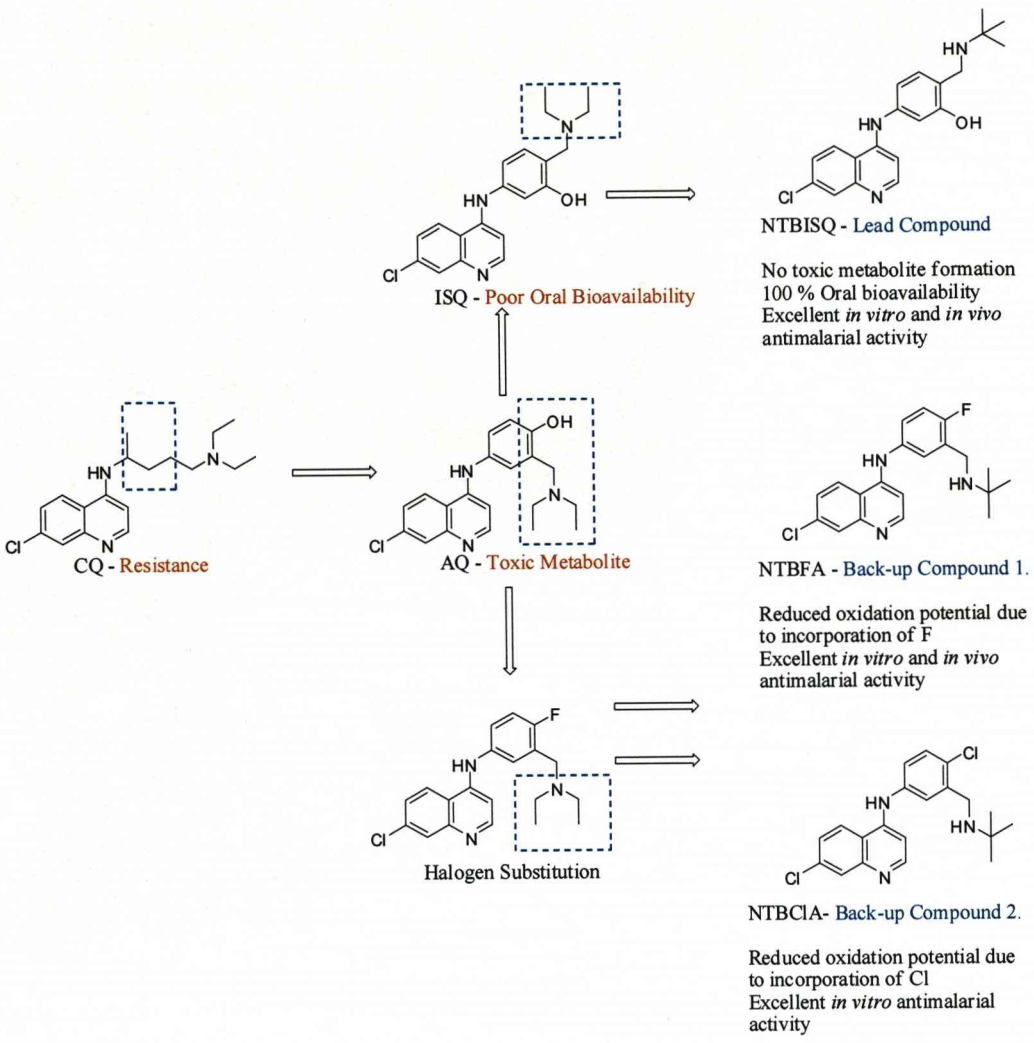

Figure 7.2 Rational re-design of old drugs for new. A summary highlighting the problems associated with current therapies and the structural changes from CQ to NTBISQ, NTBFA and NTBClA.

7.1.1 *In Vitro* Activities of NTBISQ, FAQ and ClAQ-4

A number of different analogues of ISQ and AQ have been synthesized and their antimalarial activity tested. The results of these tests saw NTBISQ, FAQ-4 and ClAQ-4 to have excellent *in vitro* activity against a number of different strains of *P. falciparum* malaria, including two CQ-resistant strains (K1 and TM6) (Table 7.1). The activities of NTBISQ, ClAQ-4 and FAQ-4 were highly comparable with that of

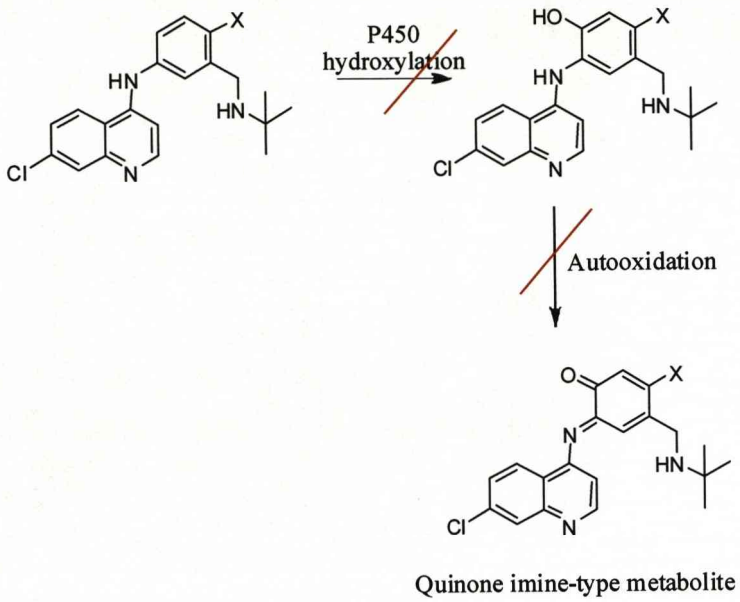

Quinone imine-type metabolite

Scheme 7.5 Possible P450-mediated hydroxylation of XAQ-4 analogues, leading to a quinone imine-type metabolite (X = Cl or F).

7.1.3.2 Distribution

The dispositional fate of each novel compound *in vivo* in rats was investigated. The importance of these studies lay in the fact that adverse effects may occur with drug accumulation due to direct toxicity. In a study by McChesney and co-workers in 1967 CQ was shown to accumulate in the tissues of rhesus monkeys (McChesney *et al.*, 1967). The study showed that after 96 hours, 35 % of the dose was present in the tissues. The liver was one of the main organs of accumulation. In our studies tissues with major affinity for radioactivity included the liver and skin. The pattern of distribution of [^{3}H]-NTBISQ, [^{3}H]-FAQ-4 and [^{3}H]-ClAQ-4 was remarkably similar, despite the differences in structure and radically different routes of metabolism (Figure 7.3). Significantly less [^{3}H]-ClAQ-4 was retained in the liver and skin as compared to [^{3}H]-NTBISQ ($p = 0.0310$ and 0.0396). The amount of radioactivity in the bile after dosing with [^{3}H]-FAQ-4 and [^{3}H]-ClAQ-4 was much

AQ and no evidence of cross-resistance between strains of *P. falciparum* was observed with any of the drugs investigated, aside that of CQ.

	IC_{50} nM			
Drug	K1	HB3	3D7	TM6
CQ	183.2 ± 11.1	14.9 ± 3.9	19.4 ± 1.9	75 ± 22.1
AQ	15.1 ± 9.4	9.6 ± 3.7	11.2 ± 1.4	7.2 ± 3.3
NTBISQ	13.2 ± 3.2	12.6 ± 5.3	11.2 ± 2.2	ND
FAQ-4	20.2 ± 4.6	13.2 ± 3.4	11.2 ± 2.5	ND
ClAQ-4	ND	10.1 ± 3.2	ND	3.0 ± 2.2

Table 7.1 ***In vitro*** **antimalarial activities of CQ, AQ, NTBISQ, FAQ-4 and ClAQ-4.** Data obtained from The School of Tropical Medicine, Liverpool. Values expressed as mean IC_{50} (nM) ± the standard deviation against four strains of the malaria parasite, *P. falciparum*: the CQ-resistant strains K1 and TM6 and the CQ-sensitive strains HB3 and 3D7. ND = No data.

7.1.2 *In Vivo* Activities of NTBISQ, FAQ-4 and ClAQ-4

Following evaluation of the therapeutic efficacy of NTBISQ, FAQ-4 and ClAQ-4 against *P. berghei* in mice the *in vivo* activity of NTBISQ was comparable with that of AQ (Table 7.2). FAQ-4 was observed to be less active and ClAQ-4 was considerably less potent than AQ (ED_{50} approximately 19 mg/kg). It was postulated that the reduced activity observed with ClAQ-4 could be a consequence of its increased lipid solubility (Table 7.3), implying that the compound may have undergone rapid first-pass metabolism in the liver resulting in less compound reaching the bloodstream. The results of these analyses showed NTBISQ to be the most potent of the three novel compounds at killing malaria parasites *in vivo*.

Compound	ED_{50} (mg/kg)	95 % Confidence Interval (mg/kg)	ED_{90} (mg/kg)	95 % Confidence Interval (mg/kg)
CQ	3.3	2.8 - 3.7	4.4	4.0 - 4.9
AQ	2.6	2.1 - 3.2	3.7	3.3 - 4.1
NTBISQ	2.8	3.3 - 4.3	4.7	4.8 - 6.1
FAQ-4	5.3	4.1 - 6.8	12.4	10.7 - 14.4
ClAQ-4	18.9[a]			

Table 7.2 The therapeutic efficacy of CQ, AQ, NTBISQ, FAQ-4 and ClAQ-4 against the *P. berghei* ANKA infection in mice. Data was taken from a study at GlaxoSmithKline, Tres Cantos, Spain using a standard 4-day test assay. [a]Preliminary data, confidence interval could not be set due to irregularities in data.

7.1.3 Metabolism and Distribution of NTBISQ, FAQ-4 and ClAQ-4

7.1.3.1 Metabolism

The mass fate and tissue distribution of each drug was investigated in rats. Each compound was labelled with a tritium atom incorporated into the quinoline ring system in order to enable analysis by radiometric HPLC and scintillation counting. Compounds were given *i.v.* at a dose of 54 μmol/kg, 20 μCi and bile, urine and plasma were analysed using LC-MS.

Administration of [^{3}H]-NTBISQ gave rise to the simplest metabolic profile of the three compounds (Scheme 7.2). In bile, [^{3}H]-NTBISQ was observed to undergo direct glucuronidation to form solely, its phenolic *O*-glucuronide. In urine, [^{3}H]-NTBISQ was excreted entirely as the parent compound. No other metabolites were observed in the HPLC trace. In a parallel *in vitro* study undertaken recently at GlaxoSmithKline, using human hepatocytes, similar results were observed. The main metabolites were the phenolic *O*-glucuronide and a quinolinone (which was not observed in out studies) (Scheme 7.2). The ultimate model for the metabolism of drugs in man is, of course, man. However the *in vitro* studies carried out by

GlaxoSmithKline showed all routes observed *in vivo* in rats were also observed in human, thus validating the use of the rat model in these studies.

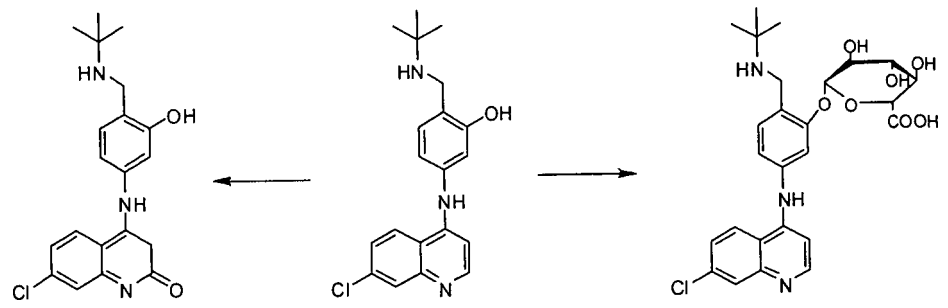

NTBISQ quinolinone **NTBISQ** **NTBISQ-*O*-glucuronide**

Scheme 7.2 ***In vitro* metabolic profile of NTBISQ in human hepatocytes.** The quinolinone was not observed *in vivo* in the rat.

Administration of [^{3}H]-FAQ-4 to rats led to a more complex metabolic profile. In bile, one major metabolite was detected by HPLC the molecular weight of which was thought to be 468. After numerous attempts, the putative metabolite could not be structurally assigned without the use of more sensitive equipment.

In urine, [^{3}H]-FAQ-4 was mainly present as the parent compound. Three other metabolites were excreted by this route also and these were the side-chain carboxylic acid, the *N*-oxide and a glucuronide of the carboxylic acid derivative (Scheme 7.3).

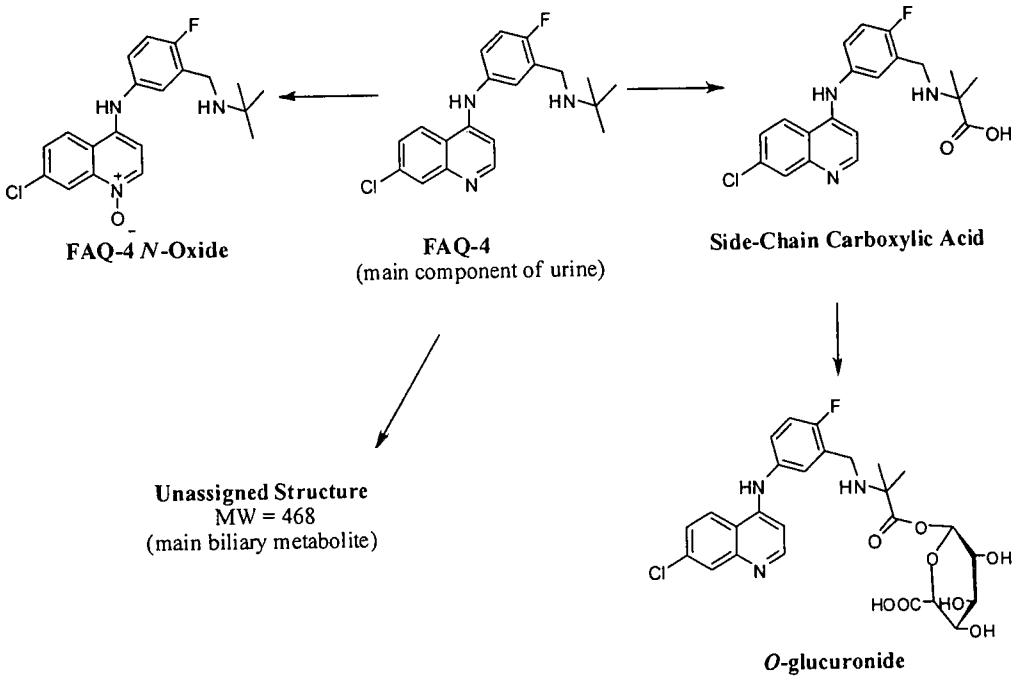

Scheme 7.3 Metabolic profile of [^{3}H]-FAQ-4, 5 hours after *i.v* administration to male, Wistar rats.

Following the administration of [^{3}H]-ClAQ-4 to rats (54 μmol/kg, 20 μCi) four major metabolites were found in bile and urine. LC-MS analysis revealed the presence of co-eluting pairs of chlorine isotopes which ultimately led to the assignment of metabolite structures (Scheme 7.4). As with [^{3}H]-NTBISQ and [^{3}H]-FAQ-4 the major component in urine was the parent compound. Similarly to [^{3}H]-FAQ-4 the side-chain carboxylic acid was formed, however conversion to this metabolite was much greater with [^{3}H]-ClAQ-4. There lies the possibility that this transformation may offer a significant route of clearance and could also explain the lower *in vivo* activity observed with [^{3}H]-ClAQ-4.

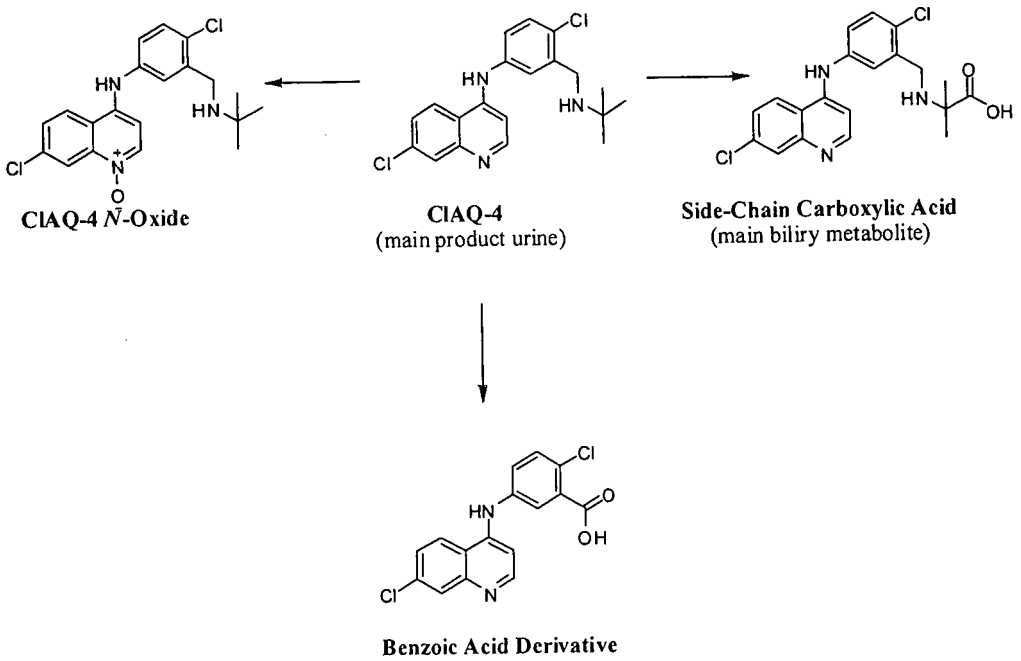

Scheme 7.4 Metabolic profile of [^{3}H]-ClAQ-4, 5 hours after *i.v* administration of male, Wistar rats.

P450 hydroxylation could potentially occur at any position of the aromatic ring of NTBISQ, FAQ-4 and ClAQ-4. This could ultimately lead to the formation of quinone imine-type metabolites (Scheme 7.5). The studies in this thesis have shown definitively that this was not the case. In addition, no glutathione conjugation was observed *in vivo* or *in vitro* with any of the compounds studied.

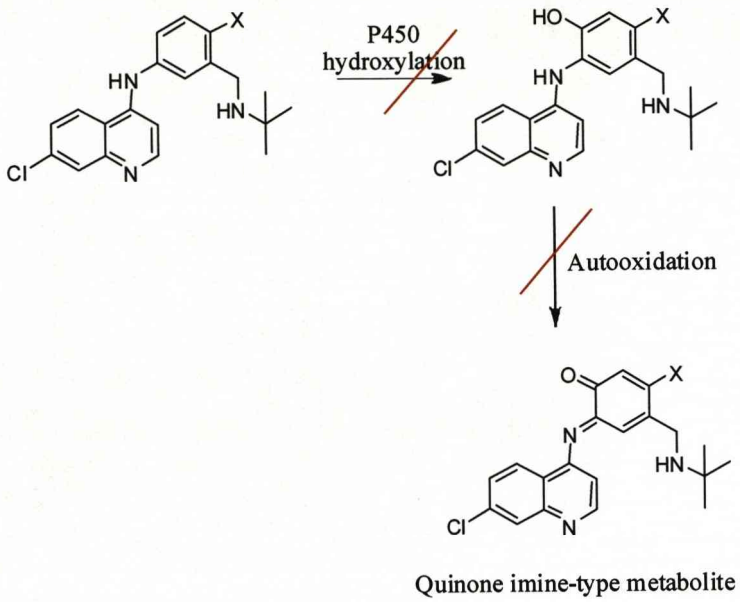

Quinone imine-type metabolite

Scheme 7.5 Possible P450-mediated hydroxylation of XAQ-4 analogues, leading to a quinone imine-type metabolite (X = Cl or F).

7.1.3.2 Distribution

The dispositional fate of each novel compound *in vivo* in rats was investigated. The importance of these studies lay in the fact that adverse effects may occur with drug accumulation due to direct toxicity. In a study by McChesney and co-workers in 1967 CQ was shown to accumulate in the tissues of rhesus monkeys (McChesney *et al.*, 1967). The study showed that after 96 hours, 35 % of the dose was present in the tissues. The liver was one of the main organs of accumulation. In our studies tissues with major affinity for radioactivity included the liver and skin. The pattern of distribution of [^{3}H]-NTBISQ, [^{3}H]-FAQ-4 and [^{3}H]-ClAQ-4 was remarkably similar, despite the differences in structure and radically different routes of metabolism (Figure 7.3). Significantly less [^{3}H]-ClAQ-4 was retained in the liver and skin as compared to [^{3}H]-NTBISQ ($p = 0.0310$ and 0.0396). The amount of radioactivity in the bile after dosing with [^{3}H]-FAQ-4 and [^{3}H]-ClAQ-4 was much

greater than after dosing with [^{3}H]-NTBISQ which could be attributed to the increased lipophilic nature of these compounds (Table 7.3).

At the time of measurement all radiolabelled drug had been cleared from the blood making it impossible to work out the relative plasma:tissue ratios.

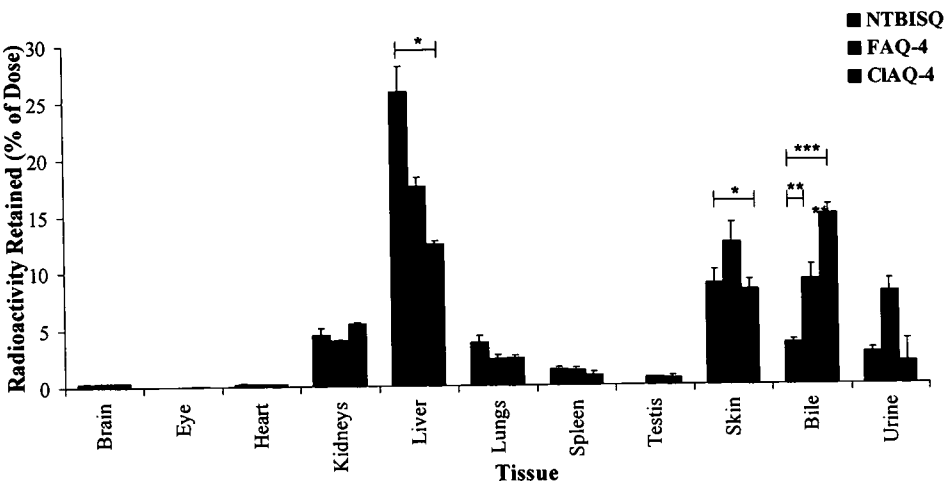

Figure 7.3 Percentage of radioactive dose recovered in tissues 5 h, after administration of [^{3}H]-NTBISQ, [^{3}H]-FAQ-4 and [^{3}H]-ClAQ-4 (54 µmol/kg, 20 µCi/rat) to male Wistar rats (n = 4). Results are expressed as mean percentage of dose ± SEM. Statistics were performed using a one way ANOVA test for parametric data and Kruskal Wallis test for non-parametric data. *P<0.05, **P<0.01, ***P<0.001

Compound	LogP	LogS	PKa (acid)	PKa (side-chain amine)
CQ	5.03 ± 0.88	-4.04 ± 0.68	NA	10
AQ	4.79 ± 0.67	-3.81 ± 1.25	10.4	9.1
ISQ	4.84 ± 0.86	-4.33 ± 0.33	7.7	9.1
NTBISQ	4.41 ± 0.83	-4.68 ± 0.68	7.7	9.1
FAQ-4	5.11 ± 0.48	-4.02 ± 1.42	NA	9.1
ClAQ-4	5.50 ± 0.59	-5.28 ± 0.93	NA	9.1

Table 7.3 In silico prediction of lipophilicity (logP), solubility (logS) and PKa of CQ, AQ, ISQ, NTBISQ, FAQ-4 and ClAQ-4 using computational software (VCCLAB, 2005). NA = Not applicable.

Investigation into the possible retention of these compounds in the organs of the rat saw that after 24 hours the majority of the radioactive dose of each compound was excreted in bile and urine (Figure 7.4). In particular, despite its increased lipophilicity ClAQ-4 displayed the least retention in all of the tissues tested.

The compounds investigated all had similar whole body disposition in the rat, despite radically different routes of metabolism. It is possible that this was due to the molecules having similar physiochemical properties as indicated in table 7.3.

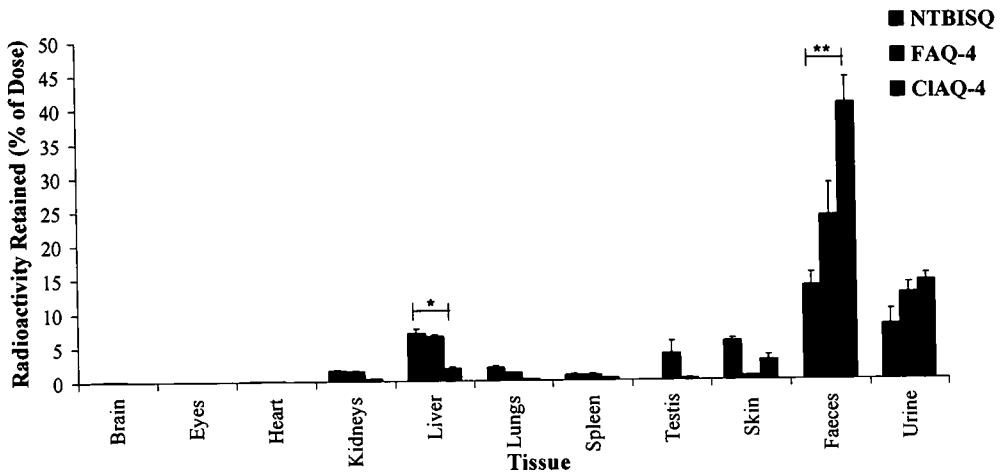

Figure 7.4 Percentage of radioactive dose recovered in tissues 24 h, after administration of [^{3}H]-NTBISQ, [^{3}H]-FAQ-4 and [^{3}H]-ClAQ-4 (54 µmol/kg, 20 µCi/rat) to male Wistar rats (n = 4). Results are expressed as mean percentage of dose ± SEM. Statistics were performed using a one way ANOVA test for parametric data and Kruskal Wallis test for non-parametric data. *P<0.05, **P<0.01, ***P<0.001

7.1.4 Toxicity

The cytotoxicity of NTBISQ, FAQ-4 and ClAQ-4 was investigated using isolated rat hepatocytes (Figure 7.5). Primary hepatocytes are only viable for a short number of hours, therefore the longevity of these preparations is too short to investigate time-dependant metabolism. However, the relative toxicities of these compounds could be compared after 6 hour incubations.

All compounds were shown to be less toxic to the rat liver cells in comparison to AQ. NTBISQ was shown to be the most cytotoxic of the three analogues tested with a Tox_{50} value of 40 μM. In comparison to the antimalarial activity of NTBISQ the *in vitro* therapeutic window remained above 3000 indicating that the compound is selective for the malaria parasite. FAQ-4 was shown to cause little damage to hepatocytes with Tox_{50} greater than 150 μM.

The results of this work show that NTBISQ may not be without its limitations clinically and it is possible it may cause some level of toxicity in humans. The cause of this toxicity may be due to the ability of the 4-aminoquinoline compounds to induce phospholipidosis in the liver.

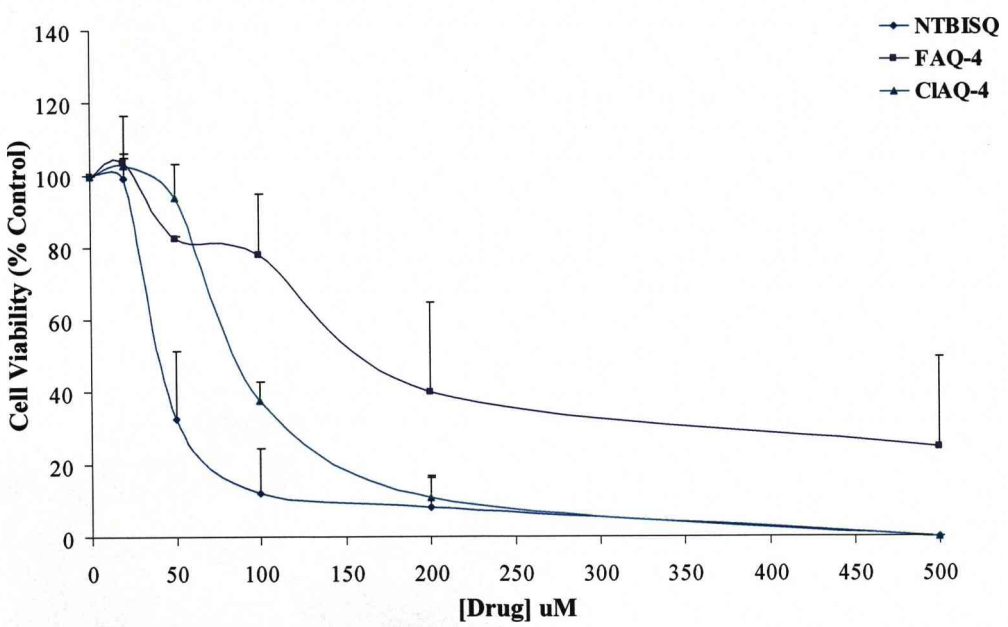

Figure 7.5 Viability of male, Wistar rat hepatocytes, incubated for 6 h with various concentrations of NTBISQ, FAQ-4 or ClAQ-4, and stained with Trypan blue dye as an indicator for cell death. Results are expressed as mean percentage of dose ± SEM. Statistics were performed using a one way ANOVA test for parametric data and Kruskal Wallis test for non-parametric data. *P<0.05, **P<0.01, ***P<0.001

7.1.5 Conclusion

This thesis has described the complete pathway of development of three novel 4-aminoquinoline compounds. Starting with the chemical synthesis, each compound has been prepared in good yield, using efficient and inexpensive routes. It is estimated that NTBISQ will cost less than $3 for a course of treatment - for a disease that is prevalent mainly in poverty-stricken areas this is essential.

The *in vitro* antimalarial activity of each novel compound has been shown to be comparable to that of AQ and NTBISQ has shown excellent *in vivo* activity. Extensive metabolism and dispositional work has been carried out resulting in complete metabolic profiles for NTBISQ and ClAQ-4. Most importantly, we have demonstrated with two chemical series that it is possible to dissociate metabolic activation from the efficacy of the 4-aminoquinolin antimalarials.

The main pathway of metabolism of NTBISQ is glucuronidation. In the absence of any bioactivation *in vivo* it is clear that by the implementation of structure-activity-design, we have successfully presented a means of metabolic escape in each compound. One major metabolite of [^{3}H]-FAQ-4 remained unresolved. It was possible that the parent ion was not identified in the spectra obtained. Further studies implementing the use of LC-NMR are required in order to elucidate the putative ion before it can be held unequivocally that FAQ-4 does not form a quinone imine metabolite *in vivo*.

At present the clinical situation, in terms of 4-aminoquinoline treatment of malaria, stands with the use of CQ being very limited due to the related resistance and AQ may only be used for acute treatment of malaria, rather than prophylaxis due to issues of toxicity. In addition, two drugs, PQ and pyronaridine are being developed as artemisinin-based combination therapies (ACTs). Whilst the

advantages of NTBISQ over AQ have been made clear, the benefits over PQ and pyronaridine still remain to be discussed. Table 7.4 shows a summary of some of the main parameters of interest of these CQ alternatives. From these data it can be seen that NTBISQ holds a clear advantage over PQ in the sense it is almost four-times more active against the K1 CQ-resistant strain of *P. falciparum.*

The use of NTBISQ in clinic is most likely to be in the form of an ACT and the preferred partner drug to be combined with NTBISQ is one with similar pharmacokinetics. The shorter half-life of NTBISQ in comparison with PQ offers a further advantage. Combination of an artemisinin-based compound with a very low half-life to a 4-aminoquinoline with a very long half-life c.f. PQ may result in the parasite being exposed to sub-lethal concentrations of one drug, resulting in the emergence of drug-resistance.

Quinoline antimalarials are potentially cardiotoxic, as observed in the rat at high doses of NTBISQ and in man after chronic dosing of CQ. Although, no clinically significant cardiovascular effects have been observed with PQ, gastrointestinal disturbances have been reported in China as a dose-limiting adverse effect (Karunajeewa *et al.*, 2004). In addition to this, resistance has developed in China before and prospective monitoring of PQ in combination with DHA will be required. Few toxicological concerns have been raised with pyronaridine except for transient electrocardiographic changes in man. This is in contrast to data reported for NTBISQ where initial findings suggest the dose-related toxicity to cardiac tissue, skeletal muscle and liver in rats. It is thought that this toxicity is due to phospholipidosis, a class effect of the 4-aminoquinolines also seen with CQ (Reasor *et al.*, 2006).

Although pyronaridine has better *in vitro* activity against the K1 strain of malaria than NTBISQ (Table 7.4), NTBISQ holds an advantage in that it has a simpler chemical synthesis and will also cost less to prepare.

The overall results of this thesis show that out of the three novel compounds tested, NTBISQ is a clear lead candidate for further development, with FAQ-4 and ClAQ-4 worthy back-ups. NTBISQ has been shown to be comparable, if not superior to two compounds currently entering phase III clinical trials as combination chemotherapy. Indeed, NTBISQ is now due to enter phase I clinical trials in man. It is only when clinical data has been obtained that we will be able to fully define the relationship between drug metabolism, drug disposition and drug safety for the novel 4-aminoquinoline antimalarials.

Drug	No. Synthetic Steps	$T_{1/2}$ (h)	F %	Toxicity	Activity versus K1 (nM)	Combined With
Amodiaquine	2	5		Hepatoxicity and agranulocytosis (man)	15.1 ± 9.4	Artesunate
Piperaquine	2	543	80-90 (mice)	Mild cardiotoxicity (rabbits). Mild heptatoxicity (dogs and monkeys) GI disturbances (man)	49 ± 1.8	DHA
Pyronaridine	>5	ND	19.7 (rabbits)	Transient electrocardiographic changes (man)	4.9 ± 1.1	Artesunate
N-tert Butyl Isoquine	2	9	100 (monkey)	Reversible cardiotoxicity, muscle toxicity and phospholipidosis (rats, high dose only)	13.2 ± 3.2	
N-tert Butyl fluoro Amodiaquine	4	ND	100 (rat) 37 (mice)	ND	20.2 ± 4.6	

Table 7.4 4-Aminoquinoline alternatives to chloroquine. Data taken from (Basco *et al.*, 2003; Davis *et al.*, 2005; Hatton *et al.*, 1986; Neftel *et al.*, 1986; Pradines *et al.*, 1998). ND = No data.

7.2 REFERENCES

BASCO, L. & RINGWALD, P. (2003). *In vitro* activities of piperaquine and other 4-aminoquinolines against clinical isolates of *Plasmodium falciparum* in Cameroon. *Antimicrobial Agents and Chemotherapy*, **47**, 1391-1394.

CHEN, Q., DENG, J. & WU, D. (1979). Study on absorption, distribution and excretion of 14C-piperaquine phosphate and 14C-piperaquine in mice. *PharmazeutischeI Industrie*, **8**, 19-23.

DAVIS, T., HUNG, T., SIM, I., KARUNAJEEWA, H. & ILETT, K. (2005). Piperaquine. A resurgent antimalarial drug. *Drugs*, **65**, 75-87.

DELARUE, S., GIRAULT, S., MAES, L., DEBREU-FONTAINE, M., LABAEID, M., GRELLIER, P. & SERGHERAERT, C. (2001). Synthesis and in vitro and in vivo antimalarial acitvity of new 4-anilinoquinolines. *Journal of Medicinal Chemistry*, **44**, 2827-2833.

HATTON, C., PETO, T., BUNCH, C. & PASVOL, G. (1986). Frequency of severe neutropenia associated with amodiaquine prophylaxis against malaria. *The Lancet*, 411-414.

HIEN, T., DOLECEK, C., MAI, P., DUNG, N., TRUONG, N., THAI, L., HOAI, D., THANH, T., STEPNIEWSKA, K., WHITE, N. & FARRAR, J. (2004). Dihydroartemisinin-piperaquine against mulitdrug-resistant Plasmodium falciparum malaria in Vietnam: randomised clinical trial. *Lancet*, **363**, 18-22.

KARUNAJEEWA, H., LIM, C., HUNG, T., ILETT, K., DENIS, M., SOCHEAT, D. & DAVIS, T. (2004). Safety evaluation of fixed combination piperaquine plus dihydroartemisinin (Artekin) in Cambodian children and adults with malaria. *British Journal of Clinical Pharmacology*, **57**, 93-99.

LEE, J., SON, J., CHUNG, S., LEE, E. & KIM, D. (2004). In vitro and in vivo metabolism of pyronaridine charectorized by low-energy collision-induced dissociation mass spectrometry with electrospray ionization. *Journal of Mass Spectrometry*, **39**, 1036-1043.

MCCHESNEY, E., FASCO, M. & BANKS, W. (1967). The metabolism of chloroquine in man during and after repeated oral dosage. *Journal of Pharmacology and Experimental Therapeutics*, **158**, 323-331.

MIROSHNIKOVA, O., HUDSON, T., GERENA, L., KYLE, D. & LIN, A. (2006). Synthesis and antimalarial activity of new isotebuquine analogues. *Journal of Medicinal Chemistry*, **50**, 889-896.

MYINT, H., ASHLEY, E., DAY, N., NOSTEN, F. & WHITE, N. (2007). Efficacy and safety of dihydroartemisinin-piperaquine. *Transactions of the Royal Society of Tropical Medicine and Hygiene*.

NAISBITT, D., WILLIAMS, D., O'NEILL, P., MAGGS, J., WILLCOCK, D. & PARK, B. (1998). Metabolism-dependant neutrophil cytoxicity of amodiaquine: A comparison

with pyronaridine and related antimalarial drugs. *Chemical Research in Toxicology*, **11**, 1586-1595.

NEFTEL, K., WOODTLY, W., SCHMID, M. & FRICK, P. (1986). Amodiaquine induced agranulocytosis and liver damage. *British Medical Journal*, **292**, 721-724.

O'NEILL, P., HARRISON, A., STORR, R., HAWLEY, S., WARD, S. & PARK, B. (1994). The effect of fluorine substitution on the metabolism and antimalarial activity of Amodiaquine. *The Journal of Medicinal Chemistry*, **37**, 1362-1370.

PRADINES, B., TALL, A., PARZY, D., SPEIGEL, A., FUSAI, T., HIENNE, R., TRAPE, J. & DOURY, J. (1998). In vitro activity of pyronaridine and amodiaquine against African isolates (Senegal) of Plasmodium falciparum in comparison with standard antimalarial agents. *Journal of Antimicrobial Chemotherapy*, **42**, 333-339.

REASOR, M., HASTINGS, K. & ROGER, G. (2006). Drug-induced phospholipidosis: issues and future directions. *Expert Opinion on Drug Safety*, **5**, 567-583.

SHAO, B. (1990). A review of antimalarial drug pyronaridine. *Chinese Medical Journal (Engl)*, **103**, 428-434.

TINGLE, M., JEWELL, H., MAGGS, J., O'NEILL, P. & PARK, B. (1995). The bioactivation of amodiaquine by human polymorphonuclear leucocytes *in vitro*: chemical mechanisms and the effects of fluorine substitution. *Biochemical Pharmacology*, **50**, 1113-1119.

VCCLAB (2005). Virtual computational chemistry laboratory. pp. http://www.vcclab.org.